Analysis of gene expression during the macrophage to foam cell transformation using cDNA arrays

Assum Gulzar

M.Phil. Thesis

Analysis of gene expression during the macrophage to foam cell transformation using cDNA arrays

By

Assum Gulzar

A thesis submitted to:

The Department of Biological Sciences

University of Durham

South Road

Durham City

DH1 3LE

United Kingdom

In accordance with the requirements for the degree of

Master of Philosophy

2006

Abstract

Analysis of gene expression during the macrophage to foam cell transformation using high-density cDNA arrays

By Assum Gulzar

Coronary heart disease (CHD) is the leading cause of death in most industrialised countries. Atherosclerosis is the major underlying cause of CHD. Atherosclerosis is a disease process in which monocyte derived macrophages enter the subendothelial space, accumulate excess amounts of cholesterol to form lipid filled foam cells. These foam cells have been found contribute significantly to the aetiology of the fatty streak and subsequent lesions involved in atherosclerosis.

The aim of this study was to gain a further understanding of the foam cell formation process by studying gene expression during the macrophage to foam cell transformation. Human THP-1 monocytic cells were differentiated into macrophages using a phorbol ester. Macrophages were subsequently exposed to either acetylated LDL or oxidised LDL to induce foam cell formation. Foam cell formation was assessed using the techniques of flow cytometry, Oil Red O staining, fluorescence microscopy and cholesteryl oleate loading.

Gene expression was examined using high density cDNA array technology. RNA was isolated from cells exposed to native or modified LDL. First strand cDNA probes were subsequently generated and applied to high-density cDNA arrays. Two different arrays were probed; an array representative of the Human I.M.A.G.E collection and a custom array containing known genes thought to be involved in the cardiovascular disease process.

The results of this study showed increased expression in CD36, a known receptor for OxLDL. In addition other genes were also identified including IL1β and fibronectin. Cluster analysis of a time series experiment showed the existence of nine distinct clusters of genes with different expression patterns. In particular two genes IL-1β and TIMP-1 were shown to have a highly correlated pattern of expression.

Declaration

I declare that the work contained within this thesis submitted by me for the degree of Master of Philosophy has not been previously submitted for a degree at this or any other University.

The work presented within this thesis is my own except where stated. Where others have contributed to this work, their contribution is clearly stated.

The thesis conforms to the word limit set out in the University Degree of Regulations.

Copyright

This thesis has been approved by Glaxo SmithKline Intellectual Property Department for publication.

Correspondence

Correspondence regarding this thesis may be addressed to the author via email to Assum_Gulzar@yahoo.co.uk.

List of Contents

Chapter 1: Introduction

Chapter 4: Differential Gene Expression Technology

Chapter 5: Gene Regulation in response to native and modified LDL

Abbreviations used in the text

ACAT	Acyl-coenzyme A cholesterol acyl transferase
AcLDL	Acetylated low-density lipoprotein
AP-1	Activator protein 1
BSA	Bovine serum albumin
bp	Base pairs
β-actin	beta actin
CHD	Coronary heart disease
cpm	Counts per minute
dpm	Disintegrations per minute
DEPC	Diethyl pyrocarbonate
DGE	Differential Gene Expression
DMSO	Dimethyl sulphoxide
dNTP's	Dideoxy nucleoside triphosphates
DTT	Dithiothreitol
ECM	Extracellular matrix
ECs	Endothelial cells
EF-1	Elongation factor-1
FBS	Foetal bovine serum
FH	Familial Hypercholesteorlemia
GAPDH	glycealdehyde 3-phosphate dehydrogenase
HDL	High density lipoprotein
HOCl	Hypochlorous acid
HSL	Hormone sensitive lipase
IL	Interleukin
I.M.A.G.E	Integrated molecular analysis of Genomes and their Expression
LDL	Low density lipoprotein
LpL	Lipoprotein Lipase
MCSF	Macrophage colony stimulating factor
MCP-1	Macrophage chemoattractant protein 1

MMPs	Matrix metalloproteinases
MOPS	3-N-morpholinopropane sulfonic acid
MPO	Myeloperoxidase
NO	Nitric oxide
NF-κB	Nuclear factor kappa b
OxLDL	Oxidised low-density lipoprotein
PBS	Phosphate buffered saline
PDGF	Platelet derived growth factor
PCA	Principle component analyis
PCR	Polymerase Chain Reaction
PMA	Phorbol 12-myristate 13-acetate
PPARs	Peroxisome proliferator activator receptors
SDS	Sodium dodecyl sulphate
SMCs	Smooth muscle cells
SMase	Sphingomyelinase
SRs	Scavenger receptors
STATs	Signal transducers and activators of transcription
TAE	Tris acetate buffer
TBE	Tris borate buffer
TIMPs	Tissue inhibitors of metalloproteinases
TLC	Thin layer Chromatography
TNF-α	Tumour necrosis factor alpha
TGF-β	Transforming growth factor beta
TGE	Temporal gene expression

Chapter 1: Introduction

1.1 Atherosclerosis

Despite many advances in cardiovascular medicine over the last few decades, coronary heart disease (CHD) still remains one of the leading cause of mortality in most industrialised nations [1]. The major underlying cause of CHD is the disease process of atherosclerosis. The term 'arteriosclerosis' was introduced in 1829 to describe the scarring and calcification seen in post-mortem arteries. Atherosclerosis was subsequently used as a term used to describe lipid-rich deposits seen in arteriosclerosis [2]. The term atherosclerosis comes from the Greek words "athero" meaning gruel and "sclerosis" meaning hard, describing the process in which the coronary arteries become narrowed with deposits of fat and these deposits of fat develop into plaques filled with cholesterol [2].

Initially atherosclerosis was thought to be a lipid related disease, however in recent years the role of inflammation has gained has gained as much importance as the lipid aspect [3,4]. The major clinical symptoms of atherosclerosis include myocardial infarction and stroke [5]. Disease progressesion occurs for many years before symptoms develop, making it difficult to follow the early development of the disease in humans. Knowledge of early atherosclerosis has thus been obtained mainly from post mortem examinations and animal studies. Plaque formation is thought to begin in early life and advanced plaques are common by the time people are in the third decade of life [6].

The earliest lesion of atherosclerosis is the fatty streak, which is characterised by the accumulation of monocyte-derived macrophages containing large amounts of lipids [7]. These cells are known as "foam cells" and are characteristic of both early and advanced lesions of atherosclerosis [8].

Atherosclerosis is a multifactorial disease with a wide range of risk factors associated with it. The major risk factors include dyslipidemia, hypertension, diabetes and the use of tobacco products [9]. Other risk factors include, raised plasma cholesterol concentrations, increasing age, the male gender, the postmenopausal state in woman, obesity, alcohol consumption, homocysteinemia and a family history of premature atherosclerosis [9].

1.2 Lipoproteins

Lipids are insoluble in aqueous solution and are therefore transported in the plasma in the form of lipoproteins. Lipoproteins are complex water-soluble molecules containing a core of cholesteryl ester and triglyceride covered by a surface monolayer of phospholipids, free cholesterol and apolipoproteins [5]. The major classes of lipoprotein found in the plasma are chylomicrons, very low-density lipoprotein (VLDL), intermediate-density lipoprotein (IDL), low-density lipoprotein (LDL) and high-density lipoprotein (HDL) [14]. Lipoproteins are synthesised in the liver or the intestine with a corresponding structural apoprotein. Table 1.1 below lists the major properties of the different lipoproteins.

Table 1.1

Properties of the plasma lipoproteins (from reference 5)

Name of lipoprotein		*Density (d; g/ml)*	*Electrophoretic mobility*	*Source*
chylomicrons		<0.95	origin	intestine
very low density lipoproteins (VLDL)		<1.006	pre-β	liver
intermediate density lipoproteins (IDL)		1.006-1.009	broad β	catabolism of VLDL & chylomicrons
low density lipoprotein (LDL)	I	1.02-1.03	β	catabolism of VLDL
	II	1.03-1.04		
	III	1.04-1.06		
high density lipoprotein (HDL)	2	1.063-1.125	α	catabolism of chylo-microns&VLDL; liver & intestine
	3	1.125-1.21		

Lipoproteins can be distinguished from one another by a variety of methods including lipid content, density, size, electrophoretic mobility and the proteins on their surfaces [5]. The different classes of lipoproteins vary in their contribution to atheorsclerotic risk. LDL, chylomicron remnants and IDL are known to be pro-atherogenic, whereas HDL levels are thought to be inversely related to risk of CHD

[10]. The main cholesterol carrying lipoproteins are LDL and HDL. In a normal individual, LDL contains approximately 70% and HDL 20% of the total plasma cholesterol [10].

1.3 Lipoprotein receptors

1.3.1 The LDL receptor

LDL is a spherical particle containing a hydrophobic core surrounded by a polar phospholipid coat. The apolipoprotein of LDL is apo B_{100}. Apo B_{100} on the surface of the LDL allows recognition binding and removal of the lipoprotein by the LDL receptor [11]. The LDL receptor was first elucidated by the experiments of Goldstein and Brown in the 1970s using cultured human fibroblasts [12]. They demonstrated that the underlying defect in the genetic disease Familial Hypercholesterolemia (FH) was an absence or impairment of function in the LDL receptor [12].

The LDL receptor can bind apoB_{100} or apoE containing ligands including chylomicron remnants, IDL and LDL (hence is also referred to as the apoB/E receptor [13]). The LDL receptor is responsible for removing approximately 75% of LDL particles from the circulation [13]. The LDL receptor pathway is a tightly regulated pathway, in which expression of the LDL receptor decreases as intracellular cholesterol levels increase.

1.3.2 LDL receptor related protein (LRP)

LRP is a receptor that has homology to the LDL receptor, however it differs from the LDL receptor in that it does not recognise apoB [14]. LRP has been found to be highly expressed in the liver, brain and placenta [14]. It is able to mediate uptake of apoE containing lipoproteins including chylomicrons and IDL [14]. LRP has has been implicated in atherosclerosis as it allows macrophages to take up lipoproteins.

1.3.3 The VLDL receptor

The VLDL receptor is a more recently discovered member of the lipoprotein receptor family [15]. The VLDL receptor is also highly homologous to the LDL receptor and like the LRP it also binds apoE but not apoB containing lipoproteins. The VLDL receptor differs from the LDL receptor in its expression pattern [15]. It is found highly expressed in heart, skeletal muscle and adipose tissue [2]. Although the exact function of the VLDL receptor remains to be determined, it is thought to be involved in the binding of triglyceride-rich lipoproteins thereby helping deliver fatty acids to tissues [2].

1.3.4 The macrophage scavenger receptors

Since LDL is the major atherogenic lipoprotein found in atherosclerotic lesions, it would be expected that incubation of macrophages with LDL would lead to foam cell formation. However this proved not to be the case, as reported by Goldstein and Brown [16]. This lead to a search for an explanation for the paradox. Again it was Goldstein and Brown who provided the answer. They reported the existence of a receptor for modified LDL using acetylated LDL as a ligand [16]. Macrophage scavenger receptors (SRs) have been found to mediate the uptake of large amounts of modified LDL in an uncontrolled fashion [17]. This occurs because unlike the LDL receptor pathway, scavenger receptor expression is not down-regulated.

In addition to binding modified LDL such as oxidised and aggregated LDL, SRs also act as binding sites for polyribonucleases and some polysaccharides (such as dextran sulphate) and anionic phospholipids such as phosphotidylserine. Six different classes of SRs have been described [18] and they have been classified as shown in table 1.2.

SR classes A and B are expressed in atherosclerotic plaques and are involved in the development of lipid laden foam cells [19, 20]. However since expression of SRs is not restricted to the cells within the arterial wall, preventing foam cell formation in atherosclerotic plaques by inhibition of SRs may not be very effective.

Table 1.2

Table showing classification of the scavenger receptors (From reference 18)

The scavenger receptors	
Scavenger Receptor Class	Members of Class
Class A	SR-AI, SR-AII, SR-AIII and MARCO (the macrophage receptor with collagenous structure)
Class B	SR-B1 and CD36
Class C	Drosophilia SR-C

Class D, E and F receptors are the most recently identified and none of them show any structural similarity with class A, B or C receptors

Class A SRs include macrophage SR types AI, AII and AIII (SR-AI, SR-AII and SR-AIII). SR-AI and II are homotrimeric membrane proteins [19], found predominantly in macrophages and activated smooth muscle cells. Ligands for class A scavenger receptors include acetylated LDL, oxidised LDL, fucoidan and caragenan [19]. An increase in SR activity has been observed during differentiation of monocytes to macrophages. This has been attributed to an increase in the expression of the SR-AI isoform [21]. Furthermore this increased macrophage SR-AI expression is thought to be important for the transformation of macrophages into foam cells [21].

Class B scavenger receptors include CD36, and SR-B1, which are found in adipose tissue, lung, liver and macrophages [22]. These receptors bind OxLDL, apoptotic cells and anionic phospholipids. CD36 has been found to be significantly expressed in atherosclerotic foam cells in human coronary arteries [23] and has been implicated to be a major receptor for OxLDL [22].

SR-BI has also been reported to be major a receptor for HDL [24]. SR-BI has been found to bind HDL with high affinity and subsequently mediate the selective uptake of cholesteryl ester [24]. Thus it is possible that SR-BI may be involved in the initial steps of cholesterol efflux from foam cells in the arterial wall [25]. A third class

of scavenger receptors has also been reported as CD68/macrosialin, a family of endosomal proteins that have a sequence homology similar to lysosomal associated membrane proteins [26].

A more recent receptor for OxLDL has also been reported. Lectin-like oxidised LDL receptor-1 (LOX-1) was found to be present on bovine vascular endothelial cells [27]. In addition to being expressed on ECs, LOX-1 has also been found to be present on smooth muscle cells (SMCs) and macrophages [28].

1.4 Structure of the normal artery wall

The main types of arteries found to have plaques leading to clinical symptoms are the coronary arteries, although lesions can also be found in other arteries [5]. Normal muscular and elastic arteries have been found to consist of three morphologically distinct layers [29], the intima, the media and the adventitia (figure 1.1).

The intima is the innermost layer and consists of a narrow region bounded on one side by a single continuous layer of endothelial cells and bound peripherally by a sheet of elastic fibres, which is known as the internal elastic lamina (shown in figure 1.2 below). The media is the middle layer. It consists of diagonally orientated smooth muscle cells, surrounded by collagen, small elastic fibres and proteoglycans.

Figure 1.1

Diagrammatic cross-sectional representation of the artery wall

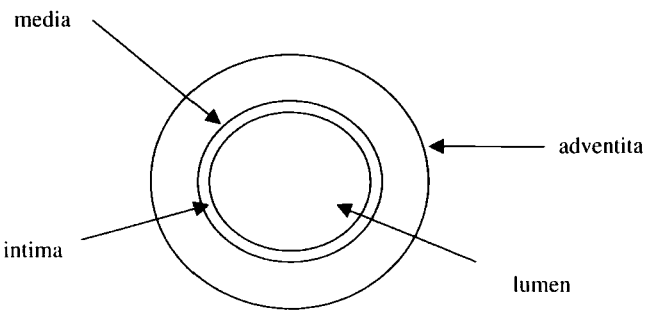

The adventitia is the outermost layer of the artery. It consists mainly of fibroblasts intermixed with SMC loosely arranged between bundles of collagen and surrounded by proteoglycan. It also contains vaso vasorum and innervation. It is separated from the media by a discontinuous sheet of elastic tissue, the external elastic lamina [29].

The intima is the initial cell layer that is involved in atherosclerosis (figure 1.2) although changes can also be found in the media during the later stages of atherosclerosis [29]. The intima itself consists of two regions. Beneath the endothelial cells is the proteoglycan layer that contains non-fibrous connective tissue, proteoglycans and a few elastic fibres. Proteoglycans interact with other matrix proteins such as collagens, elastin and fibronectin [30]. In normal human coronary arteries the content of these proteoglycans increases with age, but levels are also found to increase in atherosclerosis [30]. Below the proteoglycan layer is the musculoelastic layer that consists of SMC s of the contractile phenotype. The major component of the intima however is the extracellular matrix, which comprises around 60% of the volume of the intima [31]. It contains molecules synthesized and secreted by both ECs and SMCs.

Figure 1.2

Diagrammatic representation of the intima (adapted from reference 2)

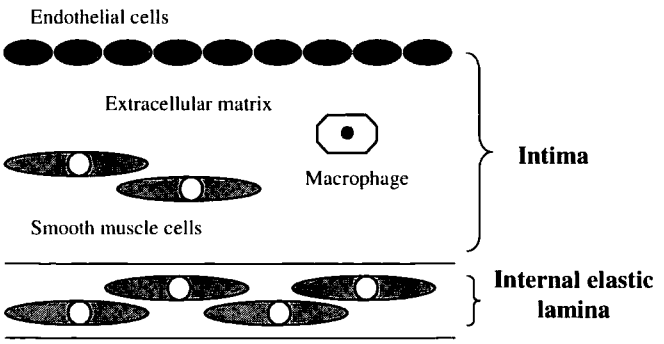

1.5 Lesions of atherosclerosis

Stary and other investigators [29, 32, 33] have reported the main types of lesion that are found during the progression of atherosclerosis, the fatty streak, the

fibrous plaque and the advanced complicated lesion (types I-Vb). The progression of lesions in experimental animals is the development of fatty streaks and later the development of fibrous plaques and more complicated lesions [34]. Studies of human disease have indicated similar patterns of lesion evolution (although it should be noted they are not identical [33]).

1.5.1 Fatty streaks

The first atherosclerotic lesions that appear are fatty streaks. Post mortem studies have shown that fatty streaks are commonly found in young children [35]. The fatty streak causes no obstruction and does not result in any clinical symptoms [35]. Fatty streaks are characterised by the accumulation of lipid filled foam cells [35]. Most of the foam cells arise from circulating monocytes that enter the subendothelial space, transform into macrophages and then take up and accumulate excess lipid and reside within the endothelium [36]. The fatty streak is found to be a yellowish colour which is associated with the presence of lipid deposits (mainly cholesterol and cholesteryl ester) found in macrophages and smooth muscle cells [29].

1.5.2 Fibrous plaques

The fibrous plaque is the most characteristic lesion of advancing atherosclerosis [29]. It is found to protude out into the vessel wall and has found to be whitish in appearance [29]. It consists of an accumulation of intimal smooth muscle cells surrounded by connective tissue matrix and containing variable amounts of intracellular and extracellular lipid.

1.5.3 Complicated lesions

The third type of lesion is the advanced complicated lesion. These advanced lesions are thought to result from fibrous plaques that become altered as a result of haemorrhage, calcification, cell necrosis and thrombosis [33]. One of the characteristics of the complicated lesion is the presence of calcification. Studies by Stary [32] indicate that a fully developed plaque can take up to 10-15 years to develop.

Advanced plaques have been found to have a very characteristic anatomy [32]. They contain a core of extracellular lipid separated from the media by SMCs and separated from the lumen by a thick cap of collagen rich fibrous tissue containing SMC. Lipid filled foam cells are found to surround the lipid core. The lipid core is thought to be largely derived from the death of macrophage foam cells and the release of their cytoplasmic content [38]. The advanced plaque is the stage at which plaque complications develop and clinical symptoms appear. Advanced plaques can be of two types, stable or unstable. Unlike the stable plaque, unstable plaques have a thin fibrous cap separating the lipid core from the lumen of the artery [39]. This thin fibrous cap is more prone to rupture leading to thrombotic events [39] (discussed below).

1.5.4 Detection of atherosclerotic lesions

Atherosclerosis is a progressive disease that takes many years to develop to the point where clinical symptoms are evident. It is not possible to determine the early stages of atherosclerosis in humans due to the fact that most atherosclerotic lesions are found in vital arteries. A number of methods are however available to examine lesions that have already formed. These include angiography and intravascular ultrasound [40].

Angiography involves the injection of an opaque dye and then subsequently X-raying the vascular system. Intravascular ultrasound involves introduction of small catheter delivered ultrasound probes (ranging from 20-50MHz), which enables visualisation of the full 360^{o} circumference of the vessel wall, rather than the 2-dimensional projection of the lumen seen by angiography. Both these techniques however, pose a certain degree of risk, as they are both invasive techniques. However non-invasive techniques such as Magnetic Resonance Imaging (MRI) and Electron-beam computed tomography (EBCT) have also been reported [41,42]. More recently Brindle and colleagues [43] reported the use of NMR-based metabnomics, (a technique in which metabolites within patients serum/plasma can be studied) as a novel, more rapid and non invasive technique for diagnosis of CHD.

1.5.5 Initiation of atherosclerosis

As discussed in section 1.2, various factors are known to predispose to the development of atherosclerosis with clinical symptoms. Elevated plasma lipoprotein concentration has been associated with increased concentrations in the intima. At such regions (referred to as as lesion prone sites) mechanical forces may favour the entry of LDL into the subendothelial space. [44]. In addition advanced lesions are more commoly found at such lesion prone sites [44]. Furthermore continued exposure to risk factors such as hyperlipidemia, cigarette smoke, high blood pressure, homocysteine, increased PAI-1 and C-reactive protein (CRP) results in a progressive endothelial dysfunction during atherosclerosis [9].

1.6 The response to injury hypothesis

The normal function of the endothelium is to form a barrier from the passage of blood constituents into the artery wall. The response to injury hypothesis of atherogenesis put forward by Russel Ross [45] proposes that injury to the endothelium is the initiating event in atherogenesis [45]. Factors such as hyperlipidemia, increased sheer stress and hypertension have been proposed to 'injure' the endothelium [45]. According to the response to injury hypothesis, restoration of the endothelial barrier eventually occurs and the lesions regress if both the injury and the tissue responses to it are limited. However further proliferation of SMC and accumulation of connective tissue and lipid occur if injury to the endothelium is continuous or repeated [45].

Loss of endothelial cells from the fatty streaks has been observed, first by Gerrity [46] in swine and then by Faggiotto [47] in primates. Studies with monkeys that were fed dietary cholesterol to induce hypercholesterolemia showed that they lose approximately 7% of their arterial endothelial surface [47]. Injury to the endothelium is though to alter endothelial cell to cell or endothelial cell to connective tissue interactions or both, resulting in the possible detachment of endothelial cells from the artery wall [45]. Detachment of endothelial cells is known as desquamation. Focal desquamation of the endothelium exposes the underlying subendothelial connective tissue to components in the circulation including platelets, macrophages and lipoproteins.

Although endothelial dysfunction has been found to be an early occurrence in atherosclerotic lesions, the appearance of actual physical damage is a later process. Thus the endothelium may be injured without actual loss of cells, yet altered enough to elicit a response that triggers the release of growth factors initiating a sequence of events that leads to the formation of an atherosclerotic lesion [45]. The injury could be mechanical or induced by immune complexes, toxins, viruses or other factors [48].

1.7 Properties of the components of the arterial wall

1.7.1 Endothelial cells (ECs)

ECs of normal arteries have a flattened and elongated structure [49]. The most characteristic feature of endothelial cells is the presence of Weibel–Palade bodies which are rod shaped inclusions that contain factor VIII related antigen and Von Williebrand factor. ECs have number of physiological functions in the normal artery wall which include [50]: -

[a] Acting as a permeability barrier

One of the most important features of the normal endothelium is to regulate the traffic of plasma proteins and lipoproteins. Transport across the endothelium can occur by transcytosis in plasmalemmal vesicles and through intracellular junctions [50].

[b] Providing a non-thrombogenic surface.

Normally cells do not adhere to the endothelial surface since ECs do not contain receptors for cells to bind. The EC membrane also contains thrombomodulin that binds thrombin and prevents clot formation [50].

[c] Synthesis of basement membrane components.

ECs are involved in the synthesis and secretion of extracellular matrix components including fibronectin, type IV and type V collagen, laminin and proteoglycans.

[d] Maintenance of vascular tone.

ECs are also involved in maintaining the vascular tone by the release of prostacyclin, nitric oxide and endothelin.

[e] Formation and secretion of growth regulatory molecules and cytokines.

Dysfunction of the endothelium is thought to result in the secretion of growth molecules and cytokines

1.7.2 Smooth muscle cells (SMCs)

In vitro studies have attributed the following functions to SMCs in the normal endothelium [51]:-

[a] Synthesis of extracellular matrix components.

SMC can synthesise collagen, elastin, and proteoglycans and thus contribute to intimal growth.

[b] Ability to proliferate.

SMC will proliferate in response to growth factors released during injury to the endothelium, since they express various growth factor receptors [45]

In addition SMCs are found in two distinct phenotypes, the synthetic phenotype and the contractile phenotype [52]. The synthetic phenotypes are rich in rough endoplasmic reticulum while the contractile phenotypes are rich in myofibrils. During atherosclerosis, SMCs are present in varying degrees in early fatty streaks, in which macrophages are the principal cell type [35]. However as fatty streaks progress to fibro fatty lesions, SMCs become more abundant. In fibrous plaques, SMCs are the predominant cell type. The role of SMC in fibrous plaques is important since their accumulation and proliferation are critical in determining the extent and characteristics of advanced lesions and whether they will lead to clinical symptoms [53].

1.7.3 Macrophages

Macrophages are present in the normal intima in very low numbers. Their function in normal intima is thought to include the following [54] :

[a] Remodelling of the intima.

Macrophages can synthesise and secrete the metalloproteinases (MMPs) collagenase and elastase and other components that can play a role in modifying the extracellular matrix [54].

[b] Inflammatory response and scavenger function.

Macrophages are responsible for the phagocytosis of bacteria and tumour cells. In the intima, macrophages are responsible for the phagocytosis and removal of dead cells and immune complexes, removal of plasma proteins and lipoproteins. Macrophages also secrete cytokines that attract lymphocytes to the sites of injury [54].

[c] Immune response.

Macrophages are involved in binding and presentation of antigens, cytokines and growth factor production related to the immune respons

1.7.4 Extracellular matrix (ECM)

The ECM is composed of mainly of proteoglycans, collagen, elastin, fibronectin and laminin [29]. The four major types of proteoglycans present in the ECM of the vessel wall are chondroitin sulphate, heparin sulphate, dermatin sulphate and keratin [29]. During atherosclerosis, there is a significant increase in the content of chrondoitin sulphate and dermatin sulphate proteoglycans. Both these molecules can bind plasma LDL and thus enhance its retention in the intima [55]. The amount of chondroitin sulphate has been shown to be positively correlated with the intimal accumulation of apoB [55].

In the normal artery wall most of the collagen exists in the form of two interstitial collagens, types I and III [7]. In children, type III collagen is the predominant form in the subendothelial space of the intima. With ageing, there is a change in the ratio of the two types of collagen in favour of type I [56]. Other types of collagen are present; but account for only 0.5-1% of the total arterial collagen content. Both collagen types I and III increase significantly in advanced lesions [29]. SMC are the major cell type responsible for collagen generation in the vessel wall [39].

Elastin is the main component of the elastic fibres, which give blood vessels their elasticity [2]. In the normal vessel, elastin is mainly located in the media and the musculoelastic layer of the intima and very little change in the elastin content in early atherosclerosis [7]. In contrast advanced lesions contain an increased amount of subendothelial, medial and adventitial elastin [29].

Fibronectin is an adhesive glycoprotein present on cell surfaces in extracellular matrix and in blood. It plays important roles in cell-cell adhesion, cell-substrate

adhesion and cell-matrix interactions [57]. Laminin is another major non-collagenous glycoprotein found in the ECM. Along with heparin sulphate proteoglycan and type IV collagen, laminin is a major component of the basement membrane that underlies the endothelium and surrounds each SMC [58]. Both fibronectin and laminin are found to be increased in atherosclerotic lesions [57, 58]. Fibronectin may promote SMC migration as well as monocyte and T-lymphocyte infiltration.

Together the components of the extracellular matrix have a number of important physiological functions. These include [2]:-

[a] Arterial Permeability.

The extracellular matrix is involved in the transfer of essential nutrients across the intima to cells within the intima and the underlying media.

[b] Maintaining the structural integrity of the intima.

The chondroitin sulphate proteoglycans provides the intima with its strength and compression properties [55]. The collagen and elastin fibres provide further structural strengthening. Cells within the intima are held in the intracellular matrix by cell associated heparin sulphate proteoglycans.

1.7.5 T-cells

Although T-cells are not normally present within the arterial wall, they are present in early lesions as part of fatty streaks [48]. In advanced atherosclerotic plaques, T-lymphocytes make up about 20% of the cells in the fibrous cap [29]. B-lymphocytes and natural killer cells are normally sparse [48]

1.8 Foam cell formation

The sequence of events leading to fatty streak formation can be summarised as follows (schematically represented in figure 1.3 below). Damage to the endothelium caused by factors such as hyperlipidemia or infectious agents results in increased adherence of blood monocytes to endothelial cells and the release of cytokines such as macrophage chemoattractant protein 1 (MCP-1) and macrophage colony-stimulating factor (M-CSF) [58,59]. It is thought that in the presence of a high level of plasma LDL, the concentration of LDL in the intima is increased where it becomes oxidised

[60]. This oxidised LDL contributes to the subsequent recruitment of circulating monocytes [61]. Once within the arterial wall, the monocyte differentiates into a macrophage [61]. OxLDL subsequently inhibits it from returning to the plasma [86]. As resident macrophages these cells express scavenger receptors, take up OxLDL and become foam cells [61]. These foam cells accumulate beneath the endothelial cell layer forming the precursor lesion of atherosclerosis, the fatty streak [35]

Figure 1.3

Schematic diagram showing formation of the fatty streak

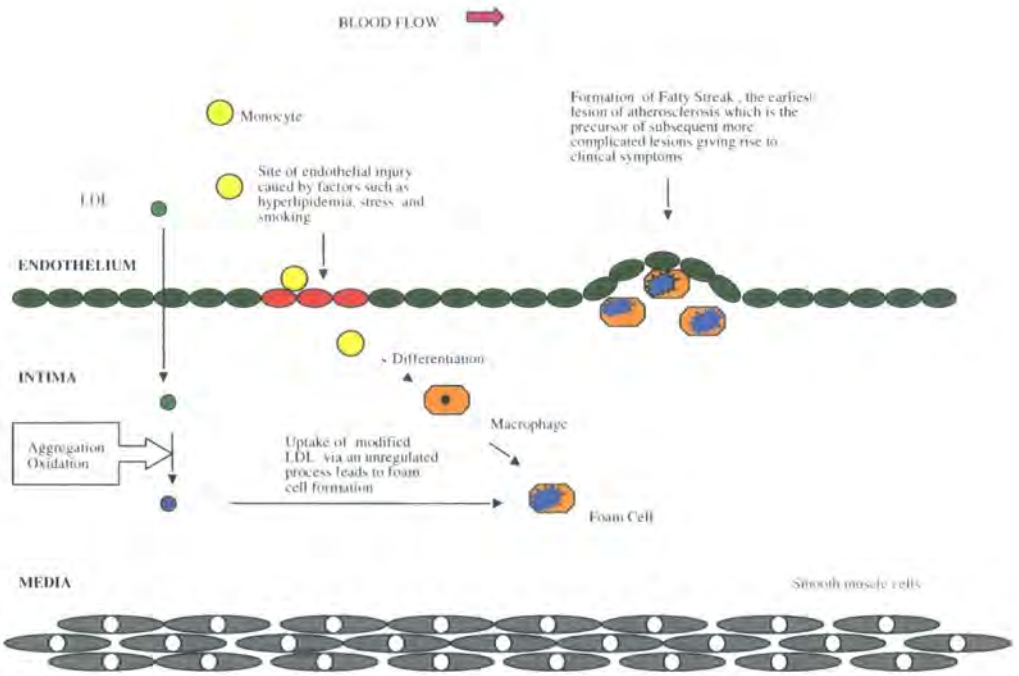

1.8.1 The role of the monocyte derived macrophage

Although smooth muscle cells can also take up lipid, monocyte derived macrophages are the major source of foam cells in all stages of human and experimental atherosclerosis [29, 33]. The macrophage derived foam cell has been implicated in multiple aspects of atherosclerotic plaque development [38, 61]. The monocyte-derived macrophage is also capable of producing growth factors for vascular smooth muscle cells thus it can also contribute to the proliferative stages of

plaque development [9]. It can also generate cytotoxic factors for neighbouring cells, leading to smooth muscle cell and endothelial cell damage and death [38].

1.8.2 Monocyte attachment

Damage to the endothelium is thought to be the initiating event that leads to monocyte adherence [45]. The recruitment of leukocytes (monocytes and T-cells) is a process that includes cell rolling, cell adhesion to the endothelium and cell migration in response to chemotactic gradients [8].

The activated endothelium expresses several proteins on its surface that attracts some of the cellular components of the bloodstream particularly leukocytes. These cellular components in turn have receptors that bind to the proteins expressed on the endothelium. These adhesion proteins expressed on the endothelial cell surface can be of two classes.

[1] The selectins.

[2] The immunoglobulin superfamily.

1.8.2.1 Endothelial selectins

The selectins are a family of glycoproteins with specific structural motifs in common. They all have an amino terminal lectin-like domain followed by an EGF-like domain, numerous cysteine rich tandem motifs, a transmembrane region and a short cytoplasmic tail [62]. These molecules are not present on unstimulated endothelial cells but appear on the surface of the endothelium after activation by several biological modifiers such as interleukin-1 (IL-1), bacterial lipopolysaccharide, thrombin, phorbol esters and TNF [62]. Two selectins have been identified on the activated endothelium, E selectin and P selectin. E selectin is thought to be involved in the adhesion of monocytes to endothelial cells [62]. Platelet selectin (P- selectin) was first shown to be present on the surface of activated platelets. It has subsequently also been shown to be present on the surface of activated endothelial cells [62]. The ligand for both P selectin and E selectin is the monocyte.

1.8.2.2 Immunoglobulin superfamily of adhesion molecules

These adhesion molecules derive their name from the fact that they contain several immunoglobulin-like domains. Three members of this family have been characterised in ECs, vascular cell adhesion molecule 1 (VCAM-1) and intracellular adhesion molecules 1 and 2 (ICAM1 and ICAM 2) [63]. VCAM 1 is a glycoprotein expressed on the surface of activated endothelial cells. Its ligand on leukocytes has been shown to be VLA 4 (very late antigen 4), which is present on lymphocytes and monocytes but not neutrophils [63]. The ligands for VCAM-1 are monocytes and lymphocytes [63]. VCAM-1 has recently gainied importance as the molecule having the major role in recruiting monocytes in early atherosclerosis [64].

1.8.3 Monocyte migration and accumulation in the intima

Once monocytes attache to ECs, chemoattractant stimuli are thought to promote their migration and entry into the intima. The chemoattractant thought to be involved in monocyte migration is MCP-1 [65]. This cytokine has been shown to be a specific chemoattractant for monocytes and is found to potently stimulate directed migration of monocytes *in vitro* [65]. ECs, SMCs and leukocytes have all been shown to inducibly express MCP-1 *in vitro* [66]. Transgenic mice deficient in MCP-1 or its receptor CCR-2 have been shown to have significantly reduced lesions, implying that the MCP-1 /CCR-2 have an important role in monocyte recruitment in atherosclerosis [66].

1.8.4 Lipoprotein uptake

The accumulation of cholesteryl esters by macrophages occurs by the uptake of modified lipoprotein particles via specific membrane receptors most notably the scavenger receptors. Macrophages can thus become heavily loaded with lipid droplets in the subendothelial space. Macrophages within human atherosclerotic lesions have been found to express scavenger receptors [67], whilst circulating monocytes do not express scavenger receptors. Differentiation of monocytes into macrophages has been found to induce expression of SRAI [22]. Macrophage colony stimulating factor (M-

CSF) can stimulate the expression of scavenger receptors whereas α-interferon can suppress expression of scavenger receptors [18].

It is now recognised that LDL must undergo some form of modification in its structural and biological properties before it can be taken up by macrophages at a rate sufficient to generate foam cells [68]. A number of chemical modifications have been shown to have this effect including acetylated LDL (AcLDL) and oxidised LDL (OxLDL). Experimentally AcLDL is used as the standard form of modified LDL to induce foam cell formation (as used by Goldstein and Brown in the discovery of the scavenger receptor [16]). *In vivo* however, the main modification of LDL is thought to be oxidation [68] (discussed below). Other forms of modified LDL also exist including aggregated LDL and glycated LDL (found in patients with diabetes). The rapid uptake of modified LDL particles leads to foam cell formation and foam cells accumulate beneath the endothelial cell layer.

1.8.5 Retention of LDL

The subendothelial aggregation and retention of LDL are key events in atherogenesis. As noted above, components of the extracellular matrix such as the proteoglycans can bind and retain LDL [60]. Specifically chondroitin sulphate and dermatin sulphate can bind plasma LDL and thus enhance its retention in the intima [60]. Studies have also shown that treatment of LDL with sphingomyelinase *in vitro* leads to formation of lesion-like aggregates that become retained by the extracellular matrix and stimulate foam cell formation [69]. Although the mechanism of lipoprotein aggregation in lesions is not known, it has been suggested that the enzyme sphingomyelinase (SMase) plays a major role [69].

1.9 Intracellular cholesterol regulation in macrophages

Once atherogenic lipoproteins have been taken up via unregulated scavenger pathways, post-receptor events that affect intracellular cholesterol metabolism are thought to play a major role in whether or not foam cell formation occurs [17]. For cholesteryl ester accumulation to occur, intracellular metabolism has to favour cholesterol esterification. The cholesterol esterification process in macrophages is a regulated process, although the nature of this regulation is still not fully understood.

The process appears to be a balance between cholesterol esterification by acyl-coenzyme A cholesterol acyl transferase (ACAT is also known as SOAT) and hydrolysis by neutral cholesteryl ester hydrolase (nCEH) [70].

Macrophages internalise LDL via receptor-mediated endocytosis [17]. These endocytic vesicles are then passed to the lysosome, where the cholesteryl esters are degraded by an acid hydrolase [71]. The free cholesterol leaves the lysosome and enters the cytoplasm where it has two fates; it can be excreted and is taken up by HDL which acts as an acceptor or it can be re-esterified by the enzyme ACAT and stored as cholesteryl ester droplets [71]. Stored cholesteryl ester droplets can be subsequently hydrolysed by a cytoplasmic enzyme (nCEH) and passed on to HDL through ABC-A1. In the absence of HDL or another acceptor for cholesterol the free cholesterol is retained in the cell and re-esterified by ACAT [72]. In addition macrophages actively secrete apoE. This may promote cholesterol efflux to HDL and thereby inhibit the transformation of macrophages to foam cells. This role of apoE has been demonstrated in apoE null mice that have been found to develop much larger lesions when compared to normal mice [113].

Thus stored cholesteryl esters are not inert; they are in a dynamic state continually undergoing a cycle of hydrolysis and re-esterification (dependent on the availability of an acceptor for free cholesterol). This cycle has been termed the cholesteryl ester cycle [73].

1.9.1 Enzymes involved in intracellular cholesterol regulation

NCEH is an enzyme which works best at a pH in the neutral range (6.5-7.5) hence its name. It has been found to be located in the cytosolic compartment part of the cell. It can be activated by a cAMP-dependent protein kinase [72]. NCEH is responsible for mobilisation of stored cholesteryl esters. ACAT is a microsomal enzyme that is responsible for esterifying intracellular free cholesterol to cholesteryl esters and promoting storage of lipid in arterial macrophages. ACAT uses long chain fatty acyl coenzyme A and cholesterol as substrates [75]. It has been shown that increased ACAT activity is responsible for the cholesteryl ester accumulation in cytoplasmic lipid droplets [76]. ACAT's role in re-esterification is of particular importance in controlling the concentration of membrane free cholesterol, which in excess can be toxic to cells.

Two separate ACAT enzymes have been identified: ACAT1 and ACAT2 [75]. ACAT 1 is widely distributed in tissues and plays a central role in cholesterol metabolism in steroidogenic tissues and macrophages [75]. ACAT 2 acts in the intestine and the liver synthesizing cholesteryl ester that are then incorporated into lipoprotein particles [75]. The role of ACAT in foam cell formation has led to the development of ACAT inhibitors that work by acting directly in the cells that form the atherosclerotic plaque [77].

Hormone sensitive lipase (HSL) is a key enzyme involved in lipolysis in adipose tissue and catalyses the rate limiting step in the breakdown of triacylglycerol. [78]. The activity of HSL is regulated by phosphorylation via a cyclic-AMP dependent protein kinase [78]. HSL has been shown to be present in macrophages where immunological studies have suggested that it is responsible for the neutral hydrolysis of cholesteryl esters [79]. This has been further supported by the fact HSL and nCEH are products of the same gene [80]. It has been shown that an increase in the cellular concentration of cholesterol in macrophages inhibits HSL activity and reduces HSL expression [81]. This loss of HSL activity leads to an imbalance in the cholesteryl ester cycle, resulting in cholesteryl ester accumulation. Thus whether a foam cell will increase or decrease its stores of cholesteryl esters depends on the relative activities of nCEH and ACAT within the cell. HSL expression has been demonstrated in both human monocyte-derived macrophages and human THP-1 cells [71].

Lipoprotein lipase (LpL) is an enzyme that plays a central role in lipid metabolism and transport by catalysing the hydrolysis of triacylglycerol rich lipoproteins [82]. LpL hydrolyses the triacylglycerol component of chylomicrons and VLDL, thereby providing non-esterified fatty acids and 2-monoacylglycerols for tissue utilisation [82]. Macrophage derived foam cells are the primary source of the LpL enzyme within atherosclerotic lesions [83]. Studies with transgenic mice have shown that macrophages isolated from atherosclerotic susceptible mice showed a higher LpL activity and mRNA levels than those from atherosclerotic resistant mice, thereby suggesting a contributive role for LpL in the progression of atherosclerosis [84].

Paradoxically evidence also exists in support of an anti-atherogenic role for LpL. LpL deficient patients and patients heterozygous for LpL mutations still develop relatively advanced atherosclerosis [83]. It is likely that the role of LpL in atherosclerosis may depend on the tissue in which it is expressed. In the arterial wall,

LpL may be pro-atherogenic whereas in muscles and adipose tissue, it may function protectively [83].

1.10 Oxidative modification of LDL

The hypothesis that oxidative stress plays an important role in the atherosclerosis process has now been well established [85]. In particular oxidation of lipoproteins by activated macrophages in the subintimal space has been postulated to be an important early step in the atherosclerosis process [61]. Lipoprotein oxidation is critically important in allowing macrophages and other cells to remove lipid from the interstitial space, as modified lipoproteins are more readily cleared by macrophage scavenger receptors. Lipoprotein oxidation could therefore also be considered a normal adaptive process to remove excess lipid. Oxidation of LDL however, has been shown to result in a modified LDL particle that is taken up rapidly by scavenger receptors on macrophages, leading to foam cell formation resulting in atherosclerosis [86]. Thus LDL oxidation is considered to be an initial and important step in atherogenesis and this has initiated interest in the mechanisms by which the LDL oxidation may occur and interventions to slow the rate of oxidation.

Oxidative modification of LDL is primarily though to occur in intima of the artery wall [87]. Significant amounts of LDL oxidation are not thought to occur in the plasma because of the presence of antioxidants such as vitamin C and E. Furthermore were sufficient oxidation to occur in the plasma, that oxidised LDL would be rapidly removed from the plasma by scavenger receptors present on hepatic Kupfer sinusoidal cells [87].

1.10.1 Evidence for LDL oxidation

Several lines of evidence support the role of oxidatively modified LDL in atherogenesis. These include

(a) Cells in the subendothelial space of a developing lesion can oxidise LDL *in vitro* in the presence of transition metals [88].

(b) A large proportion of the lipids in lesions is oxidised [87].

(c) Lesion-derived LDL particles have increased electrophoretic mobility [87].

(d) Epitopes of OxLDL have been found in plasma and atherosclerotic lesions of animals and humans [87].

(e) The presence of antibodies against OxLDL [89].

(f) Dietary supplementation with antioxidants reduces the development of atherosclerosis in experimental animals [89].

(g) Lysine-aldehyde adducts (markers of OxLDL) have been demonstrated in the macrophage rich lesions of human and rabbit aorta [87].

1.10.2 Mechanisms of LDL oxidation

The oxidation of LDL has been proposed to occur in three phases [88].

(a) An initial lag phase when endogenous LDL antioxidants are consumed.

(b) A propagation phase with rapid oxidation of unsaturated fatty acids to lipid hydroperoxides.

(c) A decomposition phase when hydroperoxides are converted to reactive aldehydes.

Results of *in vitro* experiments have proposed that there are a variety of potential mechanisms for cell mediated LDL oxidation [88] (see table 1.3).

Table 1.3

Table showing proposed mechanisms of LDL oxidation (from reference 88)

Proposed mechanisms of LDL oxidation
(1) Extracellular iron or copper Free or low molecular weight complexes Ceruplasmin bound copper
(2) Superoxide
(3) Thiols
(4) Lipoxygenase
(5) Reactive Nitrogen Species
(6) Myeloperoxidase

1.10.2.1 Metal ions

LDL oxidation has been found to require trace amounts of redox active metals (copper or iron) [91]. Evidence suggests that copper binding histidine residues on apolipoprotein B100 promote lipid peroxidation [91].

1.10.2.2 Cell induced oxidation of LDL

All three of the major cell types of the arterial lesion, ECs, SMCs and macrophages can oxidise LDL in cell culture [92]. Cells in the subendothelial space are thought to oxidise LDL by different methods. Release of superoxide anion is thought to be the major pathway in cultured fibroblasts and SMCs [92]. Generation of lipoperoxides by the action of 15-lipoxygenase is thought to be the major pathway of oxidation catalysed by macrophages and by endothelial cells [92].

Macrophages have the potential to oxidise LDL because they produce large amounts of highly reactive oxidants when they generate an inflammatory response or kill invading microorganisms and tumour cells [93]. They generate superoxide that can subsequently be broken down to form hydrogen peroxide [94]. They also secrete myeloperoxidase, which amplifies the oxidative potential of hydrogen peroxide by generating cytotoxic oxidants [95].

1.10.2.3 Lipoxygenases

Lipoxygenases are intracellular enzymes that can peroxidise polyunsaturated fatty acids [96]. There appears to be differences among the lipoxygenases with respect to their involvement in the oxidation of LDL. In humans, 5-lipoxygenase does not appear to be involved whereas 12- lipoxygenase and 15-lipoxygenase do, particularly in macrophages and endothelial cells [97, 98]. The role of lipoxygenases has been shown in mice where disruption of the 12/15 lipoxygenase gene has been shown to dramatically reduce atherosclerotic lesions [99].

1.10.2.4 Myeloperoxidase

Myeloperoxidase (MPO) is a haem-containing enzyme secreted by human phagocytes [95] which has two major activities, halogenation and peroxidation. Myeloperoxidase and MPO-derived hypochlorous acid (HOCl) have been implicated *in vivo* in LDL modification and atherogenesis [95]. Reaction of MPO derived HOCl with LDL results primarily in the modification of apoB [100]. HOCl reacts rapidly with the E amino groups of apoB lysine residues resulting in the formation of N-chloroamines [100]. Catalytically active MPO has been detected in human atherosclerotic lesions and co-localises with macrophages [101].

1.10.2.5. Role of nitric oxide

Nitric oxide (NO) released by endothelial cells of the artery wall plays an important role in normal physiology [102]. The major stimulus of nitric oxide synthesis, *in vivo* is thought to be shear stress that occurs on the surface of the endothelium by the flow of blood [102]. NO is also thought to have several functions in the normal intima including vasometric relaxation, promotion of SMC relaxation, inhibition of platelet adherence and aggregation, action as an antioxidant and as an inhibitor of smooth muscle cell proliferation [102]. NO produced by inducible nitric oxide synthases in activated macrophages is cytotoxic and is normally involved in antiviral, anti-protozoal and anti-microbial activities [93]. NO has also been shown to react with superoxide. This may represent a protective effect since superoxide can oxidise lipids [103]. However it may also be atherogenic. When NO reacts with superoxide it generates peroxynitrite, a powerful oxidising intermediate [103]. Peroxynitrite oxidises LDL lipids and converts the lipoprotein into a form recognised by the scavenger receptor. Studies using cultured cells have suggested that NO protects LDL from oxidation [104]. However the evidence is conflicting; a reduction in fatty streak formation has been reported in mice lacking nitrix oxide synthase [105].

1.10.3 Susceptibility of LDL to oxidation

The susceptibility of LDL to oxidation appears to depend on the abundance of unsaturated fatty acids in the particle [88]. Other factors may also affect the susceptibility of LDL to *in vitro* oxidation. These include variations in LDL particle size, lipid composition and the presence of Lp (a) [88]. In particular; small dense LDL particles are thought to be more atherogenic and prone to oxidation than the larger species.

1.10.4 Components of OxLDL

The components of OxLDL that results in its biological activities have still not been fully elucidated. However LDL oxidation does result in oxysterol formation which contribute to the cytotoxicity of OxLDL [106]. Several oxysterols including 7α and 7β hydroxycholesterol, 7-ketocholesterol and 2-hydroxycholesterol have been identified. [106]. Oxysterols can alter membrane permeability; inhibit cholesterol biosynthesis and suppress LDL receptor expression [106].

1.10.5 The role of antioxidants

Blood concentrations of antioxidants may affect the susceptibility of LDL and Lp(a) to oxidation [103]. The last decade has seen a number of studies performed on the hypothesis that antioxidants (such as Vitamin E, Vitamin C and β-carotene) may have a role in prevention of atherosclerosis [107]. One of the strongest lines of evidence for the oxidation hypothesis is the ability antioxidants to inhibit atherogenesis in animal models of hypercholesterolemia [108]. Thus it can be postulated that interventions inhibiting the oxidation of LDL within the artery *in vivo* wall should also inhibit the atherogenic process.

Results from human studies however, have not as yet provided clear evidence that antioxidants play a role in reducing the risk of CHD [109,110]. A recent meta-study by Topol *et al* [110] looked at seven randomised trials of vitaman E treatment and eight trials of β-carotene treatment. Their analysis concluded that vitamin E and β-carotene should not be used in patients at high risk of CHD.

1.10.6 Effects and atherogenicity of OxLD

OxLDL is not a single defined chemical entity. Depending on the extent of oxidation and on various oxidised products generated, it may show a broad range of biological effects including;-

(a) Uptake

One of the most important effects of OxLDL is that it is taken up by macrophages at a rate many times faster than native LDL [86]. Oxidatively modified LDL has been shown to be taken up by macrophages 3-10 times more rapidly than is native LDL and can therefore generate foam cells [86]. Oxidation of the lipid moiety of LDL causes modification of $apoB_{100}$ [88]. Scavenger receptors on macrophages subsequently recognise and bind OxLDL and are not down-regulated as intracellular cholesterol accumulates. As uptake continues, the macrophages become lipid laden foam cells.

(b) Chemotactic activity

OxLDL has chemotactic activity and is involved in the recruitment of blood monocytes [61]. Studies by Quinn *et al* [61] have shown that oxidatively modified LDL, but not native LDL is a potent chemoattractant for circulating human monocytes. This chemotactic activity has been attributeted to lysolecithin that is generated during oxidation of LDL [61]. Once oxidised, LDL is thought to build up in a given area of an artery and it may contribute to the further accumulation of monocytes in the same area.

(c) Cytotoxicity

Oxidised LDL is cytotoxic [106], and therefore could contribute to atherogenesis by causing cell injury and death. It also interacts with platelets, which promotes their aggregation [88].

(d) Inhibition of motility

Oxidised LDL has also been found to inhibit the mobility of tissue macrophages [61].

(e) Resistance to cathepsins

OxLDL has been shown to be more resistant than native LDL to cathepsins and can cause partial inactivation of macrophage lysosomal proteases [111]. OxLDL has been shown to inactivate cathepsin B but up-regulate cathepsin D [112]. High cathepsin D expression has been reported in human macrophage derived foam cells [112].

It has been speculated that uptake of OxLDL by macrophages in early stages of atherosclerosis may be beneficial rather than harmful [113]. By taking up OxLDL it may actually protect cells, including endothelial cells from its cytotoxic effects. Later when the macrophages have become excessively loaded with lipid and die, the effect may be harmful because of the release of cytotoxic components from lipid-laden macrophages [113].

1.10.7 Role of OxLDL in the expression of cytokines and growth factors

Cytokines, chemokines and growth factors are a set of multi-functional signalling molecules involved in regulating several cellular functions, including chemotaxis, proliferation, accumulation of lipid and synthesis of matrix components. Cytokines are thought to regulate immune function whereas growth factors are stimulators and inhibitors of cell proliferation [114]. Cytokines and growth factors can be induced by a variety of processes including damage to the endothelium and uptake of OxLDL.

Uptake of OxLDL by macrophages induces the expression of a wide range of growth factors and cytokines many of which have been localised within atherosclerotic lesions. These include transforming growth factor beta (TGF-β), fibroblast growth factor (FGF), macrophage chemotactic protein-1 (MCP-1) macrophage colony stimulating factor (M-CSF), interleukin-1 (IL-1), interleukin-8 (IL-8), tumour necrosis factor alpha (TNF-α) and platelet derived growth factor (PDGF) [115]. In addition, a number of chemokine receptors such as chemokine motif receptor 2 (CCR2), chemokine motif receptor 5 (CCR5) and the Chemokine CX3C receptor (CX3CR1) are thought to be important in the development of CHD [1].

IL-1 can sustain the inflammatory process and is a chemoattractant for T-cells [116]. Both OxLDL and 9-hydroxyoctadecadienoic acid, a breakdown product of

OxLDL can induce the expression of IL-1. IFN-γ down-regulates the expression of scavenger receptors for modified LDL on macrophages [117]. The secretion of MCP-1 (a chemoattractant for monocyes) from the endothelium has been shown to be induced by IL-1β, IL-4, TNF and IFN-γ [65]. OxLDL also induces the production of IL-8 from macrophages [118]. IL-8 is chemotactic for neutrophils and lymphocytes [119]. M-CSF stimulates the proliferation and differentiation of macrophages [120].

Many cytokines and growth factors mediate their effects via the activation of a common signal transduction pathway, the JAK/ STAT pathway (janus kinases/ signal transducers and activators of transcription) [199]. Studies show that oxidised LDL activates STAT1 and STAT3, transcription factors that can mediate the effects of cytokines and growth factors [121].

It has been shown that interaction of CD40 with its ligand CD40L (CD154) has an important role in the development of advanced lesions [122]. The binding of CD154 to CD40 particularly on macrophages results in the production of inflammatory cytokines, matrix degrading proteases and adhesion molecules [122].

1.11 The role of peroxisome proliferator activator receptors (PPARs) and the nuclear receptors LXRα and LXRβ

Perixosome proliferator activator receptors (PPARs) are ligand activated transcription factors that belong to the nuclear receptor superfamily. Three different PPAR subtypes have been indentified; PPARα, PPAR δ and PPARγ [123]. Both PPARα and PPARγ are present in human ECs, SMCs and macrophages *in vivo* [124]. In particular PPARγ has been found to be highly expressed in foam cells and OxLDL has been demonstrated to activate macrophage gene expression through PPARγ [124]. Upon activation PPARα and PPARγ regulate genes involved in lipid and glucose metabolism, cellular differentiation and inflammation control [124].

PPARs regulate gene expression by binding with 9-cis retinoic-acid X-receptor (RXR) to specific DNA sequence elements known as PPAR response elements [123]. PPARs regulate gene expression by interfering with the transcriptional activities of activator protein 1 (AP-1) and nuclear factor kappa β (NF-κB) [123]. Fatty acids such

as linoleic and arachidonic acid have been identified as natural PPAR activators that bind and activate both PPARα and PPARγ [124].

Activation of PPARγ has been shown to enhance macrophage differentiation and induce expression of the scavenger receptor CD36 leading to increased intracellular cholesterol accumulation [125]. However this is counteracted by reduced expression of another scavenger receptor SR-A [125]. Thus the net effect of PPAR activation in foam cells may be anti-atherogenic.

Both PPARγ and PPARγ activators have been found to induce the expression of the gene encoding ABC1, a transporter that controls apoA1-mediated cholesterol efflux from macrophages [124]. In contrast PPARγ activation does not affect cholesterol efflux from macrophages in patients with Tangiers disease which is caused by a genetic defect in the ABC1 transporter [126].

The nuclear oxysterol receptors LRX-α and LRX-β are involved in regulating the expression of proteins involved in the control of hepatic lipid metabolism and also in cellular cholesterol efflux [127]. The main activators of the LXR receptors are oxysterols. Activation of the macrophage LXR by free cholesterol induces the expression of the ABCA1 and also of Apo E, therby leading to cholesterol efflux from the cell [128]. Recently it has been demonstrated that LXR's and their ligands are negative regulators of macrophage inflammatory gene expression [129].

1.12 The role of the macrophage derived foam cell in advanced lesions.

Plaque rupture is the underlying cause of coronary syndromes, which include unstable angina and myocardial infarction [33]. Growth of atherosclerotic plaques can occur by outward luminal expansion and when coronary blood flow is decreased it presents itself clinically as stable angina [33].

During atherosclerosis there is a continuous dynamic balance between the influence of inflammatory cells including macrophages tending to destabilise the plaque and the influence of SMCs, which favour plaque stability [39]. Macrophage derived foam cells have been implicated in a number of processes which lead to plaque instability and subsequent acute coronary syndromes [39]. These include contributing to the lipid core, weakening the fibrous cap and being a source of tissue factor [39].

1.12.1 Composition of vulnerable plaques

The composition and vulnerability of a plaque rather than its volume is thought to be the most important determinant for the development of coronary syndromes [32]. Plaques that are vulnerable to rupture tend have thinner fibrous caps especially at the shoulder region [130]. In addition to an increased macrophage density they also have a reduced collagen and SMC content in their fibrous caps [130]. Increased macrophage density and decreased collagen content have been shown to be associated with a reduced tensile strength, which may weaken the fibrous cap [130]. Plaques less likely to lead to myocardial events tend to have thicker fibrous caps that protect the underlying thrombogenic lipid core from contact with the circulating bloodstream [32]. Although the thicker fibrous cap increases stenosis of the artery, it makes the plaque less likely to rupture.

1.12.2 The fibrous cap

The integrity of the fibrous cap overlying the lipid rich core is one of most important factors in determining the stability of an atherosclerotic plaque [131]. The fibrous cap consists of a dense fibrous extracellular matrix made up of collagens, elastins and other extracellular matrix materials like proteoglycans [131]. The SMC is the major cell type involved in the production of extracellular matrix. As would be expected, regions of the plaques fibrous cap particularly prone to disruption have been found to contain relatively few SMCs [131].

Cytokines and growth factors such as IL-1, TGF-β and PDGF can significantly induce collagen synthesis in SMC [132]. In the unstable plaque, IFN-γ secreted by activated T-cells has a number of effects on SMC [132]. It has been shown to inhibit collagen synthesis, suppress the proliferation of SMC in response to other growth factors and promote apoptosis of SMC [132]. In addition IFN-γ secreted by the T-lymphocytes can also activate the macrophage [132]. Activation of macrophages in the atherosclerotic plaque leads to the secretion of a variety of proteolytic enzymes capable of degrading the extracellular matrix [133]. Three major families of enzymes participate in extracellular matrix degradation [133]: the serine proteases (urokinase

and plasmin), cystine proteases (such as cathepsins) and the matrix metalloproteinases (discussed below).

Degradation of collagen and other matrix components contributes to the weakening of the fibrous cap, rendering it particularly susceptible to rupture. Rupture of the fibrous cap exposes the underlying core to circulating platelets in the blood [131]. Foam cells in the lesion area are subsequently capable of producing large quantities of tissue factor (a strong procoagulant), that potently stimulates thrombosis formation when in contact with blood [134]. In addition to tissue factor, the plaque core is rich in collagen and lipid, all of which are potent thrombogenic agents [131]. Thus a delicate balance exists in which SMC synthesize ECM components and macrophages break them down. When this balance is disrupted, then the plaque is more vulnerable to rupture and exposure to the bloodstream.

1.12.3 Role of lipids

The propensity of atherosclerotic plaques to rupture may also be influenced by their lipid content. Disrupted plaques have been shown to have a greater content of lipid (mainly free cholesterol and cholesteryl esters) than intact plaques [130] especially in the shoulder region. Lipid concentrations have been shown to be positively associated with macrophage accumulation in all plaque types [130].

1.12.4 Role of apoptosis

Apoptosis of both macrophages and SMC has been detected in atherosclerotic plaques [135]. Since macrophages are responsible for collagen breakdown in the plaque, loss of macrophages will lead to less MMP activity and subsequently decreased collagen breakdown [135]. This could lead to plaque stabilisation and therefore less risk of plaque rupture. This supports the idea that macrophage apoptosis may be a beneficial process, which leads to plaque stability.

However the situation may be more complex. Uptake of dying cells is an important component of the apoptotic process since it prevents the release of toxic intracellular contents and the formation of an inflammatory infiltrate [135]. If apoptotic bodies are cleared quickly, a stable fibrous plaque will form with low

atherogenicity [132]. If apoptotic SMCs or macrophages are not engulfed, however, a necrotic core with high thrombogenicity forms [135]. Thus macrophage apoptosis may actually be a detrimental process since it reduces the number of cells available to scavenge apoptotic cells. Apoptosis of SMC in the fibrous cap is also thought to be detrimental since it will lead to a loss of collagen types I and II and a weakening of the fibrous plaque. This will subsequently lead to unstable plaques that are more prone to rupture [132].

1.12.5 Effects of lipid lowering on plaque stability

Lipid lowering has been found to result in a decrease in clinical events without a substantial change in the degree of luminal stenosis [136]. This suggests that lipid lowering affects the composition of the plaque rather than its size. Lipid lowering by statin therapy is though to stabilize plaques through several mechanisms [137]: -

(a) Reduced lipid intake into the artery wall results in a less lipid-rich plaque with reduced macrophage foam cell formation.

(b) Decreased MMP activity allows a higher collagen content in the atheorsclerotic plaque.

(c) Reduced inflammatory cell proliferation appears to correlate with a reduction in apoptotic cell death in the plaque.

(d) Statins may also have an inhibitory effect on tissue factor.

1.13 The Matrix Metalloproteinases

The matrix metalloproteinases (MMPs) have been implicated in tissue remodelling in both normal and pathological conditions [138]. Changes in MMP activity have been observed in menstruation, pregnancy, wound healing, inflammation and tumour metastasis [138]. There is also evidence that the MMPs are also involved in a number of events associated with the development and progression of atherosclerosis [133].

The ECM constitutes up to 60% of the volume of the intima and it is thought to undergo continuous remodelling during atherogenesis [139]. MMPs are secreted by a number of cells including fibroblasts, SMCs, ECs and macrophages. The MMPs

have been implicated as the major molecules involved in the breakdown of the fibrous cap and subsequently plaque instability [131]. The major source of MMPs in the plaque is the foam cell [140]. Macrophages release cytokines that can activate a range of MMPs and may also regulate MMP activation via release of reactive oxygen species [140,141].

1.13.1 Biochemistry of the MMPs

The matrix metalloproteinase family in humans comprises of 22 enzymes. These are generally expressed at low levels in normal adult tissue but are up regulated during normal and pathological remodelling processes [138]. The general classification of MMP is based on substrate specificity, but several of the MMPs have overlapping substrate specificties. All MMPs share the following common features [138]: -

(a) Most are secreted as latent zymogens requiring activation for proteolytic activity.

(b) They degrade ECM components but non-ECM molecules can also be substrates.

(c) They function at neutral pH.

(d) They contain zinc at their active sites and require calcium for stability.

(e) They are inhibited by specific tissue inhibitors of metalloproteinases (TIMPs).

The MMP family can been divided into four main subgroups, based on their substrate preferences (see table 1.4 Properties of the matrix metalloproteinases) [138]: -

(a) The interstitial collagens

(b) The gelatinases

(c) The stromelysins

(d) The membrane-type MMPs (MT-MMPs)

An important control point of MMP activity is the inhibition of the activated enzyme by the tissue inhibitors. To date, four TIMPs have been identified [142]. All TIMPs inhibit MMP function by forming inhibitory non-covalent stiochiometric complexes with MMPs and blocking access to their substrate [142]. The balance between degradations by MMPs and TIMPs may regulate plaque stability.

Table 1.4

Classification of the matrix metalloproteinases (adapted from reference [138])

MMP subgroup *Name*	*MMP number*	*Substrate*
Collagenases		
Interstitial collagenase	MMP-1	Collagen types I, II, III, V, X, gelatins and proteoglycans
Nuetrophil collagenase	MMP-8	as above (for MMP-1)
Collagenase - 3	MMP-13	as above (for MMP-1)
Gelatinases		
Gelatinase A (72Kd type IV collagenase)	MMP-2	Gelatins, collagens types IV, V, VII, X and XI, elastin, fibronectin and proteoglycans
Gelatinase B (92kd type IV collagenase)	MMP-9	Gelatins, collagen types IV, V, elastin and proteoglycans
Stromelysins		
Stromelysin 1	MMP-3	Proteoglycans, fibronectin and laminin
Stromelysin 2	MMP-10	Elastin, gelatin, collagen types II, IV, V, IX and X
Stromelysin 3	MMP-11	Gelatin, fibronectin and proteoglycans
Matrilysin	MMP-7	Gelatins, collagens types 1- IV and proteoglycans
Metalloelastase	MMP-12	Elastin
Membrane type MMPs		
MT1 - MMP	MMP-14	Collagen types 1-III, gelatin
MT2 - MMP	MMP-15	Collagen type I-III, gelatin
MT3 - MMP	MMP-16	Collagen type I-III, gelatin
MT4 - MMP	MMP-17	Gelatin
MT5 - MMP	MMP-24	Gelatin
MT6 - MMP	MMP-25	Collagen type IV and gelatin
CA-MMP	MMP 23A MMP23B	Gelatin

Others

RASI-1	MMP-19	Collagen types I, IV and gelatin
Enamelysin	MMP-20	
Epilysin	MMP-28	Casein
Matrilysin-2	MMP-26	Collagen type IV and gelatin

1.14.2 MMP and TIMP expression

A number of MMPs and TIMPs are expressed by SMCs and macrophages in atherosclerotic plaques where they may participate in vascular remodelling, SMC migration and plaque disruption [140,143].

MMP-1, MMP-9 and MMP-3 have been found to be expressed in the fibrous cap, shoulders of lesions and at the base of the lipid core, whereas MMP-7 is predominantly expressed in macrophages overlying the lipid core [144]. TIMP-1, 2 and 3 have also been localised in all these areas, particularly in plaque shoulders and between the fibrous cap and the necrotic core [142]. In particular intense MMP-1 expression has been detected in macrophages located at the borders of lipid cores next to fibrous caps and shoulder regions, which are critical to plaque integrity [145]. Thus MMP-1 could contribute to plaque rupture by degradation of the two of major structural proteins of the fibrous cap, collagen types I and III collagen [146]. Both MMP-2 and MMP-9 have been found to be expressed in isolated atherosclerotic lesions [147]. MMP-2 and MMP-9 have been associated with SMC migration and proliferation *in vitro* and *in vivo* [146]. MMP-2 can degrade type IV collagen, an important component of the basement membrane to which endothelial cells attach [146]. Unlike other secreted MMPs, MMP-2 activation does not occur through proteolysis by serine proteases but rather through MT1-MMP [148].

It has been demonstrated that MT1-MMP is expressed by SMCs and macrophages in lipid rich atherosclerotic plaques [148]. Proinflammatory molecules IL-1α, TNF-α and OxLDL have been found to augment MT1-MMP expression, leading to increased activation of MMP-2 [148]. MMP-9 has emerged as one of the major members of the MMP family in the context of plaque events [149]. It has been found to be up-regulated in plaques vulnerable to rupture [149]. Several mechanisms exist for the up-regulation of expression of MMPs. TNF-α and IL-1 have been shown

to up-regulate MMP activity by macrophages [144]. In addition the interaction of macrophages with T-lymphocytes, through the interaction of CD40 with its ligand CD154 also up-regulate MMP expression [122].

TIMP-1 is synthesized and secreted by macrophages and its expression is regulated by a variety of agents including growth factors (EGF, TNF-α, IL-1 and TGF-β), phorbol esters and retinoids [150]. IL-8 is thought to play a potentially atherogenic role by inhibiting local TIMP-1 expression [150]. TIMP-2 is frequently co-localised with MMP-2 and its expression is largely constitutive and down-regulated by TGF-β [133]. *In vitro* studies have also established the human macrophage as a novel source of TIMP-3 [151]. Extracts of atherosclerotic plaques have been found to have a 5 fold higher levels of TIMP3 than non-atherosclerotic tissue [151], where it has been found to be localised with macrophages [151].

1.13. 3 Effects of statins and antioxidants on MMP and TIMP expression

Lipid lowering may produce clinical benefit by stabilising plaques against disruption. A study using pravastatin has shown that the drug decreases lipids, lipid oxidation, inflammation, MMP-2 and cell death and increases TIMP-1 and collagen content in plaques, confirming its plaque stabilizing effect in humans [137].

Plaques and foam cells taken from lesions of rabbits have showed a marked decrease in the expression of MMP-9, if the animal had been treated with the reactive oxygen species scavenger, n-acetyl cysteine [152]. Inhibition of MMP activity by antioxidants early in atherosclerotic lesion development may again contribute to plaque stability.

1.14 Inflammatory markers

Studies have indicated that levels of plasma markers of inflammation such as C-reactive protein, white cell count and fibrinogen levels are elevated in individuals at risk from CHD [153]. C-reactive protein is a liver derived protein (regulated by interleukin-6), which is produced by inflammatory cells. Data by Ridker *et al* [154] has indicated that patients with relatively low lipid levels but elevated CRP levels may benefit from statin therapy

Studies have also linked lipoprotein-associated phospholipase A_2 (Lp-PLA_2) with a risk of CHD [155]. A_2 phospholipases are a family of enzymes that can hydrolyse phospholipids at the *sn*2 position to generate lysophospolipids and fatty acids. Plasma Lp-PLA_2 levels have been found to be significantly elevated in patients with CHD, when compared with age-matched controls [153]. Furthermore a comparison of risk factors in CHD patients and normal groups has indicated that plasma Lp-PLA_2 is a clearer marker of risk on a case control basis than either plasma cholesterol or LDL cholesterol. The majority of Lp-PLA_2 has been found to be associated with LDL where it is involved in the oxidative modification of OxLDL [156]. In particular Lp-PLA_2 has been found to be highly enriched in the atherogenic small dense LDL particles [156].

1.15 Aims and objectives

1.15.1 Background to this study

Even when an atherosclerotic lesion is well advanced and the risk of plaque rupture is high, lipid lowering may stabilise the plaque and reduce the risk of thrombotic events [137]. Results from animal experiments have indicated that macrophage foam cells may be a relatively reversible component in atherosclerotic lesions [157]. CHD is a multifactorial disease with both genetic and environmental factors having an input to its progrsssion [2]. Many of the genes responsible for single gene vascular disorders, such as FH and Tangiers Disease have been described [126]. Although genes that contribute to atherosclerosis have been identified, it is likely that more remain to be discovered.

In an effort to identify other genes that are specifically induced in foam cell formation we examined genes in a human macrophage cell line (THP-1 cells) in response to native LDL (nLDL), AcLDL and OxLDL stimulation using high-density cDNA arrays. A comprehensive review of the use of gene expression profiling in cardiovascular disease has been reviewed by Henriksen *et al* [158]. A better knowledge of gene expression would be helpful in understanding the mechanisms behind foam cell formation.

1.15.2 Experimental Considerations

1.15.2.1 The THP-1 cell line

The THP-1 cell line was used as a *in vitro* model for studying foam cell formation. Human THP-1 cells have been established as a cell line for studying the lipid metabolism of human macrophages and have been reported to represent a more differentiated and committed macrophage cell line than previously available human monocytic lines [159]. THP-1 cells can be differentiated to mature macrophages after stimulation with various factors including phorbol esters and retinoic acid [160]. THP-1 cells, like mature human primary macrophages, synthesize and secrete M-CSF, and apo E. IL-8 secretion has also been described in THP-1 cells [159]. Further properties of THP-1 cells, which make them a useful model for studying foam cell formation, are discussed in chapter 3. The main reason for using an *in vitro* rather than an *in vivo* model of macrophages in this study was to minimise variability. Compared to THP-1 cells, human monocyte derived macrophages show large variability between subjects. In addition compared to human monocyte derived macrophages, THP-1 cells are easier to grow in large batches.

1.15.2.2 Use of AcLDL and OxLDL

Although AcLDL it is not a naturally occurring *in vivo* modification of LDL, Goldstein and Brown used it in their studies leading to the discovery of the scavenger receptor. Thus experimentally AcLDL is used as a modified form of LDL to induce foam cell formation as it represents a standardised particle for lipid loading.

OxLDL is more likely to represent the *in vivo* situation, although it may not be a true representation since the degree of oxidation of LDL that occurs *in vivo* remains to be determined. Importantly OxLDL is a more heterogeneous entity composed of a variety of oxidation products and having a range of biological effects. Thus OxLDL formed by in vitro copper oxidation was used to try and induce large changes in expression of key genes.

1.15.2.3 Analysing gene expression

Various molecular biology methodologies exist for the detection and quantitation of gene expression [161]. The most popular ones include RT-PCR, differential display and northern blots [161]. The last decade has seen the development of a new method for analysing gene expression namely DNA array technology [162]. The main advantage of DNA array technology is that it allows the expression levels of thousands of genes to be measured simultaneously [162] (hence the reason for using this technology in this study). High-density cDNA arrays are nylon membranes or glass slides containing cDNA sequences corresponding to individual genes/transcripts arrayed at high density.

Briefly messenger RNA was extracted from both differentiated THP-1 cells and THP1 cells exposed to nLDL, AcLDL and OxLDL. Complementary DNA was subsequently prepared from the messenger RNA and radioactively labelled. The labelled cDNAs were then hybridised to identical arrays consisting of several thousand spotted gene fragments. Phosphorimaging of the arrays revealed the genes being expressed for each treatment and the differences between differentiated THP-1 cells and differentiated THP-1 cells exposed to AcLDL or OxLDL were identified. The method is discussed in further detail in chapter 4.

1.15.3 Aims of this study

The aim of this study was to determine which genes are expressed during foam cell formation and, in particular, which genes are specifically regulated by the two forms of modified LDL used in this study, namely OxLDL and AcLDL. A number of genes have already been reported to be altered on exposure to these agents. Most of these genes have been found to be inflammatory molecules and cytokines.

1.15.4 Objectives

[1] To establish an *in vitro* model of foam cells using THP-1 cells incubated with AcLDL/OxLDL

[2] To differentiate the THP-1 monocytic cell line into macrophages using PMA and confirm this differentiation.

[3] To establish cDNA array technology (in use at Glaxo SmithKline) to compare acetylated and oxidised LDL induced changes in gene expression.

[4] To perform a temporal study of gene expression in THP-1 cells exposed to OxLDL for up to 72 hours compared to zero.

[5] To confirm these changes identified by independent means, namely quantitative RT-PCR.

Chapter 2: Methods

2.1 Human THP-1 cell line

2.1.1 Culture of human THP-1 cells

Human THP-1 cells were kindly donated by Dr Steve Yeaman, Department of Biochemistry at the University of Newcastle (original source: American Type Culture Collection [ATCC 10801], Rockville, MD). THP-1 cells were grown continuously in culture in RPMI-1640 + L-glutamine + 25mM HEPES media supplemented with 10% foetal bovine serum (FBS), 1% penicillin/streptomycin (10mg/ml), 1% L-glutamine (10mg/ml) and 10μM 2-mercaptoethanol as previously described [163]. (Media and all media components were obtained from GibcoBRL, Paisley. FBS was obtained from Sigma, Dorset). Cells were maintained in an incubator at 37°C in a humidified atmosphere containing 5% CO_2/95% air. Cells were grown in suspension to a density of 1-2 x10^6 cells/ ml over seven days (with a media change every two days) before being split back to a level of 1x10^5 cells/ml. Cells were counted as described in 2.1.4.

2.1.2 Differentiation

THP-1 cells in suspension were pelleted by centrifugation (Sigma 3-15) at 400g for 10 minutes. Cells were resuspended in RPMI 1640 + L-glutamine media supplemented with 10% FBS, 1% penicillin/streptomycin (10mg/ml), 1% L-glutamine (10mg/ml) and 10μM 2-mercaptoethanol at a concentration of 5x10^5 cells/ml. Cells were subsequently plated at a concentration of 1x10^6cells per well (2mls per well) in six-well plates (Falcon/Becton Dickinson, Oxford). Cells were differentiated using phorbol 12- myristate 13-acetate (PMA) [Sigma, Dorset] at a final concentration of 250nM (5μl of a 50nM stock solution of PMA per well, prepared as described in section 2.5). Medium containing 250nM PMA was replaced every two days.

After 7 days of differentiation, the media was removed and the cells were washed twice with 2ml of phosphate buffered saline (PBS). Cells were then exposed to RPMI 1640 + L-glutamine media supplemented with 1% L-glutamine (10mg/ml), 1% penicillin/streptomycin [10mg/ml], 0.2% bovine serum albumin (BSA)

[essentially fatty acid free A6003, Sigma, Dorset], 10μM 2-mercaptoethanol and 250nM PMA. This media contained no FBS and cleared the cells of any exogenous lipoprotein.

After 24 hours the media was replaced with RPMI 1640 + L-Glutamine media supplemented with 1% L-glutamine [10mg/ml], 1% penicillin/streptomycin [10mg/ml], 0.08 % BSA, 10μM 2-mercaptoethanol and 250nM PMA. At this stage the cells were ready for addition of lipoproteins.

2.1.3 Freezing/thawing

Cultured THP-1 cells ($50x10^6$) were pelleted at 400g for 10 minutes (Sigma 3-15) and resuspended in 1ml of freezing media (90% FBS, 10% dimethyl sulphoxide [DMSO]). Cells were immediately placed in a cryofreezing chamber (Nalgene) containing isopropanol (50ml) and placed at -70°C. After 24 hours cells were transferred to liquid nitrogen for long-term storage.

Cells were thawed in warm water (37°C) and resuspended in 20ml of RPMI-1640 + L-glutamine + 25mM HEPES media supplemented with 10% FBS, 1% penicillin/streptomycin (10mg/ml), 1% L-glutamine (10mg/ml) and 10μM 2-mercaptoethanol. Cells were then pelleted by centrifugation at 400g for 10 minutes and resuspended in fresh media to remove any remaining DMSO. Initially these thawed cells were grown at high density (one vial cells/per 20ml media) for one week to help their proliferation before being split and grown as described in section 2.1.1.

2.1.4 Cell Counting

To determine the numbers of cells in culture at any time during their growth, 100μl of cell suspension was added to 100μl 0.6% filtered trypan blue (trypan blue is excluded by live cells and stains dead cells blue). The cell suspension was placed on a counting chamber (Weber Scientific, depth 0.02mm, $1/400mm^2$). The number of cells in the four quadrants was counted (using a standard laboratory light microscope [CK Olympus, Tokyo] at x40 magnification). The total number of cells in the four quadrants was divided by four to give an average number. This average was subsequently multiplied by two (to take account of the dilution with trypan blue) and by 10^4 to give the number of cells per millilitre.

2.1.5 Oil Red O staining

Cells were stained with Oil Red O (lipid stain) as previously described [164]. THP-1 cells ($1x10^6$) in suspension were pelleted at 400g for 10 minutes and resuspended in 1ml of 40% FBS in PBS. A sample of the cells (200µl) was loaded into a cytocentrifuge chamber attached to a slide. Cells were subsequently pelleted onto the slide by spinning in a cytospin for 5 minutes at 100g and allowed to air dry for a few minutes.

Differentiated THP-1 cells were grown on culture slides (5ml; Falcon/ Becton Dickinson, Oxford) for 7 days as described in section 2.1.2 before being exposed to lipoprotein. Slides with cells were fixed in 40% calcium formal solution (see section 2.6) for one hour. The slides were then placed in 60% isopropanol for 15 minutes and subsequently stained in a solution of Oil Red O (Sigma, Dorset; see 2.6) for 15 minutes. After staining, the slides were dipped in 60% isopropanol for approximately 15 seconds and washed in deionised water. Subsequently the slides were counterstained with haematoxylin solution (Sigma, Dorset) for 3 minutes to stain the nuclei. The slides were then rinsed well in deionised water and allowed to air dry. Finally a coverslip was mounted onto the slide using glycerine jelly (BDH, Dorset) and the slides were stored at 4°C.

2.1.6 Nile red staining

THP-1 cells were differentiated as described in section 2.1.2. The cells were then exposed to varying concentrations of native, acetylated or oxidised LDL for different time intervals. After exposure to lipoprotein, cells were washed twice in PBS and incubated in 1ml of 0.27% EDTA for 10 minutes at 37°C. The cells were subsequently lifted from the well with the single stroke of a cell scraper, transferred to a microfuge tube and pelleted by centrifugation for 10 minutes at 400g. The supernatant was removed and the cells were fixed in 1% paraformaldehyde solution (see section 2.6) for 10 minutes. An automatic pipette was used to mix the cells and to disrupt aggregates by gently sucking the cell solution up and down, gently in a pipette tip. The cells were then centrifuged at 400g for 10 minutes to remove the paraformaldehyde, and the cell pellet was resuspended in 1ml PBS.

Nile red [Sigma, Dorset] (10µl from a 10µg/ml solution of nile red in acetone) was added to each sample to give a final concentration of 100ng/ml as previously described [165]. The samples were incubated with the dye for 5 minutes before running the samples on a flow cytometer.

2.1.7 Flow Cytometry

Using a flow cytometer (Coulter EPICs XL-HCL), cells (which are counted as events) were allowed to pass through the cytometer with the flow rate set to medium (around 100 cells counted per second) until 10,000 events had passed. The excitation wavelength was set to 488nm (since nile red has an excitation wavelength of 488nm).

The data was subsequently expressed as a ratio of the side scatter (granularity of the cell) versus forward scatter (size of the cell). Emission spectra were collected using four different fluorescence (FL) channels, which had different emission spectra collection ranges. These were FL1 (505-545nm), FL2 (560-590nm), FL3 (605-635nm) and FL4 (660-700nm). Cholesteryl esters were detected using a 600nm long pass filter (FL3) and triglycerides were detected using a 580nm long pass filter (FL2). The data was expressed as number of cells versus log fluorescence.

2.1.8 Estimation of cholesterol uptake

Stimulation of cholesteryl [^{14}C] oleate synthesis is commonly used as a functional assay to measure lipoprotein uptake. Loading of THP-1 cells with ^{14}C-oleate was performed as previously described [166].

2.1.8.1 Preparation of ^{14}C-oleate label

Four individual solutions were prepared as follows: Solution 1: - 150mM NaCl, 50mM Tris-HCl, pH 7.4.

Solution 2 was prepared by dissolving 12 g of BSA (essentially fatty acid free A6003; Sigma, Dorset] in 2g aliquots to 35ml of solution 1 over a five-hour period with continuous stirring at room temperature. After five hours, the solution was adjusted to pH 7.4 with 5M NaOH and the volume made up to 50 ml using solution 1.

For solution 3, 90mg of oleic acid (Sigma, Dorset) was dissolved in 2ml of ethanol and 100µl of 5M NaOH. This solution was then dried under gaseous nitrogen and re-dissolved in 10ml of solution 1. The resulting solution was heated to 60°C for 5 minutes, before the addition of 12.5ml of ice-cold solution 2. The solution was then stirred for 10 minutes before the volume was finally adjusted to 25ml with solution 1.

Solution 4 was prepared by drying 50µCi ^{14}C oleic acid (100µCi/ml) under nitrogen. The mixture was resuspended in 0.16ml solution 1, 0.16ml solution 2 and 0.87ml solution 3 and stirred gently at room temperature for 4-6 hours.

After their preparation solution 1 was stored at room temperature, whilst solutions 2-4 were stored at -20°C until required.

2.1.8.2 Preparation of ^{3}H-cholesteryl oleate internal standard

To prepare the cholesteryl oleate internal standard 50mg cholesterol, 50mg oleic acid, 50mg triolein and 10µl of ^{3}H-cholesteryl oleate (1µCi/µl) were dissolved in 10ml of a mixture of chloroform: methanol (1:2).

2.1.8.3 Lipid extraction and thin layer chromatography

To estimate cholesterol ester accumulation by THP-1 cells, amount of cholesterol esters was measured. THP-1 cells were differentiated as described in section 2.1.2. Differentiated THP-1 cells were exposed to varying concentrations of native, acetylated and oxidised LDL for varying time periods in the presence of 10µl of 10mM ^{14}C oleate (0.42µCi ^{14}C oleate) in 12% BSA (final concentration 0.1mM oleate in 0.12% BSA).

After the cells had been exposed for the relevant time period, media containing lipoproteins and ^{14}C oleate was removed. Cells were subsequently washed twice in 2ml of PBS per well and 1ml of PBS was added per well. Cells were lifted into the PBS using a cell scraper and a pasteur pipette was used to transfer the mixture into a glass tube.

To extract the lipid, 3.75ml of a solution of chloroform-methanol (1:2, v/v) was added to the cells/PBS mixture and mixed thoroughly by vortexing. This was followed by the addition of 1.25ml of chloroform and 0.25ml of water. At this stage

20µl of ^{3}H-cholesterol oleate internal standard (0.02µCi) was added to each sample to determine percentage recovery. Samples were subsequently centrifuged at 500g for 15 minutes. The upper phase and denatured proteins were removed and the lower phase was transferred to 5ml-scintillation vial. Samples were dried down in a rotary evaporator (Jouan Rotary Evaporator RC 10.22) at 50°C for 90 minutes before being redissolved in 50µl chloroform (containing 1g/ml cholesterol oleate and 1mg/ml cholesterol).

Samples were applied in 10µl aliquots as spots onto a 20cm x 20cm plastic backed silica thin layer chromatography (TLC) plate (catalogue number 01511; Anachem, Luton) using a 100µl Hamilton syringe and needle and dried using a hair dryer. An additional 50µl of chloroform (containing 1mg/ml cholesterol oleate and 1mg/ml cholesterol) was added to each tube to remove any remaining sample and again spotted onto the TLC plate. Two standards, cholesterol (1mg/ml in chloroform) and cholesterol oleate (1mg/ml) were also spotted onto the plate. The TLC plate was placed in a standard chromatography tank containing 100ml of petroleum spirit/diethyl ether (170:30, v/v) until the solvent front had reached three-quarters up the TLC plate (approximately 30 minutes).

The TLC plate was subsequently placed in an enclosed chromatography tank containing a small amount of iodine crystals until the iodine vapours allowed visualisation of the cholesterol and cholesterol oleate spots. The TLC plate was removed and the position of the spots was marked using a pencil.

Cholesterol oleate spots were subsequently cut out the TLC plate and placed in a scintillation vial containing 10ml of scintillation fluid (Ecoscint A, National Diagnostics). The vial was left for twenty-four hours to allow leaching. Samples were then counted in a liquid scintillation counter (Packard tricarb liquid scintillation analyser 2200 CA) for 1 minute using a dual ^{3}H and ^{14}C program. Each reading was taken twice and the results obtained were averaged and converted from cpm into dpm. The results in dpm were corrected by using percentage recovery of the ^{3}H cholesterol oleate internal standard. Amount of ^{14}C incorporated into cholesterol esters was calculated (0.42µCi = 932400dpm = 0.1µmol ^{14}C cholesterol oleate) and the results were expressed as micromoles of cholesterol ester accumulation per $1x10^{6}$ cells.

2.1.9 MTT assay for cell viability

Cells were seeded at a density of 3-5 x10^5 cells per well. After differentiation with PMA (as described in section 2.1.2) cells were exposed to native LDL, AcLDL or OxLDL at a concentration of 0.2mg/ml for 24, 48 and 72 hours respectively. After incubation with lipoprotein for the appropriate time period, 100µl of 5mg.ml MTT was added to each well (in 900µl media) to a give a final concentration of 0.5mg/ml. Cells were then incubated at 37°C for 3 hours. After 3 hours, water-insoluble formazan was solubilised by adding 1ml of HCl/Isopropanol (1:24) and mixed with a pipette. The OD value of the subsequent solution from each well was measured in a spectrophotometer using a test wavelength of 570nm and reference wavelength of 630nm. The MTT assay was performed by Dr Wei, (Department of Obstetrics and Gynaecology, Glasgow Royal Infirmary)

2.1.10 Statistical Analysis of Results

Statistical Analysis was performed using a computer software package called Stastica with a function called multiple dependent measures analysis. This initially tests whether these are differences across the whole time course or concentration series being studied. A post-hoc test; Tukey Honest Significant Difference (THSD) was then used to test for specific differences between different time points or concentrations. A * is used in the graphed results to indicate a significant difference between groups being compared.

2.2 Isolation of low-density lipoprotein

LDL was isolated from human plasma by density ultracentrifugation as previously described [167, 168] and as described below.

2.2.1 Preparation of density solutions

A density solution at a density of 1.006g/ml was prepared by dissolving 57g NaCl, 0.5g NaEDTA and 5ml of 1M NaOH in 5 litres of deionised water. The 1.006g/ml density solution was subsequently used as a base solution to make a further

density solution of density 1.063g/ml by addition of 74g of potassium bromide to 1 litre of 1.006g/ml density solution.

The density of the solution was assessed using the refractive index of the solutions since refractive index is proportional to the refractive index of the solution (appendix one). Density solutions at density 1.006g/ml and 1.063g/ml have refractive indexes of 1.335 and 1.344 respectively [169].

2.2.2 Collection of blood and separation of plasma

Blood was collected from laboratory volunteers at Dryburn General Hospital, Durham. Human blood was collected in tubes containing 50mM EDTA to prevent coagulation. Blood was centrifuged at 1900rpm for 10 minutes using a centrifuge with a swing out rotor to separate the plasma. The plasma layer was removed using a pasteur pipette and transferred to a new tube. The plasma was subsequently centrifuged at 3000rpm to pellet the white blood cells. Potassium bromide (43.75g) was subsequently dissolved per 100ml of plasma to give a solution of density greater than 1.063g/ml

2.2.3 Separation of LDL

Beckman Quickseal centrifuge tubes were filled with 24ml of 1.0063g/ml solution. Potassium bromide adjusted plasma (11.5ml) was placed below the density solution using a gradient former (Watson-Marlow 501). Tubes were filled to the top with 1.0063g/ml density solution, balanced to within 50mg of one another and sealed using a Beckman heat sealer. Tubes were placed in a Beckman VTi50 horizontal rotor and centrifuged at 50000g for 2.5 hours at 16°C using Beckman L-70 ultracentrifuge. Minimum deceleration, no acceleration and no brake controls were used so as not to disturb the gradient. After centrifugation the LDL layer was found to form a tight band in the middle of the tube (volume 6-10ml). This LDL band was removed using a syringe and needle (21 gauge) by piercing the tube below the LDL band

2.2.4 Concentration of LDL

LDL was concentrated using CF50 centrifuge filter cones (Amicon, Bedford, USA). LDL was loaded into filter cones placed in collection tubes (Amicon, Bedford, USA). The tubes were centrifuged (in a centrifuge with a swing out rotor), three times at a maximum speed of 1000g for 15 minutes or until the LDL volume was between 2-4ml.

To wash the LDL to ensure it was free of contaminants and other lipoproteins, 2ml of LDL was placed in a 5ml polyallomer quick seal tube (Beckman). The LDL was overlaid with 1.063g/ml density solution, tubes were sealed using a heat sealer and placed in a TLA100.4 rotor. Tubes were centrifuged at 100,000rpm for 1 hour at 16°C in a Beckman Optima TLX ultracentrifuge. After centrifugation the LDL moved to the top of the tube. The LDL band was removed using a syringe and needle (21 gauge) by piercing the tube above the LDL band.

Subsequently the LDL was desalted on a PD10 column (Pharmacia, Little Chalfont) to remove the salt. PD 10 Columns were equilibrated with PBS. LDL in a volume of 2.5ml was passed through the column and eluted with 3.5ml of PBS. Finally the LDL was dialysed extensively at 4°C in a volume of PBS that was at least 1000 times the volume of LDL.

2.2.5 Bradford assay

The concentration of LDL was expressed as mg/ml using the standard Bradford assay for protein measurement [170].

Bradford working reagent was prepared by adding 15ml of Bradford stock reagent (see section 2.6) to 85ml of deionised water. Bovine serum albumin [BSA] (1mg/ml) was used to construct a standard protein curve. Dilutions of BSA (0.1-1mg/ml) were prepared in a total volume of 100µl of deionised water. A blank sample containing no BSA was also prepared as a reagent blank. Dilutions of LDL were prepared in a range of 1 to 1/10 in a total volume of 100µl. Bradford working reagent (900µl) was added to each sample whilst mixing on a vortex. Samples were allowed to stand at room temperature for 15 minutes before being read in a spectrophotometer at 595nm. The spectrophotometer was set to zero using the reagent blank. The

readings from the standard samples were used to construct a standard curve. The concentration of the LDL was determined using the BSA standard curve.

2.2.6 Modification of LDL

LDL was modified either by oxidation or acetylation.

2.2.6.1 Oxidation

OxLDL was prepared as previously described [171] by incubating native LDL at a concentration of 1mg/ml (diluted with PBS) with 20μM copper sulphate ($1/1000^{th}$ volume of 20mM solution) for 20 hours at 37°C. Transferring the reaction to 4°C was used to stop the oxidation reaction.

2.2.6.2 Acetylation

AcLDL was prepared as previously described [172] by adding 1ml of a saturated solution of sodium acetate per ml of native LDL (irrespective of LDL concentration) in a glass beaker and stirring for 10 minutes. Acetic anhydride was then added at a volume in micro litres equal to 1.5 times the total protein concentration of LDL (in mg/ml), in small aliquots over a one-hour period with continuous stirring at 4°C. After a further 30 minutes of stirring the AcLDL was dialysed overnight against PBS to remove the sodium acetate.

Finally both Ox LDL and AcLDL were filter sterilised in a flow hood using 0.2μm filters and stored at 4°C until required. All preparations of LDL were used within two weeks of preparation.

2.2.7 Agarose gel electrophoresis of LDL

Relative electrophoretic mobility on Beckman Paragon LIPO™ gels was used to check modification of LDL.

The gel was prepared as per manufacturer's instructions; 5μl of each LDL sample was applied to the gel slots and allowed to diffuse for 5-10 minutes. The gel

was placed in an electrophoresis cell containing 30ml barbital buffer (see section 2.6) and electrophoresis performed for 30 minutes at 100 volts in a Beckman Paragon Electrophoresis kit (kindly loaned from Glaxo Wellcome). After the electrophoresis the gel was placed in fixative solution (see section 2.6) for 5 minutes and dried using a hair dryer. The gel was then stained with lipoprotein stain (Sudan black B stain 0.07% v/v; in deionised water) for 5 minutes before being placed in a destain solution (see section 2.6) for at least 5 minutes. The gel was finally washed well in de-ionised water before being dried with a hair dryer.

2.3. General Molecular Biology

2.3.1 DNA extraction

DNA was extracted from blood using the method reported by Kunkel *et al* [173].

2.3.1.1Extraction of DNA from human blood

Blood was collected in tubes containing 50mM EDTA to prevent coagulation. Blood was centrifuged at 2800rpm to separate the blood cells and the plasma. The plasma layer was removed using a sterile pasteur pipette.

Blood cells (4ml from 10ml of blood) were mixed with 80ml of lysis buffer (see section 2.6). This mixture was centrifuged at 10,500g for 10 min at 4°C using Beckman centrifuge J2-HC and rotor JA-20 to pellet the nuclei. The pellet was resuspended in 4.5ml of resuspension buffer (see section 2.6), 250µl of 10% SDS and 250µl of proteinase K (2mg/ml) and incubated overnight (18 hours) at 37°C.

After incubation, 5ml of phenol was added. The tube was mixed by inversion and the mixture was centrifuged at 3000rpm for 5 mins. This separated the mixture into two phases. The upper phase was transferred to clean tube using a bent pasteur pipette. Chloroform: isoamylalchohol (24:1; 5ml) was added to the upper phase and the tube mixed by inversion. The mixture was centrifuged at 3000rpm for 5 mins. The upper phase was again removed and the chloroform/isoamylalcohol extraction step was repeated. The upper phase was finally transferred to a fresh tube.

Pure ethanol (99%; 11mls) and 0.5ml of 3M sodium acetate solution (pH 7) were added to the upper phase and the mixture mixed gently by inversion several times. At this stage the DNA can be visualised and was hooked out using a sealed pasteur pipette and placed in a 1.5ml eppendorf tube. Excess ethanol was removed from the DNA by briefly centrifuging and removing the ethanol with an automatic pipette. The DNA was dissolved in 500µl TE buffer (see section 2.6). Dissolving was aided by aspirating the solution gently with a sterile pipette tip. DNA, once dissolved, was stored at -20°C. Typical yield obtained was about 200-500ng of DNA per 10ml of blood.

2.3.1.2 Quantitative estimation of DNA

The optical density of a 1 in 50 dilution of DNA was measured at 260nm and 280nm. The reading at 260nm is a measure of the amount of DNA present while the reading at 280nm is a measure of any protein that may be present. An optical density of 1 at 260nm corresponds to 50µg/ml of double stranded DNA. The ratio between the optical density at 260nm and 280nm gives an estimate of the purity of the DNA. A ratio of 1.8 was used as an indicator of a relatively pure preparation of DNA.

2.3.2 RNA extraction

2.3.2.1 Isolation of white blood cells from human blood

Blood was collected in tubes containing 50mM EDTA. Histopaque (4.5ml; Pharmacia, Little Chalfont) was added to a 15ml tube and overlaid with 6ml of blood. The tubes were centrifuged for 30 mins at 1500rpm. The plasma layer was aspirated to just above the cell layer using a sterile pasteur pipette. A 5ml sterile pipette was used to remove the white blood cell band to a fresh tube. The volume of the cell band was made up to 13.5ml with PBS. The tube was then centrifuged for 10 mins at 1900rpm to pellet the cells. After centrifugation the supernatant was removed leaving the white blood cell pellet.

2.3.2.2 Isolation of total RNA using TRIzol reagent

Cells isolated as described above in section 2.3.2.1, pelleted THP-1 cells or differentiated THP-1 cells grown in six well plates were lysed in 1ml TRIzol reagent (GibcoBRL, Paisley) by repetitive pipetting (TRIzol is a ready to use reagent for the isolation of total RNA from cells and tissues based on the method of Chomcyzynski and Sacchi [174]). Samples were processed according to the manufacturer's instructions. After the addition of TRIzol, samples were incubated at room temperature for 5 minutes to allow complete dissociation of nucleoprotein complexes. After 5 minutes, 200µl of chloroform were added to the tubes. The tubes were shaken vigorously by inversion and allowed to stand at room temperature for a further 2-3 minutes. Samples were then centrifuged at 12000g for 15minutes at 4°C (Beckman Avanti 30 using rotor F2402).

After centrifugation the mixture separated into a lower red phenol-chloroform phase, an interphase and a colourless upper aqueous phase. RNA remained in the upper aqueous phase. The aqueous phase was transferred to a fresh tube, 0.5ml of isopropanol were added and the sample was incubated at room temperature. After 10 minutes the samples were centrifuged at 12000 g for 10 mins at 4°C. After centrifugation the supernatant was carefully removed to avoid disturbing the RNA pellet.

The RNA pellet was washed by adding 1ml of 75% ethanol, vortexing and centrifuging at 7500g for 5 minutes at 4°C. The ethanol was removed and the RNA pellet was allowed to dry at room temperature for 15 minutes. The RNA was dissolved in 10µl of RNase-free water (Ambion, Texas, USA).

2.3.3 Reverse transcription of total RNA

RNA was transcribed into cDNA as previously described [175]. Total RNA (5µg) was made up to 11µl with DEPC treated water in a 200µl plastic thin-walled PCR tube (Scotlab). Oligo dT primer 1µl (0.5µg/µl; GibcoBRL, Paisley) was added to the samples and the samples were heated at 70°C for 10 minutes. The samples were then chilled on ice and centrifuged briefly.

For cDNA synthesis, a master mix containing all the components required was prepared and subsequently aliquoted. The master mix contained the following

components per sample; 4µl of first strand cDNA buffer (supplied with reverse transcriptase enzyme), 1µl dNTPs (10mM), 2µl DTT (0.1mM) and 1µl of MMLV reverse transcriptase (200units/µl) [all GibcoBRL, Paisley]. After the addition of components required for cDNA synthesis, samples were incubated at room temperature for 10 minutes. The samples were then incubated at 42°C for 50 minutes followed by 90°C for 10 minutes in a thermal cycler (MJ2; Roche, Lewis). After heating, samples were placed on ice for 10 minutes and centrifuged briefly in a bench top micro centrifuge. Finally 1µl of RNase H (200U/µl; GibcoBRL, Paisley) was added to the samples and the samples were incubated at 37°C for 20 minutes.

Each time the reverse transcription reaction was performed two control samples were included to check for contamination. Control 1 contained RNA but no reverse transcriptase enzyme. Control 2 contained all reverse transcription components but no RNA template. All steps were carried out using procedures that minimised risk of RNase contamination.

2.3.4 PCR

2.3.4.1 Polymerase chain reaction

PCR was performed using the protocols of Innis *et al* [176]. For each PCR reaction 1µl of DNA (50ng) was dispensed into 0.2ml thin walled PCR tubes. To minimise pipetting errors a master mix was prepared and subsequently aliquoted. When *n* number of samples was being prepared, a master mix for *n*+1 samples was prepared. The master mix contained the following components per sample; 1µl of 10x Taq polymerase buffer, 0.5µl forward oligonucleotide (5pmol/µl), 0.5µl reverse oligonucleotide (5pmol/µl), 1ul of dNTP's (10mM), 5.9µl of sterile filtered water, 0.1µl of Taq polymerase (5U/µl) [Boehringer Mannheim; Lewis]. Master mix (10µl) was dispensed into each tube and the samples were overlaid with 10µl silicon oil (Sigma, Dorset). The samples were briefly vortexed, centrifuged briefly in a bench top micro centrifuge and placed in PCR machine (MJ2; Roche, Lewis). The PCR primers being used determined the PCR programme subsequently used to run the samples.

2.3.4.2 PCR primer sequences

Table 2.1 shows primer sequences used to amplify genes of interest. The forward primer sequence anneals to the DNA in the 5'-3'direction whereas the reverse primer anneals to DNA in the 3'-5' direction. The internal standard primer was used to generate a DNA fragment that was shorter in length than the fragment produced by the original forward and reverse primers, but had the same primer binding sites [177]. In addition the base pairs at the beginning of the internal primer sequence were designed to be identical to the base pairs at the end of the forward primer sequence. All primer sequences were designed from published sequences obtained from the Genbank database (at the internet site http://www.ncbi.nlm.nih.gov/Genbank). Oligonucleotide primers were synthesized by MWG Biotech, Germany or PE-Applied Biosystems, UK.

Table 2.1

Table showing sequences of oligonucleotides used to amplify genes of interest.

Gene	*Sequence of forward primer*	*Sequence of reverse primer*	*Sequence of internal standard primer*	*Genbank accession number*
CETP	5'-CAC TAG CCC AGA GAG AGG AGT GCC-3'	5'-CTG AGC CCA GCC GCA CAC TAA C- 3'	-	From reference [178]
HPRT	5'-CCT GCT GGA TTA CAT CAA AGC ACT G-3'	5'-GTC AAG GGC ATA TCC TAC AAC AAA C-3'	5'-CAA AGC ACT GAT CAG ACT GAA GAG CTA GTG-3'	M31642
ACAT	5'-CAC CTA GTA ATG GTC GAA TTG ACA-3'	5'- GTA GAC AGG AAC ATG ATC CAC CAG-3'	5'- GAA TTG ACA TAA GTT GGC AGT CAC T-3'	L21934
IL-8	5'- GGA AGG AAC CAT CTC ACT GTG TGT A -3'	5'- AGT GTC CAC TCT CAA TCA CTC T- 3'	5'- ACT GTG TGT ACC TGA TTT CTG CAG C- 3'	D14283
β-actin	5'- TGT GAT GGT GGG AAT GGG TCA G-3'	5'- TTT GAT GTC ACG CAC GAT TTC C –3'	5'- TGT GAT GGT GGG AAT GGG TCA GGC CAA CCG CGA GAA GAT GAC CCA G-3	M31642
LpL	5'-ACA CAG CTG AGG ACA CTT GC-3'	5'- CAC TGG GTA ATG CTC CTG AG-3'	5'- GGA CAC TTG CTG GTG ATC CAT GGC T-3'	M15856

2.3.4.3 PCR product sizes

Table 2.2 shows the sizes of the products obtained after PCR and the names of the programs used for PCR. For those genes where an internal standard was prepared, the size of the internal standard and intermediate product obtained on preparing the internal standards are also given.

Table 2.2

Table showing product sizes in base pairs (bp) obtained after PCR for genes of interest and the name of the PCR programme used for their amplification

Gene	*Product size (bp) forward and reverse primers*	*Internal standard product size (bp)*	*Product size – internal standard/reverse primer (bp)*	*PCR programme*
CETP	535	-	-	B60
HPRT	351	294	314	T65
ACAT	475	392	407	T65
IL-8	210	154	169	T65
β-actin	511	318	318	B60
LpL	227	150	165	B60

2.3.4.4 PCR programs

Table 2.3 below shows the two PCR programs used for the amplification of genes of interest.

Table 2.3

Table showing the steps involved in the PCR programs used, with temperature in degrees Celsius and time in seconds

PCR programme	*Step Number*	*Temperature (^{o}C)*	*Time (sec)*
B60	1	94	15
	2	60	15
	3	72	30
	4	Go to step 1, twenty-nine more times	
T65	1	94	15
	2	70	10
	3	72	10
	4	Go to step 1, five more times	
	5	94	15
	6	65	10
	7	72	10
	8	Go to step 5, five more time	
	9	94	15
	10	60	10
	11	72	10
	12	Go to step 9, five more times	
	13	94	15
	14	65	10
	15	72	10
	16	Go to step 13, twenty-five more times	

2.3.5 Agarose gel electrophoresis of PCR products

A 1% agarose gel was prepared by dissolving 1g of agarose in 100ml of 1x TBE buffer (see section 2.6). The mixture was heated to boiling and subsequently cooled. Ethidium bromide (10µl of a 10mg/ml solution) was added to the gel solution before the gel was cast to set (gel size; 14cm x 11cm).

Loading buffer (10x; see section 2.6), 2µl was added to each 10µl PCR product and 5µl of each sample was subsequently loaded per lane of the gel. A marker 100 base pair ladder, (0.5ug; GibcoBRL, Paisley) was also loaded onto the gel to check the size of the PCR products. Electrophoresis was performed in 1x TBE buffer at 100 volts for 60 minutes. Gels were visualised using a UV trans-illuminator and photographed (Polaroid type 667; size 3¼ x 4¼).

2.3.6 Purification of DNA from agarose gels

DNA was isolated from agarose gels using the Wizard PCR Preps DNA Purification Kit (Promega Corporation) according to the manufacturer's instructions.

The PCR reaction products were separated in a 1x TAE agarose gel (low melting point agarose; Sigma, Dorset) containing ethidium bromide and visualised by UV trans-illuminator. The band of interest was isolated from the gel using a sterile razor blade. The exercised band was transferred to a 1.5ml micro centrifuge tube and incubated at 70°C with 1ml of DNA purification resin (supplied with the kit) until the gel had completely melted.

For each PCR product, one Wizard mini-column (a column containing a filter to bind the DNA) was used. A disposable syringe (with the plunger removed) was attached to each mini-column (at the opening where the needle is attached).

The DNA/resin mixture was pipetted into the syringe and pushed through the attached mini-column gently using the syringe plunger. The syringe was detached from the mini-column and the plunger removed. The syringe was reattached to the column and 2ml of 80% isopropanol were pipetted into the syringe and pushed through the column (using the plunger) so as to wash the column. The syringe was then removed and the minicolumn was transferred to a 1.5ml eppendorf tube. The mini-column was centrifuged in a bench top centrifuge for 2 minutes at 10,000g to dry the resin.

The mini-column was transferred to a fresh tube and TE buffer (50µl; see section 2.6) was added. The column was then left for two minutes and subsequently centrifuged for 20 seconds at 10,000g to elute the bound DNA fragment.

2.3.7 Quantitative RT-PCR

2.3.7.1 Oligonucleotide end labelling using gamma ^{32}P- ATP

For each oligonucleotide, 41µl water, 1.5µl of oligonucleotide to be labelled (5pmol/µl), 1ul of T4 polynucleotide kinase (GibcoBRL), 5µl "phosphorus all in one buffer"(supplied with the enzyme) and 1µl gamma-^{32}P ATP (10µCi/µl) were combined together. The mixture was incubated at 37°C for 30 minutes in a heating block. Incorporation was checked by paper chromatography. A small amount of each sample (1µl) was spotted onto 3MM paper (Whatman). The filter paper was placed vertically in a large beaker containing 100ml 0.25M ammonium formate for about 30 mins or until the solution front had travelled three quarters up the filter paper. The filter paper was allowed to air dry and subsequently covered with Saran™ wrap (cling film). The film was then exposed to film (Kodak X-OMAT; 35 x 43 cm) for 2 hours before the film was developed using a film developer (X-ograph Imaging Systems: - Compact X4).

The amount of radioactivity incorporated into the forward or reverse primer for any gene was visually compared by eye and the primer showing the most radioactive incorporation was identified. Subsequently for each PCR reaction, in addition to the normal volumes of both oligonucleotides, 0.5µl of this ^{32}P-labelled oligonucleotide was also added as a tracer to each PCR reaction.

2.3.7.2 Denaturing gel electrophoresis

For denaturing gel electrophoresis an acrylamide/urea gel was prepared by combining 42g urea, 10ml 10x TBE buffer (see section 2.6), 15ml 40% acrylamide (acrylamide: bisacrylamide; 40:1) and 37ml of water. The mixture was stirred until all the urea had dissolved. At this stage 100µl TEMED and 1ml 5% ammonium persulphate were added to allow polymerisation.

Gel glass plates were prepared by washing the glass plates with ethanol (70%) and deionised water. One of the plates (back plate) was coated with Sigmacote™ (water repellent; Sigma, Dorset) on the side that was going to be exposed to the gel and the plates were allowed to dry. Spacers (1.5 cm width) were placed between the two plates and the plates were sealed tightly using electrical tape (BDH, Dorset). The gel solution was cast into the plates in a slanted vertical position avoiding the introduction of air bubbles. A 32-tooth comb was placed in the top, and the plates and comb were clipped together using bulldog clips. The gel was subsequently allowed to set for at least an hour in a horizontal position. After the gel had set, the comb was removed and the wells were washed with TBE buffer to remove any unpolymerised acrylamide. The tape from the bottom edge of the gel plates was removed.

Radioactive PCR samples were prepared for loading onto the gel by the addition of 2µl of formamide dye (see section 2.6) to each sample. Samples (10µl) were subsequently loaded onto the gel. Electrophoresis was performed in a vertical electrophoresis gel tank (Gibco-BRL) containing TBE buffer for 2.5 hours at 1000 volts.

After electrophoresis the electrical tape and spacers were removed from the gel plates and the plates were carefully forced apart. The gel was found to stick to one of the glass plates as the other had been coated with Sigmacote™. A sheet of 3MM chromatography paper was placed on top of the gel and subsequently lifted slowly from one corner. This transferred the gel onto the chromatography paper. The gel was covered with Saran™ wrap and dried using a gel dryer [BioRad slab dryer model 483] at 80°C for one hour. The gel was then exposed to film (Kodak X-OMAT; 35 x 43 cm) overnight before the film was developed using a film developer (X-ograph Imaging Systems: - Compact X4)

For quantitation of radioactive PCR products, the dried gel was placed next to a 20cm x 25cm phosphor beta-imaging screen (BioRad, Hemel Hempstead) for one hour. The screen was scanned using a Molecular Imager (BioRad model GS-525) and the data captured and analysed using Molecular Analyst software (BioRad, version 2.1) according to the manufacturer's instructions.

2.4 Differential gene expression

2.4.1. Isolation of RNA for differential gene expression

For gene expression studies, cells were cultured in large numbers ($7x10^7$ cells) so as to provide a greater yield of RNA. Cells were differentiated in $175cm^2$ flasks (Falcon) rather than 6 well plates. RNA was isolated in two steps. Firstly total RNA was isolated from the cells and then messenger RNA was subsequently isolated from the total RNA. All steps were carried out using procedures that minimised risk of RNase contamination.

2.4.1.1 Isolation of total RNA

Total RNA was isolated using an RNeasy Midikit (Qiagen, Crawley) according to the manufacturer's instructions.

Cells were washed twice in PBS after exposure to lipoprotein. Cells were lysed by addition of 3.8ml of RLT buffer (supplied with kit) containing 38µl β-mercaptoethanol directly to the culture flask. Cells were collected using a cell scraper and the lysate was transferred to a sterile RNase free polypropylene tube. The lysate was vortexed for 10 seconds before being passed through a 10ml syringe and needle (21 gauge) between 5-10 times to homogenise the lysate. Then 3.8ml of 70% ethanol were added to the lysate and the mixture vortexed briefly.

The vortexed sample was applied in maximum volumes of 3.8ml to an RNeasy midi spin column (a column containing a filter to bind the RNA) placed in a 15ml centrifuge tube. The tube was centrifuged (Sigma 3-15) for 5 minutes at 5000rpm and the flow through was discarded. This was repeated until the entire sample had been applied to the column. A buffer RW1 (3.8mls; supplied with kit) was then applied to the column and the column was centrifuged for 5 minutes at 5000rpm, with the flow through being discarded.

To wash the bound RNA, 2.5ml of buffer RPE (supplied with kit) was added to the column and the column was centrifuged for 2 minutes at 5000rpm. This was followed with a further 2.5ml of buffer RPE and centrifugation at 5000rpm for 5 minutes. The RNA was eluted by adding 250µl of RNase free water to the spin

column membrane, allowing the column to stand for 1 minute before centrifugation for 3 minutes at 5000g. The elution step was repeated so as to maximise the yield of RNA.

2.4.1.2 Isolation of messenger RNA

Messenger RNA was subsequently isolated from the total RNA using an mRNA Midikit (Qiagen, Crawley) according to the manufacturer's instructions. Total mRNA (500µl) was mixed with 500µl of 2x binding buffer and 55µl oligotex suspension in a sterile eppendorf tube. The tube was initially incubated at 65°C for 5 minutes to allow disruption of RNA secondary structure and then left at room temperature for at least 10 minutes to allow annealing of the oligo dT to the polyA tail of the mRNA.

The tube was centrifuged for 2 minutes at 14000g in bench-top micro centrifuge to pellet the oligotex resin containing the mRNA. The supernatant was carefully removed by pipetting and the pellet was resuspended in 400µl of wash buffer by vortexing. This was applied to a spin column (a column containing a filter to capture the oligo dT resin bound to the mRNA) sitting in an eppendorf tube and the tube was centrifuged at 14000g for 30 seconds in a bench top micro centrifuge. The spin column was transferred to a fresh tube and 400µl wash buffer was applied to the column, followed by centrifugation for 30 seconds at 14000g.

To elute the bound mRNA, the spin column (containing the mRNA) was transferred to a fresh tube. Elution buffer (75µl), preheated to 70°C was applied to the column. The elution buffer was pipetted up and down several times using an automatic pipette to allow resuspension of the resin. The tube was then centrifuged for 30 seconds at 14000g. The elution step was repeated with a further 75µl of elution buffer. The isolated mRNA was stored in elution buffer at -70°C after the addition of 1µl of RNasin (40U/µl; Boehringer Mannheim, Lewis).

To precipitate the RNA in a small volume, RNA in elution buffer was mixed with 2.5 volumes of 100% ethanol, 2µl glycogen (20mg/ml; Boehringer Mannheim, Lewis) and 0.1 volumes of 3M sodium acetate. This mixture was stored overnight at -20°C, before being centrifuged for 15 minutes at 13000g. After centrifugation the supernatant was removed and the pellet was re-suspended in 500µl of 75% ethanol. This was followed by centrifugation at 13000g for 15 minutes to wash the pellet. The

RNA pellet was subsequently dried at room temperature for 10-15 minutes before being re-suspended in 9µl of DEPC treated water and 1µl RNasin (40U/µl).

2.4.1.3 Quantitation of RNA

The concentration and purity of RNA was determined by measuring absorbance of RNA in a spectrophotometer at 260nm and 280nm. Cuvettes (100µl) were washed with a solution of 0.1M NaOH/1mM EDTA followed by RNase free water to ensure that they were RNase free. The RNA was diluted 1 in 20 and the absorbance readings at 260nm and 280nm were read in a spectrophotometer (Unicam UV/VIS). The RNA concentration was calculated using the relationship that an absorbance of 1 at 260nm corresponds to 40µg of RNA per ml. The ratio between the absorbance readings at 260nm and 280nm indicated the purity of the RNA. A ratio of 1.8 or above was used as an indication of a relatively pure preparation of RNA.

2.4.1.4 Determining RNA integrity

RNA integrity can be determined by examining ribosomal RNA bands (18S and 28S) present in the RNA samples. For both total RNA and mRNA, two types of gels were prepared either an agarose/formaldehyde gel or a glyoxal gel. Initially agarose/formaldehyde gels were used however glyoxal gels were subsequently used since they represent a more advanced detection method in terms of sensitivity.

2.4.1.4.1 Agarose /formaldehyde gel electrophoresis of RNA

A 1% agarose gel was prepared by combining the following, 20ml 5x MOPS buffer (see section 2.6), 62.1ml DEPC-treated water and 1g of agarose (Sigma, Dorset). The mixture was heated until boiling to dissolve the agarose and subsequently cooled to 55°C. This was followed by the addition of 17.9ml of 37% formaldehyde, mixing the solution and casting the gel (gel size; 14cm x 11cm).

RNA samples were prepared by adding one part RNA to two parts RNA sample buffer (see section 2.6) up to a volume of 10µl. The samples were heated to 65°C for 5 minutes and cooled to room temperature. This was followed by the addition of 2µl of RNA loading buffer and 1µl of ethidium bromide (10mg/ml).

Before loading the samples on the gel, the gel was pre-run at 100 volts for 10 minutes in 1x MOPS buffer (see section 2.6). The gel was run at 100 volts for 90 minutes or until the bromophenol blue had migrated at least 10cm from the wells. The gel was visualised using a UV trans-illuminator and photographed (Polaroid type 667; size 3¼ x 4¼).

2.4.1.4.2 Glyoxal gel electrophoresis of RNA

A 1% agarose/MOPS gel was prepared by dissolving 1g agarose in 100ml of 1x MOPS buffer, heating until boiling and pouring the gel. RNA samples were prepared by combining 0.5µl of RNA (0.06µg) with 8.5µl of RNase free water and 9µl of a Glyoxal/DMSO mixture (1.5ml Glyoxal / 2.5ml DMSO). The samples were then heated at 50°C for 60 minutes and chilled on ice for one minute. This was followed by the addition of 5µl of gel loading buffer (Sigma, Dorset) before the samples were loaded onto the gel. Electrophoresis was performed for 45 minutes at 90 volts in 1x MOPS buffer.

After electrophoresis the gel was stained in 1 x MOPS buffer with a 1:10000 dilution SYBR gold stain (Sigma, Dorset) for 30 minutes with continuous shaking. The RNA was then detected using a Fluorimager (Molecular Dynamics) and the image file generated was saved.

In both cases 18S and 28S RNA markers (Sigma, Dorset) were also loaded onto the gel. The integrity of the samples was confirmed by the presence of 18S and 28S ribosomal RNA bands.

2.4.2 Preparation of high-density cDNA arrays

High-density cDNA arrays were prepared by the DGE group, Department of Genetics at Glaxo Wellcome Medicines Research Centre (Stevenage). Briefly complementary DNA (cDNA) libraries were robotically picked from 96-well format into 384-well format using a picker/gridder (Genetix, UK). PCR was performed on the library cDNA cloned inserts using a high-throughput custom-built PCR robot. PCR conditions were 95°C for one minute followed by 29 cycles of 94°C for 30

seconds, 50°C for 2 minutes and 72°C for 2 minutes and a final incubation at 72°C for 5 minutes.

PCR products were subsequently gridded in duplicate onto 20cm x 30cm positively charged nylon membranes (Boehringer Mannheim, Lewis) using a picker/gridder (Genetix, UK). The libraries used in this study were the human re-arrayed I.M.A.G.E (Integrated Molecular Analysis of Genomes and their Expression) library, and a custom atheroma library (prepared by the DGE group in collaboration with the Vascular Diseases Unit at Glaxo Wellcome). In addition luciferase cDNA and control genes were also gridded onto the arrays at set positions to be used in subsequent analysis. Gridded arrays were cut to size approximately 22.5cm by 16cm (so that they would fit into Techne Hybridisation bottles). Each grid was subsequently labelled (by pencil) with a unique experiment number and marked with a upward pointing arrow on the top left hand side of the grid (near to position 1,1 of gridding) to designate orientation

2.4.3 Quantitation of PCR products on arrays

To measure the amount of DNA per spot on the arrays, the arrays were annealed with a ^{33}P -end labelled oligonucleotide. This end labelled oligonucleotide was designed to specifically anneal to all the spotted PCR products by virtue of complementarity to the plasmid vector polylinker sequence. For the both the re-arrayed human I.M.A.G.E library and the custom atheroma, an oligonucleotide named M13F was used.

M13F sequence 5' ACG TTG TAA AAC GAC GGC CAG 3'

2.4.3.1 5' radiolabelling of M13F oligonucleotide

To prepare the DNA loading oligonucleotide probe (M13F), the following were combined together: 5µl 10x polynucleotide kinase buffer (supplied with the enzyme), 1µl DNA oligonucleotide M13F (20pmol/µl), 5µl Redivue gamma ^{33}P-dATP (10µCi/µl), 2µl polynucleotide kinase (New England Biosciences) and 37µl of deionised water. The reaction mixture was incubated at 37°C for one hour in a water bath.

After one hour the probe was purified using a sephadex G25 spin column (Pharmacia, Little Chalfont). Total number of cpm were assessed before and after purification of the probe using a bench top counter (Bioscan QC-4000, Bioscan, Washington, USA) and the percentage incorporation calculated. Only probes showing percentage incorporation in the expected range of 20-50 % were used.

2.4.3.2 Hybridisation of radiolabelled M13F oligonucleotide probe to arrays.

Arrays were placed in a shallow tray containing a small volume (10ml) of Digoxigenin Easy Hybridisation Buffer (DIG Easy Hyb; Boehringer Mannheim, Lewis). DIG Easy Hyb is a ready-to-use buffer for nucleic acid blot hybridisation. When more than one array was being used, a mesh was placed between the arrays and any resulting air bubbles were expelled. The sandwich of arrays and meshes (up to maximum of four arrays) were transferred to a Techne hybridisation bottle containing 10ml of DIG Easy Hyb buffer and allowed to pre-hybridise in a Techne oven pre-set to 45°C for at least 30 minutes.

After 30 minutes the pre-hybridisation solution in the Techne bottle was discarded and replaced with 10 ml of DIG Easy Hyb buffer pre-heated to 45°C. The labelled probe (M13F) was then added and hybridisation was performed overnight in a Techne oven at 45°C.

After overnight hybridisation, the hybridisation solution was discarded and the arrays were washed three times with a wash solution (preheated to 45°C; see section 2.5) for 15 minutes per wash. Arrays were removed from the Techne bottle and mounted in a cassette between a layer of thin plastic sheeting and Saran™ wrap. The arrays were subsequently placed next to a phosphorimaging screen (Molecular Dynamics) for two days. The data from the screen was captured using a Storm Scanner (Molecular Dynamics).

2.4.4 Complex probe preparation from mRNA

Messenger RNA isolated from experimental samples as described in section 2.4.1 was transcribed into radiolabelled 1st strand cDNA probes.

For first strand cDNA synthesis 1µl dVN (T) $_{15}$ (1.44g/ml; GibcoBRL) was added to 5µl RNA (containing 10µg total RNA or 2µg mRNA) and heated at 70°C for

10 minutes. This was followed by addition of 4µl of 5x Superscript reaction buffer, 2µl 0.1M DTT, 1µl dNTP mix [1mM dATP, dGTP, dTTP, 0.01mM dCTP), 1µl of RNasin [40U/µl] and 4µl of α^{33}P dCTP (10µCi/µl) and 2µl of Superscript II enzyme [200U/µl] (GibcoBRL, Paisley). This mixture was incubated at 42°C for 90 minutes.

After the incubation, 30µl of distilled water was added to the reaction mixture. Total cpm were assessed before purification using a bench top counter (Bioscan QC-4000, Bioscan, Washington, USA). The probe was then purified using a sephadex G50 column (Pharmacia, Little Chalfont). Total cpm were recounted after purification and percentage incorporation calculated. Only probes showing incorporation greater than 40% were subsequently used (the higher the percentage incorporation the better the probe).

2.4.5 Complex probe quality control

The length of each probe was determined by gel electrophoresis and comparing against a set of markers of known size (in the range of 500bp-1.5kb). Up to five labelled marker PCR product markers of size 500bp, 800bp, 900bp, 1.3kb and 1.5Kb were used (prepared by the DGE group in the same way as the M13F oligonucleotide probe as described in section 2.4.3.1).

Gel loading buffer II (2µl; Ambion, Texas, USA) was added to prepared cDNA probes (2µl/0.08µg mRNA) and to each standard (2µl). The samples were heated at 100°C for 5 minutes, allowed to cool and subsequently loaded onto a pre-prepared 6% polyacrylamide: TBE gel (Novex). Electrophoresis was performed at 120 volts for 90 minutes. The gel was removed from the plates, placed in an imaging cassette (with a thin plastic sheet backing). The gel was covered with Saran™ wrap and exposed to a phosphorimaging screen overnight. The image of the gel was subsequently captured using a Storm Scanner and the size of the probes in relation to the size of the markers was examined. Only probes whose length profile was between 500bp and 2kb were subsequently used for hybridisation experiments.

2.4.6 Hybridisation of complex probes to arrays

Pre-hybridisation of filters was carried out as for DNA loading as described in section 2.4.3.2. The complex probes (prepared as described in section 2.4.4) were prepared for hybridisation by combining the complex probe with 5µl poly (A) $_{80}$ (GibcoBRL, Paisley), 1µl Human COT-1 DNA (GibcoBRL, Paisley) and 435µl Dig Easy Hyb. [COT-1 DNA and poly (A) $_{80}$ were used to bind to alu sequences and T-repeat sequences respectively that are present and may interfere with hybridisation]. Radiolabelled luciferase probe (5µl) was also added to each experimental probe prepared (the luciferase probe was prepared as per complex probes described in section 2.4.4 using 2µg luciferase mRNA).

This complex probe mixture was heated at 100°C for 10 minutes followed by incubation at 45°C for 90 minutes and then added to 10ml of DIG Easy Hyb pre-equilibrated to 45°C. The DIG Easy Hyb containing the probe was subsequently added to the Techne bottle containing the pre-hybridised arrays. Hybridisation was performed in a Techne oven at 45°C for three days.

After three days, the arrays were washed three times for 15 minutes in wash solution (50ml; see section 2.5) preheated to 68°C. Arrays were then mounted in cassette (between a layer of thin plastic sheeting and Saran™ wrap) and exposed to a phosphorimaging screen for two days. The image data from the screens was then captured using a Storm Scanner (Phosphorimager).

2.4.7 Data Analysis

2.4.7.1. DGE data analysis

A more detailed account of how data analysis was performed is given in Chapter 4. The image data collected using the Storm Scanner (from section 2.4.3.2 and section 2.4.6) was subsequently processed using a software package called DGENT (developed by the DGE group, Glaxo Wellcome, Stevenage).

Briefly, two images were obtained for each filter. A DNA loading image obtained after hybridisation with M13F oligonucleotide (to assess for the amount of DNA present on the grid) and a probe hybridisation image obtained after hybridisation with the experimental probe. Images were firstly cropped to keep the

size of the image to a minimum (reduces the file size) and were labelled using the date of the experiment and the name of experimental probe.

These images were subsequently processed using DGENT. (The positions at which PCR products are arrayed are referred here to as spots, due the fact that they show up as spots on the images). The position of the corner spots and luciferase marker spots of an image was marked using the software. The software then detected the position of the remaining spots using the luciferase marker spots. In addition the position of the control spots were also marked. Once spots had been detected the software was used to find the intensity of the actual spot hybridisation.

To perform a comparison experiment the image data for the hybridisations to be compared were opened (both the DNA loading data and the experimental hybridisation data for two different experiments, four sets of data). The DNA loading data was associated with the relevant experimental hybridisation data to take into account any discrepancies in DNA loading (automatically done by the DGENT software). The expression level on each array was corrected using the expression levels of the control genes on the array. The comparison was designated a comparison identification number and the two images were compared using the DGENT software and the differences listed.

Each difference was inspected by eye to omit any false positives. Real differences were sent to the DGE database (a database containing all the gridding data). The position of spot on the array was used as a means to identify the gridded cDNA sequence from the database.

2.4.7.2 Temporal gene expression data analysis

The data generated from the temporal gene expression experiments was coloured using the tools function of Microsoft Excel. Under the tools menu, add-in was selected and the Excel data analysis tool-pack was loaded. Firstly the data was analysed using the histogram tool to get a feel for sensible minimum and maximum values for the data. These values were then used to colour the data accordingly. Colour differentiation was selected under the tools menu of Excel; this brings up the colour differentiation wizard. The minimum and maximum values of the data were entered so that at least 95% of the data was represented (these values were determined

using the Histogram tool), then sharp colour was chosen to colour the data (other options were grey and colour).

2.5 Hierarchical Clustering

2.5.1 Steps involved in correlating gene expression data and performing hierarchical clustering.

The initial gene expression data correlation in this study was performed by Dr Steve Blakemore, DGE group, Glaxo Wellcome. Figure 2.1 shows the steps in correlating gene expression data, applying hierarchical clustering and analysing the results.

Figure 2.1. Steps involved in correlating gene expression data and performing hierarchical clustering

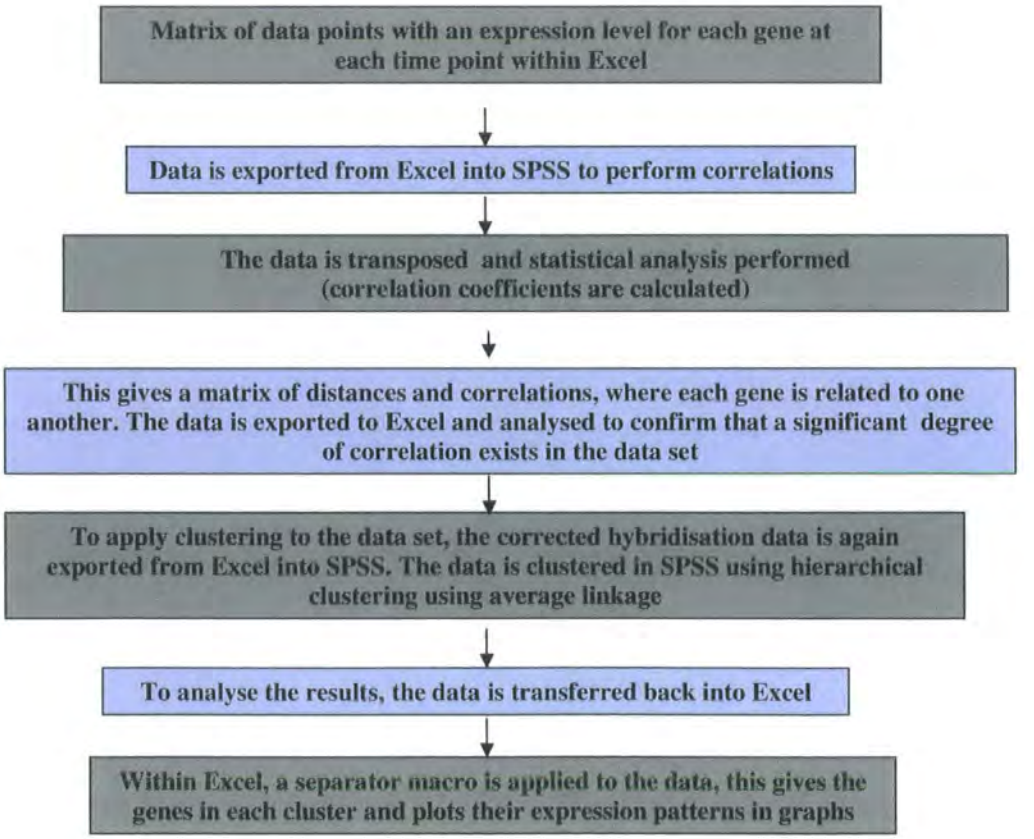

The first step in the procedure involved transferring the corrected data of expression levels (table 6.1) from Microsoft Excel into SPSS version 8.0. Next, the data was transposed so that column heading were gene names and rows were time points (this is because SPSS will only derive gene correlations if the gene names are column headings). Then from the statistics pull down menu, correlate, distances was selected. The distances were then calculated by SPSS and displayed in SPSS viewer as a correlation matrix, where each of the genes is related to one another by a similarity distance. The correlations were then calculated by SPSS and the results were displayed as correlation matrix where each gene was related to one another by a correlation coefficient.

The correlation steps were performed so as to demonstrate that the number of positive correlations observed in the data set were greater than would expected by chance alone. It would be useless to apply hierarchical cluster analysis (HCA) to a data set in which there was no significant degree of correlation especially since clustering algorithms can generate clusters even when applied to random data.

2.5.2 Cluster analysis

The cluster analysis on the temporal gene expression data set was again performed in SPSS. The corrected raw hybridisation intensity data was imported from Excel into SPSS. Under the statistics pull down menu, classify was selected followed by hierarchical clustering. This brings up the HCA processing window. Time points were then selected as the variables to cluster. Clicking on statistics brings up the statistics window from which agglomerative schedule was selected (agglomeration schedule displays the clusters joined at each stage, the distances between the clusters and the last cluster level at which a variable joined the cluster; it starts with the two most related samples and links them forming an initial cluster, the process is then repeated until all the samples have been linked).

Clicking the methods button on the hierarchical cluster analysis window brings up the methods window, from which between-groups linkage was used followed by Pearson correlation. This means that the procedure will operate an average cluster linkage clustering using a correlation matrix based on the appropriate correlation formula. Finally the data needs to be visualised graphically so the plot button from the hierarchical cluster analysis window was selected and dendogram was

selected. This completed setting the parameters involved in the clustering procedure. The results were subsequently displayed in SPSS viewer as an agglomeration schedule, which gave information on the clustering process and a dendogram plot that showed how the genes were linked into clusters.

Using the dendogram plot the appropriate cluster solution can be chosen. The clustering procedure was then repeated to take account of the clustering solution generated. In the hierarchical cluster analysis window, the save button was selected, this brings up the save new variable window under which single solution was selected and the number of clusters (cluster solution from dendogram plot) was entered. This saves the individual clusters for subsequent analysis. At this stage SPSS data editor displays the original data (genes with expression levels at each time point) with an extra variable (column) that gives the cluster membership (the cluster assigned to each gene). To analyse the results, the first step involves looking at the time course plots for the different clusters. This can be easily done in Excel so the data matrix with the new variable (cluster membership) was exported to Excel.

Once the data has been exported to Excel, plots of each of the different clusters were created. To do this a Macro called Separator was activated (this is a function of Microsoft Excel). Once activated the separator macro was chosen under the tools menu of Excel. This brings up the row separator wizard that allows you to select the area on the worksheet that you wish to analyse. Next the column containing the cluster solution was selected as the variable (to separate the plots). Finally the number of genes to plot in each chart was chosen (all the genes in the cluster were chosen so that all genes in the cluster were displayed on one graph). Separator then created a new worksheet for each cluster in Excel, into which each cluster has been copied and graphs had been created.

The worksheets were then edited to presentable form so that genes were listed alphabetically, variable names were replaced with the experimental time points and the graphs were edited to show each gene in a different colour on the graph. These worksheets showing the genes in each cluster and their plots are shown in appendix 8.

Each worksheet shows a separate cluster with a table showing the genes in the cluster (listed alphabetically) and their expression levels. A graph of the genes in the cluster is then given below the expression level table. Graph legends (gene names) are only given when there are less than 10 genes in the cluster. Where there are more than 10 genes per cluster, graph legends are not given due to the size of the graphs

generated. In this case one may determine the identity of a line on the graph by simply placing the mouse cursor on the line of interest, this will provide the gene name.

2.6 Composition of solutions

Standard solutions were prepared according to Sambrook *et al* [179].

Barbital Buffer

Barbital buffer was composed of 10mM 5,5-diethylbarbituric acid and 50mM 5,5-diethylbarbituric acid sodium salt.

Bradford stock reagent

Bradford stock reagent was prepared by dissolving 100mg Commassie Brilliant Blue G in 95% ethanol and 100ml of 85% (w/v) phosphoric acid. The stock reagent was subsequently stored at 4°C and filtered before use.

Calcium formal solution

Calcium formal solution was prepared by combining 10ml 40% formaldehyde, 10ml 10% calcium chloride and 90ml distilled water.

DEPC treated water

DEPC was added to deionised water at a final concentration of 0.01%(v/v). The resulting solution was stirred overnight before being autoclaved.

Destain solution

45ml of reagent alcohol (95% methanol, 5% methanol) was mixed with 55ml of de-ionised water.

DNA lysis buffer

DNA lysis buffer was composed of 0.32M sucrose, 10mM Tris-HCl, 5mM $MgCl_2$ and 1% Triton X-100. The resulting solution was adjusted to pH 7.5 and autoclaved.

DNA resuspension buffer

DNA resuspension buffer consisted of 0.075M NaCl and 0.024M EDTA. The pH of the final solution was adjusted to pH 8.0 and the solution was autoclaved.

Fixative solution

180ml reagent alcohol [95% ethanol, 5% methanol] was combined with 90ml de-ionised water and 30ml glacial acetic acid.

Formamide dye

Formamide dye was prepared by combining 24.5ml formamide, 0.5ml EDTA (0.5M), 12.5mg bromophenol blue and 12.5mg xylene cyanole FF.

Hybridisation wash solution

Hybridisation wash solution consisted of 0.1% SDS and 0.1x SSC.

Loading buffer for agarose gel electrophoresis of PCR products

Loading buffer was prepared by combining 5ml glycerol, 0.37g Na_2.EDTA.$2H_20$, 0.1g SDS, 0.01g bromophenol blue and 0.01g xylene cyanole FF. The resulting solution was made up to 10ml in deionised water

Membrane wash solution

6 x SSC and 0.5% SDS

Messenger RNA binding buffer (supplied with kit)

20M Tris-HCl, 1000mM NaCl, 2mM EDTA, 0.2% SDS

Messenger RNA wash buffer (supplied with kit)

10mM Tris-HCl (pH 7.5), 150mM NaCl and 1mM EDTA

Messenger RNA Elution buffer (supplied with kit)

5mM Tris-HCl at pH 7.5

5X MOPS buffer

A 5x MOPS solution was prepared consisting of 0.2M MOPS, 0.05M sodium acetate and 0.05M EDTA. The final solution was adjusted to pH 7 with 1M NaOH.

Oil Red O working solution

Oil Red O working solution was prepared by taking three parts of a stock solution of Oil Red O (Oil Red O saturated in 99% isopropanol) and mixing with two parts of distilled water to give a working solution of Oil Red O. The working solution was filtered with Whatman No.1 paper an hour before use.

Oligotex Suspension (supplied with kit)

Oligotex suspension consisted 10 % oligotex particles [w/v], 10mM Tris-HCl, 1mM EDTA, 0.1% SDS and 0.1% NaN_3.

Paraformaldehyde (1%)

A 2 % solution of paraformaldehyde was heated to between 60-70°C until a milky solution was formed. At this stage 0.1M sodium hydroxide was added drop wise until clear. This was diluted with 0.2M PBS, pH 7.4 (see below) to give a working solution of 1% paraformaldehyde.

0.2M PBS

Two separate 0.2M solutions were prepared. Solution 1 was prepared by dissolving 35.61 g of dibasic sodium phosphate in 1 litre of distilled water. Solution 2 was prepared by dissolving 31.21g of monobasic sodium phosphate in 1 litre of water. Solution 1 (40ml) was mixed with 10ml of solution 2 to give a solution of pH 7.4.

Phosphate buffered saline (PBS)

NaCl (8g), KCl (0.2g), $1Na_2HPO_4$ (1.44g) and KH_2PO_4 (0.24g) were dissolved in 800ml of deionised water. The pH of the resulting solution was adjusted to pH 7.4 with 1M HCl. The volume of the final solution was made up to one litre before being autoclaved.

Phorbol 12- myristate 13-acetate [50μM]

A stock solution of 50 μM PMA was prepared by dissolving PMA (1mg) in 1.62ml of DMSO and subsequently diluting 1 in 20 with sterile filtered PBS. The stock solution was aliquoted into 1ml cryogenic vials and stored at -70°C. Each vial was thawed and used once.

Tris borate buffer (5x TBE)

A 5x stock solution was prepared by dissolving 54g Tris base, 27.5g boric acid and 20ml of 0.5M EDTA in one litre of deionised water. The final solution adjusted to pH 8.3 using 10M NaOH.

Tris acetate buffer (50x TAE)

A 50x stock solution was prepared by dissolving 242g of Tris base, 57.1ml of glacial acetic acid and 100ml of 0.5M EDTA in one litre of water. The resulting solution was adjusted to pH 8.

RNA sample buffer

RNA sample buffer was prepared by combining 10ml of deionised formamide, 3.5ml formaldehyde (37%) and 2ml of 5x MOPS buffer.

RNA loading buffer

50% glycerol, 1mM EDTA, and 0.4% bromophenol blue in DEPC treated water.

20x SSC

A solution of 20x SSC was prepared by dissolving 175.3g of NaCl and 8.2g of sodium citrate in 800ml of deionised water. The pH was adjusted to 7 using 10M NaOH and the final volume was made up to 1litre in deionised water.

10 % SDS

SDS solution was prepared by dissolving 100g of SDS in 900ml of deionised water at 68°C. The pH was adjusted to 7.2 using 10M HCl and the final volume of the solution was made up to 1 litre using deionised water.

TE buffer

TE buffer consisted of 10mM Tris-HCl and 1mM EDTA. The resulting solution was adjusted to pH 7.4 and autoclaved.

2.7 Materials

All tissue culture plastics were obtained from Falcon/Becton Dickinson (Crowley, Oxford, UK) or Griener (Stonehouse, Gloucestershire, UK).

All inorganic chemicals were of at least AnalaR quality and were obtained from Sigma (Poole, Dorset, UK) or BDH chemicals (Poole, Dorset, UK) unless otherwise specified.

All organic solvents were obtained from Sigma (Poole, Dorset, UK) unless otherwise specified.

Molecular Biology enzymes and reagents were obtained from GibcoBRL (Paisley, Scotland, UK), Boehringer Mannheim (Lewis, East Sussex, UK) or Pharmacia Biotech (Little Chalfont, Buckinghamshire, UK) unless otherwise specified.

Cell culture media and components were obtained from GibcoBRL Life Technologies (Paisley, Scotland, UK).

RNA isolation kits were obtained from Qiagen (Crawley, West Sussex, UK)

Radioactive material was all obtained from Amersham Life Sciences (Little Chalfont, Buckinghamshire, UK).

Chapter 3: Foam Cell Formation

3.1 Introduction

As discussed in chapter one (section 1.8), one of the major events in atherosclerosis is the appearance of lipid-filled foam cells [3]. The accumulation of foam cell formation beneath the endothelium leads to the formation of the fatty streak, the earliest lesion of atherosclerosis. During the more advanced stages of atherosclerosis, foam cell death is thought to contribute to the characteristic lipid core and weakening of the thin fibrous cap found in more advanced lesions (section 1.12) [32].

Immunohistochemical studies have established that foam cells are predominantly monocytic in origin [46]. Monocytes attach and enter the intima at sites of endothelial injury. Once in the intima they differentiate into macrophages and take up large amounts of cholesterol via unregulated scavenger receptors to become foam cells. Modified lipoproteins, mainly OxLDL have been implicated as one possible source of cholesterol for cholesterol ester storage in foam cells *in vivo* [18].

Although most cells can take up lipoproteins, macrophages possess mechanisms that allow them to take up, digest and store cholesteryl esters. In addition macrophages can secrete cholesteryl esters through SR-B1 when cholesterol acceptors such as HDL are available [24]

3.1.1 The Cholesteryl Ester Cycle

Goldstein and Brown [12] were the first to show that acetylation of LDL led to its uptake by macrophages and results in foam cell formation *in vitro*. They found that patients with genetic defect FH, had a LDL receptor deficiency, however still accumulated large amounts of cholesteryl esters within macrophages of atherosclerotic plaques. They subsequently identified the scavenger receptor [16], which was found to mediate the binding and internalisation of AcLDL through a pathway they termed the scavenger pathway. A shift in balance towards cholesteryl ester formation and storage is thought to be the mechanism that leads to excessive cholesteryl ester accumulation and

foam cell formation within macrophages [71]. Under normal physiological conditions macrophages express few receptors for native LDL and these receptors are down regulated in the presence of high concentrations of native LDL [16]. Modified LDL however is taken up by scavenger receptors, which are not subject to down regulation. This results in an increase in the amount of cholesterol in the cell. This excess cholesterol is subsequently delivered to the lysosome where it is esterified by the ACAT enzyme into cholesteryl esters. In the absence of cholesterol acceptors such as HDL, the cholesteryl esters are transported to the cytoplasm of the cell for storage where excessive accumulation leads to foam cell formation. In the presence of a cholesterol acceptor such as HDL, the cholesteryl esters are transported to the liver where they are hydrolysed and the free cholesterol excreted is secreted. This cycle in which excess cholesterol is esterified and subsequently secreted through an acceptor such as HDL, or retained within the cell has been termed the cholesteryl ester cycle [74]

Although the scavenger receptor has been reported on macrophages from every species including human monocyte derived macrophages, the natural ligand for the scavenger receptor was unclear since modification by acetylation is not thought to occur under physiological conditions. Steinberg *et al* [180] showed that oxidised LDL (OxLDL) can also be taken up by the scavenger receptor. Subsequent binding studies [181] with both OxLDL and AcLDL concluded that macrophage receptors for modified LDL consist of at least three different types, a receptor that recognises AcLDL, a receptor that recognises OxLDL and a receptor that recognises both. A number of macrophage cell surface proteins have been identified that can specifically bind OxLDL. These include the class A and B scavenger receptors, CD36, CD68 and CD32 [22] (see chapter one section 1.3.4). In particular CD36 has been implicated to be a major receptor for OxLDL on human monocyte derived macrophages *in vitro* [67].

3.1.2 The THP-1 cell line

Differentiation of human blood monocytes *in vitro* has been used extensively as a model system for investigating macrophage development [54]. Both primary human monocyte-macrophage preparations and differentiated cell lines have been used *in vitro* to study foam cell formation [164,182]. The use of primary macrophage preparations can present problems such as donor variability, accessibility, a limited number of cells available for study and a finite survival period in culture. The use of a continuous cell line can overcome these limitations [183]. Commonly used monocytic cell lines include J774 cells (mouse), U937 cells and THP-1 cells. Because of the technical limitations involved, most studies of lipoprotein metabolism employ the use of cell culture models.

The human monocytic THP-1 cell line was derived from the blood of a one-year-old boy with acute monocytic leukaemia. It is considered to be a more differentiated and committed macrophage cell line than other monocytoid lines [184]. In this study the THP-1 cell line was used as an *in vitro* model for foam cell generation instead of human monocyte derived macrophages for the following reasons: -

(a) THP-1 cells have been shown to resemble human monocytes in respect to morphology, secretory products, oncogene expression, membrane antigens and receptors and the expression of genes involved with lipid metabolism [183].

(b) THP-1 cells take on macrophage like characteristics when stimulated with phorbol ester (PMA) [160].

(c) They are easy to grow in large batches.

(d) There is less likely to be variation between preparations using THP-1 cells than using human monocyte derived macrophages. Thus during experimental treatment, differences obtained are more likely to be due to treatment with lipoprotein, not due to inter-individual variability.

3.2 Experimental Design

In order to study differences in gene expression between macrophages and foam cells, a cell culture model of foam cells had to be established. Although it has been

reported by many investigators that incubation of THP-1 cells with both acetylated and oxidised LDL leads to foam cell formation [185,171], this had to be confirmed in the hands of the investigator of this study. This was done using a variety of previously described techniques that have been used to assess foam cell formation. These techniques include: -

1. Staining for lipid droplets using Oil red O staining and detection by light microscopy.
2. Staining for lipid droplets using nile red and detection by
   (a) Fluorescence microscopy.
   (b) Flow cytometry.
3. Measurement of cholesteryl ester accumulation using ^{14}C-oleic acid loading.

The aim of these experiments was to establish that:-

1. THP-1 cells that had been exposed to PMA changed in morphology from monocytes into macrophages.

2. Differentiated THP-1 macrophages took up modified LDL (either acetylated or oxidised LDL) that resulted in cholesteryl ester accumulation and foam cell morphology using qualitative analysis

3. (a) There was cholesteryl ester accumulation in differentiated THP-1 cells exposed to native, acetylated and oxidised LDL quantitatively.
   (b) Accumulation was greater in cells exposed to modified LDL than those exposed to native LDL at the same concentration.

3.3 Modification of LDL

As discussed before (section 1.8.4), LDL must be modified in order for foam cell formation to occur. The uptake of native LDL is tightly controlled by a feedback mechanism that does not result in over-accumulation. Modified LDL however is taken up by the unregulated scavenger pathway and results in cholesteryl ester accumulation. Although AcLDL is not thought to occur *in vivo*, it is the modification Goldstein and Brown used in their discovery of the AcLDL scavenger receptor [16]. It is therefore the standard used to generate foam cells. OxLDL on the other hand is the most likely *in vivo* candidate involved in foam cell formation and is thus the more physiologically relevant ligand.

In this study LDL was isolated at density 1.063g/ml from normolipaemic subjects by ultracentrifugation in potassium bromide gradients. LDL was modified either via acetylation by the addition of acetic anhydride or oxidation by the addition of copper sulphate as described in the methods (section 2.2.6). To check that modification of LDL had been successful native, acetylated and oxidised LDL were subjected to electrophoresis on a Beckman agarose LIPO gel as described in the methods (section 2.2.7)

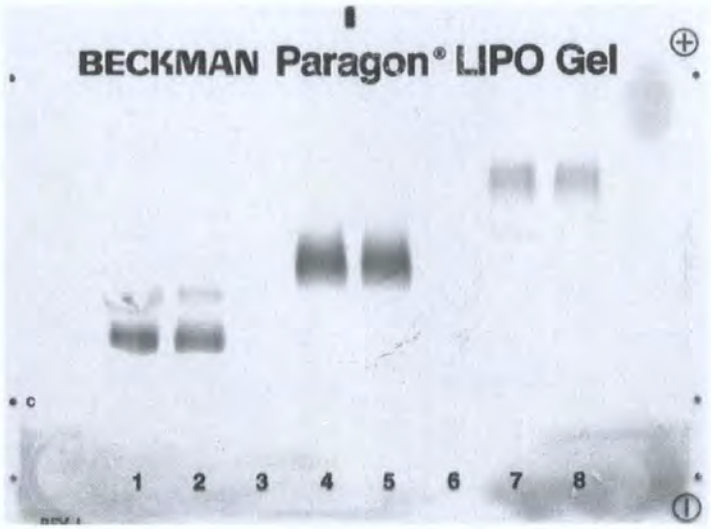

Figure 3.1

A Beckman LIPO gel showing migration of native LDL, (1mg/ml; lanes 1 and 2), oxidised LDL, (1mg/ml; lanes 4 and 5) and acetylated LDL (0.5mg/ml; lanes 7 and 8) after electrophoresis. Lanes 3 and 6 are blank.

Modification of LDL by acetylation or oxidation has been shown to abolish the positive charges on the lysine residues of LDL [91]. The resultant acetylated or oxidised LDL is more negatively charged than native LDL and therefore migrates further than native LDL during electrophoresis as shown in figure 3.1. Rf values were usually 1 for native LDL, 1.5 for OxLDL and 2.5 for AcLDL (from the origin).

Recognition of LDL by the scavenger receptor is dependent on derivatisation of the positive lysine residues found in the apolipoprotein B region of LDL [186]. It is thought that upon modification, apoB undergoes a conformational change in its tertiary structure so that there is steric display of amino acyl groups that are important for recognition by the scavenger receptor [186].

Figure 3.1 also shows that acetylated LDL has greater mobility than oxidised LDL. This may be due to the observation that apoB has been shown to be sensitive to oxidative damage and that oxidation results in the breakdown of apoB into smaller

peptides resulting in a decreased electrophoretic mobility [187]. This can be seen on agarose gels as a broader lipid band.

3.4 Differentiation of THP-1 cells

PMA treatment of THP-1 cells promotes a dramatic changes in cell morphology that results in macrophages that have the functional characteristics of tissue macrophages [159]. PMA is a hydrophobic phorbol ester that acts by binding to the cell membrane acyl side chains and activating the protein kinase C signal transduction pathway [188]. The cells stop proliferating, become adherent and develop an irregular shaped nucleus. In addition, the cells form well-developed cell organelles such as phagocytotic vacuoles, free ribosomes and golgi apparatus (which are found to be less developed in monocytes) [159]. The differentiation of monocytes into macrophages is also accompanied by a change in their capacity to recognise and accumulate modified LDL.

Both LDL and scavenger receptors on THP-1 cells have been reported [160,188]. Dividing THP-1 cells have been reported to display LDL receptors that disappear when the cells differentiate in response to PMA treatment [189]. However concomitant with the loss of LDL receptors is the appearance of scavenger receptors. PMA treatment of THP-1 cells has been shown to result in a dramatic induction of scavenger receptor activity especially scavenger receptor class AII [189], via activation of protein kinase C [189]. In addition treatment of THP-1 cells with PMA also results in the induction of specific enzymes and proteins, including tissue lipoprotein lipase and apo E [190].

Figure 3.2 shows the difference in morphology in THP-1 cells and differentiated THP-1 cells. THP-1 cells respond to PMA treatment by converting from a suspension cell line (figure 3.2A) to one that is adherent and spread (figure 3.2B).

Figure 3.2A

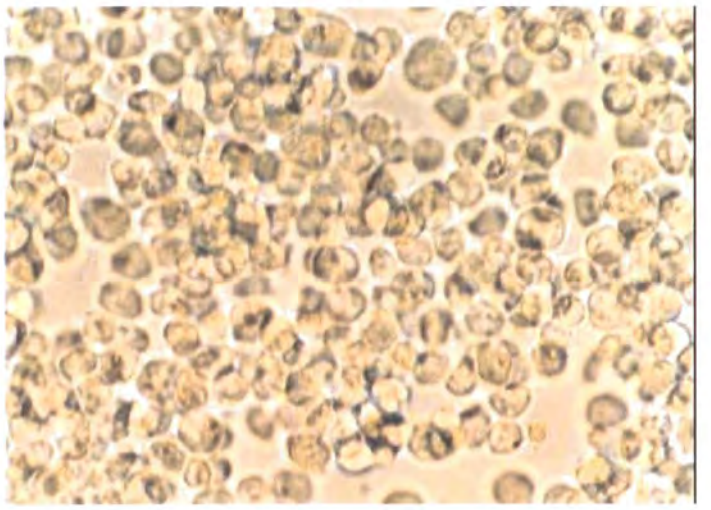

Figure 3.2B

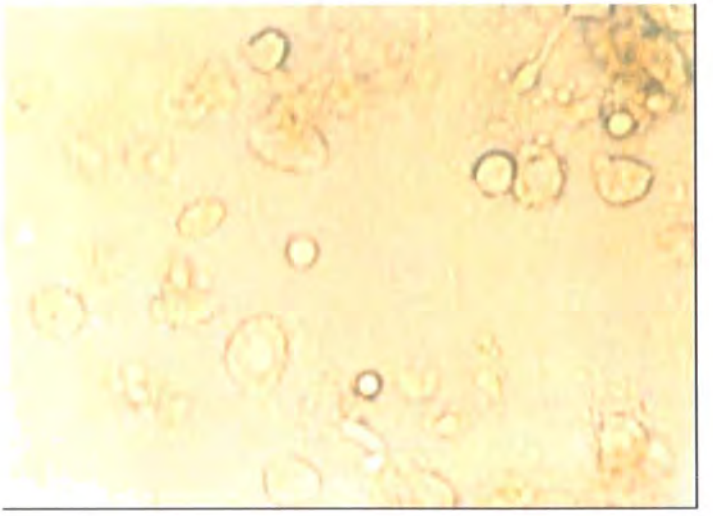

Figure 3.2

Photomicrographs showing morphology of dividing THP-1 cells in suspension (figure 3.2A) and THP-1 cells differentiated using PMA (250nM) for seven days (figure 3.2B) Cells were differentiated as described in the methods (section 2.1.2). Cells were photographed at x320 magnification.

3.5 Oil red O staining

A commonly used histological technique for examining lipid stores in tissues and cells is Oil red O staining. This technique has also been used to examine lipid stores in THP-1 derived foam cells [160]. For Oil red O staining, THP-1 cells were differentiated on microscope slides for seven days. Cells were exposed to native or modified lipoprotein (0.2mg/ml) for twenty hours. Cells were then fixed and stained with a solution of Oil red O to stain lipid droplets and subsequently counter-stained with Harris Haematoxylin to stain the cell nuclei as described in section 2.1.5. THP-1 cells in suspension were prepared for staining as described in section 2.1.5.

THP-1 cells exposed to no lipoprotein and showed no Oil red O staining as expected (figure 3.3A). When THP-1 cells were differentiated and exposed to native LDL, lipid droplets were observed in small numbers in some of the cells (figure 3.3B). On exposure to either acetylated or oxidised LDL however, a larger number of lipid droplets were found to be present in most of the cells (figure 3.3 C&D). Thus Oil red O staining confirmed that exposure of differentiated THP-1 cells to modified LDL resulted in the presence of a larger number of intracellular lipid droplets in comparison to cells exposed to native LDL.

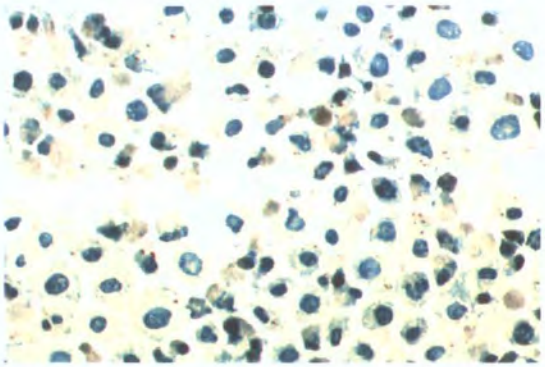

Figure 3.3 A

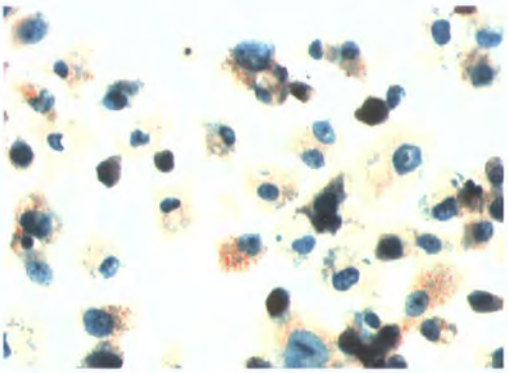

Figure 3.3 B

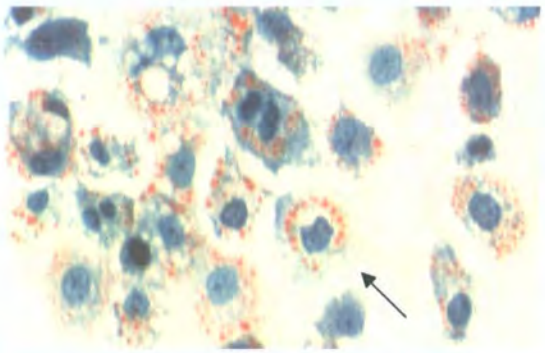

Figure 3.3 C

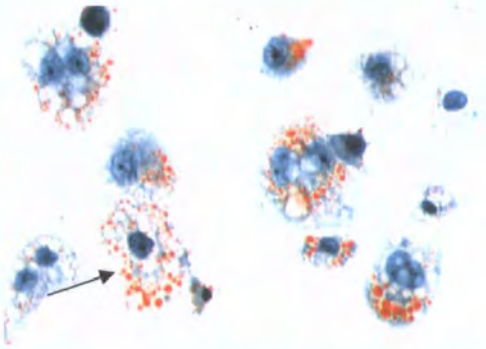

Figure 3.3 D

Figure 3.3

THP-1 cells and differentiated THP-1 cells (exposed to lipoprotein) and subsequently stained with Oil Red O and haematoxylin. Cells were photographed at x320 magnification.

Figure 3.3A THP-1 cells stained with Oil Red O and haematoxylin (as described in section 2.15)

Figure 3.3 B, C and D Differentiated THP-1 cells exposed to 0.2mg/ml native, acetylated and oxidised LDL for 24 hours respectively. Cells were stained with Oil Red O and haematoxylin (as described in section 2.15). Arrows in 3.3 C&D point to cells containing lipid deposits.

3.6 Fluorescence microscopy of nile red stained cells

Fluorescence labelling reagents can be used directly on cells to stain structures like DNA and lipids. Fluorescence dyes contain a chromophore structure, made up of conjugated bonds and related electronic structures that give the dye its colour [191]. Fluorescent dyes can produce fluorescence signals through excitation. Dyes can become excited by absorbing a photon of light. Once a dye has been excited, the intensity of the subsequent fluorescence depends on what happens to the energy of the excited chromophore. The excitation energy may be given off as heat, or emitted as a photon (fluorescence) or it could be transmitted to another dye molecule [191].

Greenspan *et al* [165] discovered nile red to be an excellent stain for lipid droplets. Nile red was found to be present as a minor component of the non-fluorescent lipid stain nile blue [165]. Nile red is a benzophenoxazone dye that is poorly soluble in water. It does, however, dissolve in a wide range of organic solvents including acetone to produce an intensely fluorescent solution [165]. Figure 3.4 shows the chemical structure of nile red.

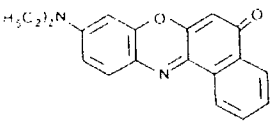

Figure 3.4 The chemical structure of nile red

Treatment of cultured cells with a solution of nile red has been shown to produce an intense staining of cytoplasmic contents of cells when viewed by fluorescence microscopy [163]. To visually examine lipid loading of THP-1 cells, THP-1 cells were stained with nile red and examined using fluorescence microscopy.

THP-1 cells were differentiated using PMA (250nM; as described in section 2.1.2). After seven days, the cells were exposed to either native or modified LDL (0.2mg/ml) for twenty-four hours. Cells were washed well in PBS, stained with nile red (100ng/ml) and examined using a Nippon episcopic inverted fluorescence microscope.

A combination of three elements; an excitation filter, a dichroic mirror and a

barrier filter affect excitation techniques in episcopic fluorescence microscopes. Two different fluorescent wavelengths, yellow-gold fluorescence (excitation wavelength 450-490nm) and red fluorescence [excitation wavelength 510-560nm] have been previously reported to be used to study nile red staining of macrophages by fluorescence microscopy. Thus here, cells were examined using these two different fluorescence wavelengths. Yellow-Gold fluorescence has been shown to be good at detecting cytoplasmic lipid droplets whereas red fluorescence has been reported not to resolve lipid droplets with a sufficient degree of clarity. In addition green fluorescence with a wavelength greater than 488nm was also used because nile red has an excitation wavelength of 488nm.

Figure 3.5 shows photographs of fluorescence microscopy of differentiated THP-1 cells exposed to native or modified LDL (0.2mg/ml for 24 hours), stained with nile red and viewed using the above three different fluorescent excitation wavelengths.

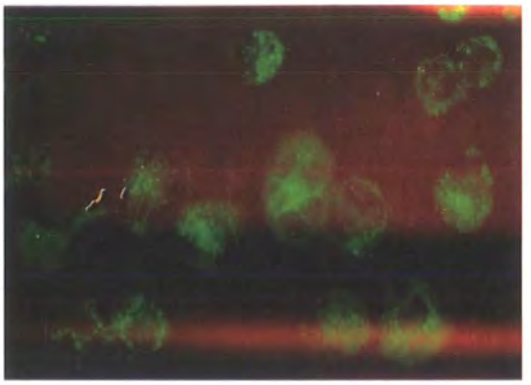

Figure 3.5 A

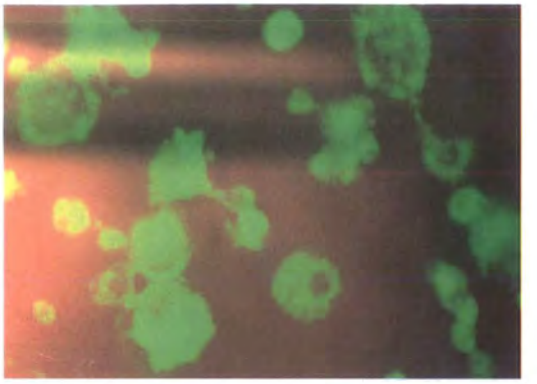

Figure 3.5 B

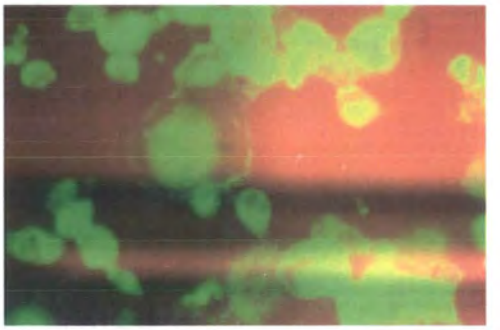

Figure 3.5 C

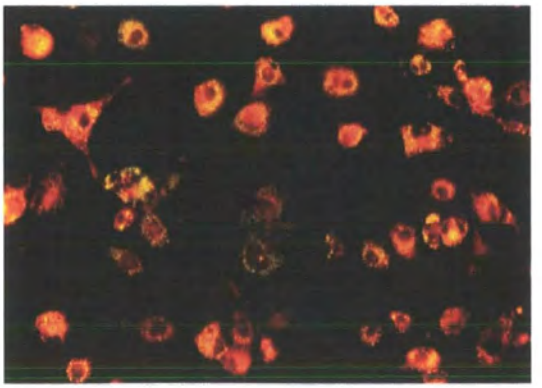

Figure 3.5 D

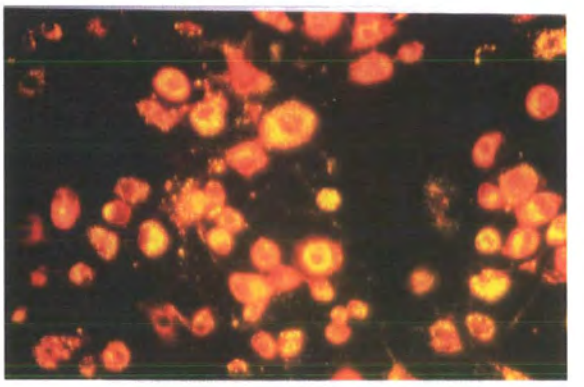

Figure 3.5 E

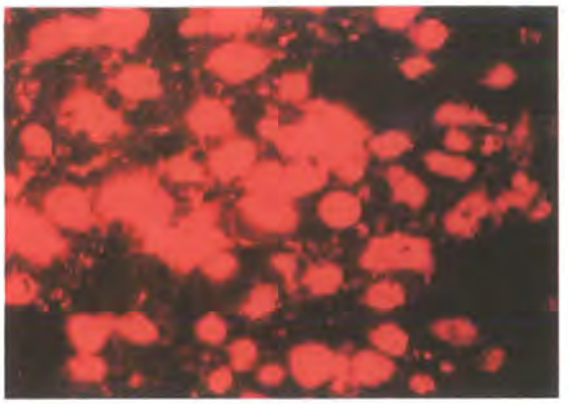

Figure 3.5 F

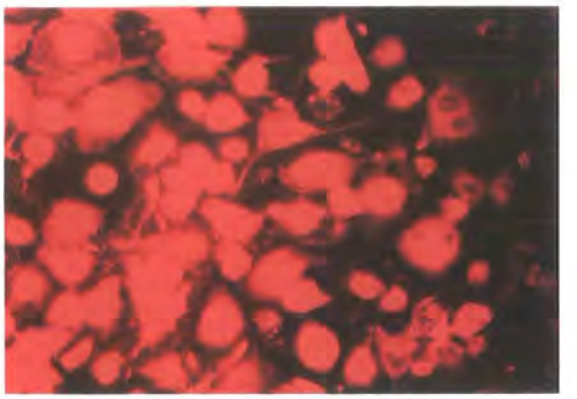

Figure 3.5 G

Figure 3.5

Differentiated THP-1 cells exposed to native LDL (3.5A, 3.5D and 3.5F), AcLDL (3.5B) and OxLDL (3.5C, 3.5E and 3.5G) at a concentration of 0.2mg/ml of lipoprotein for 24 hours. Cells were stained with nile red (100ng/ml) and viewed by fluorescent microscopy. Cells were photographed at x320magnification.

Figure 3.5 A-C	Cells viewed using green fluorescence, emission wavelength greater than 488nm.
Figure 3.5 D&E	Cells viewed using yellow-gold fluorescence, emission wavelength 450-490nm
Figure 3.5 F&G	Cells viewed using red fluorescence, emission wavelength 510-560nm.

Although fluorescence emitted was not measured, visually one could can see that from figure 3.5, cells exposed to modified LDL, stained with nile red and viewed using green fluorescence (figures 3.5B and 3.5C) or yellow-gold fluorescence (figure 3.5E) showed greater fluorescence than cells exposed to native LDL (figures 3.5A and 3.5D). Although cells exposed to native LDL (figure 3.5A and 3.5D) did show fluorescence, the intensity of the fluorescence was less than that of cells exposed to modified LDL (figures 3.5 B, 3.5C and 3.5E)

Cells viewed using red fluorescence (figures 3.5F and 3.5G) did show fluorescence but the cytoplasmic components of the cells were not resolved and therefore the difference in lipid droplets could not be examined. The results of this experiment correspond to the work of Greenspan *et al.* [165]. They found better resolution of the lipid droplets using yellow gold fluorescence than red fluorescence as is also demonstrated in this study. In addition as shown in figure 3.5 A-C green fluorescence showed good resolution of lipid droplets. This supports the fact that 488nm is the optimal excitation wavelength for nile red.

3.7 Flow Cytometry

Fluorescence activated cell sorting (FACS) is a technique that has had a major impact on both basic and clinical research in the last two decades [191]. The major advantages of FACS are that it allows the rapid collection of quantitative measurements on a large number of individual cells and it helps to identify specific cell types from a heterogeneous mixture of cells. Fluorescent dyes are used as the means of detection in flow cytometry [191]. During flow cytometry, cells in suspension are moved through a set region of the flow cytometer where they are excited by one or more laser beams. The subsequent emissions are collected, separated, processed and recorded in a computer for individual cells as they flow one by one past a set region.

Treatment of macrophages with a dilute aqueous solution of nile red has been found to produce an intense fluorescence staining of cytoplasmic lipid components (as already shown in figure 3.5). Several investigators including Hassall and Greenspan *et al* [163, 165] have thus used nile red in flow cytofluorometric analysis to assess foam cell formation.

For flow cytometric analysis, cells were differentiated using 250nM PMA for seven days. After seven days, cells were exposed to varying concentrations (0-0.3mg/ml) of native, acetylated and oxidised LDL over different time periods. Cells were fixed in paraformaldehyde and stained with nile red (final concentration; 100ng/ml) for 5 minutes. Cells were then passed through the flow cytometer and the mean nile red fluorescence of emissions representing cholesteryl esters were collected from samples in triplicate. Nile

red stained cells were analysed using a Coulter EPIC flow cytometer. For nile red, an excitation wavelength of 488nm was used (standard wavelength produced by an argon ion laser found in most flow cytometers) and the emission spectra were collected. The parameters used in these experiments were based, where possible, on those reported by Hassall and Greenspan *et al* [163,165].

The most common display method for flow cytometry data is called a dot plot. This is a two-dimensional display, in which two user selected parameters form the x and y-axis. Dot plots update the data from the samples in real time. The display data collected in these experiments was in two formats; the first display gave the shape (size of cell versus granularity of the cell). The second display format gave the fluorescence (cell count versus fluorescence). Analysis was performed routinely performed on 10,000 cells. Data was expressed as a ratio of forward scatter (size of the cell on the x-axis) and side scatter (granularity of the cell on the Y-axis). A gate was placed to include 90% of the cell population to prevent the inclusion of outlying data due to cell signal from cell debris.

Fluorescence emission spectra were collected and separated using filters of different ranges (given in section 2.1.7) to separate triglycerides and cholesteryl esters (which have different emission spectra). Emission spectra representing triglycerides and cholesteryl esters were separated using a 590nm dichroic long pass filter. Emission spectra were then collected using a 510-80nm-band pass filter for triglycerides and a 600nm long pass filter for cholesteryl esters. All fluorescence data collected was gated on forward scatter and the data was expressed as log fluorescence versus count.

3.7.1 Confirmation of differentiation

To determine whether PMA treatment resulted in differentiation of THP-1 cells from non-adherent cells to adherent cells, THP-1 cells and differentiated THP-1 cells were passed through the flow cytometer. Figure 3.6 shows dot plots of THP-1 cells (figure 3.6A) and THP-1 cells that have been differentiated into macrophages using PMA (figure 3.6B). As can be seen from figure 3.6, differentiation of THP-1 cells leads to both an increase in size (forward scatter) and an increase in granularity (side scatter). THP-1

cells are all similar in size and granularity whereas differentiated THP-1 cells show a much broader range of size and granularity. This result is in agreement with that previously reported [163]. In addition the changes matched well with the morphological changes seen under light microscopy (figure 3.2).

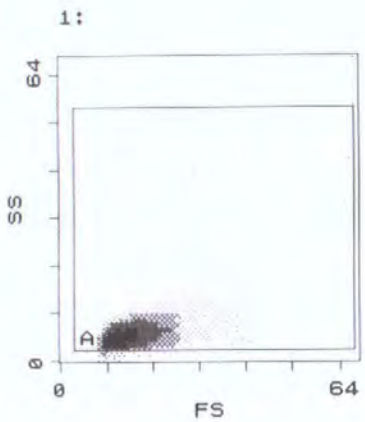

Figure 3.6A

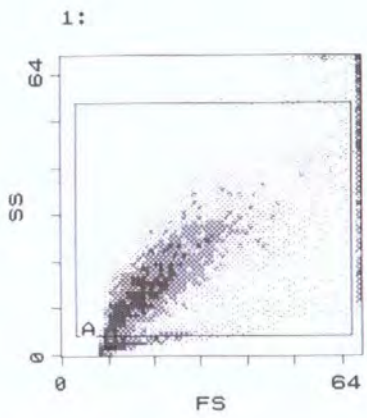

Figure 3.6B

Figure 3.6

Flow cytometry dot plots of undifferentiated THP-1 cells (figure 3.6 A) and differentiated THP-1 cells (figure 3.6 B). The cells are gated on linear forward scatter (FS) and linear side scatter (SS) The box labelled A represents the gate placed around the cells to prevent inclusion of debris and cell clumps in the analysis.

3.7.2 Nile red fluorescence staining

Figure 3.7 shows fluorescence emission profiles of THP-1 cells that have been stained with nile red and unstained THP-1 cells. The emission profiles demonstrate, as expected, that staining with nile red leads to an increase in fluorescence as shown by the

shift to the right of the peak of fluorescence. The fluorescence emission spectra shown (FL3) are those corresponding to cholesteryl esters.

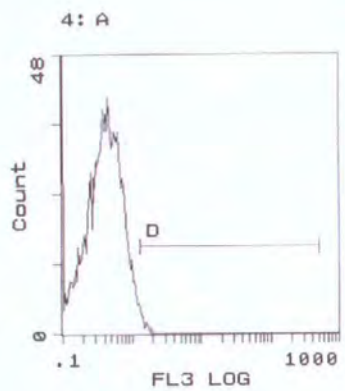

Figure 3.7A

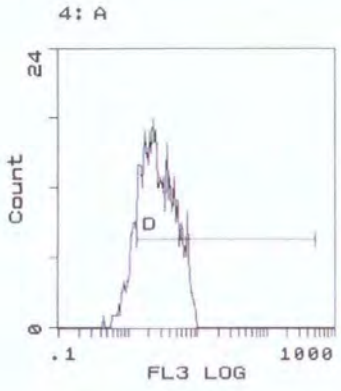

Figure 3.7B

Figure 3.7

Comparison of two fluorescence emission profiles from differentiated THP-1 cells without nile red (figure 3.7A) and differentiated THP-1 cells stained with nile red (figure 3.7B). Count represents number of cells and FL3 LOG represents log fluorescence intensity emissions over 600nm corresponding to cholesteryl esters. The shift in the peak indicates an increase in fluorescence emissions. The line D is a marker line set at fixed position from which changes can be measured.

The basis of using nile red was that as levels of cholesteryl esters increase during foam cell formation, staining with nile red would be expected to result in a greater fluorescence emission (an increase in fluorescence per cell). As cholesteryl esters accumulate, the peak of fluorescence emission shown in figure 3.7B would be expected to shift to the right. Thus measuring an increase in the mean nile red fluorescence of cells would be an indication of increased cholesteryl ester accumulation and foam cell formation.

3.7.3 Nile red staining in response to modified LDL

Figure 3.8 shows a dose response curve of mean nile red emissions representing cholesteryl esters in differentiated THP-1 cells exposed to 0.05, 0.1, 0.2 and 0.3 mg/ml of native, acetylated or oxidised LDL The zero time sample represents lipoprotein depleted cells

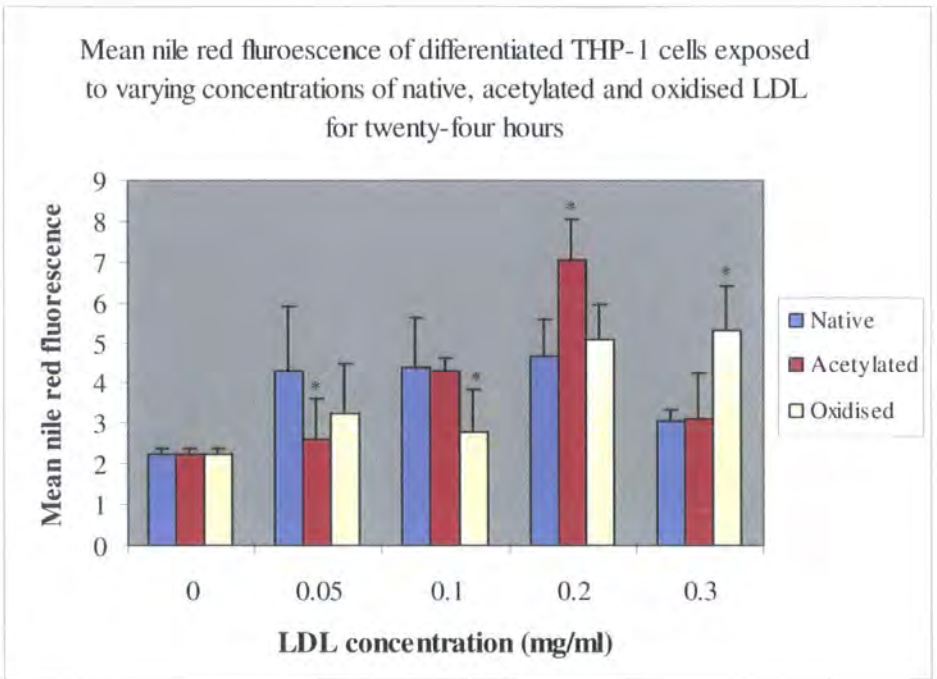

Figure 3.8

Bar chart showing mean nile red fluorescence of differentiated THP-1 cells exposed to 0, 0.05, 0.1, 0.2 and 0.3mg/ml concentrations of native, acetylated and oxidised LDL. Bars represent the mean + SD from three independent experiments in which each sample was performed in triplicate. * indicates significance difference (P= <0.05) between treatment (AcLDL or OxLDL) when compared to native sample at the same concentration

Exposure to native LDL results in an increase in fluorescence. Fluorescence levels show a significant increase ($P< 0.01$) nearly doubling on exposure to 0.05mg.ml of native LDL. This is expected as cells were cultured in lipoprotein depleted serum before the start of the experiment. With increasing concentration the levels of fluorescence remain constant eventually falling at a level of 0.3mg/ml of native LDL. This would be expected and would fit in with the model of native LDL uptake sufficient to meet the cells requirements before subsequent down-regulation of the LDL receptor. Exposure to AcLDL results in a linear increase (correlation coefficient = 0.99) in fluorescence upon increasing AcLDL concentration up to 0.2mg/ml with increase being significant between concentrations ($P <0.002$). At a concentration of 0.2mg/ml mean nile red fluorescence is significantly greater ($P< 0.0002$) in cells exposed to AcLDL than native LDL. Compared to AcLDL, OxLDL shows a slower increase in mean nile red fluorescence. This may be related in some way to the reported cytotoxic effects of OxLDL [192]. It can be postulated that the cells may have a more stringent control mechanism which limits the entry of OxLDL, however when sufficient OxLDL has entered this may override such a control mechanism. In addition other receptors may also become involved in the uptake of OxLDL. The dose response experiment demonstrated that the greatest mean nile red fluorescence was observed using a concentration of 0.2mg/ml AcLDL. To investigate this further a time course experiment was performed for up to 72 hours.

Figure 3.9 shows a time course of mean nile red fluorescence of differentiated THP-1 cells exposed to native and modified LDL at a concentration of 0.2mg/ml for seventy-two hours. Cells exposed to both native and modified lipoprotein showed a time dependent increase in mean nile red fluorescence. Exposure to native LDL resulted in a increase in mean nile red fluorescence up to 72 hours, although the increase was not significant between any of the increasing time points except 0 and 4 hours ($P < 0.001$). Exposure to AcLDL lead to a increase in mean nile red fluorescence, which peaked at 24 hours after which it began to decline. The 24 hour AcLDL time point showed a significant increase ($P < 0.0002$) in mean nile red fluorescence compared to the 8 hour AcLDL time point. In addition at 24 hours and 48 hour times points mean nile red fluorescence was significantly higher ($P< 0.03$) in cells exposed to AcLDL than native

LDL. This increase up to 24 hours followed by a decrease confirms the model that the cell may stop the uptake of lipoprotein once it has sufficient cholesterol to meet its needs.

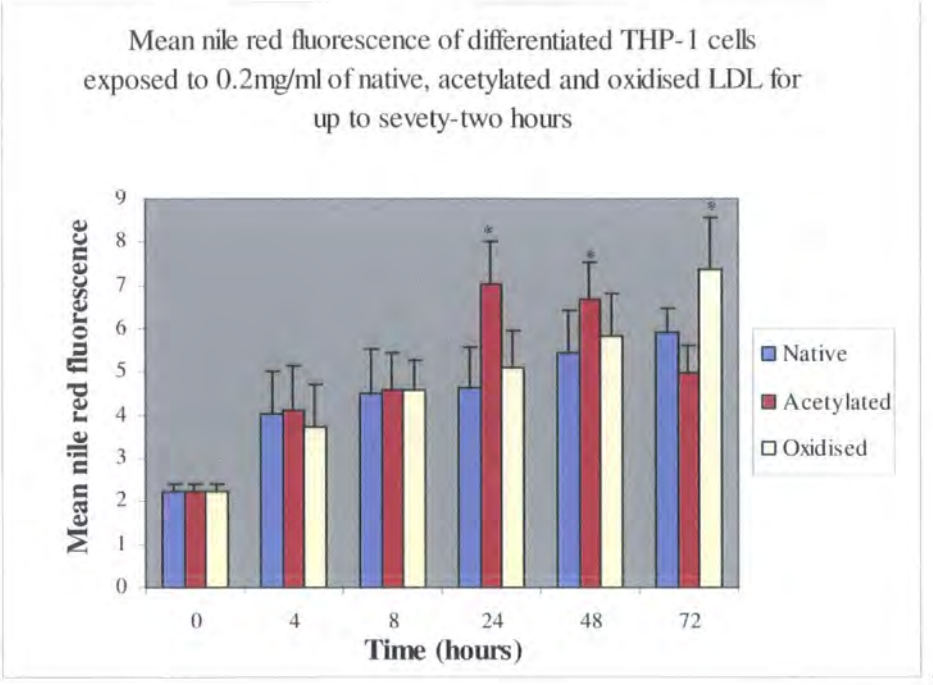

to

Figure 3.9

Bar chart showing mean nile red fluorescence in differentiated THP-cells exposed to 0.2mg/ml of either native, acetylated or oxidised LDL for 4, 8, 24, 48 and 72 hours. Bands represent the mean + SD of three independent experiments with each sample being performed in triplicate. * indicate significance difference (P= <0.05) between treatment (AcLDL or OxLDL) when compared to native sample at the same time point.

Exposure to OxLDL leads to a linear increase (correlation coefficient = 0.93) in mean nile red fluorescence up to 72 hours. However OxLDL only showed a significantly greater mean nile red fluorescence than native LDL at 72 hours ($P < 0.004$).

3.8 ^{14}C-oleate loading of differentiated THP-1 cells

To study foam cell formation, Goldstein and Brown [16] demonstrated that mouse peritoneal macrophages that were exposed to AcLDL rapidly took up and internalised AcLDL as compared to native LDL. They demonstrated this using cells incubated in the presence of ^{14}C-oleate and AcLDL and subsequently measuring the formation of cholesteryl ^{14}C-oleate. Thus stimulation of cholesteryl [^{14}C] oleate synthesis is commonly used as a functional assay to measure lipoprotein uptake. Lipoprotein uptake leads to cholesteryl ester synthesis as part of the cholesteryl ester cycle (see section 1.9).

Cells were seeded at a density of $1x10^6$ cells/per ml medium as this was the density at which maximal uptake of modified LDL has been shown to occur [194]. It has been demonstrated by Rodriguez *et al* [194] that cells plated at high density ($4x10^6$ml/well) took up five times less lipoprotein than cells that were plated at a lower density of $1x10^6$ ml/well.

THP-1 cells were differentiated into macrophages using PMA (250nM; as described in section 2.1.2). Although THP-1 cells have been shown to express scavenger receptors as early as three days [160,185], cells were routinely maintained for seven days as previously reported [163] to allow full differentiation and maximal expression of the scavenger receptor although this was not measured. After seven days of differentiation, cells were exposed to native, acetylated or oxidised LDL at varying concentrations (0-0.3mg/ml) for a time period for up to 72 hours in the presence of labelled oleate (prepared as described in section 2.1.8.1). Lipids were subsequently isolated from the cells and separated by TLC (as described in section 2.1.8.3). The amount of radioactivity in spots representing cholesteryl ester spots was counted in a liquid scintillation counter. The readings were corrected for percentage recovery using ^{3}H cholesteryl oleate as an internal standard (added during the first step of lipid extraction; see 2.1.8.3). The amount of ^{14}C incorporated into cholesteryl esters was then calculated and the results were expressed as micromoles of cholesteryl ester accumulation per $1x10^6$ cells.

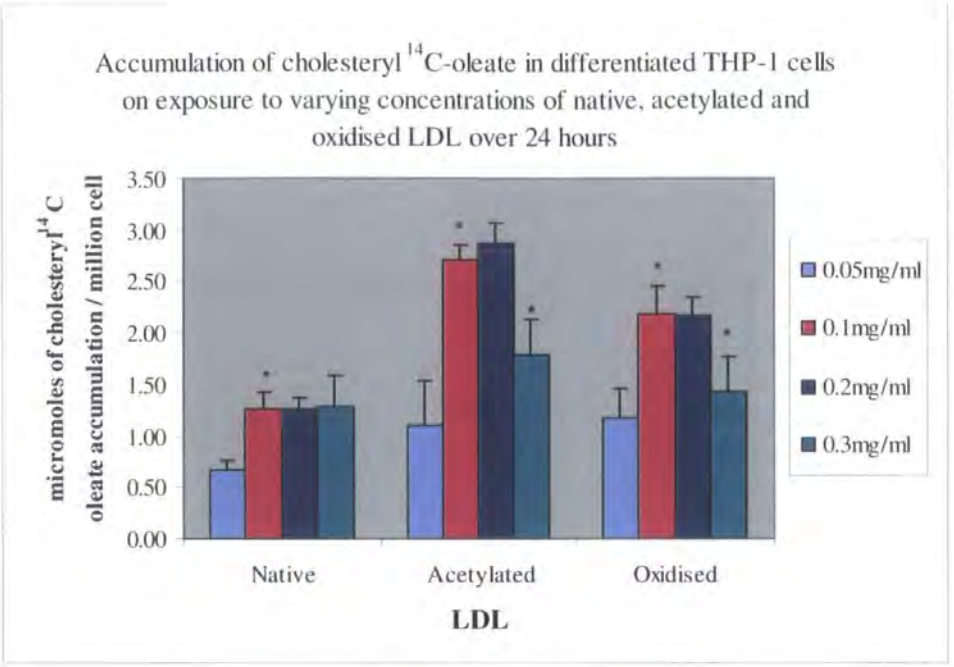

Figure 3.10

Bar chart showing accumulation of cholesteryl ^{14}C oleate accumulation in differentiated THP-1 cells exposed to 0.05, 0.1, 0.2 and 0.3mg/ml of native acetylated and oxidised LDL for 24 hours. Results are from three sets of independent experiments in which each sample was performed in duplicate. Bars represent the mean + SD (standard deviation). * indicates significance difference ($P < 0.002$) between increasing concentrations (0 to 0.05, 0.05 to 0.1, 0.1 to 0.2 and 0.2 to 0.3) of a particular treatment (native LDL, AcLDL or OxLDL).

Figure 3.10 shows cholesteryl ^{14}C oleate accumulation in differentiated THP-1 cells that were exposed to 0.05, 0.1, 0.2 and 0.3mg/ml of native, acetylated or oxidised LDL for 24 hours. At concentrations of 0.1 and 0.2 mg/ml there was a significantly greater cholesteryl ester accumulation in cells exposed to modified LDL than in cells exposed to the equivalent amount of native LDL ($P < 0.002$).

As can be seen from figure 3.10, native LDL did show a significant increase ($P < 0.001$) in cholesteryl ester accumulation when the concentration of LDL was increased from 0.05mg/ml to 0.1mg/ml, however no significant further increase was observed when

the concentration was increased to 0.2mg/ml and 0.3mg/ml. This confirms the data observed with native LDL in figure 3.8 (section 3.7.3) and probably reflects the cells prior incubation with lipoprotein depleted medium.

Although an increase of around two fold in ^{14}C oleate incorporation was observed in these experiments with modified LDL, differentiated THP-1 cells have been shown to exhibit up to a four-fold increase in the rate of ^{14}C oleate incorporation into cholesteryl esters in response to culture with AcLDL by other investigators [165]. This experiment showed a maximal cholesteryl ester accumulation using concentrations around 0.1mg/ml and 0.2mg/ml of modified LDL. At a concentration of 0.3mg/ml, both AcLDL and OxLDL showed a significant decrease in cholesteryl ester accumulation compared to a concentration of 0.2 mg/ml ($P < 0.002$).

To further study the effect of time, cholesteryl ester accumulation was assessed in differentiated THP-1 cells exposed to 0.2mg/ml native, acetylated and oxidised LDL for 24, 48 and 72 hours as shown figure 3.11

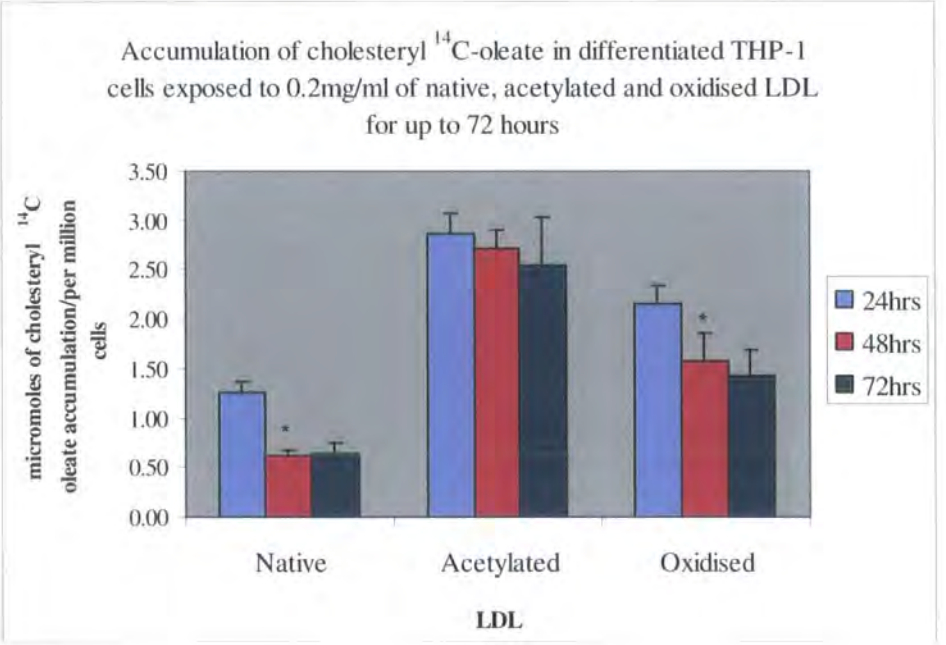

Figure 3.11

Bar chart showing accumulation of cholesterol ^{14}C-oleate in differentiated THP-1 cells exposed to 0.2mg/ml native, acetylated and oxidised LDL for 24, 48 and 72 hours. Results are from three sets of independent

experiments in which each sample was performed in duplicate. Bars represent the mean + SD for each experimental condition. * indicate significance difference (P= <0.01) between time points for a particular treatment (native LDL, AcLDL or OxLDL)

As can be seen from figure 3.11 there was significantly greater cholesteryl oleate accumulation in cells exposed to modified LDL than cells exposed to native LDL at all the time points (P< 0.0003). Cells exposed to both AcLDL and OxLDL showed maximal accumulation at 24 hours. The accumulation of cholesteryl esters in cells exposed to native LDL was limited and showed a significant decrease after 24 hours (P< 0.0002). In cells exposed to AcLDL, the level of cholesteryl esters was maintained at approximately the same level after 48 hours and 72 hours with no significant difference between the time points.

In cells exposed to OxLDL the cholesteryl ester accumulation decreased significantly after 24 hours (P <0.0002). At the 48 and 72 hour time points, the levels of cholesteryl ester accumulation was decreased by approximately 25% of the level after 24 hours. This may be due to some of the cytotoxic effects of OxLDL including lipid peroxidation, which prevents the accumulation of cholesterol and results in cell death [192].

3.9 Assay for assessing cell viability

A 3-(4,5-dimethylthiazol-2-yl)-2, 5-diphenyltetrazolium bromide MTT) assay for cell viability was performed. MTT can be cleaved by mitochondrial enzymes, mainly succinate-dehydrogenase, to form a dark blue crystalline product, formazan. This cleavage only takes place in living cells. The amount of formazan generated has been demonstrated to be directly proportional to the cell number [193].

Figure 3.12 shows that the percentage cells alive decreases in cells exposed to both AcLDL and OxLDL over time, however the decease is greater with OxLDL. This indicates there is more cell death on exposure to OxLDL, again consistent with its reported cytotoxic effects [192].

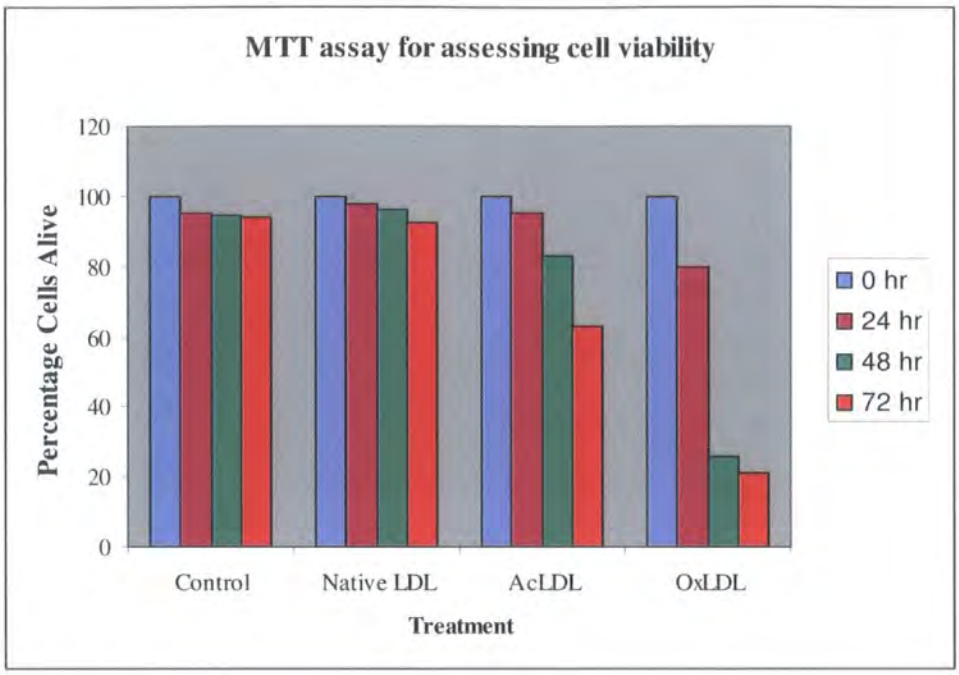

Figure 3.12

Bar graph showing percentage cells alive in differentiated THP-1 cells exposed to no LDL, native LDL (0.2 mg/ml), AcLDL (0.2mg/ml) and OxLDL (0.2mg/ml) for 0, 24, 48 and 72 hours respectively. After incubation with lipoprotein, cells were exposed to MTT (0.5mg/ml) for three hours at 37°C. The water-insoluble formazan was solubilised by adding HCl/Isopropanol(1:24). The OD value of each sample was measured using a test wavelength of 570 nm and a reference wavelength of 630nm. Results were expressed as % cells alive using the the zero time point to represent 100%

3.10 Discussion

The foam cell is the main constituent of the fatty streak, the earliest recognisable lesion of atherosclerosis. It also has been implicated to play a role in plaque stability in more advanced plaques and thus may be an appropriate therapeutic target.

The overall aim of these experiments was to assess foam cell formation in the human THP-1 cell line. The human monocytic THP-1 cell line was used because of its close homology to human monocytes and because exposure to PMA leads to its differentiation into a cell line with human macrophage characteristics [184]. Lipid loading of THP-1 cells was examined using native, acetylated and oxidised LDL because modified LDL is the major contributor of cholesterol for foam cell formation *in vivo*. The purpose of these experiments was to demonstrate that THP-1 cells could be differentiated using PMA and that these differentiated THP-1 cells could subsequently take up modified LDL and accumulate more cholesteryl esters than native LDL.

Exposure of THP-1 cells to PMA was shown to result in their differentiation into THP-1 macrophages as shown by light microscopy (figure 3.2). Flow cytometry demonstrated that differentiation of THP-1 cells leads to both an increase in size and granularity of the cells (figure 3.6). Thus flow cytometry confirmed the changes observed in cell morphology by light microscopy when THP-1 cells were differentiated with PMA.

Subsequently after confirmation of differentiation, four different methods were used to assess foam cell formation. Two of the methods; Oil red O staining and fluorescence microscopy were qualitative. The other two methods, nile red fluorescence staining and cholesteryl ^{14}C oleate accumulation were quantitative.

Oil red O staining showed that lipoprotein deficient THP-1 cells had no detectable lipid stores (figure 3.3A). In contrast both differentiated THP-1 cells exposed to native LDL and modified LDL both showed the presence of lipid droplets (figure 3.3B-3.3D). THP-1 cells exposed to modified LDL however, visually showed a larger number of cells with lipid droplets and a greater number of lipid droplets when compared to cells exposed to native LDL. Again visually no detectable difference in lipid stores between the different forms of modified LDL used, namely AcLDL and OxLDL was observed.

Similarly cells exposed to lipoprotein, stained with nile red and viewed using fluorescence microscopy showed increased fluorescence staining in cells exposed to modified LDL (figure 3.5 B, C&E) as compared to cells exposed to native LDL (figure 3.5 A&D). This was only observed in cells viewed for yellow-gold and green fluorescence (figure 3.5 A-E), as red fluorescence was found not to resolve the cytoplasmic contents of the cells (figure 3.5 F&G). This is in agreement with previously reported data [163].

Flow cytometry of nile red stained cells demonstrated an increase in mean nile red fluorescence in cells exposed to increasing concentrations of native and modified LDL (figure 3.8). Mean nile red fluorescence was found to be significantly higher in cells exposed to AcLDL over native LDL at a concentration of 0.2mg/ml lipoprotein. For OxLDL mean nile red fluorescence was found to be higher than native LDL at a concentration of 0.3mg/ml of lipoprotein. Time course data demonstrated an increase in mean nile red fluorescence in cells exposed to both native and modified LDL for up to 72 hours (figure 3.9). Cells exposed to AcLDL showed a significantly greater mean nile red fluorescence than cells exposed native LDL by 24 hours. OxLDL however did not demonstrate this effect until 72 hours.

Flow cytometry data from nile red stained cells showed that exposure to AcLDL lead to cholesteryl accumulation, which was greater than native LDL at a concentration of 0.2mg and at 24 hours. It also showed that accumulation of cholesterol esters was slower and required longer when OxLDL was used as the modified form of LDL. This may be due to the proposed cytotoxic effects of OxLDL that may result in a slower uptake of OxLDL by the cells, or in some cell death as demonstrated in figure 3.11.

Loading with labelled cholesteryl oleate demonstrated a dose dependent increase in cholesteryl ^{14}C oleate accumulation in differentiated THP-1 cells exposed to acetylated and oxidised LDL as compared to native LDL. However at high concentrations of lipoprotein (0.3mg/ml) there was significant decreased accumulation.

Cholesterol loading data also demonstrated that a concentration of 0.2mg/ml of lipoprotein resulted in maximal cholesterol accumulation (in agreement with the flow cytometry results). Cholesteryl ester accumulation was lower using OxLDL than

equivalent concentrations of AcLDL. This is consistent with previously reported data and the possible cytotoxic effects of OxLDL.

Time course data of cholesteryl oleate accumulation demonstrated maximal cholesteryl accumulation by 24 hours (again consistent with flow cytometry results). At longer exposure times there was a decrease in cholesteryl ester accumulation again possibly due to cytotoxic effects of excess lipoproteins. The cytotoxicity assay data suggests that data generated from cells exposed to modified LDL (especially OxLDL) for longer than 24 hours should be interpreted with caution.

Both quantitative and qualitative methods used demonstrated that in our hands exposing differentiated THP-1 cells to modified LDL resulted in an increased accumulation of cholesteryl esters within the cytoplasm of the cell and foam cell formation when compared to native LDL. Furthermore the experimental data presented showed that maximal cholesteryl loading occurred at a concentration of 0.2 mg/ml of modified lipoprotein and after 24 hours, thus these two parameters were used in subsequent experiments aimed at identifying the alteration in gene expression induced by lipid loading in macrophages. In addition a 4-hour time point was also included to identify genes that are differentially regulated relatively early upon exposure to lipoprotein.

Chapter 4: Differential Gene Expression

4.1 Introduction to the concept of gene expression

The discovery of messenger RNA in the early 1960s led to the deciphering of the genetic code and the reporting of the protein synthesis pathway. It was at this time that the concept of gene expression was also introduced. RNA has a central role in allowing DNA to be translated to protein. As such it has often been seen as only an intermediary molecule or 'the servant' to DNA. However the recent discovery of RNA interference, has highlighted that RNA may have a more superior role than that attributed to it in the past [196].

Regulation of gene expression is a hallmark of many cellular processes [197]. Gene expression can specify cellular fate and define responses to stimuli [197]. Inappropriate expression of cellular genes, loss of tumour suppressor genes or expression of genes during interactions with pathogens can contribute to disease processes [197].

The theory behind identifying differentially expressed genes in disease processes is in fact an attempt to understand the underlying molecular mechanisms that may be involved. Identification of differentially expressed genes in experimental models could help understand biochemical pathways involved and reveal potential therapeutic targets [5].

Various methods are currently available for detecting and quantitating gene expression levels. The most commonly used include northern blots, differential display, quantitative RT-PCR and more recently serial analysis of gene expression (SAGE) [198] and microarray technology [197]. Newer techniques such as micorarray technology have largely resulted from the completion of sequencing projects which have included sequencing of the human genome [199]. As PCR revolutionised molecular biology in the late 1980s so array technology has had a major impact on molecular biology in the late 1990s and is likely to do so in this decade.

In the early 90's several groups including Southern [200], Lennon [201], Drmanac [202] and Fodor [203] all simultaneously and independently proposed DNA arrays. Foder's group used an approach similar to that used in the manufacture of computer chips. They combined the process of combinatorial chemistry with

photolithography and produced high density oligonucleotide microarrays. These arrays are manufactured in a series of cycles utilising masks and light directed synthesis. Short 25-mer oligonucleotide fragements are synthesised on a silicon wafer one nucleotide at a time. Each nucleotide carries a photo-labile protection group protecting the oligonucleotide from growing further. This photo labile group can be removed and further nucleotides added by illuminating with light [204]. The precise location of synthesis is determined by the mask.

Utilising this approach the Californian based biotechnology company Affymetrix built the first commercial DNA array and registered the brand name GeneChip®. GeneChip probe arrays can contain as many as 1.3 million different 25-mer oligonucleotide sequences and are now widely utilised within the scientific community.

Since then, the array technology field has exploded with numerous companies and academic institutions providing arrays to the scientific community. In addition to oligonucleotide arrays, other variations of arrays have also been produced. These include arrays containing cDNA clones and PCR products arrayed on glass slide or nylon membranes at high density. Methods other than photolithography to manufacture arrays have also been reported. The company Agilent produces arrays using an inkjet synthesizer analogous to a inkjet colour printers where the dyes are replaced with oligonucleotide bases [205]. Several companies are using digital light processors where light is directed through mirrors rather than through a mask [206].

The main contributors to filter and glass based array technology have been the I.M.A.G.E consortium [207] and Patrick Brown's laboratory at the University of Stanford [208]. Others include Jeff Trent (National Human Genome Research Institute), Alan Robinson (European Bio-informatics Institute) and Geoff Childs (Albert Einstein College of Medicine) and Hans Lehrach (Max Plank Institute). In this study nylon membranes containing PCR products gridded at high density were used as previously reported [209] and will thus be the main focus. Two major supplements 'The Chipping Forecast' and 'The Chipping Forecast II' have been published in Nature Genetics [210, 211]. These provide excellent reading to those unfamiliar with the area of microarray technology.

4.2 Introduction to array technology and differential gene expression

Array technology is one of several approaches to comparatively analyse genome patterns of mRNA expression. The molecular basis of array technology is nucleic acid hybridisation [197]. The main advantage of array technology is that it allows investigators to study the expression of thousands genes in one experiment [197].

Briefly, messenger RNA is isolated from cells or tissues in the conditions to be compared. The isolated RNA is transcribed into cDNA probes and labelled. The labelled cDNA probes are subsequently hybridised to arrays containing cDNA sequences (either cDNA clones or PCR products) gridded at high density (gridded cDNA sequences correspond to genes and ESTs) or oligonucleotide sequences corresponding to a transcript of interest.

There are numerous applications and potential applications of array technology including target discovery, pharmacogenomics, toxicogenomics and diagnostics [210-212]. Microarray technology has also been utilised for SNP discovery [213], resequencing [214] and studying the role of RNA interference [215].

4.3 Designing cDNA arrays

One of the first steps in the manufacture of a cDNA array is to obtain cDNA sequence data in the form of cDNA clones. The most commonly used sources are directly from public sequence databases including I.M.A.G.E. Genbank, dbEST or Unigene [207,216]. Once clones have been obtained, clones or PCR products (obtained from amplification of cloned inserts) representing specific genes or EST sequences are spotted onto a matrix to produce high-density cDNA arrays. The main types of matrix used for producing high-density cDNA arrays are nitrocellulose or nylon charged membranes and glass slides [208].

Single stranded DNA has been found to bind strongly to nitrocellulose membranes. In addition the binding occurs in a way that prevent the DNA strands from re-associating with each other but permits hybridisation to complimentary DNA [217]. Once the DNA has been arrayed it is usually cross-linked to the matrix by ultraviolet irradiation and then rendered single stranded by heat or alkali treatment before use [218].

4.4 Experimental probe preparation and hybridisation

Once cDNA arrays have been prepared, they are hybridised to labelled probes. Probes can be generated from either mRNA or total RNA isolated form the samples of interest. The purity and quality of the isolated RNA is a critical factor in the process [219].

Reverse transcription of the RNA is performed using an oligo dT primer, in the presence of a label to produced labelled 1st strand cDNA [220]. This produces a labelled product from the 3'end of the gene, directly complementary to immobilised cDNA targets. The probe is then applied to the array for hybridisation to occur. For rare samples various amplification procedures can be utilised such as those reported by Eberwine *et al* [221].

4.5 Detection

Hybridisation can be detected by radioactive methods, although fluorescently labelled probes such as Cy 3 and Cy 5 are also commonly used [220]. For radioactive detection, ^{33}P dCTP is used as it has been found to produce a more defined spot image during phosphor imaging than ^{32}P [209].

Hybridisation data of arrays hybridised with radiolabelled probes is captured using phosphorimage screens and a Phosphorimager. During analysis, local sampling of background is used to specify a threshold above which the signal must exceed. Computer software programs are then used to compare arrays from different samples and allow identification of differentially expressed genes. This methodology where differentially expressed genes between different samples are identified after hybridisation to identical cDNA arrays is referred to here as Differential Gene Expression (DGE).

4.6 Overview of Differential Gene Expression

This overview will describe how the cDNA arrays were prepared for the current work described in this thesis

DGE can be split into five main stages as shown in Figure 4.1 (stages A-E).

Figure 4.1 Overview of the steps involved in performing a DGE experiment

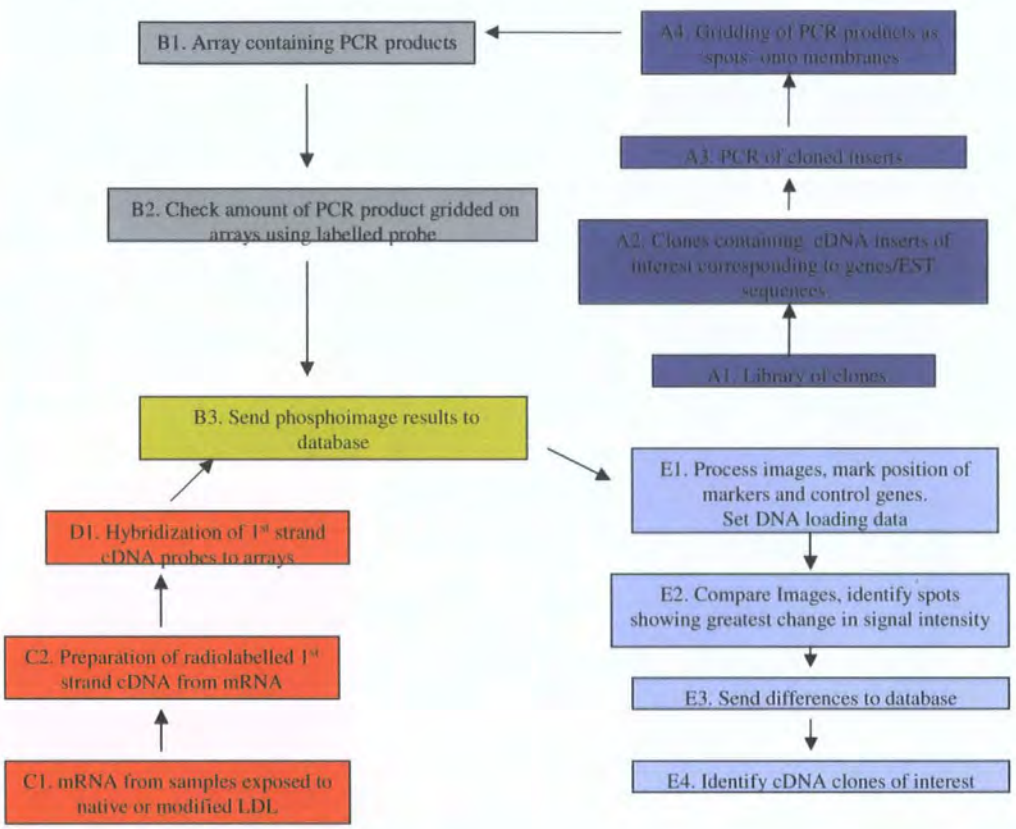

4.6.1 Preparation of cDNA Arrays

As discussed above the first stage (Figure 1; A1-A4) involves preparation of membranes with cDNAs arrayed at high-density (referred to as 'arrays') [209]. The arrays used in these experiments were prepared by the DGE group, Glaxo Wellcome.

The first step in this process involves choosing the cDNA library or libraries that you interested in studying (in these experiment a re-arrayed human I.M.A.G.E library and a custom atheroma library were used; discussed below). The libraries

consisted of vectors that have cloned inserts corresponding to genes or EST sequences. The cloned inserts were amplified by PCR in 384-plate well format. The PCR products were subsequently gridded onto nylon membranes using a robotic arrayer (arrays a large number of PCR products to a very small set area) to produce identical arrays.

All information regarding the library used, PCR conditions and gridding information are stored in a database that links every gridded product to an annotation giving the Gene/EST sequence information. After arraying, the DNA on the membranes is denatured to produce single stranded DNA and cross linked, to fix the DNA onto the arrays.

The arraying of DNA was performed using an arraying robot (Genetix). A three axis controlled drive system carries a 384-pin head, which can be positioned at a resolution of 5μm. PCR products can be arrayed in two patterns, a 5x5 pattern or a 4x4 pattern (depending on the size of the library being used) see figure 4.2.

Each 5x5 pattern contained a central ink guide dot surrounded by twelve PCR products spotted in a duplicate pattern. After hybridisation to experimental probe, the guide dot enabled automatic grid finding and subsequent automatic image analysis using computer software. When a smaller library was used, PCR products were spotted in a 4x4 duplicate pattern. Each 4x4 pattern contained eight PCR products arrayed in duplicate. Luciferase cDNA was also gridded at set positions on the array to be used as a marker and thus assisting image analysis. The 5x5 pattern and 4x4 pattern of arraying are shown below. More information about arraying parameters is given in appendix 2.

3	12	10	5	8
2	11	7	3	4
12	4	X	11	9
6	10	6	8	5
2	1	9	7	1

8	5	8	2
1	3	6	4
6	7	2	5
1	4	3	7

Figure 4.2

Arraying patterns

5x5 arraying pattern
Numbers denote position of arrayed products 1-12
Luciferase DNA is at position 3
X denotes central ink spot

4x4 arraying pattern
Numbers denote position of arrayed products 1-8
Luciferase DNA is at position **8**

4.6.2 The human I.M.A.G.E collection and the custom atheroma array

Gene and EST sequences are commonly deposited in Genbank (a publicly available database for sequence information). The human Unigene database [216] is an experimental system for automatically assigning Genbank sequences into a set of gene-orientated clusters. Some ESTs correspond with known genes, others represent partially sequenced novel genes. The aim of the Unigene project is to have one cluster corresponding to one gene, however this aim has only been partially successful as there is a large degree of redundancy within the database.

The Human I.M.A.G.E collection was started by four academic groups with an aim to share resources on arrayed cDNA libraries from the Unigene collection and make these libraries available in the public domain [207]. The Unigene collection was used to create a master array containing a representative cDNA clone for each gene.

Two separate sets of arrays were used in this study. The first set known as the human I.M.A.G.E arrays, represented a subset of the publicly available Human

I.M.A.G.E library. The clones for this library were obtained from the human I.M.A.G.E collection and re-arrayed (by the DGE group) to produce a collection of clones of interest, representative of the human I.M.A.G.E collection. This was done in an attempt to reduce the level of redundancy. The size of this library resulted in this library being gridded over three separate membranes. Clones (45,000) were arrayed in duplicate in 5x5 patterns on 22cm x 22cm nylon membranes.

Each human I.M.A.G.E array was also gridded with four commonly used housekeeping genes, β-actin, elongation factor 1 (EF-1), glyceraldehyde phosphate dehydrogenase (GAPDH) and ribosomal protein L3 (RL-3) at a range of DNA concentrations. These genes were used as controls between arrays. As noted above, each PCR product was also gridded in duplicate; this was to enable examination of the reproducibility of the results obtained. Using the human I.M.A.G.E library in these experiments allowed a significant proportion of the human genome (that had been sequenced to date) to be studied.

A second set of arrays referred to as the 'custom atheroma' arrays were also used in this study. The custom atheroma arrays contained a range of 769 genes/EST sequences chosen by the Vascular Diseases Unit at GlaxoWellcome as being of interest to their studies (a list of these genes is given in appendix 3). These clones were again chosen from the human I.M.A.G.E collection. In preparing the custom atheroma arrays, all PCR inserts amplified from the I.M.A.G.E clones were also sequenced after being gridded onto arrays (a list of genes whose sequence was confirmed are given in appendix 3). This was done to produce an array on which all the genes gridded had been sequenced to confirm their identity.

The custom array contained 769 genes that were represented by 1035 clones. (Both the custom and I.M.A.G.E arrays contained genes that were represented by more than one PCR product). Including luciferase clones (luciferase cDNA was used as a marker) and blank controls, the custom atheroma array was represented by 1438 PCR products. In addition, each PCR product was arrayed in duplicate and the whole library was gridded twice onto each membrane. Thus the custom atheroma arrays contained 5752 (1438x2x2) PCR products in total, and each PCR product was gridded in quadruplicate. The custom atheroma array was gridded in a 4x4-arraying pattern. Again control genes were also gridded onto the arrays.

4.6.3 Checking for amount of PCR products on arrays

Stage two (Figure 4.1 B1-B3) involves checking the amount of DNA gridded onto the arrays as variation in the amount of PCR product between sets of arrays could generate false changes in gene expression. Before hybridisation is performed with the experimental probes, all arrays are hybridised with a ^{33}P end labelled oligonucleotide specific to the cDNA flanking regions used in the cDNA library. This oligonucleotide specifically anneals to all the spotted PCR products on the array via complimentary binding to part of the plasmid vector sequence. The oligonucleotide used in this case for both the I.M.A.G.E and custom arrays was called M13F (sequence given in section 2.4.3). M13 F (20 pmoles) was radiolabelled for each set of arrays as described in section 2.4.3.1. The amount of label incorporated was determined by measuring radioactive emissions (cpm) before and after purification of the probe as shown in table 4.1. Although DNA loading probes were prepared independently, the probes were pooled and split before being hybridised to each set of arrays to provide an equal amount of DNA loading label across all the arrays.

After hybridisation, the arrays were exposed to phosphorimaging screens and the phosphoimage analysis data was captured. This yields a measure of the DNA loading for every spot on the array. Therefore any differences in DNA loading can be accounted for between different arrays on a spot per spot basis.

Figure 4.3 shows the phosphoimage of a human I.M.A.G.E array after hybridisation with the DNA loading oligonucleotide M13F whilst figure 4.4 shows the phosphoimage of a custom atheroma array after hybridisation with a DNA loading oligonucleotide M13F. After processing, the DNA loading images are assigned experiment numbers and stored in the DGE database until required.

Table 4.1

Table showing percentage incorporation of label for DNA loading probes M13F

Experiment	Counts before purification (cpm)	Counts after purification (cpm)	Percentage incorporation (%)
(A) Control (no LDL)	5220	2705	52
(B) Control (no LDL)	6820	2928	43
(C) 24hr Native LDL	6308	3133	50
(D) 24hr Native LDL	5850	3308	56
(E) 4hr OxLDL	6189	1677	27
(F) 4hr OxLDL	5339	1677	31
(G) 24hr OxLDL	5271	2241	43
(H) 24hr OxLDL	5965	1577	26
(J) 4hr AcLDL	5234	1772	34
(K) 4hr AcLDL	6201	1951	31
(M) 24hrAcLDL	5157	2121	41
(N) 24hr AcLDL	6217	2145	35

Figure 4.3

Phosphoimage of a Human I.M.A.G.E array after hybridisation with DNA loading oligonucleotide M13F (which binds to every arrayed PCR product on the array). Each spot on the array is a PCR product. Arrows points to control genes (which are arrayed in a 2-fold decreasing concentration).

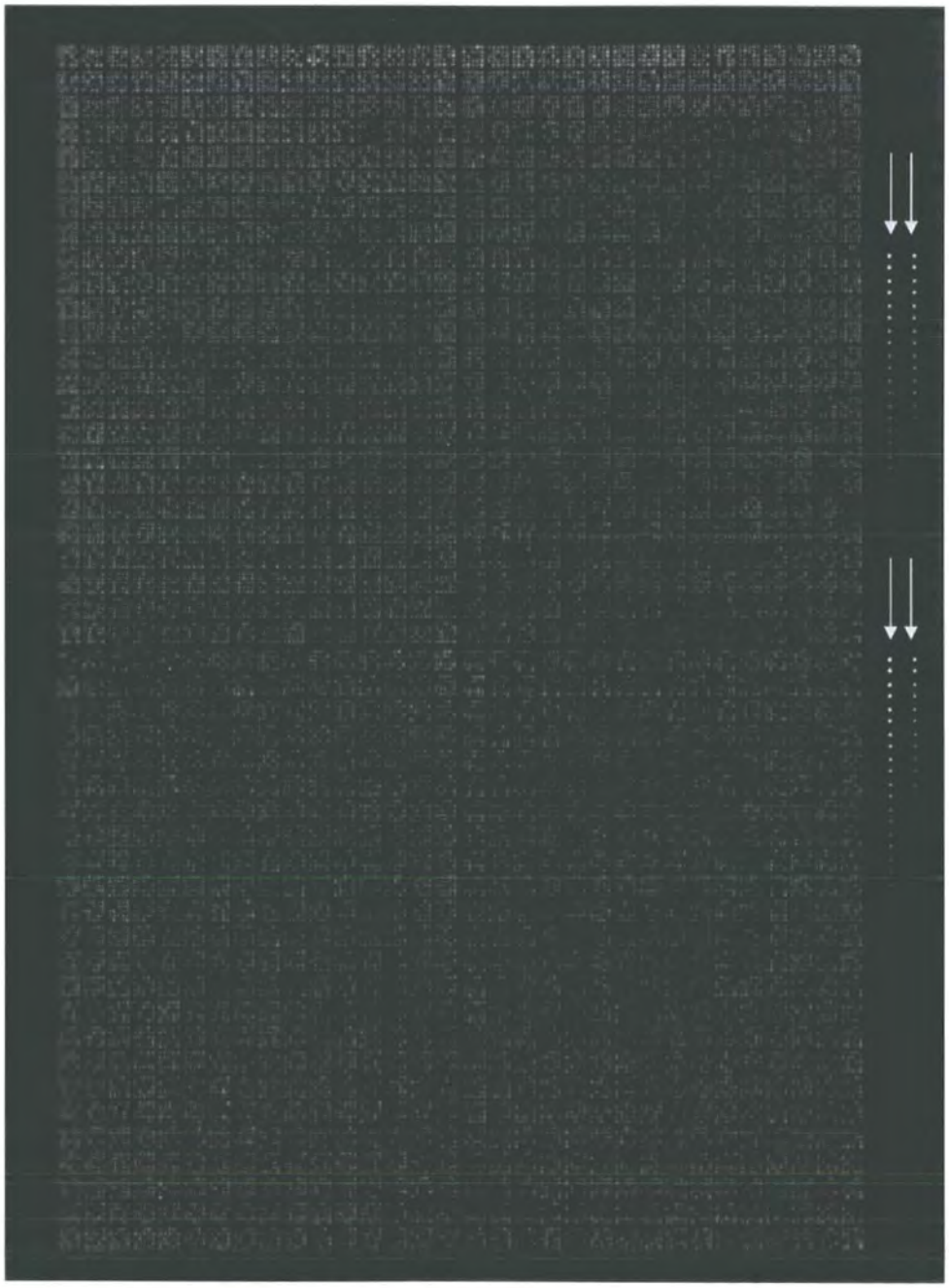

Figure 4.4

Phosphoimage of custom atheroma array after hybridisation of DNA loading oligonucleotide M13F. Each spot on the array represents a PCR product. Arrow indicates control genes (arrayed in a 2-fold decreasing concentration).

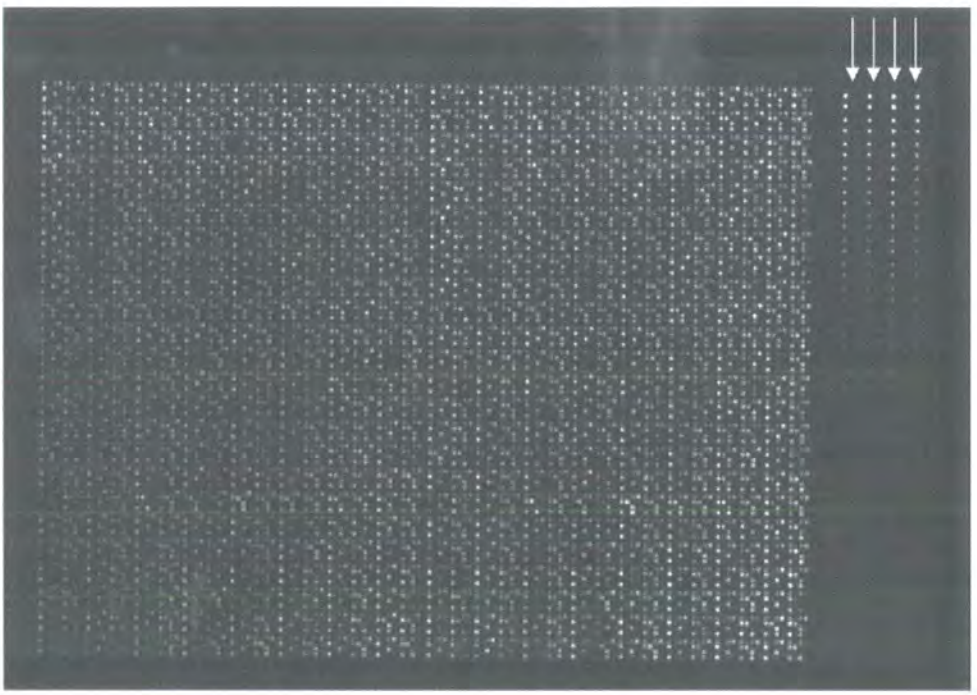

4.6.4 Isolation of mRNA

Stage three (Figure 1 C1-C2) involves the preparation of the cDNA probes. This involves isolating messenger RNA from the samples of interest. RNA preparation from most cell lines is usually a straightforward procedure. Tissue samples and micro-dissections can be more difficult [222]. The problems of having rare amounts of starting material have been overcome by using strategies such as PCR amplification of total cDNA (using random primers) before labelling [223]. In this study direct messenger RNA isolation from samples resulted in a low yield of RNA that was of poor quality (data not shown). To obtain a good yield of RNA of high quality, RNA was isolated in two steps (as described in section 2.4.1). Firstly total RNA was isolated from the samples and subsequently messenger RNA was isolated from the total RNA.

After isolation the RNA was quantified by spectrophotometry to determine concentration and purity. This was to ensure that equal amounts of mRNA were used in cDNA probe preparation. Table 4.2 shows the yields obtained and the A_{260}/A_{280} ratio used as a measure of purity (A_{260}/A_{280} ratio greater than 1.8 used as a measure of a relatively pure preparation of mRNA).

Table 4.2

Table showing RNA spectrophotometer readings at A_{260} and A_{280} and estimation of RNA concentration and purity.

Sample	A_{260} reading	A_{280} reading	A_{260}/A_{280} ratio	RNA yield µg/µl	Total mRNA yield (µg) per $1x10^7$ cells
Control	0.586	0.285	2.05	0.47	4.7
24hr Native LDL	0.580	0.280	2.07	0.46	4.6
4hr OxLDL	0.926	0.448	2.06	0.74	7.4
8hr OxLDL	0.606	0.321	1.89	0.49	4.9
16hr OxLDL	0.490	0.254	1.92	0.39	3.9
24hr OxLDL	0.387	0.188	2.06	0.31	3.1
48hr OxLDL	1.117	0.542	2.06	0.89	8.9
72hr OxLDL	1.773	0.860	2.06	1.42	14.2
4hr AcLDL	1.253	0.604	2.07	1.00	10.0
24hr AcLDL	0.385	0.190	2.02	0.31	3.1

The isolated RNA was also subjected to agarose/formaldehyde electrophoresis to check its integrity (as described in section 2.4.1.4). Figure 4.5 shows mRNA isolated from differentiated THP-1 cells exposed to native and modified LDL that has been subjected to denaturing gel electrophoresis and subsequently stained with Syber Gold (as described in section 2.4.1.4.2). The presence of the 18S and 28S ribosomal bands confirms its integrity. Degraded RNA would be expected to show a smear below the 18S band. Rabbit heart total RNA was used a control marker.

Figure 4.5

Agarose/formaldehyde gel electrophoresis of isolated mRNA showing 18S and 28S bands of RNA after staining with Syber Gold (each lane contains 0.5µg mRNA, except lane 11 which contains 0.6µg total RNA)

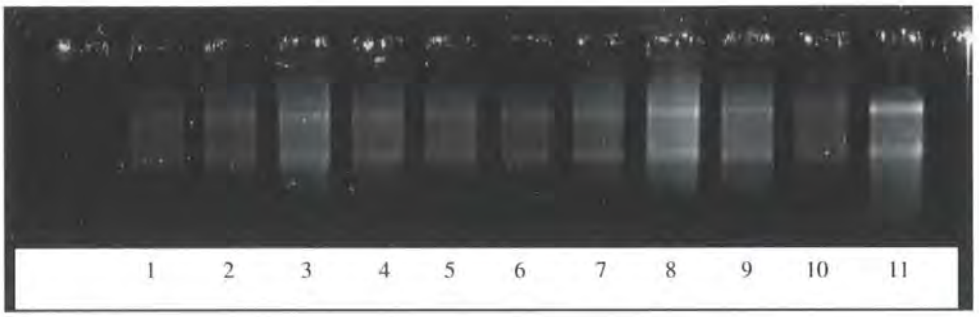

Lane 1	mRNA isolated from differentiated THP-1 cells exposed to no LDL
Lane 2	mRNA isolated from differentiated THP-1 cells exposed to native LDL
Lanes 3-8	mRNA isolated from cells exposed to OxLDL for 4, 8, 16, 24, 48 and 72 hours respectively
Lanes 9-10	mRNA isolated from differentiated THP-1 cells exposed to AcLDL for 4 and 24 hours
Lane 11	control human heart total RNA

4.6.5 Experimental probe preparation

After mRNA isolation, 2µg of mRNA (determined by spectrophtometry) from each sample was transcribed into radiolabelled cDNA probes as described in section 2.4.4. The probes were purified and amount of radiolabel incorporated was measured by determining radioactive emission before and after purification of the probe. Table 4.3 shows percentage label incorporated for the experimental probes.

Table 4.3

Table showing percentage incorporation of label in experimental probe samples

Experimental probe	Counts before purification cpm	Counts after purification cpm	Percentage incorporation (%)
Control A (no LDL)	5860	826	68
Control B (no LDL)	6100	3956	65
24hr Native C	5943	4833	81
24hr Native D	5947	3731	63
4hr OxLDL E	15239	7851	52
4hr OxLDL F	13027	7575	58
24hr OxLDL G	12784	7905	50
24hr OxLDL H	14242	10472	73
4hr AcLDL J	18224	10865	60
4hr AcLDL K	14573	8954	61
24hr AcLDL L	24365	14921	61
24hr AcLDL M	13186	6203	47

After preparation, the cDNA probes were subjected to formaldehyde gel electrophoresis (section 2.4.5) to check that they were intact and their size profile was of full length. Figure 4.6 is a phosphoimage of a gel with experimental cDNA probes. PCR products of known lengths (800bp, 900bp, 1.3kb and 1.5Kb) were run on the gel alongside the samples as markers. As the probes are larger in size (>1.3Kb) than the PCR products they can be confirmed to be of full length. The intensity and location of the radioactive signal also indicates that the probes are intact.

Figure 4.6

Phosphoimage of denaturing/formaldehyde gel showing full-length cDNA probes. Probe preparation (0.08µg mRNA per lane) was loaded in each well of the gel.

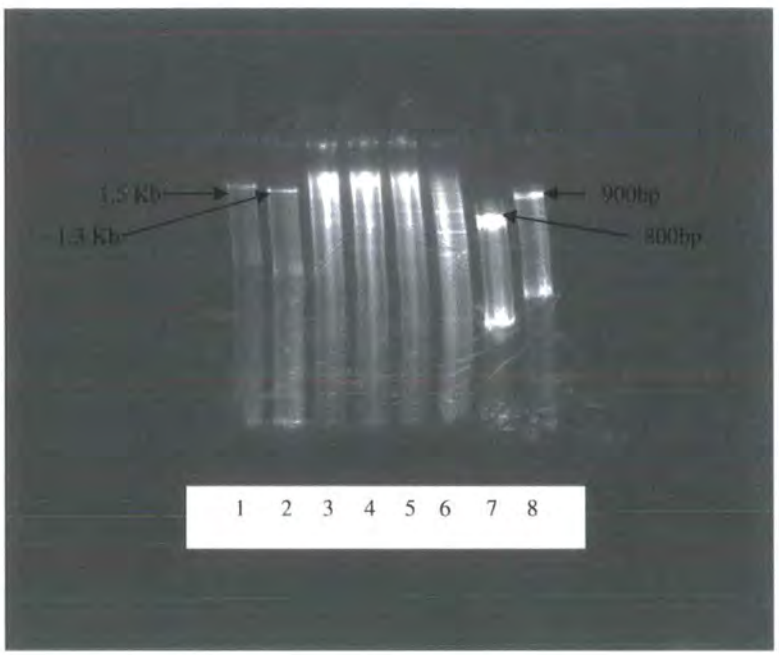

Lane 1, 2, 7 and 8	Control markers; PCR products of size 1.5Kb, 1.3Kb, 800bp and 900bp respectively (as indicated by arrows)
Lane 3	4hr OxLDL cDNA probe
Lane 4	24hr OxLDL cDNA probe
Lane 5	4hr AcLDL cDNA probe
Lane 6	24hr AcLDL cDNA probe

All information regarding amount of mRNA used (2µg of messenger RNA for each probe), its source (differentiated THP-1 cells) and other relevant information such as experimental treatment (native, acetylated or oxidised LDL), name of investigator were entered into a database where each probe was automatically assigned a unique identity number.

4.6.6. Hybridisation

Stage four involves the actual hybridisation (Figure 4.1 D1). The full-length cDNA probes were allowed to hybridise to the arrays for 3 days as described in section 2.4.6.

After hybridisation and washing, arrays were placed between a plastic sheet and cling film in developing cassettes and placed next to a phosphorimage screen for two days. The data on the phosphorimage screens was then captured using a Phosphorimager and edited using a computer software program called Image Quant. Unedited and edited files are given different names and stored in the DGE database until required. The unedited image files provided a back up should there be problems with the edited image files during comparisons. Raw data unedited image files were named according to the following convention

- the experimenter's initials (2 characters).
- day and month (4 characters).
- 1 character (a, b, c, d, etc...) for indicating more than one image generated by the same person on the same day.
- the last character was an L or H signifying either DNA loading (L) or cDNA hybridisation (H) image.
- Files were always named and stored as .gel files.

4.6.7 Data Analysis

Stage five involves data analysis (Figure 1E). The data captured from the phosphorimaging screens were edited and stored as described above. The electronically captured data files (for DNA loading or cDNA hybridisation) were analysed using DGENT, a PC based piece of software developed by the DGE group at Glaxo Wellcome.

The positions of all the corner spots of a hybridisation image were marked. Other parameters such as the position of the luciferase spots were also set (processing parameters are given in appendix 2). The DGENT application subsequently identifies the location of cell spots present (using the central ink spot and the luciferase marker spots) and then predicts where spots would have been present for those that did not generate a significant signal. Thus by this method every co-ordinate where a DNA

spot was gridded can be located. The intensities of all spot co-ordinates are measured and local background is subtracted. The intensities of all the co-ordinates of an image are then saved to the DGE database.

4.7 Analysing DGE results

Two different hybridisation images of interest were compared using the DGENT application (this piece of software also enables comparisons between arrays to be performed). Before a comparison was performed, the DNA loading image data was associated with the corresponding hybridisation data so that any differences in DNA loading are corrected for on a spot to spot basis when the comparison was performed. Normalisation was then set using either housekeeping genes, or the median array intensity. This ensures standardisation between arrays. Figure 4.7 shows DGE Windows software generated image for analysis of the control genes. Figure 4.7 shows two graphs one for the control genes, elongation factor-1 and β-actin (top graph) and one for GAPDH and RL-3 (bottom graph). As can be seen from the graphs, EF-1 and β-actin showed a linear relationship between DNA spot loading and cDNA hybridisation whereas GAPDH and RL-3 did not. Thus subsequently EF-1 and β-actin were chosen as the control genes for normalisation between arrays.

Once DNA loading and normalisation steps had been performed within the DGE application, the two images of interest could be compared. The DGE software presented the results of such a comparison as a table showing the largest differences in cDNA hybridisation at the top. In the comparison table image spots were subsequently viewed a pair at a time, to verify that there was a clear difference as opposed to artefacts on the image.

Figure 4.8 below shows a comparison between two I.M.A.G.E arrays. The table shows the largest differences found between the two arrays. Differences were sent to the DGE database where the co-ordinates of clones relating to observed differences can be identified. The link between a spot location on an array and the plate/well location and identity of the PCR product and cDNA clone it was derived from were deciphered using another piece of computer software called filter modules (software developed by the DGE group) as shown in Figure 4.9.

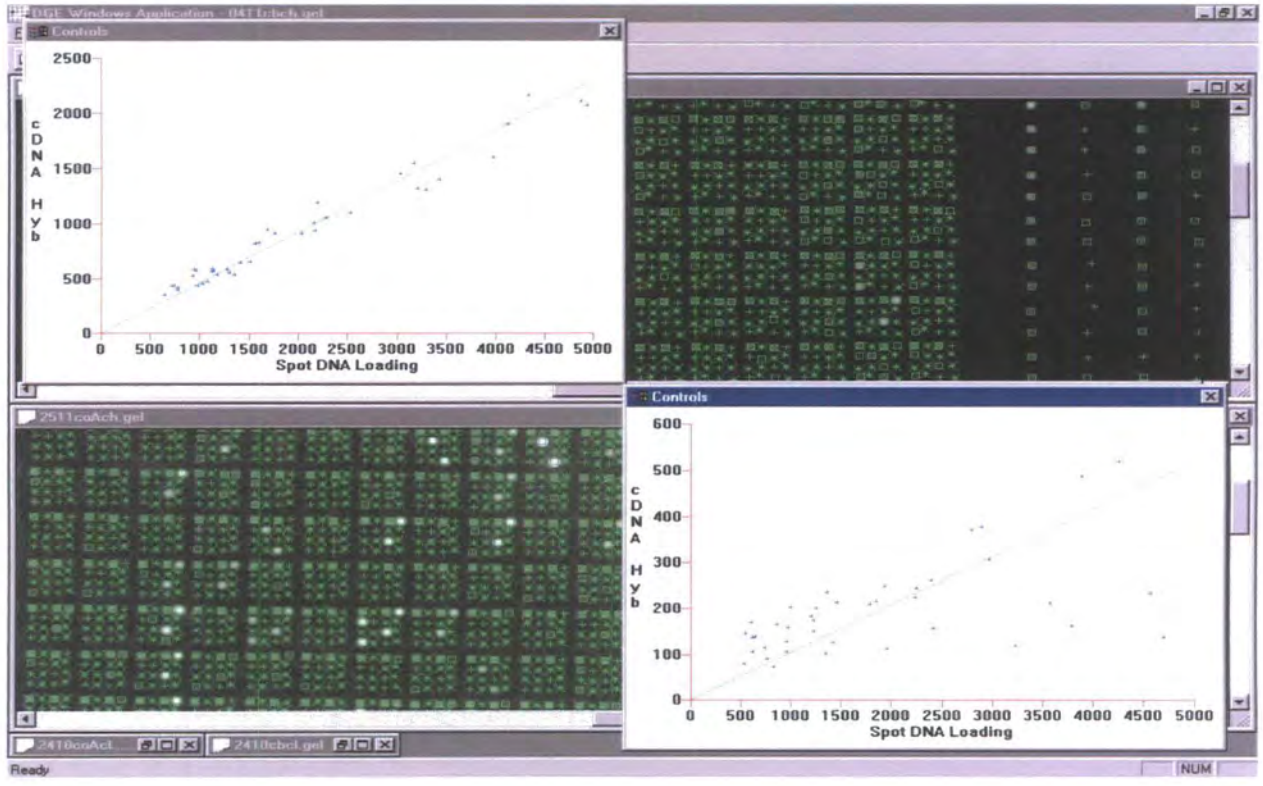

Figure 4.7

DGE Windows application image showing processed custom atheroma arrays in the background and graphs for control genes automatically generated by the DGE software. Top graph shows the genes elongation factor-1 and β-actin. Bottom graph shows the genes GAPDH and RL-3.

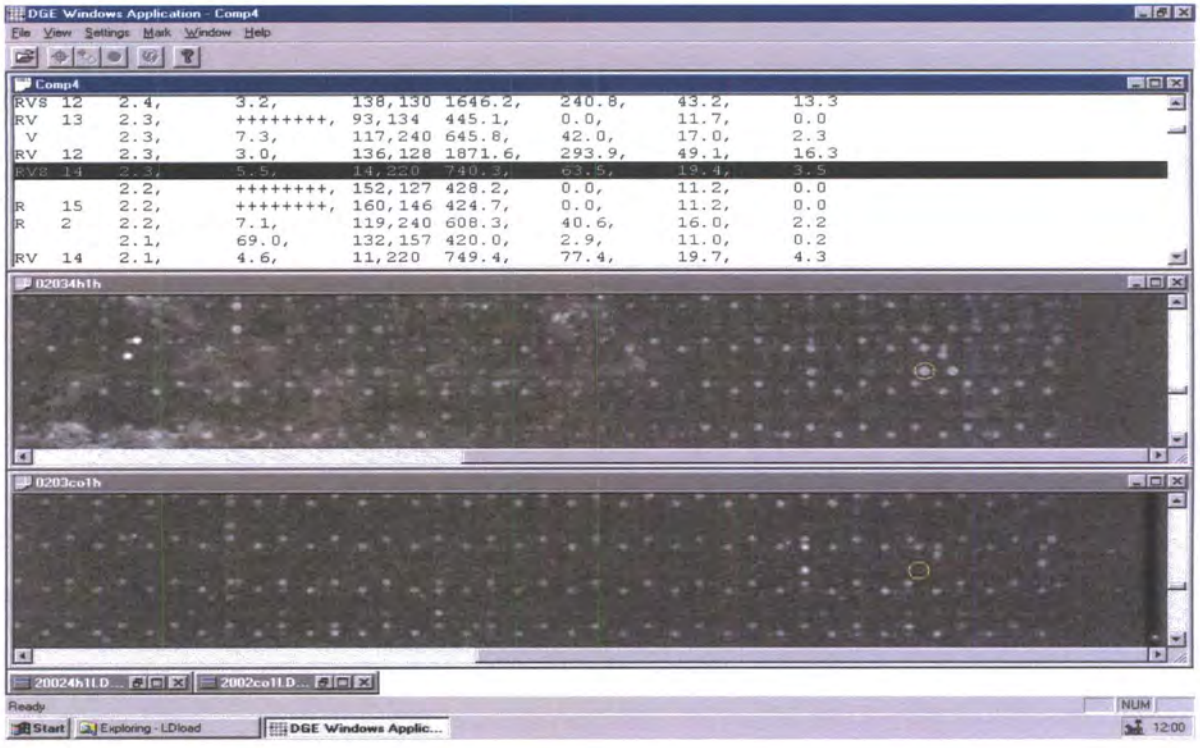

Figure 4.8

DGE application showing two I.M.A.G.E arrays being compared. Two circles indicate spot being compared with top circle a spot present and bottom circle showing a spot absent. The software automatically presents the differences found as a table shown at the top. Luciferase marker spots are indicated and are clearly visible.

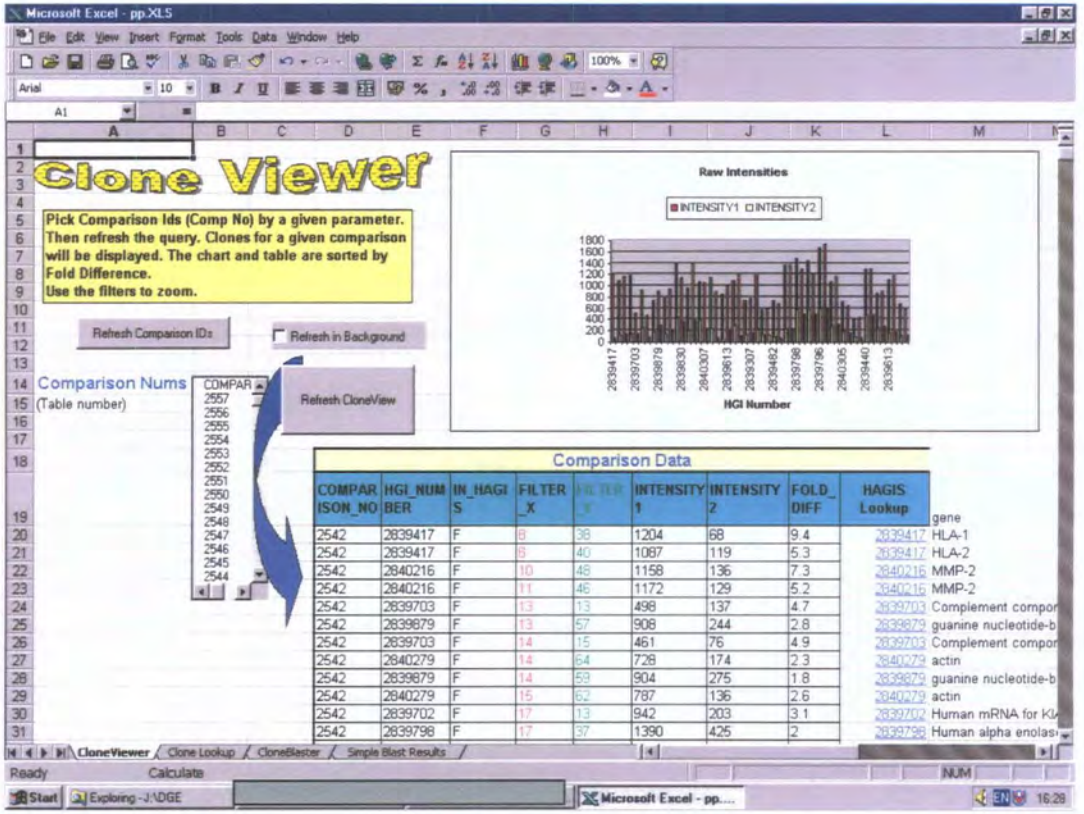

Figure 4.9

Image showing example of software used to interpret array comparison results. Comparison data is given in a table. The software also automatically generates a graph of raw intensity data.

The software lists the results in both table and graph format. The results were presented in table format sorted by the largest fold difference. The table also shows the unique database identifier (HGI number) for a cDNA clone, position of the spot (X, Y coordinates) in the filter and spot intensities 1 and 2 (these are uncorrected intensities, which are also plotted on a graph automatically generated by the software). The HGI number is subsequently used to find the identity of the clone and the gene/EST to which it corresponds. For the sequence verified atheroma arrays, the gene name could be determined immediately. However for 'hits' identified from the Human I.M.A.G.E arrays, it was necessary to identify the clones, prepare the PCR products and have them sequenced to determine their identity.

4.8 DGE database access and features

All information regarding cDNA library picking and arraying formats of PCR products was maintained within a database called the DGE database. The DGE database was maintained on a computer in the UK that was a central repository for all DGE data collected worldwide for Glaxo Wellcome. Data input into the central DGE database was performed through web based modules. These web-based modules were of four main types.

(a) DGENT Image processing

This was a windows based software package (developed by the DGE group), which processes arrays images, allows array comparisons and downloads the results to the database.

(b) Bioinformatics spreadsheets

These were Excel spreadsheets that are downloaded over the web and used in Excel 97. They allow the investigator to look at data in the database relating to comparisons, libraries, probes, blast results, arraying and plate/well locations of cDNA clones (as shown in Figure 4.9)

(c) Acquire on the Web

These were data input modules that allow the investigator to input data into the DGE database including entering probe information, the library used for arraying, the name of the experimenter and comparisons performed.

(d) Expression Profiling

These link DGE comparisons and raw data to information about the clone, including descriptions from Unigene, Genbank and Blast searches.

4.9 Discussion

The work presented in this chapter has demonstrated in detail the steps involved in performing a DGE experiment. In addition the results obtained at each stage of the process have been presented. The results showed that mRNA isolated was successfully isolated from differentiated THP-1 cells exposed to native, AcLDL and OxLDL and was used to synthesize 1st strand cDNA probes. These cDNA probes were then hybridised to high-density cDNA arrays. Finally the hybridisation data obtained was processed and stored in a database for subsequent analysis to identify differentially expressed genes.

Chapter 5: Gene Regulation in response to native and modified LDL

5.1 Introduction

The aim of this study was to compare genes being regulated on exposure of differentiated THP-1 cells to native and modified LDL. A relatively new technique, referred to here as Differential Gene Expression (DGE) technology (but also referred to in the literature by a variety of terms including cDNA array technology and DNA chips) was used, rather than other commonly used molecular biology techniques to examine gene expression (such as differential display or RT-PCR). DGE technology has the advantage of allowing the expression of thousands of genes/EST sequences to be analysed simultaneously [197]. It should be noted that this technology was still in a developmental stage during the course of this thesis. This posed the challenge of using a technology that was not fully established. DGE experiments however were successfully performed as demonstrated in Chapter 4. In addition, the technology has now become widely accepted within the scientific community.

5.2 Experimental design

THP-1 cells were differentiated as described in the methods (section 2.1.2) Cells were then exposed to medium containing BSA but without FBS. This cleared the cells of any exogenous lipoprotein (section 2.1.2). At this stage the cells were ready for the addition of lipoprotein. Differentiated THP-1 cells were then exposed to native LDL, AcLDL and OxLDL (all at concentration of 0.2 mg/ml) for 24 hours. A sample of differentiated THP-1 cells exposed to media only (no lipoprotein) for twenty-four hours was used as a control sample. In addition two samples were also prepared from differentiated THP-1 cells exposed to AcLDL and OxLDL for four hours with the aim of identifying genes that were expressed early on after exposure to modified lipoprotein. Messenger RNA was isolated and labelled 1st strand cDNA probes were prepared for the following samples (as described in sections 2.4.1. and 2.4.4): -

Control sample	Differentiated THP-1 cells. This sample represented lipoprotein-depleted cells (cells were incubated in lipoprotein deficient medium; section 2.1.2.)
Native sample	Differentiated THP-1 cell exposed to 0.2 mg/ml native LDL for 24 hours. This sample represented lipoprotein replete cells (compared to the control sample) since exposure to native LDL results in the availability of cholesterol.
Acetylated samples	Differentiated THP-1 cells exposed to 0.2 mg/ml of AcLDL for 4 and 24 hours. These samples represented a non physiological ligand taken up specifically by scavenger receptors and a mild form of lipid loading
Oxidised samples	Differentiated THP-1 cells exposed to 0.2 mg/ml of OxLDL for and 24 hours. These samples represented a more extreme and toxic form of lipid loading.

The prepared probes were then applied to both custom atheroma arrays and human I.M.A.G.E arrays described; section 2.4.6. All mRNA samples were prepared from duplicate experiments and applied to duplicate sets of arrays independently as shown in figure 5.1 (two identical probes were separately prepared from two independently isolated mRNA samples obtained from two identically treated sets of cells: the probes were then applied to two separate but identical arrays). Arrays were then edited and processed using DGENT software as described (section 2.4.7). After processing, DNA loading images were associated with the experimental hybridisation images and normalisation set using control genes β-actin and RL-3. Comparisons were then performed using DGENT software.

Table 5.1 below lists the comparisons performed (for both the I.M.A.G.E and custom arrays). For each set of comparisons, samples were compared in both directions to determine up-regulated and down-regulated genes. As all samples were prepared in duplicate, 4 sets of data lists were generated for each comparison direction performed. (For array A being compared against array B there will also be the

duplicate samples C and D respectively, therefore comparisons performed will be A/C, A/D, B/C and B/D).

Figure 5.1

Diagram showing steps involved in performing array comparisons.

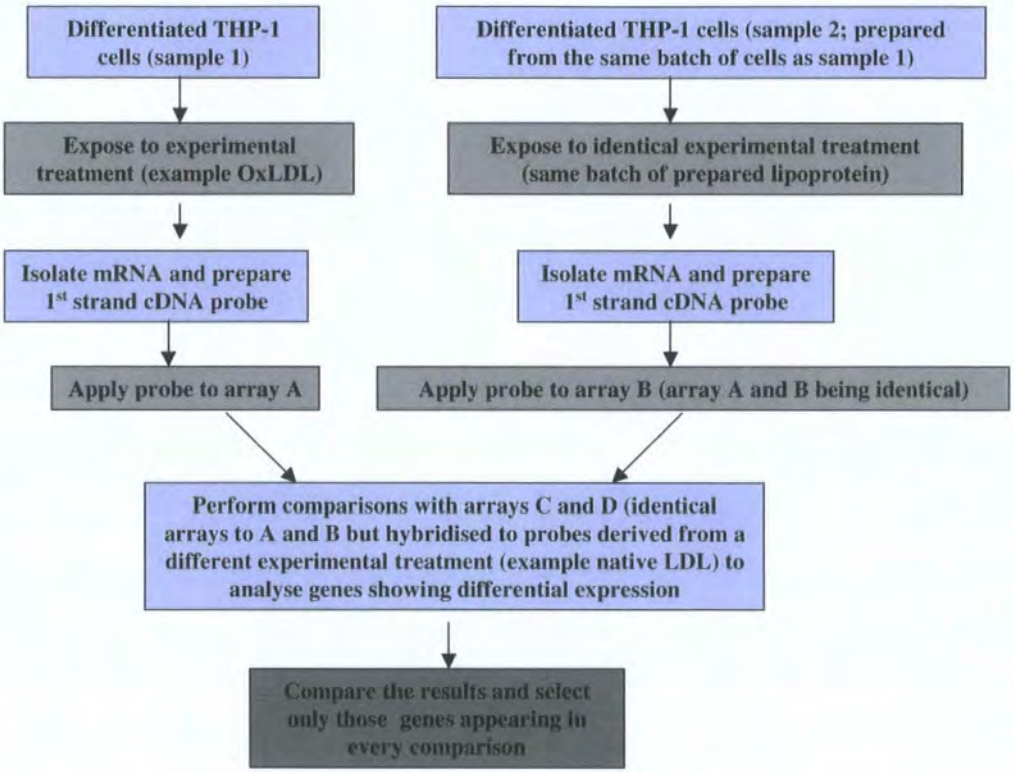

The four lists of data obtained for each comparison were compared against one another and only differences that appeared in each of the data sets were identified as definite differences for that comparison. Thus a final comparison list of genes was compiled and this final comparison list was assigned a unique comparison identification number. A list of comparisons performed and the comparison identification numbers assigned is given in appendix 4.

Table 5.1 Table showing a list of the comparisons performed and the aim of performing these comparisons.

Comparsion	To aim to identify
Native versus control	Genes regulated by native LDL (lipid homeostasis)
24hr OxLDL versus control	Genes regulated by OxLDL
24hr AcLDL versus control	Genes regulated by AcLDL
24hr OxLDL versus native	Genes regulated specifically due to OxLDL
24hr AcLDL versus native	Genes regulated specifically due to AcLDL
24hr OxLDL versus 24hr AcLDL	Genes regulated by OxLDL and not AcLDL and *vice versa*
24hr OxLDL versus 4hr OxLDL	Genes regulated on early and late exposure to OxLDL
24hr AcLDL versus 4hrAcLDL	Genes regulated on early and late exposure to AcLDL
4hr OxLDL versus 4hr AcLDL	Genes regulated on early exposure to by OxLDL only and not AcLDL and *vice versa*

5.3 Reproducibility of results

As stated above, each sample used in this experiment was prepared in duplicate and applied to two sets of identical arrays (for both I.M.A.G.E and custom arrays). For each duplicate sample, the only common source was starting material (namely differentiated THP-1 cells) and lipoprotein preparation (native, acetylated and OxLDL). Messenger RNA preparation, cDNA probe preparation and hybridisation were all performed independently for each of the duplicate samples. This meant that each comparison could be performed four times in each direction and only those results appearing in every one of the four lists generated for that comparison were taken as definite differences for that comparison.

All genes on the arrays were gridded in a duplicate pattern (for both the custom atheroma and I.M.A.G.E arrays) therefore each gene was gridded at least twice. In addition for the custom atheroma array, some genes were gridded up to sixteen times (full gridding details given in appendix 3). In general, genes were included only when both 'spots' representing the gene were differentially expressed. Each array used in these experiments also contained commonly used housekeeping genes, β-actin, GAPDH, RL-3 and EF-1. These housekeeping were used as controls between samples so that any variation in expression between arrays was normalised using the expression of levels of housekeeping genes. In these experiments, β-actin and EF-1 were used.

5.4 Sensitivity of detection

The minimum fold difference used for detecting a change in expression of a gene in a particular comparison was 1.5 fold. Although this meant that genes showing a smaller fold difference were not detected, genes that were detected were more likely to be real changes rather than artefacts on the array. The DGE group has been able to detect changes as small as 1.2 fold; routinely however a 1.5 fold difference level was used. (The minimum fold change detectable was determined by the DGE group by comparing the expression levels of samples containing genes with a known fold difference [determined by northern blots and RT-PCR]. Messenger RNA was labelled into cDNA probes and hybridised to arrays. Arrays were subsequently analysed to determine the minimum fold difference that could be detected).

During processing of arrays, background noise on the arrays was minimised using a threshold signal of 200 pixels. Thus only genes being expressed over the threshold value were automatically identified. This had the effect of excluding low abundance genes. A gene for example showing a change from 20 to 200 pixels has the same fold difference as one showing a change from 10 to 100 pixels, however the latter would be excluded due to the threshold value used. Using a threshold value however has the advantage of excluding background signal generated by the hybridisation image and subsequently following through a large number of false positives. Using messenger RNA rather than total RNA also increased the sensitivity of detection.

5.5 Results from custom atheroma array comparisons

Due to the relatively large amount of data generated from these studies, the data obtained is not presented in its entirety in this chapter but has been given in final form in appendix 5 and appendix 6 (see attached CD). The data instead has been summarised overall in respect to total numbers of genes up- and down-regulated, genes showing highest up and down regulation, genes of interest, genes regulated specifically by OxLDL and AcLDL and possible function/roles of the genes during foam cell formation. The results presented here have focused on the custom atheroma arrays. Results from the human I.M.A.G.E arrays have been presented but are not discussed in detail.

The genes on the custom atheroma arrays were chosen by the Vascular Diseases Unit at Glaxo Wellcome who were interested in studying gene expression in atherosclerotic plaques from patients who had died from myocardial ischemia. Thus, although this array was not designed specifically to look at genes thought to be regulated during foam cell formation, the array did contain genes with relevance to atherosclerosis such as inflammatory molecules, signalling molecules, lipoprotein/modified lipoprotein receptors and cytokines.

As noted in chapter 4 the custom atheroma gird consisted of 769 genes represented by 1054 clones. The custom array results tables given in appendix 5 (Excel workbook; named "appendix 5 custom array results") lists all the genes found to be differentially expressed for the comparisons performed. Each table lists the comparison, the name of the gene, the mean fold difference (since most of the genes on the array were gridded, and therefore detected, more than once), the standard deviation of the mean and the comparison number. As noted above, each PCR product was gridded at least twice on each array for both the I.M.A.G.E and custom arrays. In addition, for the custom atheroma array, most of the PCR products were arrayed 4 or 8 times. Full arraying details are given in the atheroma array template (Appendix 3 Excel workbook containing worksheet labelled "array template"; appendix 3.3).

For the custom atheroma arrays, the arrays hybridised to the 4hr AcLDL probe did not produce hybridisation data of sufficient quality that could be processed. The reason why the custom arrays hybridised to the 4hr AcLDL probe producing poor hybridisation data is unclear, since mRNA was successively isolated and the cDNA for AcLDL probes was sufficiently labelled. However the failure could be attributed

to a number of other reasons including poor hybridisation of the probe to the array, problems with arraying of PCR products onto the membrane or problems with fixing and denaturing the DNA on the arrays. The 4hr AcLDL custom arrays were subsequently excluded from the comparisons on the basis that no data was produced from them. This meant that two of the comparisons that were intended to be performed were not performed. These were the AcLDL (24) versus AcLDL (4) and OxLDL (4) versus AcLDL (4) comparisons. Note that this only applies to the custom atheroma arrays. These comparisons were performed for the human I.M.A.G.E arrays. Unfortunately repeating the experiment for this time point was not within the remit of the time slot allocated to perform DGE experiments.

5.5.1 Total number of regulated genes

Graph 5.1 below shows the numbers of genes showing up and down regulation for each of the comparisons performed using the custom arrays. For example for the native versus the control comparison, 54 genes showed a greater expression level on the arrays hybridised to the native LDL probe that the arrays hybridised to the control probe. Similarly 13 genes showed a greater expression on the arrays hybridised to the control probe when compared to the arrays hybridised with the native probe.

Due to software limitations arrays could only be assessed in one direction, namely those that were up regulated (for example it was not possible for the software to determine when expression level of genes on arrays exposed to native LDL were less than that of genes on arrays exposed to control LDL). To determine these genes, one had to compare the level of genes on arrays exposed to control probe showing higher expression than genes on arrays exposed to native LDL probe. In other words only native > control and control > native comparisons could be performed and not native < control or control < native comparisons.

An important point to note here is that the DGE experiments do not give absolute levels of expression; rather they simply compare levels of expression between two samples and look for differences between the levels which are then presented as a fold difference. Thus although the system detects expression levels (via the hybridisation intensities) these are not presented to the end user who receives only a fold difference due to software limitations.

Graph 5.1 Graph showing number of genes up-regulated and down-regulated for each comparison performed using the custom atheroma arrays

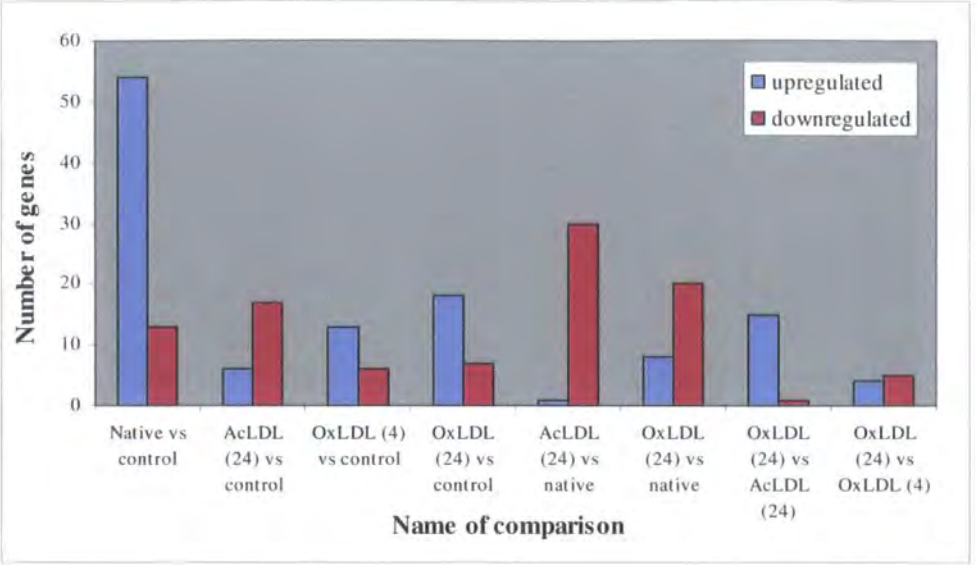

As can be seen from graph 5.1, of all the comparisons performed, the greatest number of genes up-regulated are due to native LDL (when compared to control).The greatest number of down-regulated genes were due to AcLDL (24), (when compared to native LDL). When OxLDL (24) was compared with AcLDL (24), there were more genes up-regulated due to OxLDL (24) than due to AcLDL (24). This could be consistent with the fact that OxLDL is thought to be a more potent ligand than AcLDL due to the presence of oxysterols in OxLDL. However when compared to native LDL both AcLDL (24) and OxLDL (24) showed more genes down-regulated than up-regulated.

The tables below (Table 5.2 – Table 5.9) show the top five up- and down-regulated genes for each of the comparison performed (where there were less than five genes found, all the genes are listed). Gene functions, where known, are given in brackets and were derived from the Genecards database (at the internet site http://www.nciarray.nci.nih.gov/cards; reference [224]). The tables also give the mean fold difference and the standard deviation. Full tables of results in are given in appendix 5.

5.6. Genes regulated on exposure to lipoprotein

5.6.1. Native LDL versus control

This comparison compared cells exposed to native LDL (the physiological form of LDL, found *in vivo*) with control cells that were depleted of lipoprotein. This represents a lipid-depleted and lipid-replete situation where exposure to lipoprotein results in the availability of cholesterol and triglyceride to some extent. As would be expected in such a situation, this comparison contains a large number of up-regulated genes. This comparison showed 53 genes up-regulated (native > control) and 16 down-regulated (control > native). The top up and down regulated genes are given in table 5.2. It is worth nothing that GAPDH, a commonly used housekeeping genes in expression studies showed a 4.2 fold change in expression.

5.6.2. AcLDL (24) versus control

This comparison compared expression levels of genes in cells exposed to AcLDL (at 24 hours) with control cells (lipid-depleted cells). This comparison showed 6 genes up-regulated and 17 genes down-regulated on exposure to AcLDL for 24 hours. Table 5.3 shows the most highly up- and down-regulated genes. The aim of this comparison was to identify genes being regulated by AcLDL, however it does not take into account that native LDL may also regulate these genes. Genes showing expression specifically due to AcLDL are identified through the AcLDL versus native comparison (given below).

Table 5.2 Table showing up and down-regulated genes when comparing native LDL with control

Comparison: native versus control		
Name of gene	*Fold difference*	*Standard deviation*
up-regulated		
Activator-1, 37kD subunit	8.30	0.99
Human mRNA for KIAA0201 gene (human protein; unknown function)	8.25	2.35
Homo sapiens $GlcNH_2$-3-0-SO_4 sulphoT	8.20	0.42
Human mRNA for XP-C repair complementing protein (p58/HHR23B)	7.45	0.78
Human ribosomal protein L37a mRNA sequence (*ribosomal protein*)	7.35	1.12
down-regulated		
HLA-2	7.35	2.90
Matrix metalloproteinase 2 (collagenase type IV) (*involved in tissue and ECM degradation*)	4.85	1.98
Complement component 1, S subunit	4.80	0.28
β -cantenin	4.20	1.46
GAPDH (*housekeeping gene*)	4.15	1.46

Table 5.3 Table showing up- and down-regulated genes when comparing AcLDL (24) with control

Comparison AcLDL (24) versus control		
Name of Gene	*Fold Difference*	*Standard deviation*
up-regulated		
IL-1β (*inflammatory molecule; chemoattractant and sustains the inflammatory response*)	3.73	1.21
Human ribosomal protein L37a	2.70	0.36
Lymphocyte cytosolic protein 1 (L-plastin)	2.25	0.07
Human mRNA for translationally controlled tumour protein (*found in healthy and tumor cells*)	2.02	0.15
Thymosin beta10 (*thymic hormone*)	2	0.00
down-regulated		
MMP-2 (type IV collagenase)	20.10	9.90
GAPDH	8.05	1.77
Human alpha enolase mRNA (*glycolysis enzyme*)	7.00	0.57
Moesin	5.60	2.55
β actin mutant (*Ubiquitously expressed gene*)	1.75	0.71

5.6.3 OxLDL (24) and OxLDL (4) versus control

These comparisons compare expression levels of genes in cells exposed to OxLDL (at 4 and 24 hours with the control (lipid-depleted cells). This comparison showed 13 genes up-regulated on exposure to OxLDL for 4 hours and a higher number, 18 genes up-regulated on exposure to OxLDL for 24 hours. Both time points showed similar numbers of genes down-regulated (6 and 7 for the 4 and 24 hour time points respectively). Thus although the number of genes regulated by OxLDL is less than

those by native LDL it is higher than the number regulated by AcLDL. In addition, as would be expected there are more genes up-regulated by OxLDL after 24 hours than 4 hours. Table 5.4 and 5.5 show the most highly up and down-regulated genes for the 4 hour and 24 hour OxLDL time points respectively. These comparisons aim to identify genes being regulated by OxLDL however similar to the AcLDL versus control comparison these comparisons do not take into account that these genes may also be regulated by native LDL. Those genes showing expression specifically due to OxLDL are identified through the OxLDL versus native comparisons (shown below).

Table 5.4

Table showing up- and down-regulated genes when comparing OxLDL (4) with control

Comparison OxLDL (4) versus control		
Name of gene	*Expression level*	*Standard deviation*
Up-regulated		
GAPDH	11.85	9.83
Epithelin 12	10.50	7.92
Guanine nucleotide binding protein Rho	6.25	1.20
Profilin	5.15	0.07
Urokinase (uPA)	3.75	0.49
Down-regulated		
Lipocortin II (*calcium regulated; involved in exocytosis, may have an anti-inflammatory role)*	5.15	0.64
Wnt-13 (*involved in cell/tissue development*)	3.45	0.95
p21 homologue	3.35	1.11
β2 microglobulin gene	2.20	0.14
23 Kd highly basic protein (*60s ribosomal protein*)	2.05	0.07

Table 5.5

Table showing up- and down-regulated genes when comparing OxLDL (24hr) with control

Comparison: OxLDL (24) versus control		
Name of Gene	*Fold difference*	*Standard deviation*
up-regulated		
Metallothionein (*binds various heavy metals*)	26.2	4.53
Homo sapiens Wnt-13 mRNA	10.0	0.88
Human mRNA for KIAA0312 gene (*human protein; unknown function*)	6.30	1.76
Human mRNA for lymphocyte function associated antigen-3 (LFA-3)	5.55	0.07
CD36 (*macrophage scavenger receptor; binds OxLDL*)	4.55	0.64
down-regulated		
MMP-2 (collagenase type IV)	6.10	0.57
β -actin	6.05	0.78
GAPDH	5.38	3.15
Human alpha enolase mRNA	4.74	1.67
Profilin (J03191)	3.8	0.14

5.6.4 Genes regulated specifically by AcLDL

This comparison compared expression levels of genes in cells exposed to AcLDL (for 24 hours) with cells exposed to native LDL (for 24 hours) in order to identify genes being regulated specifically by AcLDL. This comparison showed only 1 gene up-regulated and 30 genes down regulated on exposure to AcLDL. Table 5.6 shows the most highly up and down-regulated genes over 24 hours.

Table 5.6 Table showing up- and down-regulated genes when comparing AcLDL (24) with native LDL (24)

5.6.5 Genes regulated specifically by OxLDL

Comparison AcLDL(24) versus native		
Name of gene	*Expression level*	*Standard deviation*
up-regulated		
Interleukin- 1β	1.60	0.00
down-regulated		
Human mRNA for fibronectin (*involved in cell adhesion, cell motility, wound healing and maintaining cell shape*)	6.25	1.71
14-3-3 protein, theta isoform	5.90	3.25
CD36	5.80	0.64
Human RPS3a gene (ribosomal protein)	5.78	0.94
Human cyclophilin like protein mRNA	5.5	2.12

This comparison compared expression levels of genes in cells exposed to OxLDL (at 24 hours) with cells exposed to native LDL in order to identify genes specifically regulated specifically by OxLDL. This comparison showed 8 genes up-regulated and 20 genes down regulated. Table 5.7 shows the top highly up and down-regulated genes. Note that the 4hr OxLDL was not compared to the native sample as the native sample had been prepared by exposing cells to native LDL for 24 hours. (A sample of cells exposed to native LDL for 4 hours would be required to perform this comparison, which was not prepared for this study due to limitations in the number of DGE experiments that could be performed).

Table 5.7

Table showing up- and down-regulated genes when comparing OxLDL (24) with native LDL (24)

Comparison Ox LDL(24) versus native		
Gene name	*Fold difference*	*Standard deviation*
Up-regulated		
Metallothionein	7.30	3.29
Human c-jun proto oncogene	3.75	1.10
Homo sapiens mRNA for alpha (1,2) fucosyltransferase	2.75	0.07
MMP-2 (type IV collagenase)	2.55	0.49
Proliferation associated gene (pag) (enhances natural killer cell activity)	2.25	0.07
down-regulated		
Fibronectin	7.38	2.04
Human mRNA for fibronectin precursor	7.18	1.21
Human Mac-30 mRNA	6.28	1.28
Myosin regulatory light chain	5.44	0.94
Profilin	5.00	0.28

5.6.6 Genes regulated specifically by AcLDL and OxLDL

This comparison compared expression levels of genes in cells exposed to OxLDL (24 hours) with cells exposed to AcLDL (24 hours) in order to identify genes being regulated specifically by OxLDL or AcLDL. This comparison showed 15 genes up-regulated (OxLDL > AcLDL) and 1 gene down-regulated (AcLDL > OxLDL). Table 5.8 shows the most highly up and down-regulated genes over 24 hours.

Table 5.8

Table showing up- and down-regulated genes when comparing OxLDL(24) with AcLDL(24)

Comparison OxLDL(24) versus AcLDL(24)		
Name of gene	*Expression level*	*Standard deviation*
up-regulated		
LFA-3 transmembrane variant	6.55	2.67
CD36	5.70	1.98
β - tubulin	4.98	1.71
Human mRNA for KIAA0312 gene	4.80	0.57
Wnt-13	4.25	0.21
Down-regulated		
Interleukin-1β	1.55	0.07

5.6.7 Genes regulated after early and late exposure to OxLDL

This comparison compared expression levels of genes in cells exposed to OxLDL at 24 hours with cells exposed to OxLDL at 4 hours in order to identify genes being regulated early and late after exposure to OxLDL. This comparison showed 4 genes up-regulated [OxLDL (24) > OxLDL (4)] and 5 genes down-regulated [OxLDL (4) > OxLDL (24)]. Table 5.9 shows the most highly up- and down-regulated genes over 24 hours.

Table 5.9

Table showing up- and down-regulated genes when comparing OxLDL (24) with OxLDL (4)

Comparison OxLDL(24) versus OxLDL(4)		
Gene Name	*Expression level*	*Standard deviation*
Up-regulated		
β - tubulin	3.35	0.49
Lymphocyte cytosolic protein 1 (L-plastin)	3.30	1.41
Wnt-13	2.25	0.21
Human B2 microglobulin gene	2.10	0.57
Vimentin	1.55	0.07
down-regulated		
Interleukin-1β	2.10	0.42
Human collagenase inhibitor mRNA *(inhibitor of* MMPs)	1.83	0.17
p53 activated fragement-1 (*found in tumours*)	1.68	0.18
Human ribosomal protein L37a mRNA (ribosomal protein)	1.61	0.16

5.6.8 Discussion of results from the custom atheroma arrays

As can be seen from tables 5.2 - 5.9 and appendix 5 there are some genes that appear in more than one of the comparisons performed. Of interest with relevance to foam cell formation these genes included CD36, TIMP-1, interleukin-1β. CD36 is a member of the scavenger receptor family that is a major receptor for OxLDL. TIMP-1 is an inhibitor of the MMP family. IL-1β is produced as part of the inflammatory response.

As noted above when a comparison was performed, four lists of genes were generated for each direction in which the comparison was performed. Subsequently only genes appearing in all four lists were included in the final list of genes for the comparison in the direction performed. This did however mean that there was a high

'drop out rate' of genes, which were excluded from the final results. In addition it meant that in some cases that genes did not appear in comparisons or across all comparisons that they would have been expected to appear in. However it does mean that the results listed can be taken with high degree of confidence.

5.7 Genes regulated by native and modified LDL

5.7.1 Genes regulated by native LDL

Exposure of lipoprotein-depleted differentiated THP-1 cells to native LDL resulted in a larger than expected number of regulated genes (Graph 5.1; when compared to AcLDL and OxLDL). This may be attributed to the control used in these experiments (differentiated THP-1 cells that were depleted of lipoprotein). Genes up-regulated on exposure to native LDL included cytokines such as platelet-derived growth factor A, interferon γ and IL-1β. In addition cytokine receptors such as the interleukin-1 receptor and tumour necrosis factor 1 were also found to be up-regulated. Other genes of interest found to be up-regulated included thrombomodulin, fibronectin, stromelysin, collagenase, collagenase inhibitor, protein kinase C inhibitor and osteonectin. Genes of interest that were found to be down-regulated on exposure to native LDL include alpha enolase, fibronectin receptor beta subunit and MMP-2. (all genes up- and down-regulated are listed in appendix 5 atheroma results). Some of these genes such as IL-1β and MMP-2 have been implicated in the atherosclerotic process so it was interesting to determine whether subsequent comparisons of the native sample with OxLDL and AcLDL samples resulted in an increased or decreased level of expression of these genes. In addition the expression of these genes could suggest that THP-1 cells (and possibly macrophages *in vivo*) may (to a certain degree) be already sensitised to the subsequent assaults produced by the modified forms of LDL (namely AcLDL, the mild form of lipid loading and OxLDL the more toxic form of lipid loading).

5.7.2 Genes regulated by modified LDL

Table 5.10 below lists the genes showing differential expression specifically on exposure to AcLDL, OxLDL or both. This list is derived from comparing genes regulated in the AcLDL and OxLDL with native LDL comparisons

Table 5.10 Table showing a list of genes differentially expressed on exposure showing specific regulation by either OxLDL/AcLDL or both.

Genes regulated by AcLDL	Genes regulated by OxLDL	Genes regulated by both OxLDL and AcLDL
Interleukin -1β	23kd highly basic protein	TIMP-1
Human RPSA3A gene	CD36	Nidogen
Lipocortin II/Annexin II	Metallothyonein	Thymosin beta 4
Human Ferritin H chain	Proliferation association gene	Alpha enolase
	Fibronectin	Translationally controlled tumour protein
	Wnt-13	

5.7.3 Genes regulated specifically by AcLDL

Uptake of modified LDL by macrophages induces the expression of a range of growth factors and cytokines many of which have been localised within atherosclerotic lesions such MCP-1, TNF-α, MCP-1, IL-8, IL-1 and M-CSF [114]. In this study we did not detect any of these cytokines except IL-1β. This could be due to a number of reasons; including the fact that in general, cytokines tend to be expressed at low levels. Furthermore as these cytokines are involved in the initiating the earliest events of atherosclerosis, their expression is likely to occur very early on after exposure to lipoprotein. The time point (24 hours) used in this study may thus be too late to detect their expression or alternatively the concentration of native LDL used (0.2 mg/ml) may be too low or too high to induce their expression at detectable levels.

AcLDL also represents a 'pure' ligand with no pathology and simply demonstrates the scavenging function of macrophages.

(a) IL-1β

IL-1β is produced as part of the inflammatory response. It is a chemoattractant for T-cells and is known to sustain the inflammatory response. In addition it has also been reported to induce the expression of MCP-1 from the endothelium [225]. Thus IL-1β plays an important role during the initial stages of atherosclerosis by acting as a chemoattractant and during the later stages by sustaining the inflammatory process.

When comparisons were performed, the AcLDL (24) sample showed an increased fold expression in IL-1β when compared to both the native sample and OxLDL (24) samples. A 1.6 (+/- SD 0.00) fold higher expression was found in AcLDL (24) sample compared to the native sample. Furthermore when compared with the OxLDL (24) sample, there was a 1.6 (+/- SD 0.07) fold higher expression in the AcLDL (24) sample compared to the OxLDL (24) sample. IL-1β was also found to show 2.1 (+/- SD 0.42) fold higher difference in the OxLDL (24) sample when it was compared with the OxLDL (4) sample. This indicates that levels of IL-1β increase over time on exposure to OxLDL.

(b) Annexin II

Another gene found to be regulated specifically due to exposure to AcLDL was annexin II. Annexin II is calcium regulated membrane-binding protein whose affinity for calcium is greatly enhanced by anionic phospholipids. It may also cross-link plasma membrane phospholipids with actin and the cytoskeleton and be involved with exocytosis. Furthermore annexins are also thought to play a role in inflammation by acting as anti-inflammatory molecules.

When comparisons were performed, the AcLDL (24) sample showed a decreased fold expression of Annexin II when compared to both the native and OxLDL (24) samples. A 3.75 (+/- SD 0.86) fold higher expression was found in the native sample compared to the AcLDL (24) sample. Similarly when the AcLDL (24)

was compared to the OxLDL (24) sample, a 3.10 (+/- SD 0.38) fold higher expression was found in the OxLDL (24) sample. These results indicate that exposure of cells to AcLDL results in a decrease in annexin when compared to native LDL and OxLDL over 24 hours. As noted above, the annexins are thought to act as anti-inflammatory molecules thus a decrease in their expression (when compared to native LDL) is not surprising since atherosclerosis is known to be an inflammatory process.

(c) Ferritin

Another gene also found to be specifically regulated on exposure to AcLDL was ferritin. Ferritin is an intracellular molecule that stores iron in a soluble, non-toxic readily available form. It is also an acute phase reactant.

Similar to Annexin II, ferritin also showed a decreased expression in the AcLDL (24) sample when compared to the native and OxLDL samples. A 4.10 (+/- SD 0.57) fold higher expression was found in the native sample compared to the AcLDL (24) sample. When the AcLDL (24) was compared to the OxLDL (24) sample, a 3.5 (+/- SD 0.70) fold higher expression was found in the OxLDL (24) sample. These results indicate that exposure of cells to AcLDL results in a decrease in ferritin when compared to native LDL and OxLDL over 24 hours.

5.7.4 Genes regulated specifically by OxLDL

(a) CD36

CD36 is a glycoprotein that has been found to be a scavenger receptor for OxLDL. It is a member of the scavenger receptor family class B and has been reported to be expressed in THP-1 cells [22]. In addition CD36 has been found to be significantly expressed in atherosclerotic foam cells from coronary arteries [23]. When comparisons were performed, the OxLDL (24) sample showed an increased expression in CD36 when compared to both the control sample and AcLDL (24) samples. A 4.55 (+/- SD 0.64) fold higher expression was found in the OxLDL (24) sample than the control sample. When compared with the AcLDL (24) sample, there was a 5.70 (+/- SD 1.98) fold higher expression in the OxLDL (24) sample. Furthermore when the native LDL sample was compared with AcLDL (24), there was

a 5.80 fold (+/- SD 0.64) higher expression found in the native LDL sample. These results indicate that exposure of cells to OxLDL leads to a specific increase in CD36 levels when compared to control and AcLDL (24) samples. In addition the native versus AcLDL (24) comparison suggests that CD36 levels decrease on exposure to AcLDL. A possible explanation for the decrease seen in the AcLDL (24) sample could be that there is an increase in the expression of other receptors for AcLDL resulting in a decrease in CD36 expression.

This result for CD36 gives credence to the validity of our model as it suggests that foam cell formation has occurred in the experimental system under investigation (differentiated THP-1 cells exposed to modified LDL). Furthermore it provides confidence that the experimental array technology being used here is capable of detecting this change.

(b) Wnt-13

Another gene showing increased levels on exposure to OxLDL was Wnt-13. The precise role of Wnt-13 is unknown, however it is thought to be involved in cell/tissue development. It thought to be a signalling molecule, which affects the development of discrete regions of tissues. It may also be associated with the extracellular matrix and be involved in normal development or differentiation as well as in carcinogenesis.

When comparisons were performed, the OxLDL (24) sample showed an increased fold expression in Wnt-13 when compared to native, AcLDL (24) and OxLDL (4) samples. A 1.7 (+/- SD 0.14) fold higher expression was found in the OxLDL (24) sample when compared to the native sample. When compared with the AcLDL (24) sample, there was a 4.25 (+/- SD 0.21) fold higher expression in the OxLDL (24) sample. Finally when compared to the OxLDL (4) sample there was a 2.25 (+/- SD 0.21) higher fold expression in the OxLDL (24) sample. These results indicate that exposure of cells to OxLDL (24) leads to an increase in Wnt-13 levels when compared to native, AcLDL (24) and OxLDL (4). Since the function of this gene has not been fully elucidated it and the results presented here indicate an increase in its expression, it would be of interest to perform further *in vitro* experiments with respect to this gene.

(c) Metallothionein

Another gene found to show increased expression in response to OxLDL was metallothionein. Metallothioneins have a high content of cysteine residues that bind various heavy metals; they are transcriptionally regulated by both heavy metals and glucocorticoids. The member of the metallothionein family expressed here binds to zinc.

When comparisons were performed, the OxLDL (24) sample showed an increased fold expression in metallothionein when compared to the control and native samples. A 26.2 (+/- SD 4.53) higher fold expression was found in the OxLDL (24) sample than the control sample. When compared with the native sample, there was a 7.30 (+/- SD 3.29) fold higher expression in the OxLDL (24) sample. These results indicate that exposure of cells to OxLDL (24) leads to an increase levels when compared to control and native samples. This result may be expected since the OxLDL used here was prepared from native LDL by modification using metal ions (copper sulphate solution).

The gene did not however appear in the OxLDL (24) versus AcLDL (24) comparison, indicating that it may be expressed at similar levels in the AcLDL (24) sample (If this was the case, then it would be expected to appear up-regulated in the AcLDL (24) versus native LDL comparison which it did not). A more likely explanation is that it did not confirm in all 4 lists generated for the OxLDL (24) versus AcLDL (24) comparison.

(d) Proliferation associated gene

Another gene showing increased expression on exposure to OxLDL (24) was proliferation associated gene (pag). Pag enhances natural killer cell activity. When comparisons were performed the OxLDL (24) sample showed an increased expression of pag when compared to the control, native and AcLDL (24) samples. A 3.56 (+/- SD 0.42) fold higher expression was found in the OxLDL (24) sample than the control sample. When compared with the native sample, there was a 2.25 (+/- SD 0.07) fold higher expression in the OxLDL (24) sample. Furthermore when compared to the AcLDL (24) sample, the OxLDL (24) showed a 3.5 (+/- SD 0.00) fold higher expression. These results indicate that exposure of cells to OxLDL (24) leads to an

increase level of pag when compared to the control, native and AcLDL samples. Its expression by OxLDL may reflect the pro-inflammatory nature of atherosclerosis and the more toxic effects that OxLDL is thought to have.

(e) MMP-2

MMP-2 showed increased expression on exposure to OxLDL(24). MMP-2 is also known as 72 Kda type IV collagenase precursor. MMP-2 is involved in the cleavage of gelatin type I and collagen types IV, V, VII and X. It cleaves the collagen-like sequence pro-gln-gly and requires calcium and zinc for activity. MMP-2 is a member of the MMP family (discussed in chapter 1). MMPs have been implicated in determining plaque stability. When comparisons were performed an increase in MMP-2 expression was found in the OxLDL (24) sample compared to the native sample. A 2.55 (+/- 0.49) fold higher expression was found in the OxLDL (24) sample compared to the native sample indicating an increased level of MMP-2. This result is not surprising since MMP-2 has already been shown to be expressed in atherosclerotic plaques [147]. Levels of MMP-2 have been reported to be increased in shoulder regions of plaques where the majority of macrophages are found [147]. Furthermore lipid lowering therapy with pravastatin has been shown to result in a decrease in MMP-2 levels in plaques [137]. Thus this result is consistent with previous observations.

(f) Fibronectin

A gene that was found to show decreased levels on exposure to OxLDL was fibronectin. Fibronectins binds cell surfaces and various compounds including collagen, fibrin, heparin, DNA and actin. Fibronectins are involved cell adhesion, cell motility, opsonization, wound healing and maintenance of cell shape. When comparisons were performed, the OxLDL (24) sample showed a decreased expression of fibronectin when compared to native LDL. A 7.38 (+/- SD 2.04) fold higher expression was found in the native sample than the OxLDL (24) sample. This result indicates that exposure of cells to OxLDL results in a decrease in fibronectin when compared to native LDL over 24 hours.

5.7.5 Genes regulated by both OxLDL and AcLDL

(a) TIMP-1

The metalloproteinases and their inhibitors (TIMPs play a central role in tissue remodelling (especially in disease states such as cancer. They have also been implicated a play a role in plaque rupture. As discussed in chapter one the MMPs are a family of structurally related proteases that are capable of degrading the virtually all components of the extracellular matrix. The level of MMPs is tightly controlled by the MMP: TIMP ratio. In addition to identifying a higher fold expression in MMP-2 in the OxLDL (24) sample when compared to the native sample as described above, TIMP-1 was also found to be regulated by both forms of modified LDL used in this study.

When comparisons were performed, the native sample showed a higher TIMP-1 expression when compared to the AcLDL (24) and OxLDL (24) samples. A 2.68 (+/- SD 0.31) fold higher expression was found in the native LDL sample when compared to the OxLDL (24) sample. Furthermore when compared with the AcLDL (24) sample, there was a 2.83 (+/- SD 0.19) fold higher expression in native samples.

In addition when the OxLDL (24) sample was compared with the OxLDL (4) sample there was a 1.83 (+/- SD 0.17) fold higher expression in the OxLDL (24) sample suggesting that levels of TIMP-1 increased over time from 4 to 24 hours on exposure to OxLDL (although at the 24 hours the levels still remain less than those observed with native LDL at 24 hours as shown by the higher fold difference in the native LDL sample when compared to the OxLDL).

These results suggest that exposure to modified LDL leads to a decrease in levels of TIMP-1. When both AcLDL and OxLDL are compared to the native sample, the native sample shows a higher expression level of TIMP-1. This may reflect the morphological changes taking place within the cell upon lipid loading that result in decreased levels of TIMP-1. The OxLDL (24) versus OxLDL (4) comparison indicates that there is an increase in TIMP-1 levels between 4 and 24 hours.

(b) Alpha enolase

Another gene that was found to be decreased on exposure to both OxLDL and AcLDL was alpha enolase. Alpha enolase catalyses the breakdown of 2-phospho-d-glycerate into phosphoenolpyruvate and water and is an enzyme of the glycolytix pathway.

When comparisons were performed the native sample was found to show a higher expression than both the OxLDL (24) and AcLDL (24) samples. A 3.75 (+/- SD 1.20) fold higher expression was found in the native sample when compared to the OxLDL (24) sample. Similarly a 4.15 (+/- SD 0.58) fold higher expression was found in the native sample when compared to the AcLDL (24) sample. These results suggest that when OxLDL (24) and AcLDL (24) are compared to the native sample there is a decrease in expression of alpha enolase with both OxLDL and AcLDL provoking a decrease of similar magnitude. An increase in alpha enolase has been reported in mouse macrophages during cholesteryl ester accumulation [226]

(c) Thymosin beta-4

Another gene showing decreased expression when comparisons were performed was thymosin beta 4. The exact physiological role of thymosin beta-4 is not yet known. However it is a thymic hormone that can bind to actin monomers and thus inhibit actin polymerisation. It can be induced by alpha-interferon and fibroblast growth factors thus it is another gene that merits further investigation *in vitro*. When comparisons were performed the native sample was found to show a higher fold expression than both the OxLDL (24) and AcLDL (24) samples. A 1.85 (+/- SD 0.35) fold higher expression was found in the native sample when compared to the OxLDL (24) sample. When compared to the AcLDL (24) sample a 3.52 (+/- SD 0.84) fold higher expression was found in the native sample. Thus the native versus OxLDL showed a smaller fold difference than the native versus AcLDL comparison. This smaller difference was confirmed in the OxLDL (24) versus AcLDL (24) comparison sample where the OxLDL (24) showed a 2.65 (+/- SD 0.35) fold higher expression than the AcLDL (24) sample. These results suggest that exposure to modified LDL leads to decrease in thymosin beta-4 expression, the decrease being greater on exposure to AcLDL that OxLDL.

(d) Nidogen

Another gene showing decreased expression was nidogen. Nidogen is a sulphated glycoprotein that is found widely distributed in basement membranes. It is found tightly associated with laminin and also binds to collagen and may play a role in cell-extracellular matrix interactions. Again a decrease in its expression levels on exposure to modified LDL may reflect the morphological changes taking place within the cell upon lipid loading.

When comparisons were performed the native sample was found to show a higher fold expression than both the OxLDL (24) and AcLDL (24) samples A 3.20(+/- SD 0.57) fold higher expression was found in the native sample when compared to the OxLDL (24) sample. When compared to the AcLDL (24) sample a 3.10 (+/- SD 0.00) fold higher expression was found in the native sample. These results suggest that exposure to modified lipoprotein results in a decrease in nidogen gene expression.

5.7.6 Conclusions from atheroma array results

The atheroma arrays were much smaller in size than the human I.M.A.G.E arrays (in terms of the number of genes/ESTs), however contained what were thought to be a more relevant set of genes thought to be involved in cardiovascular disease. Surprisingly, the results demonstrated the largest number of genes regulated in differentiated THP-1 cells were due to native LDL rather than OxLDL and AcLDL. A possible number of explanations for this include

(a) The control used in this sample was a sample of differentiated THP-1 cells that had been exposed to lipoprotein deficient media, therefore exposure to native lipoprotein resulted in replete situation and the availability of cholesterol. In other words there was a large physical change taking place in cells when going from a lipid depleted to lipid repleted situation.

(b) The genes differentially expressed during foam cell formation (on exposure of differentiated THP-1 cells to modified LDL) were not represented on the

arrays. It is possible other pathways or mechanisms, previously unidentified could be involved.

(c) That other genes were differentially expressed on the arrays but were not detected due to the very small changes that may have occurred in their expression

(d) The criteria set for threshold and background values may have excluded these genes

(e) The number of genes regulated on exposure to modified LDL is in fact less than the number regulated on exposure to native LDL. As with uptake of native LDL, uptake of modified LDL could be considered a 'normal' scavenging function of macrophages and may a represent a protective effect which macrophages may have evolved to cope with.

In general, results from the custom atheroma arrays indicate that genes regulated on exposure to modified LDL in comparison to native LDL can be split into five classes of genes; lipoprotein receptors, inflammatory signalling molecules & cytokines, metal binding proteins, ribosomal proteins and cell structure & motility proteins as listed below

Lipoprotein receptor: -	CD36
Inflammatory signalling molecules and cytokines: -	IL-1β, translationally controlled tumour protein, proliferation association gene, annexin II and Wnt -13
Metal binding proteins: -	metallothionein, ferritin heavy chain
Ribosomal proteins: -	23KD highly basic protein, RPSA 3A
Cell structure and motility proteins: -	Fibronectin, TIMP-1, nidogen, and thymosin-beta 4,
Enzymes	Alpha enolase

As noted above, due to the number of genes found to be differentially expressed, the results presented above provide a summary of some of the genes found. A few of the genes that were found to be specifically expressed by AcLDL, OxLDL and by both AcLDL and OxLDL were selected have been discussed above (section 5.6). Further experimental work will be necessary to validate and determine the role that these genes play in foam cell formation.

5.8 Results from the human I.M.A.G.E arrays

The I.M.A.G.E arrays used in these experiments were representative of the human I.M.A.G.E collection, which in turn was representative of the human genome [207]. Due to the high amount of redundancy that is found in the I.M.A.G.E collection, the DGE group at GlaxoWellcome had rearrayed clones from the human I.M.A.G.E collection working on basis of representing each gene or EST sequence by one or a few clones.

Comparisons were performed as for the custom atheroma arrays and final differences identified in comparisons were sent to the DGE database. For the I.M.A.G.E arrays, all genes identified as differentially expressed were sequenced. The differentially expressed 'spot' on the array was deciphered to give the plate and well location of the clone from which it was derived. Subsequently this clone was repicked and grown up. The cloned insert were amplified by PCR and the PCR products were sequenced (by the Sequencing Group, Department of Genetics, GlaxoWellcome, Stevenage, UK) so as confirm their identity. Due to the large size of the files, the results obtained from the I.M.A.GE arrays are given in appendix 6

Graph 5.2 below shows the number of up- and down- regulated genes found for each comparison using the I.M.A.G.E arrays. As for the custom atheroma arrays the number of genes up-regulated are highest in the native versus control comparison. The highest number of genes down-regulated are found in the AcLDL (24) versus AcLDL (4) comparison. There are more genes up-regulated by OxLDL than AcLDL after 24 hours, as shown in the OxLDL(24) versus AcLDL (24) comparison. However at 4 hours the numbers of genes up- and down-regulated by OxLDL and AcLDL are relatively similar.

In general the human I.M.A.G.E array results indicate that there are more genes up-regulated by exposure to modified LDL than are down-regulated. This is in

contrast to the results from the custom atheroma arrays that indicate that there are more genes down-regulated on exposure to modified lipoprotein than are up-regulated. This can be explained by the fact that there are more genes on the I.M.A.G.E arrays than the custom atheroma arrays. In addition the I.M.A.G.E arrays are more representative of the human genome whereas the custom atheroma arrays contain a relatively limited number of selected genes with reference to cardiovascular disease. Furthermore the I.M.A.G.E. arrays contained a large number of ESTs. These results could suggest that there may be more, as yet undiscovered genes/transcripts that play a role during foam cell formation

Graph 5.2 Graph showing number of genes up regulated and down regulated for each comparison performed using the human I.M.A.G.E arrays

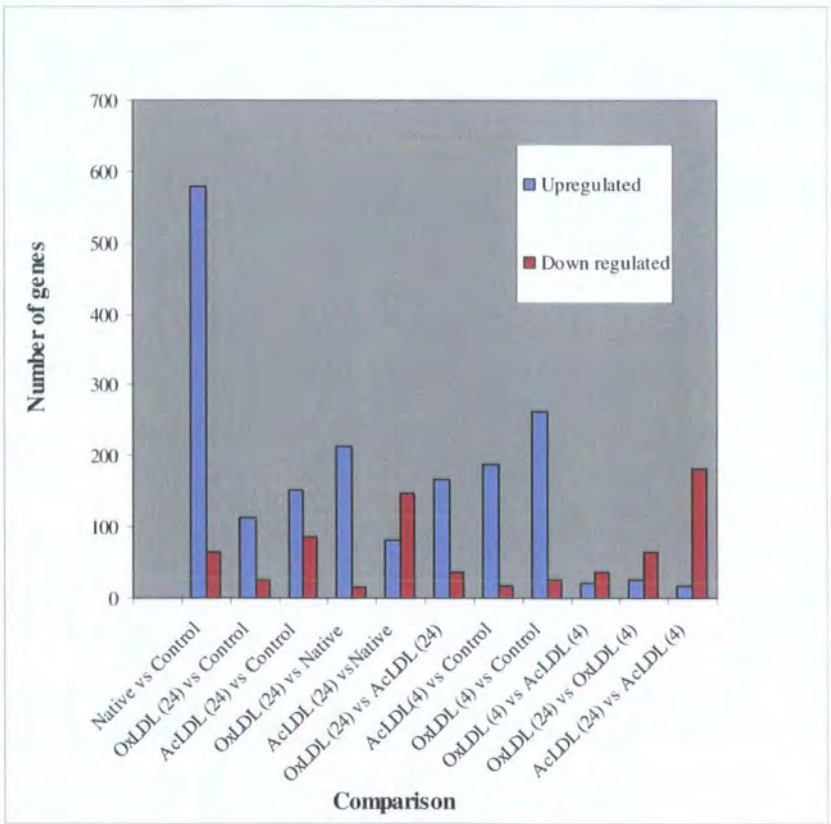

Results obtained from the IMAGE arrays are given in appendix 6 due to the amount of data generated. The first worksheet in appendix 6 entitled 'summary of results' lists the tables of genes identified in the comparisons performed. These tables do not represent the most highly up- and down-regulated genes (since in many cases, these are EST sequences of unknown function) but rather known genes. The number of ESTs found to be differentially expressed give another lead to follow in the identification of novel genes involved in the process of foam cell formation.

The tables below (table 5.11-5.21) show five up and down differentially regulated genes/EST of interest that are expressed for each comparison performed using the human I.M.A.G.E arrays.

Table 5.11 Table showing up and down-regulated genes when comparing native LDL with control

Upregulated	Fold difference
Homo sapiens clone similar to protein phosphatase PP2A, 65Kd regulatory subunit, alpha	12.3
Homo sapiens cDNA clone similar to elongation factor 1 gamma (human)	10.7
Homo sapiens clone similar to transforming protein RhoA (Human)	8.4
Homo sapiens clone similar to ATP synthase A chain	7.3
Homo sapiens clone similar to aceyl lactosamine synthase (Human)	6.1
Downregulated	Fold difference
Homo sapiens cDNA clone similar to elongation factor-1 gamma (human)	3.6
Human MAP kinase activated protein kinase 2	2.8
Eukaryotic translation elongation factor -alpha-1 (human)	2.4
Human mRNA for fibronectin (FN precursor)	2.4
NADH dehydrogenase Fe-S protein 3	2.4

Table 5.12 Table showing up- and down-regulated genes when comparing OxLDL (24hr) with control

Upregulated	Fold difference
Homo sapiens cDNA clone similar to RAS-related protein RAP-1A (human) mRNA sequence	10.9
Homo sapiens thyroid receptor interactor protein (TRIP)	8.6
Cysteine protease 1	8.2
stearoyl-coA desaturase	7.7
Homo sapiens mRNA for RALDH2-T	7.5
Downregulated	Fold difference
Homo sapiens cDNA clone similar to elongation factor 1 alpha-1 (human)	7.1
Homo sapiens cDNA clone similar to P68 protein (Human)	6.5
Homo sapiens cDNA clone similar to tubulin alpha-1 chain (human)	4.9
Homo sapiens cDNA clone similar to ferritin light chain	4.2
Homo sapiens cDNA clone similar to heat shock cognate 71Kd protein (Human)	4.2

Table 5.13 Table showing up- and down-regulated genes when comparing AcLDL (24hr) with control

Upregulated	Fold difference
Homo sapiens cDNA clone similar to prostaglandin E receptor EP1 subtype (human)	8.6
Homo sapiens cDNA clone similar to Acetyl lactosamine synthase (human)	5.7
Homo sapiens cDNA clone similar to Interleukin1-beta precursor	5.7
NADH dehydrogenase (ubiquinon 1)	4.7
Homo sapiens cDNA clone similar to NADH-ubiquinone oxidoreductase	4.5
Downregulated	Fold difference
Chloride intracellular channel 1	7.1
Heat shock 70kd protein 10	6.7
Transforming growth factor beta stimulated protein (TSC-22)	5.8
Ferritin, light polypeptide 5 (RNA helicase)	4.5
Dead/H box polypeptide 5 (RNA helicase)	4.1

Table 5.14 Table showing up- and down-regulated genes when comparing comparing OxLDL (24 hr) with native LDL (24hr)

Upregulated	Fold difference
Homo sapiens cDNA clone similar to elongation factor-1-alpha-1 (human)	5.6
Human heart mRNA for shock protein 90	5.5
Transforming protein RhoA (human)	4.5
Homo sapiens cDNA clone similar to Glia activating factor precursor (human)	3.5
Homo sapiens cDNA clone similar to protein phosphatase PP2A , 65Kd, regulatory subunit, alpha (human)	3.2
Downregulated	Fold difference
Human mRNA for fibronectin (FN precursor)	3.7
EST similar to KIAA 0313	3
Cathepsin B	2.5
ATPase family gene AFG-2	1.8
Nuclear phosphoprotein p130	1.6

Table 5.15 Table showing up- and down-regulated genes when comparing AcLDL (24hr) with native LDL (24hr)

Upregulated	Fold difference
Homo sapiens cDNA clone similar to laminin alpha-1 chain precursor	4.5
Human retinoblastoma susceptibility gene exons 1-27	4.1
Homo sapiens cDNA clone similar to Cathepsin O precursor	3.9
Homo sapiens cDNA clone similar to aldehyde dehydrogenase	3.8
Homo sapiens cDNA clone similar to madiamine acetyl transferase (human)	3.7
Downregulated	Fold difference
Homo sapiens cDNA clone similar to psoriasis-associated fatty acid binding protein homolog (human)	4.6
Fatty acid binidng protein 5 (psoriasis associated)	4.6
Human kinase suppressor of ras-1 (KSR1) mRNA	4.2
Ras homolog gene family, member E	3.8
Human glucose-6-phosphate dehydrogenase	3.7

Table 5.16 Table showing up- and down-regulated genes when comparing OxLDL (24hr) with AcLDL (24hr)

Upregulated	Fold difference
Homo sapiens cDNA clone similar to protein phosphatase PP2A	5.2
Homo sapiens cDNA clone similar to actin, cytoplasmic 2 (Human)	5
Homo sapiens cDNA clone similar to ferritin light chain (human)	3.9
Homo sapiens cDNA clone similar to elongation factor 1 -gamma	3.8
Homo sapiens cDNA clone similar to transducin-like enhancer protein 3	3.5
Downregulated	Fold difference
Homo sapiens mRNA for KIAa1372 protein	3.2
Homo sapiens cystatin B	2.7
Solute carrier family 2 (facilitated glucose transporter member 1)	2.6
Human mRNA for KIAA 0205	2.6
Homo sapiens cDNA clone similar to ribosomal protein L26	2.1

Table 5.17 Table showing up- and down-regulated genes when comparing AcLDL (4hr) with control

Upregulated	Fold difference
Homo sapiens cDNA clone similar to transforming protein Rho A	30.3
Homo sapiens cDNA clone similar to ATP synthase A chain	17.3
Homo sapiens cDNA clone similar to L-MYCp2 protein (Human)	16.9
Homo sapiens cDNA clone similar to NADH-ubiquinone oxidoreductase KFY1 subunit precursor	16
Homo sapiens cDNA clone similar to elongation factor 1 gamma	13
Downregulated	Fold difference
Human ferritin L chain mRNA	6.1
NADH dehydrogenase (ubiquinone) Fe-S protein-3 (NADH coenzyme Q reductase)	2.7
Annexin A1	2.2
Homo sapiens retinoldehydrogenase gene 2	2
Eukaryotic translation elongation factor 1 alpha 1	1.9

Table 5.18 Table showing up- and down-regulated genes when comparing OxLDL (4hr) with control

Upregulated	Fold difference
Homo sapiens cDNA clone similar to elongation factor 1 gamma (human)	22.2
Homo sapiens cDNA clone similar to PP2A, 65 kd regulaory subunit, alpha	18.4
NADH ubiquinone oxidoreductase KFY1 subunir precursor	17.8
Homo sapiens cDNA clone similar to transforming protein Rho A (Human)	14.6
Homo sapiens cDNA clone similar to trans-1,2, dihydrobenzene 1,2 diol dehydrogenase (human)	11
Downregulated	Fold difference
Human ferritin light chain mRNA	3.9
NADH-coenzyme Q reductase	3.7
Eukaryotic translation elongation factor 1, alpha 1	3.5
Annexin A1	3.5
Human MAP kinase activated protein kinase 2	2.8

Table 5.19 Table showing up- and down-regulated genes when comparing OxLDL (4hr) with AcLDL (4hr)

Upregulated	Fold difference
Homo sapiens cDNA clone similar to epidermal growth factor receptor	3.8
Ribosomal protein L25	2.6
Homo sapiens cDNA clone similar to human cysteine rich protein	2.3
Homo sapiens mRNA KIAA 0870 protein	1.8
Homo sapiens cDNA clone similar to ferritin light chain	1.8
Downregulated	Fold difference
Human cis acting sequence	4.4
Homo sapiens cDNA clone similar to retrovirus -related pol polyprotein	3.2
Ribosomal protein L27a	2.8
Homo sapiens cDNA clone similar to interleukin-12 beta chain precursor	2.7
EST highly similar to CREB-binding protein	2.7

Table 5.20 Table showing up- and down-regulated genes when comparing OxLDL (24hr) with OxLDL (4hr)

Upregulated	Fold difference
EST weakly similar to KIAA 0636 protein1 (natural resistance associated macrophage protein 2 gene)	4.9
Homo sapiens cDNA clone similar to four and a half LIM domains 2	4.1
CDW52 antigen (Campath-1 antigen)	3.8
EST weakly similar nucleoporin p62 homolog	3.2
Actin, gamma 1	3.2
Downregulated	Fold difference
Homo sapiens cDNA clone similar to human ribosomal protein S10	3.7
Human lambda-immunoglobulin constant region complex	3.7
Homo sapiens cDNA clone similar to 40S ribosomal protein S25	3.6
Homo sapiens cDNA clone similar to rat cytochrome P450	3.2
Homo sapiens cDNA clone similar to ribosomal protein L27	3.2

Table 5.21 Table showing up- and down-regulated genes when comparing AcLDL (24hr) with AcLDL (4hr)

Upregulated	Fold difference
EST	2.6
Ribosomal protein S25	2.5
Homo sapiens cDNA clone similar to putative ATP-dependent helicase	1.8
Human interleukin 1 beta	1.5
Downregulated	Fold difference
Homo sapiens cDNA clone similar to L-MYC-2 protein	6.6
Copine 1	5.7
Homo sapiens cDNA clone similar to ATP synthase A chain	5.1
Chromobox homolog1	5.1
Eukaryotic translation elongation factor 1 gamma	5.1

5.8.1 Discussion of results from human I.M.A.G.E arrays

As expected there were a larger number of genes regulated using the I.M.A.G.E arrays than using the custom arrays. The advantage of using the I.M.A.G.E arrays were that as well as containing known genes representing the human genome, the I.M.A.G.E arrays also contained novel EST sequences. This provides an opportunity to discover novel EST sequences that play a role in the foam cell transformation.

Table 5.22 below gives some of the genes specifically regulated by AcLDL, OxLDL or both AcLDL and OxLDL. This table is derived by comparing genes expressed when comparing OxLDL and AcLDL with the native sample.

Table 5.22 Table showing genes regulated by AcLDL, OxLDL or both using the human I.M.A.G.E arrays

Genes regulated by		
OxLDL	AcLDL	Both
Cathepsin B	Vitamin D3 receptor	Protein phosphatase 2A
Transforming protein RhoA	Psoriasis-associated fatty acid binding protein	Ferrtin light chain
Immunoglobulin Fc receptor	Interleukin 1beta	Tubulin alpha 1 chain
Heat shock protein 90	Prostaglandin E receptor	Elongation factor 1 gamma
Lysozyme C precursor	Macrophage inflammatory protein alpha	Fibronectin
Leukosialin precursor	Cytokine receptor related protein (cytoR4)	
	Cathepsin O	
	Glucose transporter, type 1	
	TIMP-1	

The results showed that the same genes were not found to be differentially expressed from the custom arrays and the I.M.A.G.E arrays. This could be due to a number of reasons including:-

[1] Strict criteria were used to ident ify genes being expressed by the custom atheroma arrays. As discussed above, a gene had to appear in the all four lists of a comparison formed, where it did not this gene was not included in the final list. These strict criteria resulted in a large number of genes being dropped but ensured that those included in the final list were definite differences.

[2] Both custom and I.M.A.G.E array clones were sequenced after arraying which resulted in removal of genes from both comparisons. For example although cathepsin B was identified as being differentially regulated by the custom atheroma arrays and the I.M.A.G.E arrays. It was not sequence- confirmed on the custom arrays and therefore had to be removed from the final results. It was however identified as being differentially expressed by the I.M.A.G.E. arrays and when sequenced matched its original identity.

[3] The I.M.A.G.E arrays were derived from a much larger library containing a high degree of redundancy. Due to its size this meant that it was more prone to errors in picking of cloning

5.8.2 Genes regulated by native LDL using human I.M.A.G.E arrays

As for the custom atheroma arrays the largest number of genes up-regulated were due to native LDL. Of interest these genes include interleukin-1 beta, interleukin-12, acyl hydrocarbon receptor, a psoriasis associated fatty acid binding protein, a cDNA clone similar to the prostaglandin E receptor and cytokine receptor related protein (cyto R4).

5.8.3 Genes regulated by AcLDL using human I.M.A.G.E arrays

As also shown by the results of the custom atheroma arrays, interlukin-1 expression is increased on exposure to AcLDL. In addition a number of other genes including cathepsin O, psoriasis associated fatty acid binding protein and macrophage inflammatory protein 1 (MIP-1) are regulated on exposure to AcLDL. Of particular interest is MIP-1, a chemokine implicated during the progression of CHD [227]. The receptor for MIP-1; chemokine motif receptor 5 (CCR5) is found to be expressed on macrophages and T lymphocytes [227]. Another gene of potential interest is psoriasis associated fatty acid-binding protein. OxLDL has been reported to induce expression of an adipocyte lipid binding protein [228]

5.8.4 Genes regulated by OxLDL using human I.M.A.G.E arrays

Genes specifically regulated by OxLDL include heat shock protein 90, transforming protein RhoA, cathepsin B and lysozyme C precursor. Members of the cathepsin family (including cathepsin S and K) have been found to be expressed in monocyte-derived macrophages [229]. In addition accumulation of oxidised esters has been reported in lysosomes [230], which may suggest a role the lysozome C precursor.

5.9 Conclusions from results of human I.M.A.G.E arrays

As expected a greater number of changes were found using the IMAGE arrays when compared to the custom atheroma array. This can mainly be attributed to the greater number of sequences represented on these arrays. The genes regulated again included some that have been previously implicated in the atherosclerotic process, such as onterleukin 1β and macrophage inflammatory protein. In addition several members of the cathepsin family including cathepsin B and cathepsin O were found to be regulated by modified LDL. As other members of the cathepsin family these are likely to be involved in remodelling of the extracellular matrix. A number of genes were also identified whose function in the atheroslcerotic process is not yet determined but may be of interest. These include heat shock protein 90 (heat shock

protein 60 has shown to be induced in monocytes by OxLDL [231]), cytokine receptor related protein and psoriasis-associated fatty acid binding protein.

The results from the I.M.A.G.E array of the genes being regulated by modified LDL fit into the role of inflammatory molecules and tissue remodelling genes having a role in early atherosclerosis.

5.10 Discussion of array technology

Technology is now moving so fast that since starting this study, arraying of cDNA samples is now more commonly performed on glass slides than nylon membranes although both have their own advantages and disadvantages. Filter arrays can be more cost effective because they require no special equipment except phosphoimager screens [209]. Filters are also useful for rare mRNA; as a smaller amount is required than for the preparation of fluorescent probes to glass slides. The major disadvantage of filters is that comparison of expression between two samples requires hybridisation of each sample to separate duplicate filters [209].

It should be noted that this study was performed during the development stages of the technology when methodology was constantly being improved. Some developmental data has not been shown in this thesis. For example probes were first strand cDNA probes were prepared from both messenger RNA and total RNA. The results showed that although cDNA probes derived from both mRNA and total RNA incorporated similar amounts of label, the hybridisation results obtained were of a higher standard in terms of clearer hybridisation to individual spots on the array when mRNA was used as the starting material.

One of the major challenges of using filter arrays has been ensuring clones represent the sequences they intend to. Due to the numerous steps involved (production of clones, PCR, gridding to arrays) and the large number of clones used, the method is highly prone to error. It is therefore essential that workflow is performed using strict quality control criteria which should assist in minimising such errors. For small labs intending to use limited numbers of arrays it is may be more cost effective to buy commercially available arrays or use core micoarray facilities, than set up their own microarray facility. For facilities where large number of arrays will be used, it is likely to be more cost effective and provide increased flexibility to manufacture their own arrays.

Chapter 6: Temporal Gene Expression

6.1. Introduction

6.1.1 Temporal gene expression

Although array technology allows biologists to simultaneously study the expression of thousands of genes, it has also provided a challenge in the form of the amount of data that it has generated. Assigning biological relevance to the changes in gene expression observed and organising the data obtained in a functional and meaningful manner is still a major hurdle. One approach to finding and displaying features of large sets of gene expression data has involved building maps representing gene expression data [232]. Making gene expression maps involves two main steps

(a) The data is firstly organised by a method (usually statistical), which finds orderly features within the data.

(b) The ordered data is then displayed graphically, in a way that allows biologists to assimilate the patterns of gene expression.

6.1.2 Initial work on temporal gene expression

Early work on large-scale temporal gene expression was reported in two biological systems; during spinal cord developments in the rat and in yeast during the shift from fermentation to respiration [233, 234]. Somogyi and colleagues [233] produced a gene expression map, which contained the expression levels of 112 genes at nine stages during rat cervical spinal cord development. They found that that the 112 genes clustered into 4 major waves of expression. Each of the four groups was found to have a distinct expression profile. De Resi *et al* [234] reported temporal gene expression in yeast (*Saccharomyces cerevisiae*) during the shift from anaerobic (fermentation) to aerobic (respiration) metabolism. De Resi's group used oligonucleotide arrays to look at expression across 7 time points. They found several distinct patterns of expression that correlated well with previously published data in the same organism [234]. Genes that

showed similar expression profiles were grouped by correlation clustering and five distinct temporal patterns of gene expression were observed [234].

Thus such clustering approaches demonstrated potential methods to deal with large data sets. This therefore also allows one to utilise such approaches in this study with some degree of confidence; with the aim of identifying genes or clusters of genes that show similar patterns of expression. Clusters can be useful because they can lead to associations of poorly characterised genes with genes whose function and regulation are better understood [235].

6.1.3 Introduction to clustering methodologies for analysing large data sets

A general overview on current strategies used to analyse microarray data has been reported by several authors including John Quackenbush [236] and Donna Slonim [237].Two clustering methods are generally taken to analyse large data sets; supervised methods and unsupervised methods. A brief overview of these methods is given below.

Before any clustering method (supervised or unsupervised) is applied on a data set, it is essential to perform a dissimilarity measure between two genes [238]. A dissimilarity measure indicates the degree of similarity between two genes. The subsequent clustering method then uses these dissimilarity measures to create clusters of genes with similar patterns. Commonly used dissimilarity measures are Euclidean Distance [233] and the Pearson correlation coefficent [235]. These are discussed further below

6.1.3.1 Supervised Methods

The supervised approach aims to identify genes that fit into a predetermined pattern. Supervised methods are useful for finding genes with expression levels that are significantly different between groups of samples and finding genes that are characteristic of a sample. In particular supervised methods have been reported and are useful for finding groups of genes that may be able to predict one type of cancer from another [232]. Supervised methods include; nearest neighbour analysis, neural networks decision

trees and support vector machines. The most popular of these are nearest-neighbour analysis and support vector machines.

6.1.3.1.1 Nearest Neighbours.

This technique is commonly used in a supervised approach to find genes with patterns of expression that are indicative of particular sample. It involves constructing a set of genes that show a particular pattern (for example a gene showing low expression in a normal state but showing increased expression in a disease state). Subsequently other samples can be compared to this pattern of gene expression and ranked by their similarity. This method has been successfully used by Golub *et al* [239] to distinguish between two types of childhood leukaemia.

6.1.3.1.2 Support Vector Machines

Support vector machines (SVM) are one the most recently reported methods [240] and are useful for finding combinations of genes that split sets of biological samples. They use a training set of samples in genes in which genes are known to be related to a particular class. The training set is used by the SVM to learn to distinguish between a members and non-members of a class, based on their expression pattern. Each gene is viewed as an expression vector in a multidimensional space. SVM is a classifier that attempts to separate the genes into two classes by defining an optimal hyperplane (a N-dimensional analogy which divides N+1 dimensional space into two).

6.1.3.2 Unsupervised methods

The unsupervised approach aims to find relationships or some degree of internal structure within a dataset without using any existing prior biological information on possible relationships between genes. Within unsupervised methods there are three classes of techniques [238] :-

(a) Feature determination; where genes with interesting properties are identified without looking for specific patterns. One such method is principle component analysis (PCA).

(b) Cluster determination; determining groups of genes with specific patterns of expression. Such methods include hierarchical clustering, self-organising maps (SOMs) and k-means clustering.

(c) Network determination; determining graphs which represent gene-gene or gene-phenotype interactions. Such methods include Bayesian networks and relevance networks.

The most common unsupervised techniques are PCA, hierarchical clustering, k-means clustering, SOMs and relevance networks.

6.1.3.2.1 Hierarchical clustering

Hierarchical clustering is one of the most commonly used methods among biologists and has been widely reported [232, 235, 241]. The greatest advantage in using this method is that it is simple and the number and size of expression patterns can be quickly estimated [235]. During hierarchical clustering single expression profiles are joined to form groups. These groups are further joined together until all profiles are linked forming a single hierarchical tree. Dendograms are subsequently used to visualise the results of the hierarchical clustering. Hierarchical clustering is referred to as an agglomerative approach as opposed to a divisive method [236]. (The agglomerative approach starts with single/few genes per cluster and then links them together. The devisive approach begins with all the genes in a single cluster and breaks down this single cluster into smaller clusters [236]). One of the disadvantages of hierarchical clustering is that it ignores negative correlations even when the dissimilarity measure used supports a negative correlation [238]. In addition; genes that are incorrectly linked early on in the process cannot later be linked to their correct cluster as the tree is constructed.

6.1.3.2.2 *k*-means clustering

In *k*-means clustering, the user defines the number of clusters (*k*) and the data is subsequently assigned to this number of clusters [242]. The aim being to end up with clusters where data within individual clusters is similar but between clusters is dissimilar. To achieve this, the data is initially randomly assigned to one of k clusters. An average expression vector is then calculated for each cluster and this is used to compute distances between clusters. Data is then moved between clusters and intra and inter distances between clusters is measured on each move. Data is assigned to a new cluster only if it is closer to it than it was in the previous cluster. This shuffling continues until moving any more data points would make the clusters more variable.

6.1.3.2.3 Self-organising maps (SOMs)

A SOM is a divisive clustering approach where genes are assigned to a series of partitions depending on how similar their expression vectors are relative to a reference vector (where the reference vector represents a particular partition) [243]. The user defines a configuration for the partition (usually a 2-dimensional rectangular grid; such as 3x3 giving 9 clusters). A random vector is then assigned to each partition. A gene is randomly selected and is assigned to the reference vector closest to it. The reference vector is then adjusted so that it is closer to the vector of the assigned gene. At the same time other nearby vectors are adjusted so that they are more similar to the vector of the assigned gene. The process continues until all the genes are mapped to partitions depending on their similarity to a reference vector of a particular partition. With both k-means clustering and SOMs, it is often useful to use PCA to estimate the number of clusters represented within the data before applying the aforementioned techniques. The use of SOMs have been successfully reported by Tamayo *et al* for clustering of genes from a time series of differentiating haematopoietic cells [244].

6.1.3.2.4 Relevance Networks

This method allows networks of features to be built, where the features can represent not only genes but also factors such as phenotype or clinical measurement [245]. The initial part of the technique is similar to hierarchical clustering. For example, two genes are compared to each other on a scatter-plot containing all the samples; with the expression levels of the two genes being used as coordinates. A correlation coefficient is then calculated for the features in the samples. This is compared to a chosen threshold value and only features with values greater than the threshold value are kept. They are then displayed in graph form where features are nodes joined by lines (of varying size and colour) representing the relationship between different nodes.

The advantage of relevance networks is that features showing negative correlations can be visualised [238]. One disadvantage is that at lower thresholds many features may be linked in a single network creating a high degree of complexity which is difficult to interpret.

6.1.3.2.5 Principle Component Analysis

PCA is used largely as a visualisation technique [246]. Genes or samples are represented in a multidimensional space as points. Principle components are a set of vectors in this multidimensional space that capture the variation seen in these points. As the vectors are in the same multidimensional space, the principle components are linear combinations of the points [247]. It can be compared to looking at a 3 dimensional cloud of data points and rotating the cloud so you can view from different angles [236]. Certain views would separate the data better than others. PCA finds those views and gives the best separation of the data. Although on its own PCA can make it difficult to define accurate boundaries between clusters within data sets; it is a powerful technique when used together with k-means clustering or SOMs [236].

6.2 Temporal gene expression in macrophages exposed to OxLDL

6.2.1 Experimental design

The initial aim of this work was to identify genes that were differentially expressed during exposure of differentiated THP-1 macrophages to modified LDL. Results from the previous chapter indicated that time was an important factor to take into consideration when looking at differentially expressed genes. Furthermore results from the lipid loading experiments in chapter 3 indicated that cholesterol ester accumulation occurred at a slower rate in differentiated THP-1 macrophages exposed to OxLDL (compared to native and AcLDL), with maximal accumulation occurring at 72 hours. Additionally it would be of interest to obtain a 'global picture' of gene expression that was taking place within macrophages on exposure to OxLDL to gain an understanding on the effects that this ligand has.

In an attempt to achieve this goal; a time series experiment was performed in which differentiated THP-1 macrophages were exposed to 0.2 mg/ml of oxidised LDL for up to 72 hours. Differentiated THP-1 macrophages were exposed to OxLDL for 4, 8, 16, 24, 48 and 72 hours. A sample of differentiated THP-1 macrophages exposed to no OxLDL was used as a zero time control point.

The temporal expression of genes after treatment was examined with the aim of identifying genes showing distinct patterns of expression (for example genes showing maximal expression at a particular time point). A further aim was to identify groups of genes showing similar patterns of expression (co-expressed genes) over the course of exposure to OxLDL. A point to note here is that this part of the study does not eliminate that these same genes may also be affected by native LDL; but simply allows genes being expressed on exposure to OxLDL to be identified. The identification of genes differentially expressed using different forms of LDL was the aim of the DGE experiments reported in the previous chapter.

The study was divided into two parts. The first part of the study was simply to identify the genes being expressed at each time point on exposure to OxLDL when compared to the control (no OxLDL) sample. The second part of the study used the method of hierarchical clustering (discussed above) to group those genes that showed

similar patterns of expression into clusters. The clusters were examined to find which genes had correlated expression patterns.

6.2.2 Data collection

Figure 6.1 below gives an overview of the steps involved performing and collecting temporal gene expression data. Differentiated THP-1 macrophages were exposed to OxLDL for 4, 8, 16, 24, 48 and 72 hours, with each sample being prepared as a biological replicate. Messenger RNA was extracted from the cells and 1st strand labelled cDNA probes were prepared as described (section 2.4.4.). The probes prepared were applied to the custom atheroma arrays only. I.M.A.G.E arrays were not used due to several reasons, including limited time, limited resources and subsequent data analysis limitations. In addition the genes gridded on the custom atheroma array had been checked to confirm their sequence identity (as previously described; see appendix 3). This ensured that the analysis of the data was easier because the results obtained did not have to be confirmed by sequencing. Hybridisation to atheroma arrays was performed as previously described (section 2.4.6) and the data was captured using phosphorimaging.

6.2.3 Data analysis

The first step involved processing the phosphorimaging data obtained for each array and correcting for DNA loading (amount of DNA gridded onto the arrays) using DGEnt software. This produced a hybridisation intensity for every gridded spot on the array. As biological samples were prepared and applied to arrays in duplicate, results from the duplicate arrays were averaged (mean value was calculated).

Data was archived and processed in Quanta DGE (a piece of software developed by the DGE group, Glaxo Wellcome, UK). Quanta DGE provides data management and analysis for gene expression arrays. Quanta DGE was used to provide an average mean expression level for each gene at each time point (since each gene was present on the array at least four times and two biological replicates were performed per sample, the minimum number of data points contributing to the average expression level was 8).

Figure 6.1

Overview of the steps involved in collecting temporal gene expression data

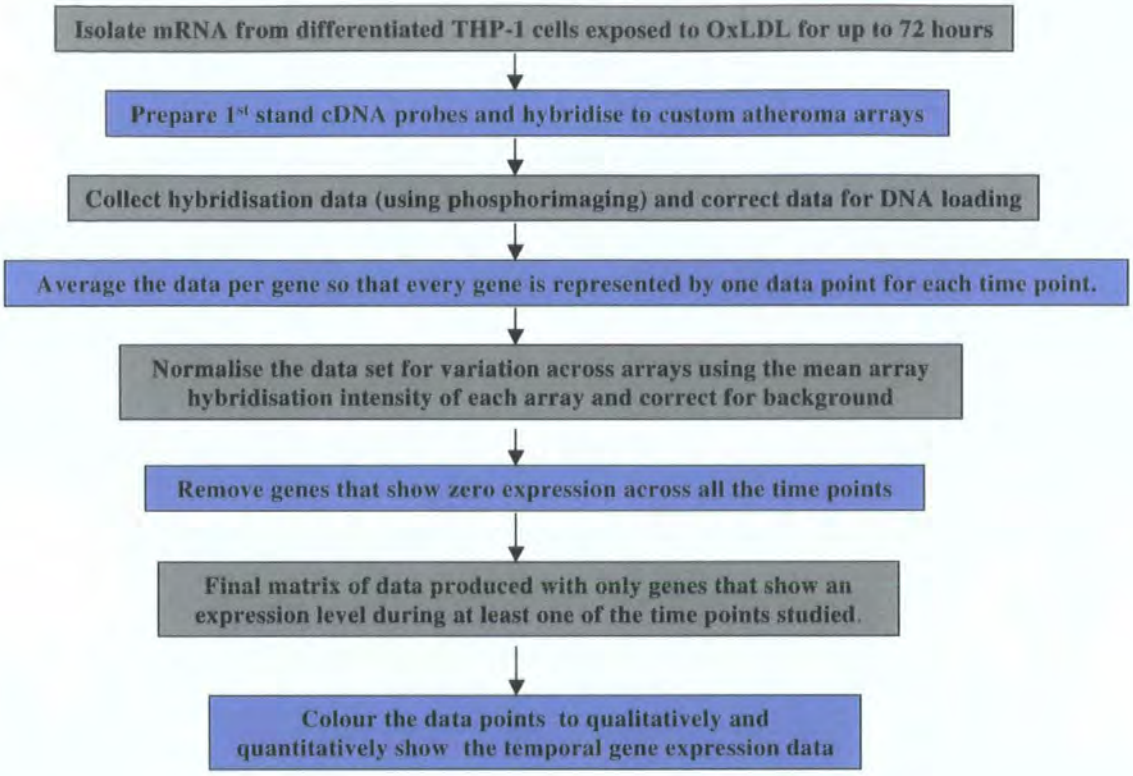

At this stage the data (which consists of a expression level for each gene at each time point) could be exported to a Microsoft Excel workbook. This data, referred to here to as 'raw data' is listed in appendix 7 (Excel workbook labelled 'appendix 7', worksheet labelled 'data analysis'. This worksheet contains 4 data tables labelled appendix 7.1, appendix 7.2, appendix 7.3 and appendix 7.4). The raw data was subsequently corrected for the mean hybridisation intensity of each array to correct for variations between arrays (appendix 7.2) and background was subtracted (appendix 7.3). This gave a corrected data set that gave an expression level for every gene at each time point (appendix 7.3). This data set consisted of 769 genes with expression levels across 7 time points, giving a total of 5383 data points. Finally the corrected data set was analysed and genes with expression levels below background across all of the time points were removed, as were any genes whose sequence was not confirmed. This ensured that all the results obtained were for those genes whose sequence had been confirmed.

6.3 Results

6.3.1 Quantitative and qualitative analysis of genes showing temporal expression

Of 769 genes on the array, 216 genes (28%) showed an expression level (greater than background) during at least one time point. These 1512 data points were analysed further (appendix 7.4). To make this matrix of expression levels (effectively a table of numbers) easier to interpret, the expression level of each gene at each time point was colour coded depending on the degree of expression. Genes showing a low expression (0-1.10) at any given time point were coloured blue, those showing moderate expression (1.11-3.86) were coloured green and those showing high expression (3.87-11.33) were coloured red as shown below in table 6.1 (and appendix 7.4). This allows one to easily visualise the data and select genes showing low, moderate and high levels of expression without having to a go through a large list of numbers. The data was coloured using the tools function of Microsoft Excel (see methods section 2.4.7.2).

Table 6.1

Table showing the 216 genes identified as expressed during at least one time point in differentiated THP-1 macrophages exposed to OxLDL for up to 72 hours. Each cell is coloured depending on the degree of expression. Blue corresponds to a low expression level (0 - 1.10), green to an average expression level (1.11 - 3.86) and red to a high expression level (3.87 - 11.33). The table is also given in appendix 7.4

	Time (hours)						
Gene Name	0	4	8	16	24	48	72
14-3-3 protein, theta isoform X56468	0.55	0.00	0.00	0.00	0.05	0.00	0.00
14-3-3 protein, theta isoform X80536	0.29	0.00	0.14	0.00	0.00	0.00	0.00
14-3-3 protein, zeta isoform U28964	1.13	0.00	0.02	0.25	0.00	0.27	1.33
23KD highly basic protein	4.67	7.61	5.28	2.26	8.51	6.30	3.80
a3integrin Very Late Antigen-3 (VLA-3); collagen	0.35	0.00	0.24	0.00	0.00	0.00	0.15
actinin, alpha non-muscle X55187	2.97	0.00	1.32	1.74	0.34	0.71	1.64
activator-1, 37 kD subunit	0.00	0.00	0.00	0.11	0.00	0.00	0.00
alpha 5 integrin (fibronectin rec)	1.73	0.31	1.68	2.84	1.73	1.93	3.14
Annexin I (lipocortin I)	0.00	0.00	0.34	1.02	0.87	0.00	0.01
Annexin II	4.14	1.42	3.18	3.76	6.91	1.71	4.10
b catenin	1.97	0.00	0.31	0.73	0.00	0.00	0.19
b-ACTIN	4.23	0.00	7.68	11.21	0.00	8.47	9.30
Basement membrane 40/SPARC (secreted protein acidic	0.00	0.00	0.00	0.00	0.21	0.00	0.00
Beta 1 adrenergic receptor	0.26	0.00	0.00	0.00	0.14	0.00	0.00
beta actin mutant	8.91	0.43	7.88	5.35	2.89	10.77	6.87
beta-actin mutant	7.20	0.00	8.92	7.72	2.16	11.05	6.62
Calcineurin B	0.33	0.00	0.27	0.00	0.01	0.16	0.02
Cathepsin L	2.23	0.00	2.63	1.75	0.46	7.35	5.39
Cathepsin S	0.56	0.00	0.00	0.00	0.00	0.00	0.00
CD106 VCAM	0.00	0.00	0.11	0.12	0.00	0.00	0.00
CD151 (PETA-3)	0.09	0.00	0.00	0.00	0.00	0.00	0.00
cd29 Fibronectin receptor beta subunit	0.15	0.00	0.00	0.65	0.00	0.00	0.00
CD36	0.57	0.00	0.00	0.00	1.45	1.77	0.90
CD36 antigen (collagen type I receptor, thrombospondin	0.00	0.00	0.00	0.00	0.12	0.00	0.00
CD44 antigen (cell adhesion molecule)	1.18	0.00	0.93	1.91	0.00	0.38	0.95
CD44E	1.50	0.00	0.61	1.21	0.00	0.53	0.90
CD44H	1.08	0.00	0.46	1.09	0.41	1.16	2.14
CD54 ICAM-1	1.03	0.00	0.33	0.39	0.00	0.00	0.03
Cell division cycle 42 (GTP-binding protein, 25kD)	0.00	0.00	0.00	0.00	0.84	0.00	0.00
Ceramidase	0.00	0.00	0.00	0.38	0.00	0.00	0.00
CHD036	0.41	0.00	0.00	0.00	0.00	0.00	0.00
Chi (Human class III alcohol dehydrogenase (ADH5) chi	0.02	0.00	0.00	0.22	0.15	0.00	0.00
c-myc binding prot	0.55	0.00	0.00	0.00	0.00	0.00	0.20
C-MYC BINDING PROTEIN MM-1.	0.40	0.00	0.33	1.21	0.05	0.00	0.36
collagenase	1.87	0.00	1.16	0.47	0.46	0.28	0.00
collagenase type IV J03210	0.39	0.00	0.00	0.00	0.49	0.11	0.00
Complement component 1, s subcomponent	1.15	0.00	1.11	0.58	0.00	1.97	0.42
COX1	0.13	0.00	0.00	0.00	0.00	0.72	0.00
CREB-2	0.98	0.00	0.74	0.70	1.30	0.51	1.25

cyclin D3 (CCND3)	0.83	0.00	0.87	0.25	0.00	1.30	0.12
cyclin G1	0.01	0.00	0.00	0.00	0.00	0.00	0.00
cyclin G1 interacting protein, putative	0.57	0.00	0.01	0.00	0.00	0.00	0.00
cyclin I	0.00	0.00	0.00	0.00	0.00	0.20	0.00
cyclin-dependent kinase 4 (cdk4)	0.17	0.00	0.16	0.00	0.00	0.75	0.16
cyclin-dependent kinase activating kinase	0.09	0.00	0.00	0.00	0.00	0.00	0.00
Cytohesin	0.94	0.00	0.00	0.03	0.00	0.00	0.00
DEFENDER AGAINST CELL DEATH 1	0.93	0.00	0.00	0.25	1.30	0.00	0.16
DNA replication licensing factor	0.57	0.00	0.00	0.00	0.00	0.00	0.00
E2F transcription factor 4, p107/p130-binding	0.00	0.00	0.14	0.00	0.00	0.00	0.00
epithelin 1 2	0.90	0.00	0.00	0.47	0.00	0.32	0.58
FEG-1	0.00	0.00	0.00	0.00	0.21	0.00	0.00
fibrillarin	0.02	0.00	0.00	0.00	0.00	0.00	0.00
fibronectin	1.70	0.00	0.54	2.21	0.23	0.28	0.84
Fibronectin 1	2.94	0.00	1.12	1.91	0.00	0.31	0.89
FN Fibronectin	0.60	0.00	0.09	0.26	0.00	0.00	0.00
FN-Rb Fibronectin receptor beta subunit	1.30	0.00	0.00	0.00	0.00	0.00	0.55
fos	0.11	0.00	0.00	0.00	0.00	0.00	0.00
G3PDH	3.38	0.00	1.74	3.06	0.00	5.94	3.20
G9 sialidase	0.03	0.00	0.00	0.04	0.00	0.00	0.16
GDP-dissociation inhibitor rho X69549	0.51	0.00	0.34	1.34	0.00	0.21	0.31
glutamine synthetrase	0.20	0.00	0.21	0.00	0.00	0.37	0.33
glutathione peroxidase	2.11	0.00	0.87	1.05	0.06	3.04	1.96
GRK3	0.00	0.00	0.00	0.00	0.00	0.09	0.00
GTPase-activating protein gap M23612	0.22	0.00	0.00	0.00	0.30	0.00	0.00
guanine nucleotide-binding protein rab1 M28209	0.92	0.00	0.03	1.22	0.00	0.00	0.00
guanine nucleotide-binding protein rho X05026	3.54	0.00	2.02	2.66	0.00	1.46	1.66
H.sapiens homeobox protein (HOX-11) mRNA, complete	0.00	0.00	0.00	0.00	0.13	0.00	0.00
H.sapiens mRNA for extracellular matrix protein collagen	0.00	0.00	0.00	0.00	0.00	0.99	0.00
H.sapiens mRNA for ragA protein	1.10	0.00	0.00	0.00	0.00	0.00	0.00
Heat shock 10 kD protein 1 (chaperonin 10)	0.30	0.00	0.08	0.00	0.94	0.08	0.00
Hexabrachion (tenascin C, cytotactin)	0.51	0.00	0.00	0.00	0.00	0.00	0.00
HLA-1	4.76	0.00	2.11	1.24	0.00	0.26	0.46
Homo sapiens interleukin-1 receptor-associated kinase	0.56	0.00	0.00	0.00	0.07	0.00	0.00
Homo sapiens mRNA for alpha(1,2)fucosyltransferase,	0.00	0.00	0.00	0.00	0.33	0.01	0.00
Homo sapiens mRNA for NB thymosin beta, complete	0.00	0.00	0.00	0.00	0.20	0.00	0.00
Hu. 1-8U gene for interpheron ind.	1.67	0.00	0.00	0.00	0.19	0.00	0.21
Human alpha enolase mRNA, complete cds.	5.19	0.00	3.88	3.24	0.00	1.69	1.58
Human alpha-2 collagen type VI mRNA, 3' end	0.30	0.00	0.00	0.26	0.30	0.00	0.00
Human CDK6 inhibitor p18 mRNA, complete cds	0.00	0.00	0.20	0.00	0.00	0.00	0.00
Human collagenase inhibitor mRNA, comple	6.13	3.33	8.12	11.33	5.82	4.54	6.87
Human cyclin-dependent kinase inhibitor p27kip1	0.13	0.00	0.00	0.00	0.00	0.00	0.00
Human ferritin H chain mRNA, complete cd	1.08	0.00	0.20	0.56	1.46	0.37	0.28
Human focal adhesion kinase (FAK) mRNA, complete	0.04	0.00	0.00	0.00	0.00	0.00	0.00
Human HepG2 partial cDNA, clone hmd3f02m	4.86	1.41	6.61	4.28	4.69	7.13	7.61
Human major histocompatibility class II	0.94	0.00	0.50	0.14	0.23	0.64	0.00
Human MAPKAP kinase (3pK) mRNA, complete cds	0.00	0.00	0.00	0.49	0.00	0.00	0.00
Human mRNA for fibronectin (FN precursor	0.92	0.00	0.79	2.62	0.09	0.50	0.69
Human mRNA for HLA class II DR-beta 1 (D	0.84	0.00	0.00	0.14	0.00	0.00	0.00
Human mRNA for KIAA0120 gene, complete c	3.09	0.00	3.53	1.60	0.10	3.98	1.57
Human mRNA for KIAA0201 gene, complete cds	0.00	0.00	0.00	0.00	1.81	0.00	0.00
Human mRNA for KIAA0233 gene, complete cds	0.00	0.00	0.00	0.00	1.37	0.00	0.00
Human mRNA for KIAA0246 gene, partial cds	0.09	0.00	0.00	0.00	0.00	0.00	0.00

Human mRNA for lipocortin II, complete c	2.97	0.91	2.51	5.00	4.83	1.92	2.97
Human mRNA for MRP-1.	0.21	0.00	0.00	0.26	0.00	0.00	0.00
Human mRNA for ORF, Xq terminal portion	0.08	0.00	0.00	0.00	0.00	0.00	0.00
Human mRNA for ornithine decarboxylase antizyme,	2.17	0.23	2.79	2.18	3.20	3.51	1.71
Human mRNA for proteasome subunit z, complete cds	0.04	0.09	0.00	0.00	0.18	0.00	0.00
Human mRNA for protein D123, complete cds	0.00	0.00	0.00	0.34	0.00	0.00	0.00
Human mRNA for protein homologous to elo	4.38	0.50	4.22	2.31	1.45	6.51	4.15
Human mRNA for stromelysin.	0.00	0.00	0.00	0.00	0.02	0.00	0.00
Human mRNA for translationally controlle	4.50	2.39	4.21	2.14	5.04	5.60	3.85
Human mRNA for U1 small nuclear RNP-specific C	0.02	0.00	0.00	0.00	0.00	0.37	0.00
Human myosin regulatory light chain mRNA, complete	2.28	0.00	0.53	0.64	0.27	0.00	0.93
Human protective protein mRNA, complete	2.06	0.00	0.70	0.33	0.51	0.40	0.51
Human putative protein kinase C inhibitor (PKCI-1)	0.73	0.00	0.00	0.00	1.06	0.00	0.36
Human RHOA proto-oncogene multi-drug-res	1.64	0.00	0.62	1.30	0.00	0.08	0.81
Human Rho-associated, coiled-coil containing protein	0.35	0.00	0.00	0.25	0.95	0.00	0.00
Human ribosomal protein L37a mRNA sequen	3.58	3.88	3.03	5.92	10.88	2.56	3.39
Human RPS3a gene.	3.17	0.38	0.76	1.39	3.08	0.00	1.01
Human saposin proteins A-D mRNA, complet	5.95	0.00	3.62	3.42	0.84	2.75	3.87
Human SPARC/osteonectin mRNA, complete c	0.00	0.00	0.13	0.00	0.00	0.00	0.00
hxfl2 t64438	0.00	0.00	0.00	0.00	0.01	0.00	0.00
hxfl3	0.26	0.00	0.00	0.00	0.00	0.00	0.00
IFN gamma R alpha	0.48	0.00	0.00	0.00	0.00	0.00	0.00
IFNg Rb	0.31	0.00	0.00	0.64	0.00	0.00	0.00
IL-1 beta	2.05	2.58	6.94	8.71	3.86	2.29	2.36
IL-10	0.08	0.00	0.00	0.00	0.00	0.00	0.00
IL-1Ra	1.57	0.36	1.29	1.82	2.00	0.78	0.80
IL-2Rg	0.00	0.00	0.00	0.00	0.00	0.04	0.00
IL-4*	0.05	0.00	0.00	0.00	0.00	0.00	0.00
IL-7R	0.01	0.00	0.00	0.00	0.00	0.00	0.00
IL-8	0.98	0.00	3.44	0.93	0.00	0.48	0.29
insulin-like growth factor binding protein 3 X64875	1.82	0.00	1.76	0.00	0.00	0.49	0.00
integrin alpha 3	1.07	0.00	0.42	0.43	0.00	1.41	0.33
Integrin beta-4 subunit	0.00	0.00	0.00	0.00	0.09	0.00	0.00
integrin-linked kinase (ILK) U40282	0.57	0.00	0.00	0.35	0.00	0.00	0.00
jun	0.00	0.00	0.00	0.00	0.28	0.00	0.00
jun-B protein X51345	0.74	0.00	0.00	0.00	0.23	0.00	0.09
KRAB zinc finger protein {alternative products}	0.11	0.00	0.00	0.00	0.00	0.00	0.00
laminin B2 J03202	0.10	0.00	0.28	0.00	0.00	0.23	0.00
laminin S B3 chain L25541	0.00	0.00	0.00	0.00	0.00	0.01	0.00
LFA-3 GPI-linked variant	0.05	0.00	0.00	0.00	0.00	0.00	0.00
LFA-3 trans-membrane variant	0.16	0.00	0.00	0.00	0.60	0.16	0.00
Lipocortin	0.35	0.00	0.96	1.66	1.34	1.27	0.79
lipocortin II M14043	2.23	2.29	2.28	2.10	5.62	3.53	4.10
Lymphocyte cytosolic protein 1 (L-plastin)	3.23	0.85	3.21	2.07	5.04	4.65	3.43
lynA	0.05	0.00	0.00	0.00	0.00	0.00	0.00
Matrix metalloproteinase 12 (macrophage elastase)	0.07	0.00	0.00	0.00	0.00	0.00	0.00
Matrix metalloproteinase 2 (gelatinase A; collagenase	5.04	0.00	3.22	3.65	0.00	2.21	2.88
matrix metalloproteinase MMP-18 Y08622	0.43	0.00	0.82	0.95	0.00	0.00	0.53
M-CSF	0.00	0.00	0.00	0.00	0.00	1.12	0.08
metalloprotease/disintegrin/cysteine-rich protein	0.49	0.00	0.00	0.35	0.00	0.00	0.02
Metallothyonein	0.00	0.00	0.13	1.25	2.93	2.90	1.99
MIP-1b Macrophage Inflammtory Protein-1b	0.25	0.00	0.00	0.00	0.00	0.00	0.00
mitogen-activated protein kinase activated protein kinase	0.93	0.00	0.42	0.51	0.00	2.45	0.81
mitotic feedback control protein madp2 homolog U31278	0.08	0.00	0.00	0.00	0.00	0.00	0.00
moesin	2.05	0.00	0.43	0.91	0.00	0.29	1.57

myosin light chain kinase (MLCK) U48959	1.20	0.00	0.00	0.09	0.05	0.00	0.36
myosin regulatory light chain X54304	2.27	0.00	0.39	1.43	0.06	0.00	1.39
nidogen (nid) M30269	0.09	0.00	0.00	0.00	0.00	0.00	0.00
Nip2	0.00	0.00	0.00	0.00	0.04	0.00	0.00
Nip3	0.24	0.00	0.00	0.00	0.00	0.00	0.00
osteopontin J04765	3.30	0.00	1.24	3.12	3.58	1.93	3.34
P21 homolog X64899	2.40	2.22	2.91	1.76	4.62	3.78	4.09
p53 activated fragment-1	3.36	2.20	3.11	4.69	5.30	2.08	3.97
p55CDC U05340	0.66	0.00	0.00	0.23	0.00	0.33	0.61
p85MCM	0.22	0.00	0.00	0.00	0.00	0.00	0.00
pag (proliferation associated gene)	1.71	1.60	1.59	0.24	2.31	3.35	1.24
paxillin U14588	0.19	0.00	0.09	0.00	0.00	0.87	0.11
PECAM	0.46	0.00	0.00	0.00	0.00	0.32	0.00
pla2 Phospholipase A2	0.96	0.00	0.01	0.32	0.00	0.11	0.87
Platelet glycoprotein IX	0.28	0.00	0.00	0.21	0.00	0.00	0.00
profilin J03191	3.44	0.00	1.47	1.79	0.00	0.47	1.41
prohibitin S85655	0.73	0.00	0.00	0.21	0.07	0.00	0.00
protein kinase p58 M88563	0.11	0.00	0.00	0.43	0.00	0.00	0.00
PROTEIN PHOSPHATASE INHIBITOR 2	0.00	0.00	0.00	0.00	0.00	0.04	0.00
prothymosin alpha M14483	3.99	6.66	2.10	1.96	8.07	4.65	2.33
proto-oncogene c-myc K01905	0.00	0.00	0.00	0.00	0.00	0.00	0.00
proto-oncogene c-src tyrosine kinase X59932	0.21	0.00	0.00	0.00	0.00	0.00	0.00
proto-oncogene c-syn M14333	0.00	0.00	0.00	0.00	0.00	0.02	0.00
proto-oncogene c-yes-1 M15990	0.09	0.00	0.00	0.00	0.00	0.00	0.00
proto-oncogene RHOA, multi-drug-resistance protein	1.96	0.00	1.06	2.50	1.10	0.34	0.89
Radixin	0.00	0.00	0.00	0.00	0.12	0.00	0.00
ras-related GTP-binding protein Krev-1 M22995	1.87	0.00	0.38	1.32	0.44	0.00	0.60
ras-related GTP-binding protein rap1a X12533	0.00	0.00	0.00	0.00	0.00	0.02	0.00
ras-related GTP-binding protein RIT Y07566	0.00	0.00	0.00	0.35	0.00	0.00	0.00
ribosomal protein S17	0.59	0.00	0.88	2.28	1.67	0.00	0.74
serine/threonine kinase FAST X86779	0.15	0.00	0.03	0.00	0.00	0.24	0.00
serine/threonine kinase rac, alpha M63167	0.54	0.00	0.00	0.28	0.00	0.00	0.01
serine/threonine phosphatase PP-1d isolog D90164	0.01	0.00	0.00	0.00	0.00	0.00	0.00
serine/threonine phosphatase PPPIA, alpha subunit	0.44	0.00	0.56	0.00	0.00	1.34	0.31
SHC, p52 isoform X68148	0.47	0.00	0.30	0.00	0.00	0.43	0.03
signal transducer and activator of transcription 6 (Stat6)	0.81	0.25	0.00	0.00	0.62	1.06	0.30
sox12	0.00	0.00	0.00	0.00	0.51	0.17	0.00
syk B-cell protein tyrosine kinase associated with	0.10	0.00	0.00	0.00	0.00	0.00	0.00
Syndecan 2 (heparan sulfate proteoglycan 1, cell surface-	0.26	0.00	0.00	0.00	0.00	0.00	0.00
talin isolog X56123	0.14	0.00	0.00	0.14	0.00	0.00	0.00
Thrombin Receptor	0.00	0.00	0.00	0.00	0.00	0.00	0.18
thrombomodulin	0.00	0.00	0.60	0.00	0.15	0.15	0.00
THYMOSIN BETA-10	2.78	0.68	1.13	0.96	3.85	1.25	2.35
TIMP-1 MMP-11	1.87	2.68	8.12	10.43	4.63	4.65	3.33
TIMP-3	0.00	0.00	0.00	0.03	0.00	0.00	0.00
TM4 family : CD9	0.48	0.00	0.00	0.00	0.00	0.00	0.00
TNF-R II	0.83	0.00	0.00	0.24	0.03	0.00	0.00
TNFR type I	0.78	0.00	0.19	0.49	0.57	0.00	0.14
transcription factor BTF-3	1.91	0.00	0.54	1.06	0.34	0.00	0.78
translationally controlled tumor protein	3.13	0.37	1.30	2.86	4.19	0.87	2.05
Tropomyosin alpha chain (skeletal muscle)	0.25	0.00	0.00	0.00	0.00	0.00	0.00
Tropomyosin beta chain (skeletal muscle)	0.22	0.00	0.00	0.12	0.00	0.00	0.00

tryptase I Serine protease produced in mast cells	0.00	0.00	0.00	0.00	0.00	0.00	0.65
TUBULIN ALPHA-4 CHAIN	0.00	0.00	0.00	0.00	0.00	0.29	0.00
tubulin, alpha K00557	1.50	0.00	1.32	2.50	0.00	0.77	1.38
tubulin, beta X79535	1.46	0.00	0.67	0.63	0.00	2.90	0.86
tubulin, gamma M61764	0.28	0.00	0.00	0.31	0.00	0.00	0.00
tymosin beta-4	5.28	0.95	0.90	2.55	10.21	2.52	5.93
tyrosine kinase src-like kinase (srk) M14676	0.01	0.00	0.00	0.00	0.00	0.32	0.00
tyrosine phosphatase hPRL-1N homolog U69701	0.18	0.00	0.00	0.00	0.00	0.00	0.00
tyrosine phosphatase hR-PTPu X58288	0.10	0.00	0.00	0.20	0.00	0.00	0.00
tyrosine phosphatase PTP1C X62055	1.28	0.00	0.11	0.59	0.00	0.00	0.31
UBCH5C (E2 ubiquitin conjugating enzyme)	0.61	0.00	0.00	0.24	0.15	0.00	0.29
u-PAR	0.86	0.00	1.39	0.62	0.00	2.04	1.44
urokinase (uPA)	0.66	0.00	0.00	0.00	0.00	0.45	0.00
vimentin	6.82	6.39	6.78	5.16	10.23	7.32	7.12
VLA-5 CD49a:Very Late antigen-5; Fibronectin receptor;	1.78	0.00	0.49	1.25	0.00	0.76	1.02
Wnt-13 Z71621	0.11	1.28	0.00	0.00	4.27	0.00	0.00
zyxin X94991	4.06	0.00	2.54	2.47	1.09	4.63	2.57

As can be seen from table 6.1, the majority of genes show a low level expression. However colouring the values does allow one to easily select out those genes showing moderate and high levels of expression. Table 6.2 below lists some of the genes taken from table 6.1 that show a low to moderate, moderate to high and high level of expression.

From a biological perspective; genes seen to be switched on by OxLDL again seem to be those implicated in inflammatory response (IL-1β and Annexin), in cell structure (fibronectin, thymosin and vimentin) and cell membrane remodelling (MMPs and TIMP). In addition several genes such as p53 and translationally controlled tumour protein were also identified which could be due to some of the potentially cytotoxic effects of OxLDL.

Table 6.2

Table showing some of the genes found to have low to moderate, moderate to high and high levels of expression on exposure of differentiated THP-1 cells exposed to OxLDL over 72 hours

Genes showing a low to moderate expression level	Genes showing a moderate to high expression level	Genes showing a high expression level
Actinin	Annexin II	23Kd highly basic protein
Fibronectin/fibronectin receptor	Cathepsin L	β-actin
CD36	Lipocortin II	Human collagenase inhibitor
Alpha enolase	Human saposin proteins A-D	TIMP-1
MMP-2	L-plastin	IL-1β
Metallothionein	p21	Prothymosin alpha
Oesteopontin	Translationally controlled tumour protein	Thymosin B4
Thymosin B10	P53 activated fragment 1	Vimentin

6.3.2 Analysis of genes of interest showing temporal expression

Graph 6.1 shows the expression profile of the annexins (also known as lipocortins). Annexins are calcium/phospholipid-binding proteins that are involved in membrane fusion and exocytosis. They also play a role in inflammation acting as anti-inflammatory agents. As can be seen from the graph the Annexin II group shows a much higher level of expression than Annexin I.

There are three cDNA clones representing the annexin II gene, 2 of which (annexin II and lipocortin II) show a peak of expression at 24 hours however the two

genes are not strongly correlated (R=0.65). A stronger correlation, however was observed between annexin II and human mRNA for lipocortin II; R= 0.81. The two versions of annexin I show a peak of expression at 16 hours; however again the pattern is not highly correlated (annexin 1 and lipocortin; R= 0.743). The strongest correlation (R = 0.865) was observed between Annexin and human mRNA for lipocortin II. This could indicate that the clones representing the annexins may not be specific enough to distinguish between the two genes.

Graph 6.1

Graph showing expression pattern of annexins in differentiated THP-1 macrophages exposed to OxLDL for up to 72 hours

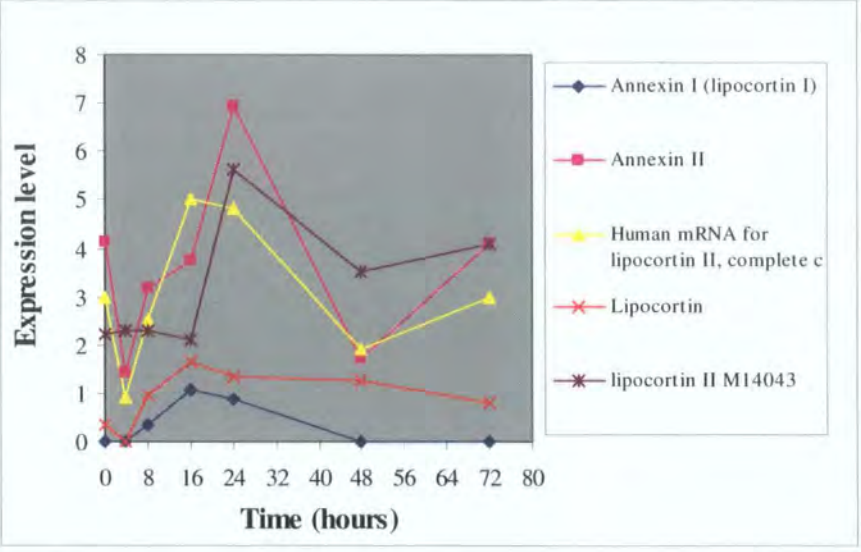

Graph 6.2 shows the expression pattern of β-actin. Actins are highly conserved proteins that are involved in various types of cell motility and are ubiquitously expressed in all eukaryotic cells. The ubiquitous expression of the β-actin means that it is often used as a housekeeping gene. In general it is assumed that the level of a housekeeping gene remains relatively constant. As can be seen from the graph however, β-actin levels in our experiments did not remain constant. They show a decreased level at 4 and 24 hours. Two of the different clones representing this gene did however show a similar pattern of expression (R= 0.94 for the two beta actin mutant clones).

Graph 6.2

Graph showing expression pattern of β-actin in differentiated THP-1 cells exposed to OxLDL for 72 hours

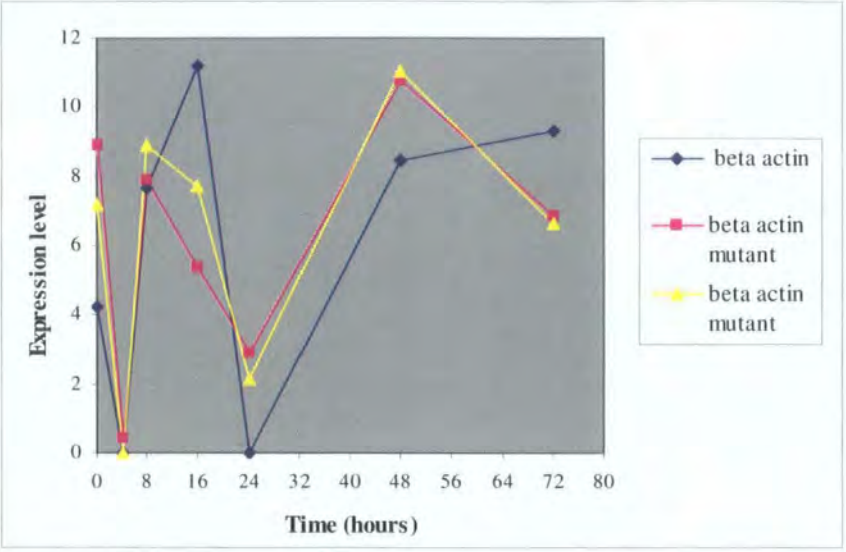

Graph 6.3 shows expression pattern of myosin light chain. Myosin light chain kinase phosphorylates a specific serine in the N-terminus of a myosin light chain. As can be seen from the graph all forms of the myosin light chain showed a peak of expression at 16 hours, decreasing and then showing an increase in expression between 48 and 72 hours. In addition the pattern of expression was similar with the R value ranging from 0.86 to 0.96 between the different clones.

Graph 6.4 shows the expression pattern of tubulin. Tubulin is the major constituent of microtubules. As can be seen from the graph, the different types of tubulin show different patterns of expression. The alpha and beta forms of tubulin show the highest levels of expression. Both tubulin alpha and gamma show a peak of expression at 16 hours whereas tubulin beta shows maximal expression at 48 hours. However a stronger correlation was observed between tubulin alpha-4 chain and tubulin beta (R= 0.86) compared to tubulin alpha and tubulin gamma (R= 0.73).

Graph 6.3

Graph showing expression pattern of myosin light chain in differentiated THP-1 macrophages exposed to OxLDL for 72 hours

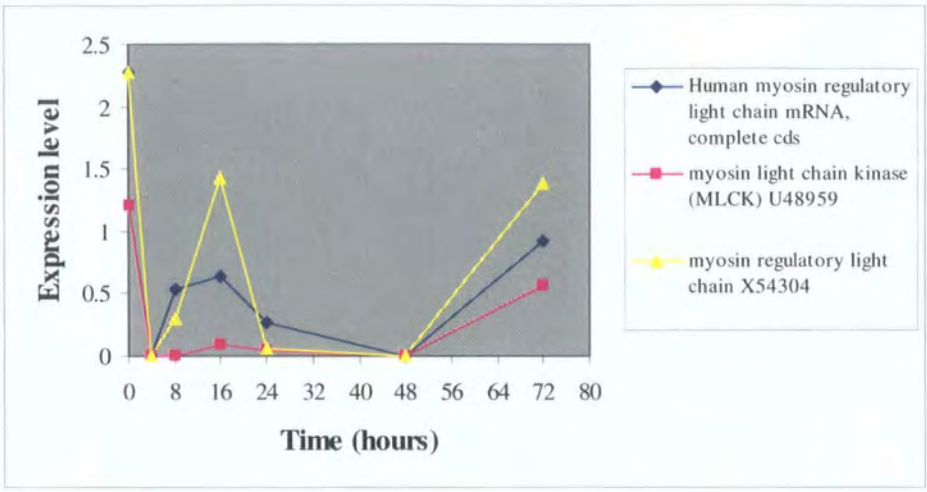

Graph 6.4

Graph showing expression pattern of the tubulin family of genes in differentiated THP-1 cells exposed to OxLDL for 72 hours

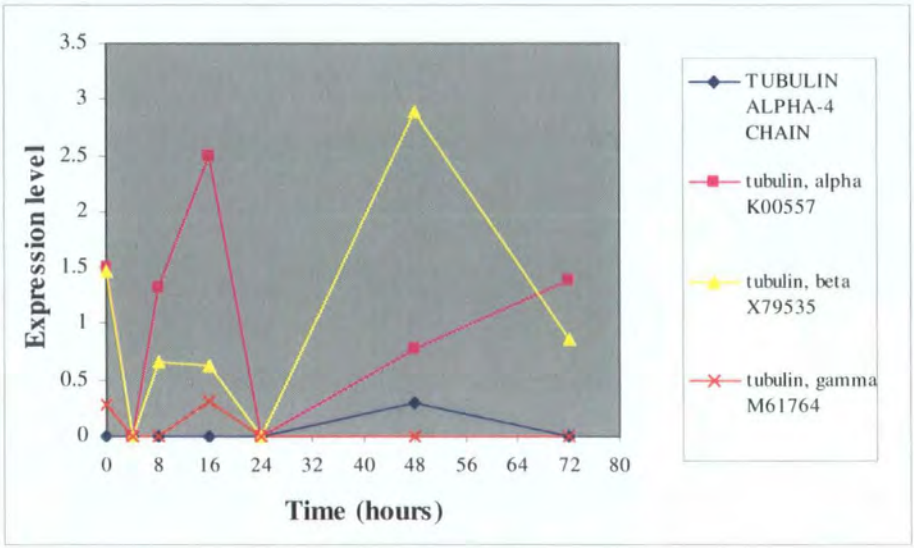

Graph 6.5 shows the expression pattern of the thymosins. The thymosins are thymic hormones. Thymosin beta-4 can bind to actin monomers thus inhibiting actin polymerisation. It also has an inhibitory effect on the proliferation of haematopoietic stem cells. As can be seen from the graph thymosin beta-4, thymosin beta-10 show a highly similar pattern of expression (R= 0.96) showing maximal expression at 24 hours. Although prothymosin alpha also shows a similar pattern of expression with maximal expression at 24 hours, a correlation with either thymosin beta-4 and beta-10 was not observed (R <0.45) .

Graph 6.5

Graph showing expression pattern of the thymosins of genes in differentiated THP-1 macrophages exposed to OxLDL for 72 hours

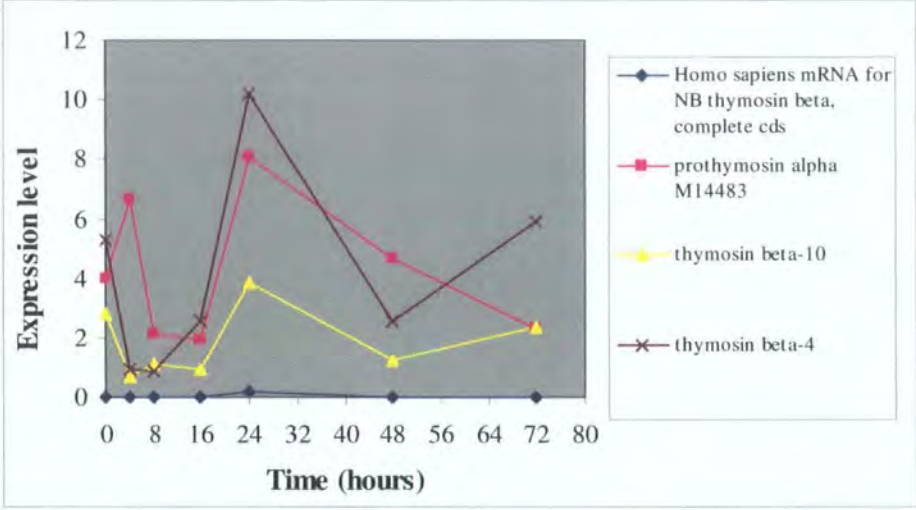

Graph 6.6 shows the expression profiles of the CD molecules. CD molecules are cluster determinant molecules present on the membranes on cells. As already discussed in the introduction CD36 is receptor capable of binding OxLDL. CD151 antigen is an integral membrane protein. CD54 is also known as intracellular adhesion molecule-1 (ICAM-1). ICAM proteins are thought to be involved in the binding of monocytes to the endothelium (one of the earliest steps of the atheorsclerotic process. CD29 (also known as beta 1 integrin) associates with different alpha polypeptides to form different receptors such as the collagen and laminin receptor. CD44 is the main cell surface receptor for

hyaluronate and also for type I and VI collagen. It is involved in matrix adhesion, and lymphocyte activation. An epithelial isoform (CD44E) is expressed by cells of the epithelium. A haematopoietic isoform (CD44H) is expressed by cells of mesodermal origin. As can be seen from the graph most of the CD molecules showed an expression pattern peaking at sixteen hours. The exception is CD36, which shows a different expression pattern peaking at 48 hours. As CD36 has been shown to be a receptor for OxLDL [22] CD36 expression would be expected to increase with time. CD44H shows the highest level of expression at 72 hours. This correlates well with the fact that the cells used is this study (THP-1 macrophages) are haematopoietic in origin [159]. The two CD molecules showing the strongest correlation were observed to be CD49a and CD44E (R= 0.93). A correlation (R= 0.90) was also observed to occur between CD44E and CD44 antigen; and also between ICAM-1 and CD44E (R= 0.84).

Graph 6.6

Graph showing expression pattern of cluster determinant molecules in differentiated THP-1 macrophages exposed to OxLDL for 72 hours

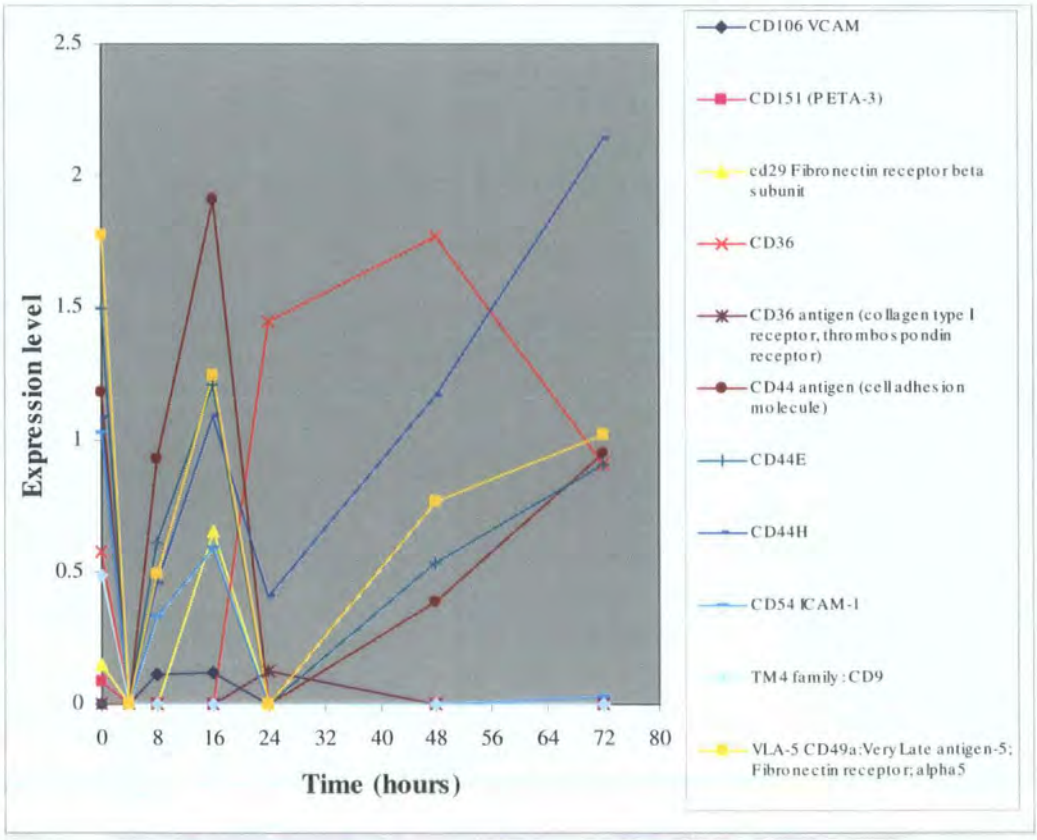

Fibronectins bind cell surfaces and various compounds including collagens, fibrin, heparin, DNA and actin. Fibronectins are thus involved in cell adhesion, cell motility, opsonization, wound healing and maintenance of cell shape. As can be seen from the graph the different variants of fibronectin and fibronectin receptors all show a pattern of expression in which expression levels peak at 16 hours, decrease at 24 hours and then showing an increase again between 24 and 72 hours. The fibronectins show a very similar pattern to the CD molecules. The strongest correlations were observed for the different clones representing fibronectin (R value range 0.77-0.94). The clone representing human mRNA for fibronectin precursor also showed a strong correlation (R= 0.89) with the fibronectin represented by dark blue in the graph but not with the other two fibronectins (represented by pink and yellow in the graph; R< 0.65). Finally a strong correlation (R= 0.90) was also observed between clone representing human mRNA for the fibronectin precursor and CD49a.

Graph 6.7

Graph showing expression pattern of fibronectin in differentiated THP-1 cells exposed to OxLDL for 72 hours

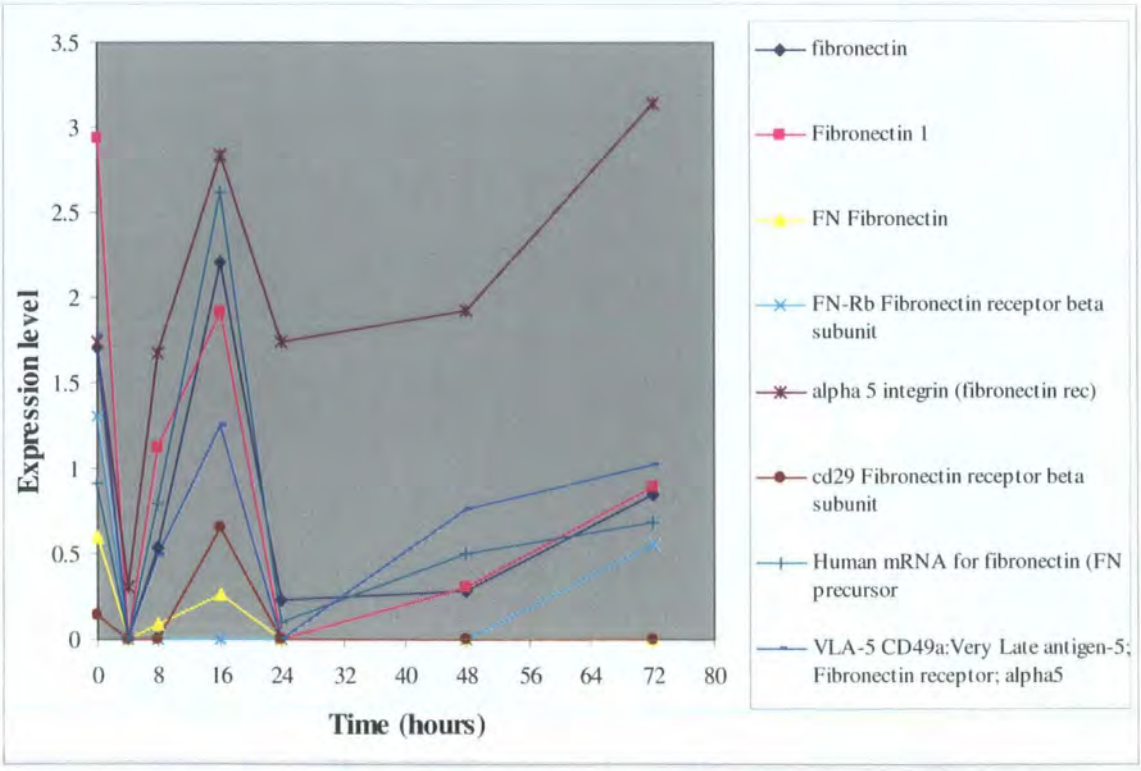

Graph 6.8 shows the expression pattern of the interleukin family. Interleukin molecules are involved as part of the inflammatory response. As can be seen from the graph, most of the interleukins show a barely detectable level of expression. However IL-1β, IL-1 receptor α and IL-8 all show a much higher level of expression. IL-1β shows the highest expression level peaking at 16 hours and falling back to near basal level by 72 hours. IL-1 receptor α shows maximal expression between 4 and 48 hours. IL-8 shows a peak of expression at 8 hours.

IL-1β is produced by activated macrophages and is an important mediator of various immunological and inflammatory reactions. It stimulates thymocyte proliferation, B cell maturation and proliferation, and fibroblast growth factor activity. IL-8 is a chemotactic factor that attracts neutrophils, basophils and T-cells. IL-8 can be produced by macrophages. It is also a mitogenic stimulus for smooth muscle cells. IL-8 has previously been reported to be increased on exposure of differentiated THP-1 cells to OxLDL [247]. This study confirms this result as well as showing an expression pattern identical to that already reported [118]. In addition the early expression of IL-8 suggests it could be involved in the interaction and regulation of other members of the interleukin family

Graph 6.8

Graph showing expression pattern of interleukin molecules in differentiated THP-1 cells exposed to OxLDL for 72 hours

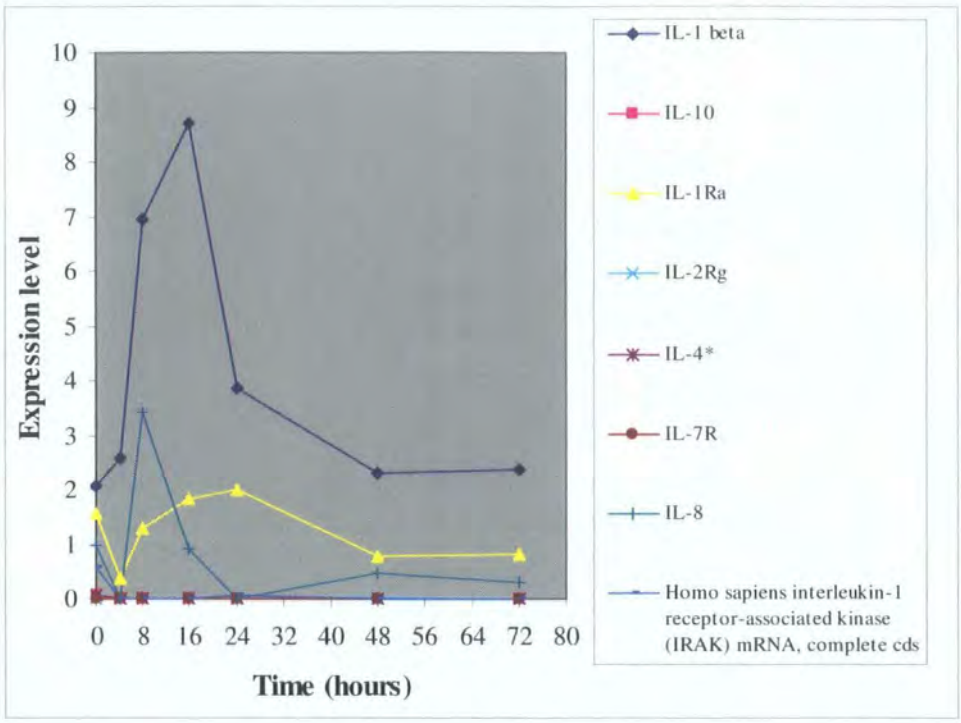

Graph 6.9 shows the expression pattern of the MMPs. The MMPs as discussed in chapter 1 are involved in the remodelling of connective tissue as well as in disease states associated with inflammation They have also been implicated in the tumour metastasic processes. MMP-2 is involved in the cleavage of gelatin type I and collagen types IV, V, VII and X. Collagenase and MDC9 are both involved in the cleavage of specific types of collagen.

As can be seen from the graph MMP-2, MMP-18 and collagenase show a higher expression level than the other MMPs, with MMP-2 showing a higher level of expression than MMP-18 than collagenase. No strong correlations were observed in expression patterns between members of the MMP family showing the highest levels of expression (MMP-2, MMP-18 and collagenase; $R < 0.68$).

Graph 6.9

Graph showing expression pattern of the MMP family of genes in differentiated THP-1 macrophages exposed to OxLDL for 72 hours

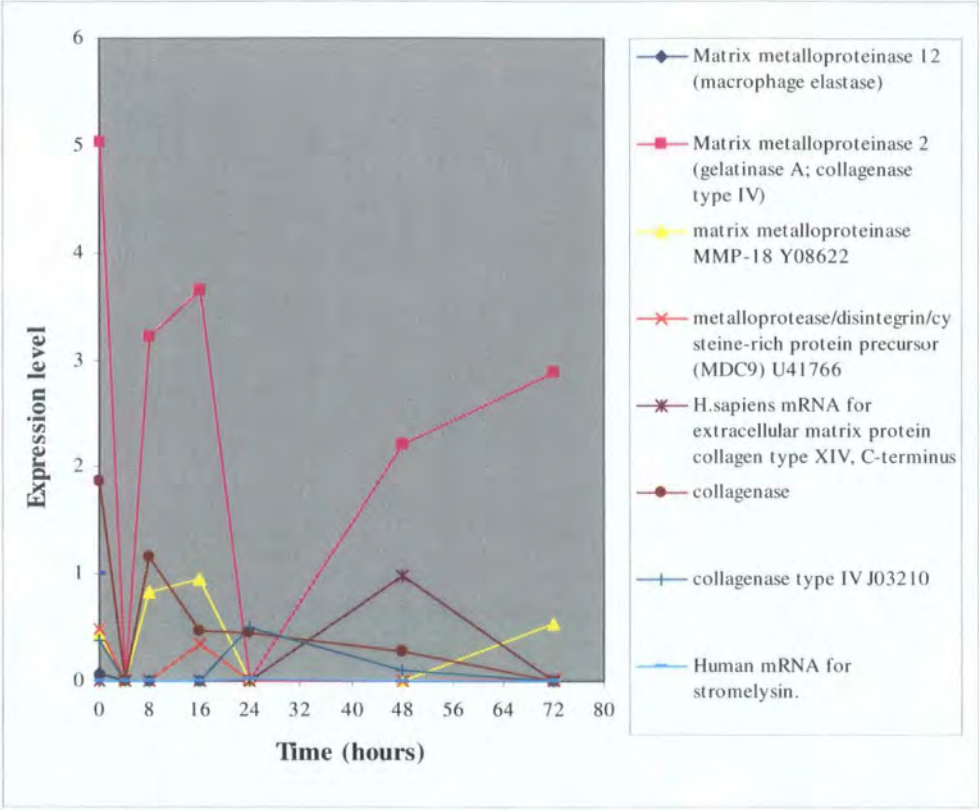

Graph 6.10 shows the expression pattern of the tissue inhibitors of the MMPs (TIMPs). TIMP-1 and TIMP-3 can complex with MMPs and irreversibly inactivate them. As can be seen from the graph, TIMP-3 shows a very low level of expression whilst TIMP-1 and collagenase inhibitor show a much higher level of expression peaking at 16 hours. In addition a correlation (R = 0.83) was observed between TIMP-1 and the collagenase inhibitor.

Graph 6.10

Graph showing expression pattern of the TIMP family of genes in differentiated THP-1 macrophages exposed to OxLDL for 72 hours

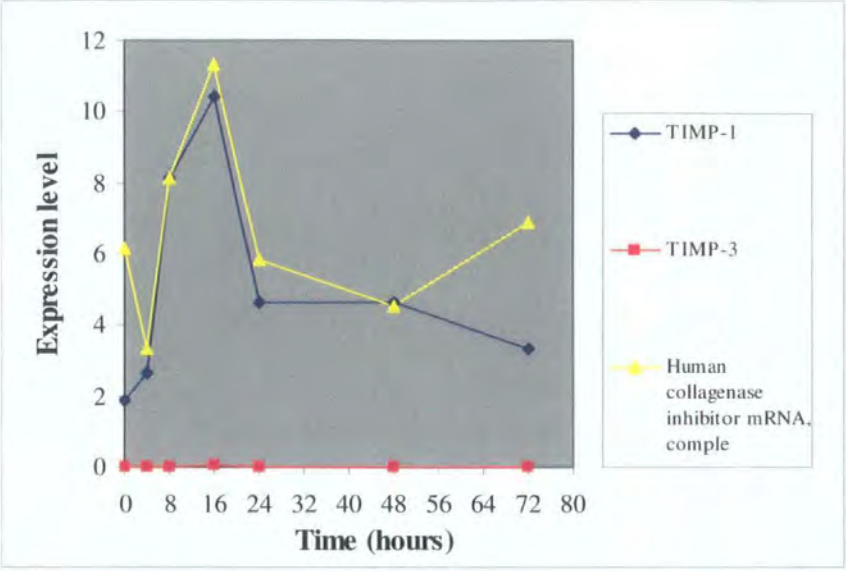

Graph 6.11 shows the expression of the cyclins. As can be seen from the graph only cyclin D3, cyclin dependent kinase 4 (cdk4), cyclin I and a cyclin dependent kinase inhibitor showed an expression level over most of the time points. Cyclin D3 is a regulator of progression through the G1 phase of the cell cycle. Cdk4 is involved in the regulation of the G1 to S phase of the cell cycle. The other cyclins showed very low or no expression. Both cyclin D3 and cdk4 showed a similar pattern of expression (R= 0.83) showing peaks of expression at 8 and 48 hours, with cyclin D3 showing a higher level of expression than cyclin D3. Cyclin I showed a peak of expression after 48 hours but not after 8 hours. Of interest, the expression level of these cyclins was minimal at precisely the time point (24 hours) where cyclin inhibitor expression was maximal (an inverse correlation).

Graph 6.11

Graph showing expression pattern of cyclins and cell cycle molecules in differentiated THP-1 macrophages exposed to OxLDL for 72 hours

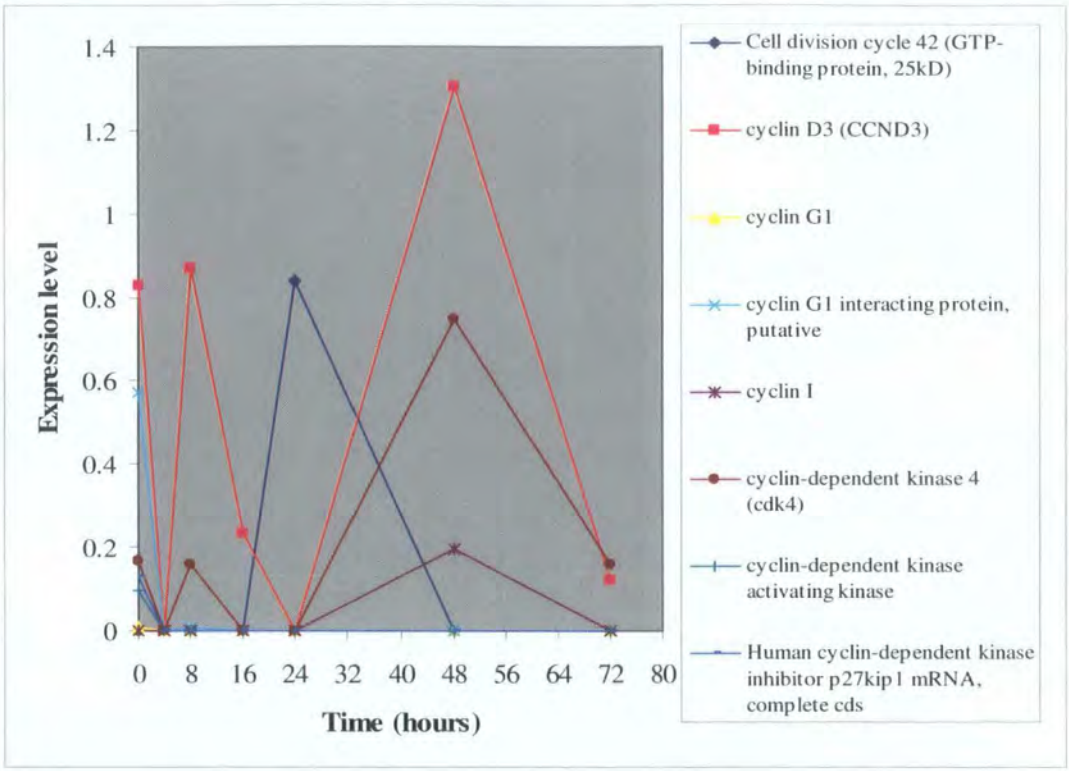

6.3.3 Conclusion from expression patterns of gene families

The results from this part of the study have shown that members of some gene families show correlated patterns of expression whereas others do not. Those with members showing similar patterns of expression include some of the CD molecules (in particular CD44E with ICAM-1 and CD49a), fibronectin, myosin regulatory light chain, the thymosin family and some members of the cyclins. Gene families not showing similar patterns of expression include the annexin family, the interleukins, the MMPs and tubulin.

6.3.4 Data analysis of genes of interest

The next stage in this study was to look at the matrix of genes (table 6.1) and using knowledge of the atherosclerosis field (and those genes showing high levels of expression) to analyse the expression of genes that have been implicated in some part of the atherosclerotic process. All these genes (around 35) were plotted onto one graph (not shown) and visually inspected. From this graph genes that showed similar patterns of expression were plotted together as shown in the graphs below.

Graph 6.12

Graph showing expression pattern of CD36, STAT 6 and ornithine decarboxylase

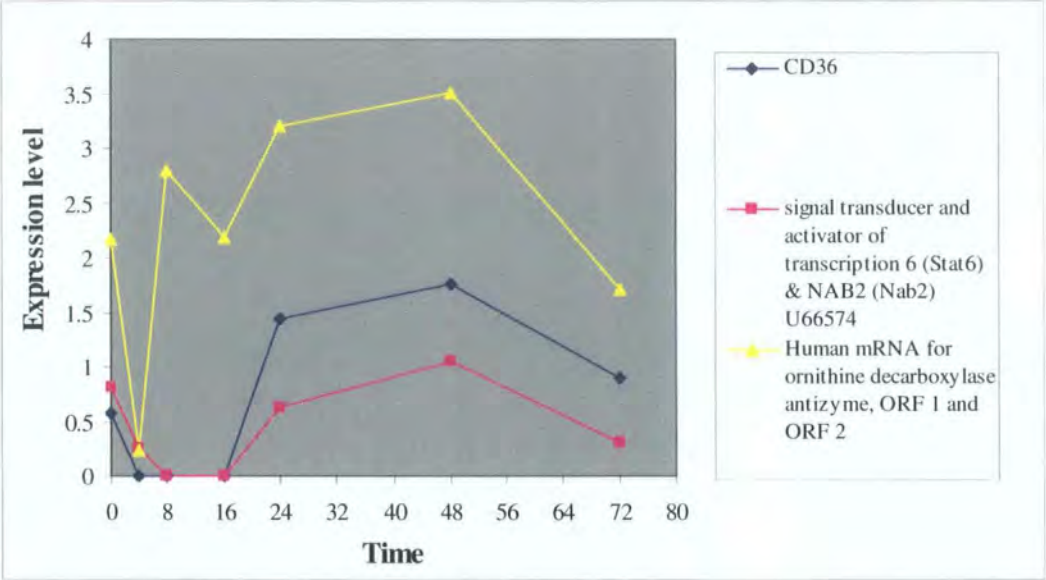

Graph 6.12 shows the expression pattern of CD36, STAT 6 and ORF 1. As can be seen from graph, CD36, STAT 6 and ornithine decarboxylase all show a very similar patterns of expression especially between 16 and 72 hours. As already mentioned CD36 is a major receptor for OxLDL. In addition it is thought to regulate gene expression of inflammatory molecules and cytokines through activation of transcription through the STAT family [121]. STAT 6 has a dual role, it is involved in signal transduction and activation and it is involved in IL-4 signalling [248]. CD36 showed a correlation with

STAT 6 (R= 0.82) whereas a poor correlation was observed when ornithine decarboxylase was compared to CD36 and STAT 6 (R < 0.63).

Graph 6.13

Graph showing expression pattern of alpha enolase, IL-8, u-PAR and thrombomodulin

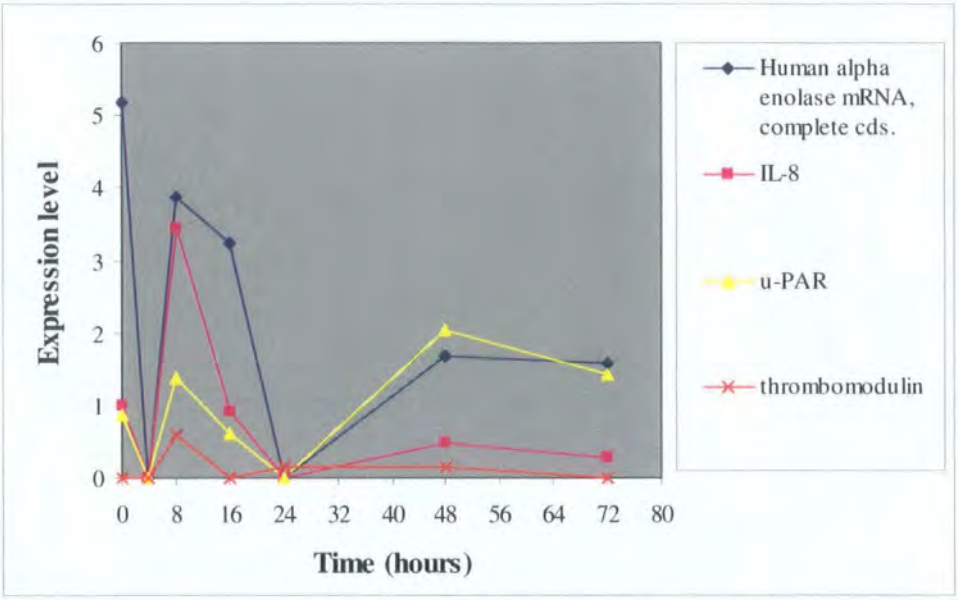

Graph 6.13 shows the expression pattern of alpha enolase, IL-8, urokinase plasminogen activator receptor and thrombomodulin. All the genes show a similar pattern of expression, showing a peak of expression at 8 hours, after which expression levels decrease before increasing again after 24 hours. As already mentioned IL-8 is involved as part of the inflammatory response and is a chemotactic factor that attracts neutrophils, basophils and T-cells. Alpha enolase is involved in the glycolysis pathway. Urokinase plasminogen activator receptor is a receptor for urokinase plasminogen activator. It plays a role in localizing and promoting plasmin formation. Thrombomodulin is a specific cell receptor that forms a 1:1 stoichiometric complex with thrombin. This complex in turn reduces the amount of thrombin generated. The basis of a similar expression pattern between these genes is not clear however it can be hypothesized that since IL-8 is expressed early on, it may play a role in the activation of the other genes that are

expressed at the later time points. Of these genes only IL-8 showed a correlation with thrombomodulin (R= 0.85).

Graph 6.14

Graph showing expression of expression pattern of TNF-RII, phospholipase A2, platelet glycoprotein and IFN gamma receptor beta

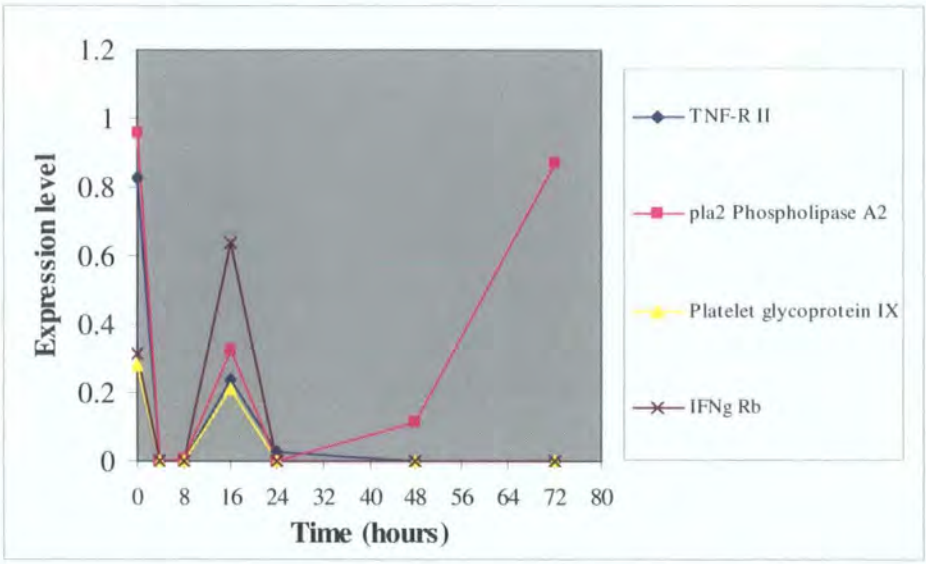

Graph 6.14 shows the expression pattern of the TNF receptor, phospholipase A2, platelet glycoprotein IX and the IFNγ receptor. As can be seen from the graph all the genes show a similar pattern of expression showing peak of expression at 16 hours. Expression levels then fall for all the genes except phospholipase A2 that shows an increase between 24 and 72 hours. Of the genes represented; strong correlations were observed between IFNγ receptor and platelet glycoprotein IX (R= 0.85) and also between TNF receptor and platelet glycoprotein IX (R= 0.92).

The TNF receptor has high affinity for TNF alpha. Phospholipase A2 catalyses hydrolysis of the 2-acyl groups in 3-sn-phosphoglycerides. Platelet glycoprotein IX plays a role in platelet adhesion and IFNγ is receptor for IFN. The reason why these genes show a similar pattern of expression is unclear but the TNF and IFN receptors may have some effect on the expression of platelet glycoprotein IX.

Graph 6.15

Graph showing expression pattern of IL-1β, human collagenase inhibitor and TIMP-1

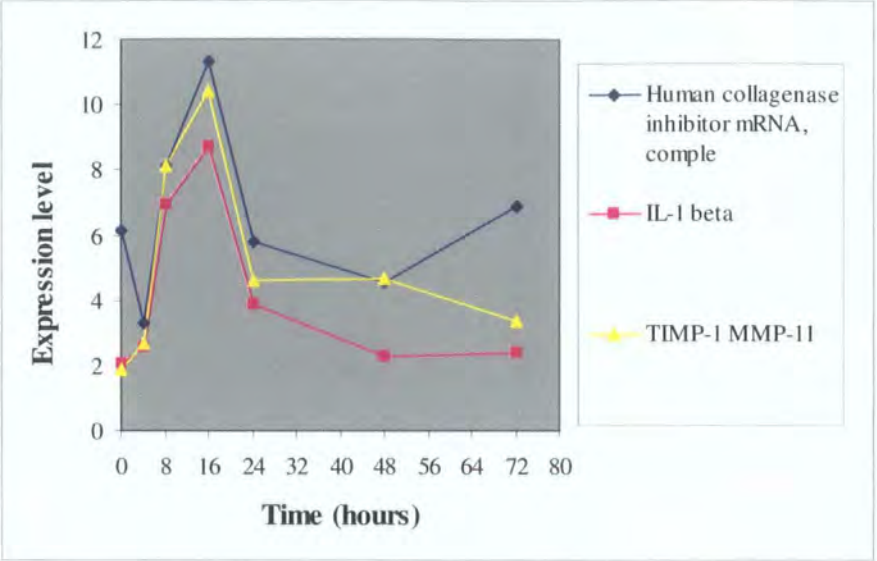

Graph 6.15 shows the expression pattern of IL-1β, TIMP-1 and collagenase inhibitor (effectively TIMP-1). As can be seen from the graph the genes show a similar pattern as well as level of expression showing a peak of expression at 16 hours. IL-1β showed a highly correlated pattern of expression in particular with TIMP-1 (R= 0.96) but also with the other form of TIMP-1 represented (collagenase inhibitor; R= 0.86) As already noted TIMP-1 is an inhibitor of the MMPs. IL-1 is an inflammatory cytokine. Cytokines have been reported to have a role in regulating the expression of the MMPs and the TIMPs [141].

Graph 6.16 shows the expression pattern of IL-1β, IL-8, MMP-2, TIMP-1 and CD36. As can be seen from graph 6.17 and as already noted, IL-8 shows the earliest expression peaking at 8 hours, this is followed by the expression of IL-1β, TIMP-1 and MMP-2 that all show peak expression at 16 hours. CD36 shows a later expression pattern starting to increase after 16 hours and showing peak expression between 24 and 48 hours. All these genes have been implicated in atherosclerosis, so one could hypothesize that IL-8 is the triggering factor, which activates one or more of the genes showing peak

expression at 16 hours (IL-1β, TIMP-1 and MMP-2). One or more of these genes could in turn activate or affect the expression of CD36.

Graph 6.16

Graph showing the expression pattern of IL-1β, IL-8, TIMP-1, MMP-2 and CD36

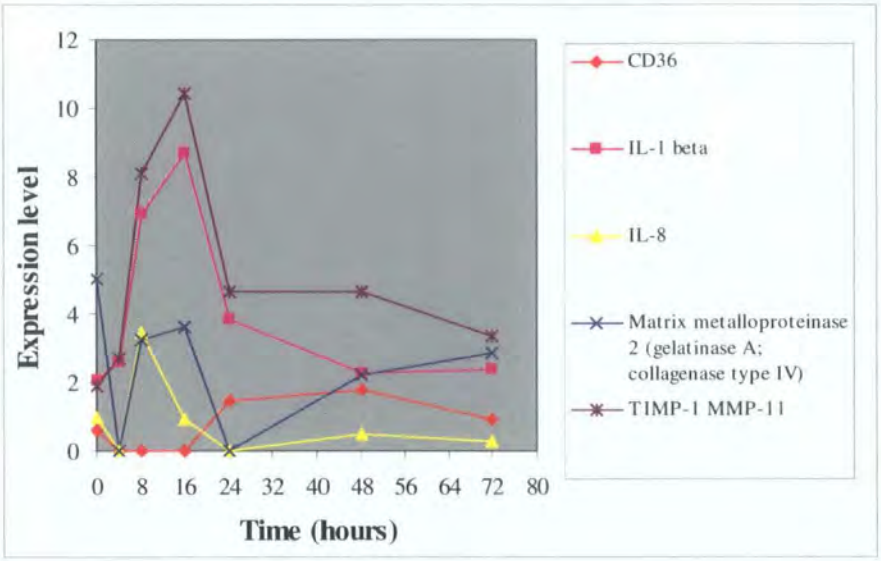

6.3.5 Conclusion from expression patterns of gene of interest

The data presented in this section demonstrates that genes of interest such as CD36 and TIMP-1 show highly correlated patterns of expression to other genes. Furthermore the graphs shown above (section 6.3.5) form a basis for hypothesising mechanisms that might be tested further experimentally. However this method of analysing the data relies completely on knowledge of genes and processes that may be involved during atherosclerosis. It does not allow the identification of other genes that are co-expressed unless one simply randomly chooses genes and see how they fit into particular expression profiles; this would involve further painstaking examination of expression of each gene. To overcome this problem, the method of hierarchical clustering was applied to the data matrix (table 6.1) to further identify genes showing similar patterns of expression.

6.4 Hierarchical cluster analysis

6.4.1 Data correlation

As discussed in the introduction to this chapter a natural basis for organising gene expression data is to group together genes with similar patterns of expression. The first step in this process is to adopt a mathematical description of similarity and show that a degree of correlation exists within the dataset. For any series of measurements, a number of measures of similarity in the behaviour of two genes can be used such as Euclidean distance, Pearson Correlation Coefficent and Mutual Information. Of these, the Euclidean distance and the Pearson Correlation Coeffient are the most commonly used [235, 244].

In Euclidean distance, each gene is seen as a point in a multidimensional space, with each axis representing a different biological sample and the coordinate on on each axis represents the level of gene expression in that sample. Euclidean distance is useful for identifying genes that have positive correlations, however it is not useful for identifying gene that do not have a positive correlation even though they may be correlated in another way (for example inversely correlated genes) [238] .For this reason in this study we used the other commonly used dissimilarity measure, the Pearson Correlation Coefficient. In addition this method is also sensitive to outliers.

The Pearson Correlation Coefficient is measured between two genes; where the two genes are treated as vectors of measurements. Disadvantages of using the Pearson Correlation Coefficient are that firstly it assumes a normal distribution of the measurements. Secondly since it uses a linear model, it assumes that genes interact in this linear model [238].

Figure 2.1 (Chapter 2; section 2.5.1) shows the steps in correlating gene expression data, applying hierarchical clustering and analysing the results. The results obtained are given in appendix 8.

6.4.2 Results of Clusters obtained

Hierarchical cluster analysis of the 216 genes showing expression during at least one time points in differentiated THP-1 cells exposed to OxLDL over 72 hours showed that the genes could be clustered into nine distinct groups. A nine-cluster solution was chosen as it best represented individual clusters

Graphs 6.17-6.25 show the general shape of the clusters assigned to the 216 genes using the Pearson correlation procedure. These graphs for each cluster are derived from the average gene expression at each time point of all the genes assigned to that cluster. From the graphs given in appendix 8; it can be seen that the nine clusters can be classified as follows: -

One cluster showing a peak of expression at 8 hours (cluster 9)

Four clusters show peak of expression at 16 hours (clusters 1, 3, 4 and 5)

Two clusters show a peak of expression at 24 hours (clusters 2 and 6)

Two clusters showing maximal peak of expression at 48 hours (clusters 7 and 8)

The two cluster showing peaks of expression at 48 hours (clusters 7 and 8) were also found to show smaller peaks of expression at 8 hours.

Graph 6.17

Graph showing average expression pattern of genes assigned to Pearson cluster 1

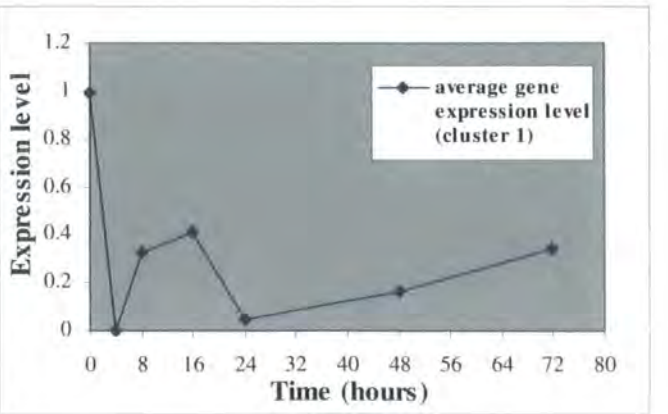

Cluster 1 contains 86 genes all of which showed the general expression pattern shown in graph 6.17, with an initial increase in expression which peaked at 16 hours fell back by 24 hours and then showed a steady increase in expression from 24 to 72 hours.

This cluster contained the largest number of genes 86 out of the 216 (40%) temporally expressed genes. Genes of interest in this cluster include some of the fibronectins, MMPs, and some of the CD molecules (CD151, CD53 CD44; discussed above). Some of the fibronectins have already been shown in the graph above (graphs 6.7) to show highly correlated patterns of expression, thus it is not surprising that these genes have been assigned to one cluster. The three genes showing the highest levels of expression in this cluster were MMP-2, alpha enolase and human saposin proteins.

Genes in cluster 2 showed the general expression pattern shown in graph 6.18. The expression level falls approximately 25% between 0 and 8 hours and remains constant between 8 and 16 hours. After 16 hours there is a sharp increase in expression levels peaking at 24 hours (approximate tripling) before the expression level falls back to pre-peak levels at between 48 and 72 hours. This cluster contained 35 out of the 216 genes (16%) showing temporal expression and was the third largest cluster. Genes in this cluster included all the thymosin genes, which have already been show to have a similar pattern of expression as shown in graph 6.5 above. In addition a member of the lipocortin family (lipocortin II) has also been included in this family, as has metallothionein. This cluster seems to contain cell morphology related genes, including the thymosins, vimentin and ferritin. The three genes showing the highest level of expression in this cluster are human ribosomal protein L37, vimentin and thymosin beta 4.

Graph 6.18

Graph showing average expression pattern of genes assigned to Pearson cluster 2

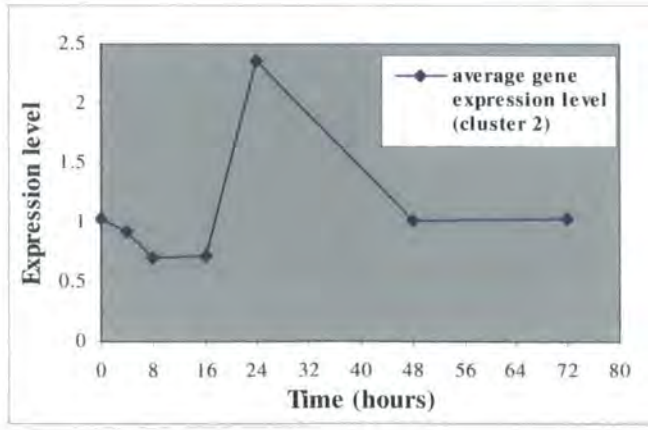

Genes in cluster 3 showed the general expression pattern shown in graph 6.19. Expression level showed an increase from 4 to 16 hours (approximate 4-fold) peaking 16 hours before falling back to pre-peak levels by 24 hours and staying at this level between 24 and 72 hours. This cluster contained 26 out of the 216 genes (12%) showing temporal expression. Genes in this cluster included IL-1β and the TIMPs that have already been shown to have a similar pattern of expression as shown above (graph 6.15). Other genes in this group some of the CD molecules (CD106, CD44, CD29) and members of the tubulin family. The three highest expressed genes in this cluster are two forms of the TIMP-1 gene and IL-1β.

Graph 6.19

Graph showing average expression pattern of genes assigned to Pearson cluster 3

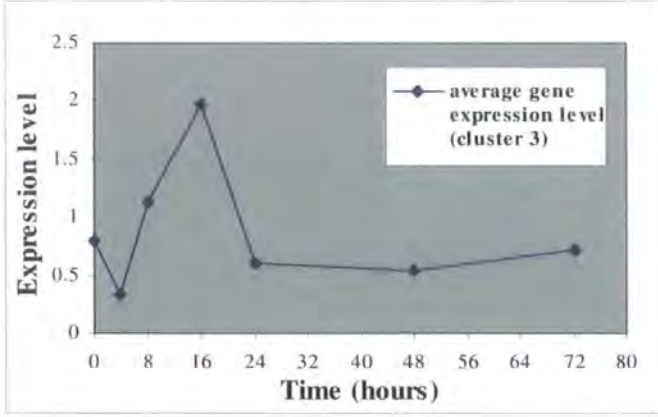

Genes in cluster 4 showed the general expression pattern shown in graph 6.20. There was an increase in expression between 4 and 16 hours (approx 4 fold) with the expression level peaking 16 hours before falling between 16 and 24 hours. The expression level then showed a steady increase between 24 and 72 hours. By 72 hours the expression level was at approximately the same level as at 16 hours. This cluster contained 6 of the 216 genes (3%) showing temporal expression. Genes in this cluster included β-actin, CD44H and the thrombin receptor. The three highest expressed genes were β actin, fibronectin and CD44H.

Graph 6.20

Graph showing average expression pattern of genes assigned to Pearson cluster 4

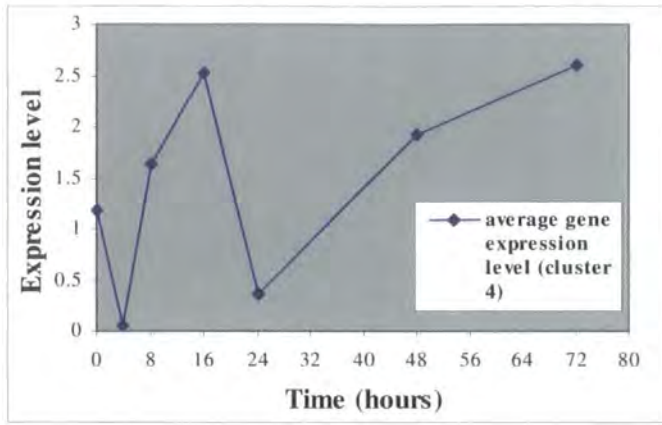

Genes in cluster 5 showed the general expression pattern shown in graph 6.21. There was an approximate 4-fold increase in expression between 4 and 16 hours with expression levels peaking at 16 hours. This was followed by a steady decrease in expression levels between 16 and 48 hours. Expression levels then increased slightly between 48 and 72 hours. This cluster contained 6 out of the 216 genes (3%) showing temporal expression. Genes in cluster 5 included members of the lipocortin family as well as p53 and ribosomal protein S17. The three genes showing the highest levels of expression were p53 activated fragment-1, human mRNA for lipocortin II and ribosomal protein.

Graph 6.21

Graph showing average expression pattern of genes assigned to Pearson cluster 5

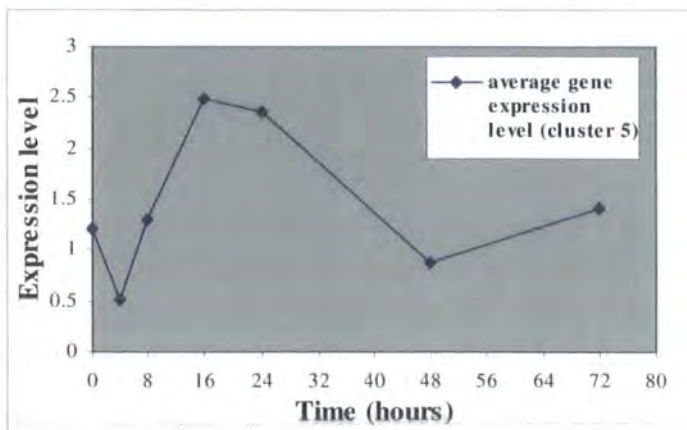

Genes in cluster 6 showed the general expression pattern shown in graph 6.22. The expression level showed a steady increase between 4 and 24 hours peaking at 24 hours (approximately 5 fold). Expression levels then fell back at 24 hours falling to pre-peak levels by 48 hours. The expression level then showed an increase (approximately doubling) between 48 and 72 hours. This cluster contained 8 out of the 216 genes (4%) showing temporal expression. Genes expressed in cluster 6 include a member of the lipocortin family (annexin II), two cytokine receptors (IL-1R and TNF-R). The three most highly expressed genes include annexin II, translationally controlled tumour protein and osteopontin.

Graph 6.22

Graph showing average expression pattern of genes assigned to Pearson cluster 6

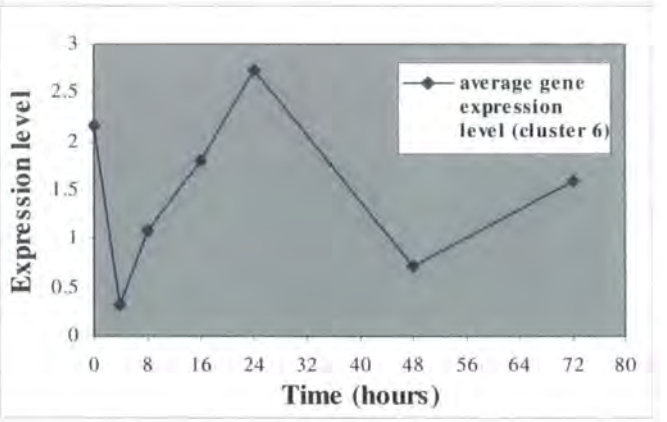

Genes in cluster 7 showed the general expression pattern shown in graph 6.23. Expression levels increased between 4 and 8 hours, peaking at 8 hours before falling between 8 and 24 hours. The expression level again increased between 24 and 48 hours peaking at 48 hours (at approximately twice the level of the expression peak at 8 hours). The expression level then fell between 48 and 72 hours. This cluster contained 37 out of the 216 genes (17%) showing temporal expression, and was the second largest cluster. Genes in this cluster included β–actin, members of the tubulin family (alpha and beta) as well as a number of cyclins and kinases. This cluster in general seemed to consist of cell cycle and cell regulation genes. The three genes showing the highest levels of expression were two genes for β-actin and a cDNA clone similar to β-actin.

Graph 6.23

Graph showing average expression pattern of genes assigned to Pearson cluster 7

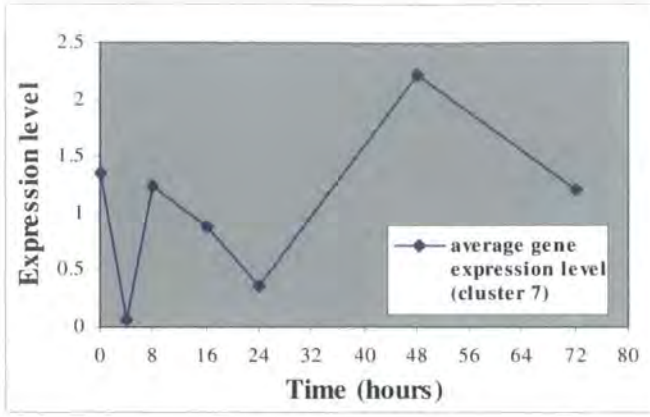

Genes in cluster 8 showed the general expression pattern shown in graph 6.24 Expression levels showed a zigzag pattern of expression between 0 and 16 hours. Expression levels then increased between 16 and 48 hours (approximately tripling) peaking at 48 hours before showing a decrease between 48 and 72 hours. This cluster contained 6 out of the 216 (3%) genes showing temporal changes in expression. Genes of interest in cluster 8 included CD 36, L-plastin and STAT 6 and translationally controlled tumour protein. Some of the genes in this cluster such as CD36 and STAT 6 have already been shown to have a similar pattern of expression as shown above (graph 6.12). Others such as L-plastin, proliferation association gene and translationally controlled tumour protein were not. The three genes showing the highest patterns of expression were translationally controlled tumour protein, L-plastin and ornithine decarboxylase.

Graph 6.24

Graph showing average expression pattern of genes assigned to Pearson cluster 8

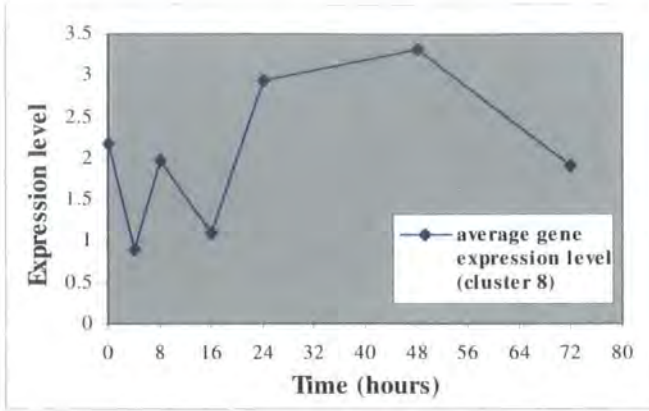

Genes in cluster 9 showed the general expression pattern shown in graph 6.25 Expression levels increased between 4 and 8 hours (approximately 8 fold), peaking at 8 hours before falling between 8 and 24 hours. The expression level then remained relatively low and steady between 24 and 48 hours. This cluster contained 6 out of the 216 (3%) differentially expressed genes. Genes in this cluster included IL-8 thrombomodulin and a transcription factor. The three genes showing the highest level of expression were IL-8, thrombomodulin and laminin. These early expressed genes are interesting because they may the signals that determine or influence the genes switched on during the later stages of exposure to OxLDL. Indeed IL-8 has already been reported to play a major role as a part of the inflammatory response by acting as a chemo-attractant for lymphocytes and T-cells, it seems plausible to hypothesize that it may also affect/regulate the expression level of other genes.

Graph 6.25 Graph showing average expression pattern of genes assigned to Pearson cluster nine

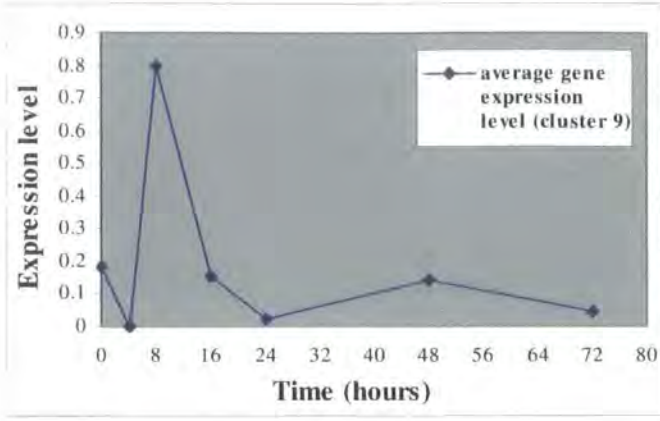

6.5 Discussion

Although clustering genes on the basis of their expression is not a new phenomenon, the development of array technology and the subsequently large amount of data generated using the technology has made clustering an important tool for the interpretation of the results. The obvious advantage in using cluster analysis is that it allows some degree of interpretation of large data sets. In particular, cluster analysis of results from multiple experiments can help to identify genes that behave similarly.

The aim of this part of the study was to identify genes showing correlated expression in differentiated THP-1 macrophages exposed to OxLDL over 72 hours. This time scale was chosen based on lipid loading experiments with OxLDL (chapter 3) that indicated cells accumulated OxLDL up to 72 hours. Cells were not exposed for longer than 72 hours because of the potentially toxic affects of oxysterols that are present in OxLDL. Another aim of performing a temporal gene expression study was to obtain an overall or 'global pattern' of gene expression of 769 genes in differentiated THP-1 cells exposed to OxLDL and to then look at these genes and identify those showing similar patterns of expression.

Hybridisation experiments were performed using the custom atheroma arrays and probes generated at 7 time points; 0, 4, 8, 16, 24, 48, and 72 hours. A final total of 5600 hybridisation intensities were collected (expression levels of 769 genes at 7 time points).

The results showed that 216 genes (1512 data points) from 769 genes on the array showed an expression level significantly above background at one of the 7 time points analysed. This still gave 1512 data points to analyse (of which, 202 data points showed a greater than 2 fold change, 58 showed a greater than 5 fold change and 7 showed a greater than 10 fold change). On its own this was a table of numbers, which would have to be painstakingly analysed. However using previously reported methodology [234], the data was represented by colours in a way that was both quantitative and qualitative. This allowed easier identification of low, medium and highly expressed genes. Although the majority of the 216 genes showed a low level of expression across the time series, some genes did show moderate and relatively high levels of expression at one more time points (table 6.2). Genes showing high levels of expression included interleukins-1β, TIMP-1, thymosin beta 4 and vimentin.

The list of genes was then analysed and gene families were selected and plotted on graphs to examine their expression patterns. This demonstrated that some gene families such as the fibronectins, thymosins, actins and some of the cyclins showed highly similar patterns of expression. However this was not always the case as shown by the expression pattern of the interleukins and MMPs.

Using knowledge of the atherosclerosis field, all relevant genes known or thought to be involved in response to OxLDL were selected and plotted to determine if any of them showed similar patterns of expression. This demonstrated that some of these genes although showing different levels of expression showed highly similar patterns of expression over 72 hours. Of particular interest CD36, which is known to be a receptor for OxLDL [18], was shown to have a pattern of expression similar to STAT 6, which is a transcription factor (graph 6.12). Since OxLDL has also been implicated to affect the expression of cytokines and inflammatory molecules this transcription factor may have a key role in this process. Two other genes showing a highly similar pattern of expression were IL-1β and TIMP-1 (graph 6.15) both of which have already been shown to play important roles in the atherosclerotic process [142, 150].

Although looking at genes of interest and those known to have a role in atherosclerosis did show genes showing similar patterns of expression, this methodology of selecting does not allow analysis of the whole data set of 216 genes to identify if there are any major patterns of expression within the data set. To address this issue hierarchical

clustering analysis was performed on the data. The cluster analysis attributed the 216 genes to nine clusters. The general expression pattern of the clusters showed that they all showed a peak of expression at one or more of the time points studied. In particular the 16 and 24 hour time points were the most prominent points for peaks of expression. Analysing the clusters further showed that most of the genes were in 4 clusters (clusters 1, 2, 3 and 7). These 4 clusters accounted for 184 (85%) of the 216 genes. The remaining 5 clusters (clusters 4, 5, 6, 8 and 9) accounted for only 32 (15%) of the 216 genes.

In general the results from the clustering correlated well with the patterns of expression observed when genes of interest or genes families were selected and plotted on graphs. Although the clustering did cluster gene families together, this was not always obvious. For example although the vast majority of fibronectin gene variants were assigned to Pearson cluster 1 some forms of fibronectin were assigned to Pearson cluster 3. This, of course, does not mean that the clustering algorithm is wrong since slightly different sequences of the same gene or different sequence regions of the same gene could easily show slight differences in expression patterns as indeed is the case if the gene graph for fibronectin family is examined further (graph 6.7). Furthermore if one examines the two sets of clusters which contain the majority of the fibronectin and CD molecules (clusters 1 and 3), one can see that they both show a similar pattern of expression, both showing peaks of expression at 16 hours but differing slightly at what happens at the other time points.

Thus it can be concluded that the clustering technique used here (HCA), was able to identify clusters of genes showing similar patterns of expression. This database provides a valuable tool, which can be used as a starting point for further analysing genes showing similar patterns of expression to genes that have already been implicated in the atherosclerotic process. The expression levels of these genes can then be analysed under different conditions by going back and performing *in vitro* experiments.

Chapter 7: Quantitative RT-PCR

7.1 Introduction

Messenger RNA provides the link between the genetic material, DNA, and the biologically functioning material, protein, in a cell. While the genes of an organism are relatively fixed, the mRNA population represents how genes are expressed under any set of given conditions [161]. RNA synthesis is thus central to the flow of genetic information in eukaryotic and prokaryotic cells and isolated mRNA has become the target for a diverse array of analytical and diagnostic techniques. The aim of this part of the study was to attempt to confirm some of the differentially expressed genes identified by the array experiments by other independent means. Due to time limitations however, this part of the study was not completed.

7.1.1 Current methods for analysing mRNA expression

Current methods for analysing mRNA expression include northern blots, array technology, ribonuclease protection assays (RPAs), quantitative RT-PCR and more recently the use of RNA interference.

7.1.1.1 Northern blots

Northern blotting is a method in which RNA is transferred to a filter and detected by hybridisation to a labelled probe [249]. The RNA of interest is separated according to size by electrophoresis, and then immobilized by capillary transfer to sheets of nitrocellulose or nylon membranes. The blot is subsequently washed in a buffer containing the labelled probe (usually labelled radioactively). The probe selectively hybridises to the RNA molecules that are complementary to the nucleotide sequence of the probe. The major limitations of using northern blotting is that it is the least sensitive of the currently available techniques. In addition it is the technique in which the RNA is most vulnerable to degradation.

7.1.1.2 Array technology

As already described (chapters 4 and 5), array based experiments allow the simultaneous study of the expression of thousands of genes in a single experiment. This technology has now become widely used for analysing mRNA expression and was the methodology employed in this study.

7.1.1.3 Ribonuclease protection assay (RPA)

RPA allows the quantitation and detection of specific mRNAs in a complex mixture of total cellular RNA. The basis of RPA is solution hybridisation of an antisense RNA probe (radiolabelled or non isotopically labelled) to a complex mixture of RNA. The reaction can be 10 to 100 fold more sensitive than northern blot analysis [250]. RPA is also less sensitive to partial RNA degradation than northern analysis. The main disadvantage of RPA is the lack of transcript size information and the lack of probe flexibility. Fragment size is determined by the homologous region of the probe, which is usually only several hundred nucleotides long. RPA only allows the use of antisense RNA probes unlike northern blots, which allow the use of DNA, RNA and oligonucleotide probes.

7.1.1.4 RNA interference

RNA interference (RNAi) is thought to be an evolutionary defence mechanism against foreign double stranded RNA [196]. Briefly RNAs called small interfering RNA (siRNA), which are around 21-23 nucloetides are cleaved from longer dsRNA chains by an enzyme called Dicer. The antisense strand of the siRNA is then used by an RNA-induced silencing complex (RISC) to allow mRNA cleavage, thus resulting in mRNA degradation [251]. RNAi is relatively novel technique which aims to identify the function of individual genes through gene silencing. The use of RNAi in mammalian cells involves the transfection with double stranded siRNAs corresponding to a region of a gene of interest. The siRNA then bind specifically to the corresponding cellular RNA

leading to the degradation of the mRNA and a subsequent decrease in the levels of the corresponding protein. Thus RNAi can specifically downgrade the expression of genes of interest. Already RNAi has been used together with microarray technology to identify genes involved in diseases such as cancer [215].

7.1.1.5 RT-PCR

The polymerase chain reaction first reported in 1986 [252] is a powerful and sensitive technique whereby DNA is quickly and reliably amplified many thousand to million fold. A variant of PCR, RT-PCR was subsequently reported and can be used for studying gene expression in tissues and cells [253]. There are two main methodologies that use RT-PCR for the analysis of gene expression. These are differential display and quantitative RT-PCR.

7.1.1.5.1 Differential Display

The basis of differential display is to perform RT-PCR using sets of primers, which enables the detection of all mRNA species present in the sample [254]. Oligo dT primers that anneal to the poly A tails of mRNA present are used. The anchored oligo dT primers consists of 11 or 12 Ts plus two additional 3' bases that provide specificity. These are used together with a set of random decamer primers. Theoretically the combination of all the primer pairs used should ensure that all the mRNA species present are transcribed during the reverse transcription reaction and subsequently amplified by PCR.

Typically one of the primers used in the reaction is radioactively labelled and PCR products are resolved by denaturing polyacrylamide gel electrophoresis. Comparison of relative intensities of PCR products obtained from a control and test sample using the same primer pairs helps to reveal sequences that are differentially expressed in the test sample. The major disadvantages of differential display are that rare mRNA species may not be efficiently displayed. In addition it is a very labour intensive method in which there is usually a high frequency of false positives to follow up [255].

7.1.1.5.2 Quantitative RT-PCR

RT-PCR is the most sensitive of the RNA detection methods. It has been shown to be 1000-10,000 times more sensitive than the classical methods for analysing gene expression (northern blots and RPAs) [256]. The main problem with RT-PCR is the difficulty in obtaining quantitative data. This arises from the exponential nature of PCR where small changes in amplification efficiency can lead to large changes in the yield of product [257]. An additional problem is that during the later stages of PCR, there is a plateau effect in which the amount of product generated plateaus due to the limitation of necessary components and generation of inhibitors [257].

7.1.2 Use of standards

To correct for variations in amplification efficiency and allow quantitation, investigators have used a range of RNA controls. A typical approach has been to co-amplify a control gene in the same tube and then to correct the experimental sample with respect to the control. In general there have commonly been two different types of control used; a control RNA already present in the sample or spiking in a synthetic control [258].

7.1.2.1 Use of housekeeping controls

These are RNA species that are already present within sample [258]. These are usually housekeeping genes such as β-actin and GAPDH, which are ubiquitously and constitutively expressed [259]. A second set of primers designed to amplify the mRNA of the housekeeping gene are normally used either in the same the same tube or a separate tube. However it has been shown that the mRNA levels of these genes do not always remain constant [259]. One disadvantage is that multiple sets of primers in the same tube often interfere with amplification of target and control gene [259].

The ideal control for RT-PCR would be ribosomal RNA since its levels remains essentially constant from sample to sample. The major problem however in using rRNA is its abundance. Ribosomal RNA tends to be very abundantly expressed thus cannot be

used as a control since the endogenous control must be expressed at roughly the same level as the RNA under study [258].

7.1.2.2 Use of Internal Standards

An alternative to using housekeeping controls is to use synthetic controls prepared by the investigator. These also are referred to as 'competitors' or 'internal standards. The advantage of using internal standards is the initial amount of standard added can be more accurately determined. Internal standards can be of two types, DNA standards [260] or RNA standards [261] and are added to the RT-PCR reaction. DNA standards tend to be stable and are easier to construct and quantify, however they do not control for the RT step of the RT-PCR reaction since they are added during the PCR step. RNA standards control for the RT step but more steps are involved in their construction and they tend to be more prone to degradation. Internal standards are designed to share the same primer binding sites as the target sequence of interest and have the same intervening sequences except for a small insertion, deletion or mutation [262]. This helps to distinguish the standard from the target sequence. Once a standard has been prepared it is co-amplified with the gene of interest using competitive RT-PCR.

7.1.3 Competitive PCR

Competitive RT-PCR is the standard method for quantitative RT-PCR [263]. During competitive RT-PCR a dilution series is made of the prepared internal standard and is co-amplified in the presence of target [263]. The internal standard competes with the target for primers (since it has the same primer binding sites) and also for enzyme. When the internal standard is in excess, there is reduced signal from the target. As the amount of internal standard decreases, the target signal increases. Quantification is performed after competitive amplification of an entire series of dilution reactions. The relative amounts of target and internal standard product in each sample are compared. A graph is constructed plotting log ratio of internal standard signal/target signal versus the log of internal standard added [261]. From this graph the amount of initial target RNA

can be found at the equivalence point. The initial amounts of target and internal are assumed to be equal in those reactions when the ratio is one to one, as then the target equals the competitor

When the ratio of internal standard/target is plotted against the log of the internal standard added, a straight line with a slope of one should be the result as shown in graph 7.1 (adapted from reference 261). If the slope is less than 1, the target has higher efficiency and if the slope is greater than 1, the standard has a higher efficiency [261]. The linearity of the slope indicates that there is a relationship between the efficiencies and that relative levels can be determined. A slope of one indicates that the efficiencies are equal and constant [261].

Graph 7.1

Model graph for quantitative competitive RT-PCR showing relationship linear relationship between log amount of internal standard added versus log ratio of internal standard to target. The equivalence point shown by the arrow is the point at which the both target and IS are present in a 1:1 ratio

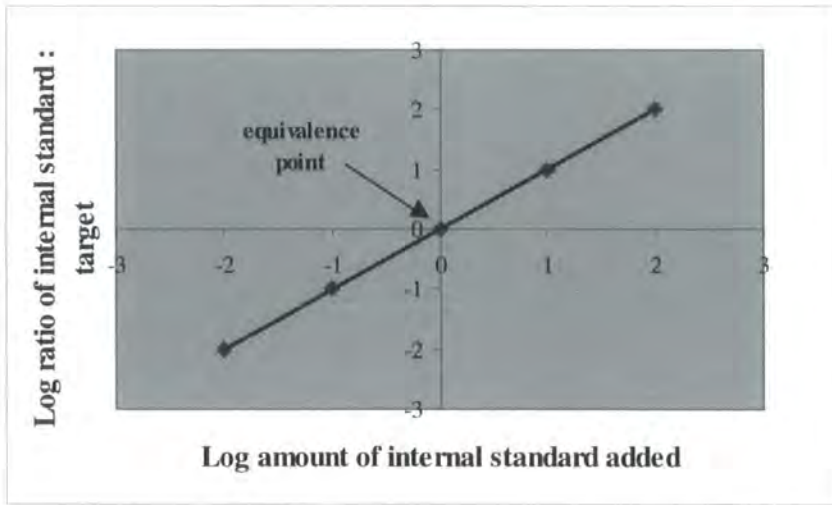

7.2 Experimental Design

In this study array technology was used to identify for differentially expressed genes in differentiated THP-1 cells exposed to native and modified LDL. In an attempt to confirm some of these changes by other independent means, the method of quantitative competitive RT-PCR was performed. The internal standards chosen were DNA standards as they are easier to prepare and are more stable than RNA standards. However it should be acknowledged that DNA standards do not control for the RT step as discussed above. The initial aim was to successfully set up quantitative RT-PCR for five genes in the THP-1 foam cell model. Two of the genes selected were normal housekeeping control genes, β-actin and HPRT; two of these genes were positive control genes for foam cell formation, IL-8 and ACAT (expected increase in levels during foam cell formation). Finally lipoprotein lipase was used as negative control gene for foam cell formation (expected decrease in levels during foam cell formation). Internal standards were prepared for the 5 genes and quantitative experiments were performed.

7.2.1 Steps involved in performing quantitative RT-PCR

The main steps involved in performing mRNA quantification include

(a) Isolation and quantification of RNA
(b) Preparation of internal standard
(c) Reverse transcription
(d) Spiking equal amounts of cDNA with a dilution series of internal standard
(e) PCR
(f) Quantitation

7.2.1.1 Isolation of RNA

Total RNA was isolated from differentiated THP-1 cells and differentiated THP-1 cells exposed to native and modified LDL using a commercially available ready to use solution (TRIzol™; as described in the methods section 2.3.2.2). Isolated total RNA was then subjected to denaturing agarose gel electrophoresis to visually verify the intensity of the RNA by the presence of 18S and 28S ribosomal RNA bands (section 2.4.1.4.1). This checks that the RNA has not been degraded during the isolation process. Quantitation was performed using spectrophotometry (section 2.4.1.3).

7.2.1.2 Internal standard preparation

DNA internal standards can be prepared using primers for the gene of interest and an additional composite primer (herewith referred to as the internal standard primer). Primer sequences were designed from published sequences obtained from the Genbank database and are given in section 2.3.4.2. Figure 7.1 shows a schematic diagram showing steps involved in internal standard preparation (adapted from reference 177). These steps include

(1) The forward and reverse primers were used to amplify the target gene of interest. The product was then separated on an agarose gel (section 2.3.5) and the product isolated from the gel as described in section 2.3.6. PCR conditions are given in section 2.3.4.4.

(2) The isolated product was then amplified using the original forward primer and a internal standard primer. The internal standard primer was designed to bind the target sequence at an upstream region (of about 40-100bps) from the original reverse primer site. Furthermore the composite primer is designed to contain a tail of about 10 bps that is identical to the first 10 base pairs of the original reverse primer. Again the PCR product obtained was separated on an agarose gel and the

product isolated. (Sequence of internal standard primers) are given in section 2.3.4.2; table 2.1)

(3) During the final amplification step, isolated product from step two was amplified with the original forward and reverse primers. The reverse primer binds to the tail on the intermediate PCR product from step 2 (since it is complementary).

(4) This produces a product that is of shorter length that target but which contains the same primer binding sites as the target sequence

A list of product sizes for targets, intermediate products and internal standards are given in section 2.3.4.3. A large quantity of each internal standard was prepared for each gene using PCR and the products separated on an agarose gel and isolated. Each batch of internal standard was aliqouted into smaller amounts and stored at 20°C until required. Each time subsequent quantitative experiments were performed; spectophotometric measurements were made to determine the concentration of the internal standard.

Figure 7.1

Schematic diagram showing steps involved in internal standard generation (adapted from reference 177)

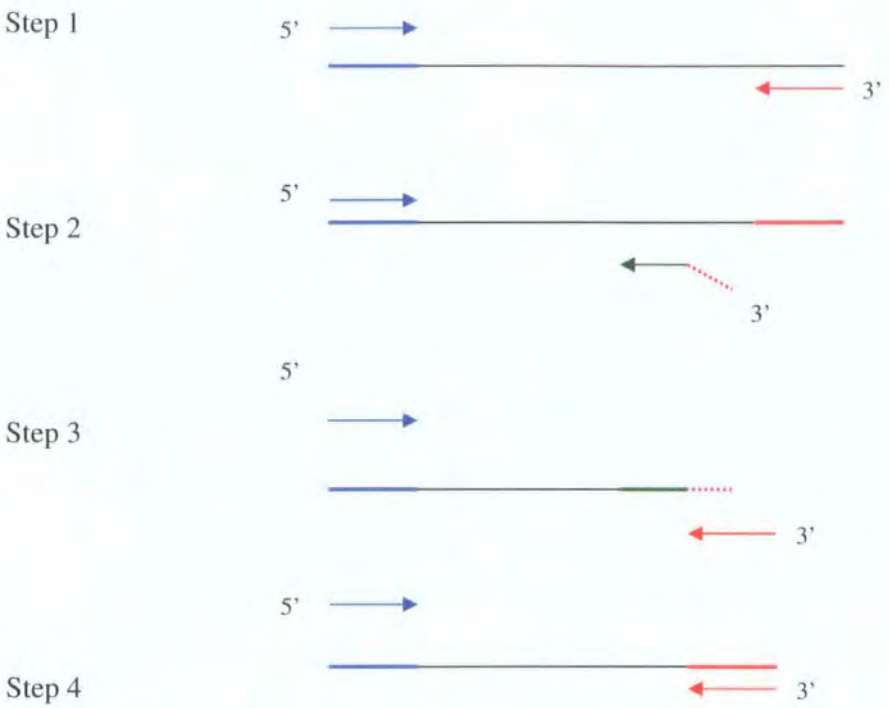

7.2.1.3 cDNA synthesis

The initial step in RT-PCR is the production of single stranded complementary DNA copy (cDNA). An oligonucleotide dT primer is used to initiate cDNA synthesis by annealing to the polyadenylated 3' tail found on mRNA. The mRNA is then transcribed through the action of the retroviral enzyme reverse transcriptase. Reverse transcription of isolated RNA was performed as described in section 2.3.3. The RT step is a enzymatic reaction, there is no amplification and the only variable is the amount of RNA, which is converted into cDNA. It can be represented by an equation cDNA = RNA x efficiency [261] (where efficiency is measured as the amount of RNA transcribed into cDNA).

7.2.1.4 PCR

After preparation and quantitation, dilutions of internal standard were prepared and spiked into identical amounts of sample cDNA. The cDNA and internal standard were then amplified using the PCR reaction (section 2.3.4.1). PCR is a three-step process consisting of denaturation, annealing and elongation. Due to its exponential nature the PCR reaction is more complex than the RT step [258]. Theoretically the amount of cDNA is doubled after every cycle. This can be represented by $P = T (1+E)^n$ where P is the product (measured after n cycles) and T is the template (amount of cDNA from the RT reaction). E is the efficiency (% of cDNA copied in a PCR cycle) and n is the cycle number [261]. Small errors in the PCR step can lead to large changes in the amount of final product obtained. Use of an internal standard however takes this into account.

In addition to the use of an internal standard, which can control for amplification efficiency during the PCR step, several additional control steps were used during the RT and PCR steps to ensure that PCR products obtained were from target genes. Two negative controls were included in the RT step. These consisted of a control containing no RNA and all other RT reagents except RNA template and a control containing all RT reagents except RT enzyme. These ensured that there was no DNA contamination of the original and subsequent cDNA preparations. Similarly during PCR, a negative control that consisted of all PCR reagents except cDNA template was used to ensure that there was no cDNA contamination of PCR products. In addition the PCR primers used were designed so that they spanned an intron. The idea behind this is that that only products from cDNA are likely to amplified. If a product is obtained from the intron containing DNA it will give a product of larger size than produced by the corresponding cDNA that allows it to be distinguished.

7.2.1.5 Quantitation

The final step in the process was the detection and quantitation of the amplification products. Reaction products were separated so that the target and internal standard could be detected and quantified. This was achieved by electrophoresis through

an agarose gel (section 2.3.5) or by polyacrylamide gel electrophoresis as described in section 2.3.7.2. Quantitation was initially performed through ethidium bromide staining to allow a range of internal standard concentrations where both target and internal standard were amplified in approximately equal amounts to be determined. More accurate quantitation was achieved through the measurement of incorporated radioactivity using labelled primers.

Both forward and reverse primers were radiolabelled as described in section 2.3.7.1. The primer showing the most radioactive incorporation was subsequently used during PCR reactions. The labelled PCR products were separated on polyacrylamide gel and the amount of label in target and internal PCR products was determined by phosphorimaging as described in section 2.3.7.2.

7.3 Results

7.3.1 Internal standard preparation

As discussed above, one of the initial steps involved the preparation of internal standards for genes of interest. Internal standards were prepared for the following genes: HPRT, ACAT, interleukin 8, β-actin and lipoprotein lipase. Internal standards were prepared by using a composite primer containing a tail with homology to the reverse primer as described above and shown by Figure 7.1 except for β-actin which was prepared according to protocol of reference [264]. Table 7.1 lists the internal standards prepared and the size in base pairs of the target gene and corresponding internal standard product.

Table 7. 1

Table of internal standards prepared and size of target and internal standard (bp)

Name of Target Gene	Target Gene Product Size (bp)	Internal Standard Product Size (bp)
HPRT	351	314
β–actin	520	320
Interleukin -8	210	164
Lipoprotein lipase	227	160
ACAT	475	407

Figures 7.2 below shows photographs of ethidium bromide stained gels showing the products obtained during internal standard preparation for two of the genes HPRT and IL-8. As discussed above (figure 7.1), three products were obtained, the target product (from the gene of interest), an intermediate product (using the composite primer) and the internal standard. As can be seen from figure 7.2, the products although being very similar in size (especially the intermediate product and the internal standard) can nevertheless be distinguished from one another during agarose gel electrophoresis.

Figure 7.2

Photographs of two ethidium bromide stained gels showing products obtained during internal standard preparation for HPRT (lanes 2 - 4) and IL-8 (lanes 5 - 7)

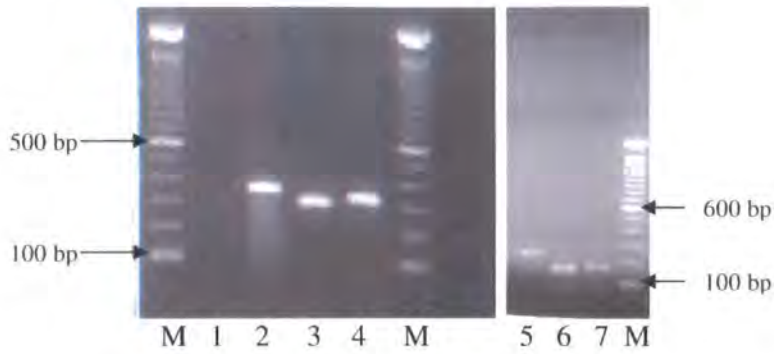

(M = 100bp marker)

Lanes labelled M are marker lanes, each containing 0.5μg of 100bp ladder.
Lanes 1-4 shows products obtained during preparation of the HPRT internal standard.
Lanes 6-8 show products obtained during preparation of the IL-8 internal standard

Lane 1 is a negative control for the PCR. Lane 2 is the target HPRT sequence (351bp). Lane 3 is the intermediary HPRT product (product from lane 2 amplified with 5' forward primer and 3' composite HPRT reverse primer; 294bp). Lane 4 is the HPRT internal standard (product from lane 3 amplified using the original 5' forward and 3' reverse HPRT primers; 314bp). Lane 5 is the target IL-8 sequence (227bp). Lane 6 is the intermediary product (product from lane 5 amplified with 5' forward primer and 3' composite IL-8 reverse primer; 150bp). Lane 7 is the IL-8 internal standard (product from lane 6 amplified using the original 5' forward and 3' reverse IL-8 primers; 160bp). As can be seen from figure 7.2 internal standards were successfully prepared for the IL-8 and HPRT genes and could be easily distinguished form their target sequences during separation by agarose gel electrophoresis. Similarly internal standards were prepared for LpL, β actin and ACAT (data not shown).

7.3.2 Initial quantitation of internal standards using ethidium bromide staining

After internal standards had been generated and quantified, a dilution series of each internal standard was prepared and added to an equal amount of cDNA. Subsequently PCR performed as described in section 2.3.4. The PCR products were separated by electrophoresis on an agarose gel, and the gel stained with ethidium bromide and photographed under UV light (section 2.3.5). This step was performed in order to determine an initial range of concentrations of internal standard, in which the internal standard and target sequence competed for PCR reagents. Furthermore so as to determine a range of concentrations at which the product and internal standard were amplified at a 1:1 ratio before the procedure was performed radioactively.

Figure 7.3 below shows a photograph of an ethidium bromide stained agarose gel after separation of PCR products obtained after performing competitive PCR using a dilution series of the IL-8 internal standard. Similarly figure 7.4 shows a photograph of an ethidium bromide stained agarose gel after separation of PCR products using a dilution series of the β-actin internal standard. In both cases an increasing amount of internal standard was added to a constant amount of cDNA (section 2.3.4).

Figure 7.3

Photograph showing ethidium bromide stained agarose gel after separation of competitive PCR products for IL-8. Product sizes are 210 bp for the target sequence and 164 bp for the internal standard. (M = marker, IS= internal standard and pg = picograms)

Lane 1 = PCR negative control
Lane 2 = DNA
Lane 3 = 80 pg cDNA only
Lane 4 = 80 pg cDNA + 25pg IS

Lane 5 = 80 pg cDNA + 31.25pg IS
Lane 6 = 80 pg cDNA + 62.5pg IS
Lane 7= 80 pg cDNA + 125pg IS
Lane 8 = 80 pg cDNA + 250pg IS
Lane 9 = 25µg IS only
M=100bp marker (0.5µg)

Figure 7.4

Photograph of ethidium bromide agarose gel after separation of competitive PCR products for β–actin. Product sizes are 520 bp for the target sequence and 320 bp for the internal standard (M = marker, IS = internal standard and pg = picograms)

Lane 1 = PCR negative control
Lane 2 = 80 pg of cDNA only
Lane 3 = 80 pg of cDNA + 1.6pg IS
Lane 4 = 80 pg of cDNA + 3.2 pg IS
Lane 5 = 80 pg of cDNA + 8pg IS
Lane 6 = 80 pg of cDNA + 16pg IS
Lane 7 = 80 pg of cDNA + 32pg IS
Lane 8 = 80 pg of cDNA + 320pg IS
Lane 8 = 80 pg of cDNA + 960pg IS
Lane 10 = 16 µg IS only
M= 100 bp marker (0.5µg)

As can be seen from figures 7.3 and 7.4, the range of concentrations used for the internal standards resulted in both the target and internal standard competing for PCR reagents. As expected at low internal standard concentrations, the amount of target amplified was greater than the amount of internal standard amplified. However as the concentration of internal standard added was increased, the amount of target amplified decreased and the amount of internal standard amplified increased. In addition there were low concentrations of internal standard where only target was amplified and *vice versa* higher concentrations of IS where only the internal standard was amplified. Similarly

dilutions were prepared of the internal standards for the other genes (ACAT, LpL and HPRT) and competitive RT-PCR was performed to estimate concentration ranges of internal standard to use (data not shown).

7.3.3 Quantitation using phosphorimaging

After initial quantitation with ethidium bromide staining that produced only visual results, quantitation was performed using phosphorimaging, which allowed a quantitative form of measurement (although quantitation using ethidium bromide has been reported, it has a poor dynamic range [265]). Both forward and reverse primers were radioactively end labelled as described in section 2.3.7.1. Subsequently one of the primers was spiked into each tube during competitive PCR. The decision on which primer to use was taken by end labelling both primers and assessing which primer incorporated the most label as described in section 2.3.7.2. Competitive PCR was then performed in the presence of ^{32}P labelled primer. Subsequently PCR products were separated on a denaturing gel as described in section 2.3.7.2. After electrophoresis the gel was dried and exposed to photographic film to determine the position of the radiolabelled PCR products (section 2.3.7.2). This section of the gel was removed and exposed to a phosphor beta-imaging screen. The screen was scanned and the relative amounts of products of target and internal standard were calculated using BioRad Molecular Analysis software as described in section 2.3.7.2. The results were subsequently exported to Microsoft Excel for analysis. The ratio of IS target was calculated and graphs were then plotted of log IS standard concentration versus log IS: target ratio for the internal standards.

Figures 7.5 to 7.7 show sections of film of radioactive PCR products obtained using competitive PCR in the presence of ^{32}P end labelled primer for the genes HPRT, β-actin and IL-8. Quantitation using this method was also performed for ACAT and LpL (data not shown). As can be seen from the from the films, at the concentration of internal standards used both target and IS competed for PCR which resulted in two products corresponding to target and internal standard being formed. In addition, as also shown by ethidium bromide staining there were also concentrations of IS used that were too low so that only target was amplified and concentrations of IS used that were too high so that

only IS was amplified. Graphs 7.2 – 7.4 show plots of log IS standard concentration versus log IS: target ratio for each of the internal standards (IL-8, HPRT and β-actin). As can be seen from these graphs, HPRT showed an S-shaped pattern, IL-8 a linear pattern and β-actin a curved pattern. However for each of the graphs there is a region which is linear if one selects a specific range of IS concentration added. Thus a region of linearity was observed with all the standards as required and shown in the model graph for PCR (figure 7.1). The results for all the genes however show that the slope of the graphs is greater than one, resulting in the slope not passing through the origin. This means that there are different amplification efficiencies between the target and IS at the concentrations of IS used.

Figure 7.5

Film showing products of competitive PCR between HPRT target and HPRT IS

1 2 3 4 5 6 7 8 9 10

Lane 1= 80pg cDNA only
Lane 2= 80pg cDNA +41pg IS
Lane 3= 80pg cDNA +41pg IS
Lane 4= 80pg cDNA +82pg IS
Lane 5= 80pg cDNA + 102.5pg IS
Lane 6= 80pg cDNA +205pg IS
Lane 7= 80pg cDNA +0.41μg IS
Lane 8= 80pg cDNA +0.82μg IS
Lane 9= 80pg cDNA +8.2μg IS
Lane 10 = 82μg of IS only

Graph 7.2

Graph showing log internal standard concentration versus log internal standard: target ratio of PCR products after competitive PCR for HPRT

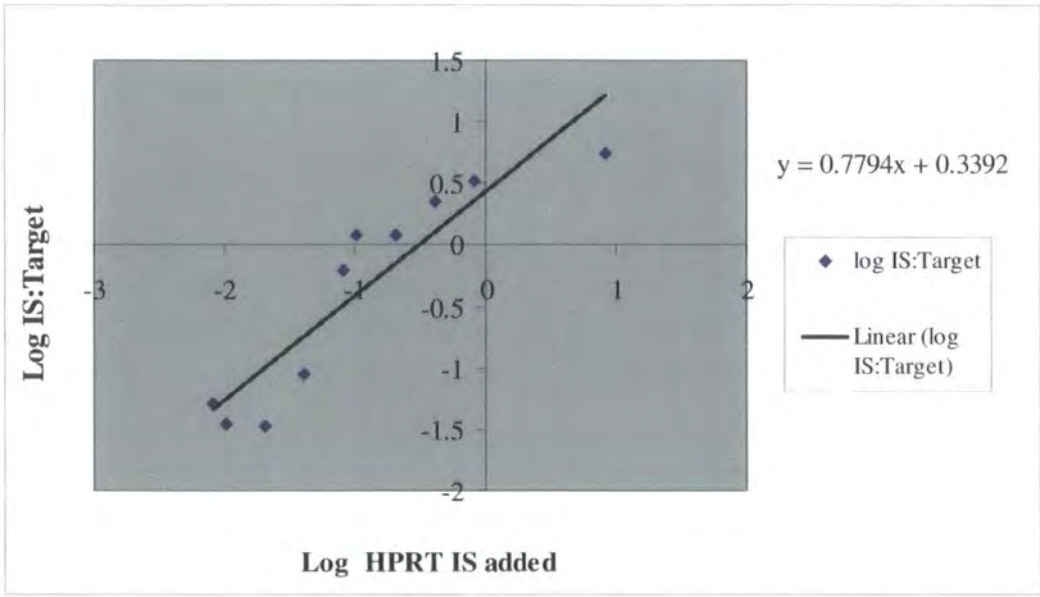

Figure 7.6

Film showing products of competitive PCR between IL-8 target and IL-8 IS

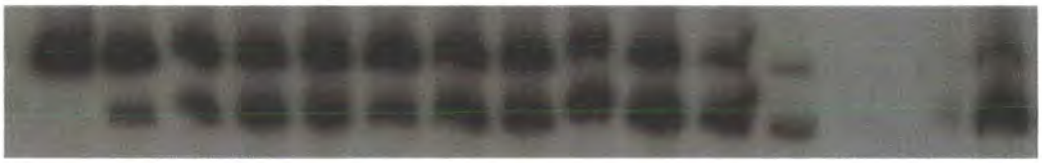

1 2 3 4 5 6 7 8 9 10 11 12 13

Lane 1= PCR negative control
Lane 2= 80pg cDNA only
Lane 3= 80pg cDNA + 0.05ug IS
Lane 4= 80pg cDNA + 0.13ug IS
Lane 5= 80pg cDNA + 0.25ug IS
Lane 6= 80pg cDNA + 0.28upg IS
Lane 7= 80pg cDNA +0.31ug IS
Lane 8= 80pg cDNA + 0.36ug IS
Lane 9= 80pg cDNA + 0.42ug IS
Lane 10= 80pg cDNA + 0.5ug IS
Lane 11= 80pg cDNA + 0.63ug IS
Lane 12= 80pg cDNA + 0.83ug IS

Lane 13= 80pg cDNA + 1.25ug IS

Graph 7.3

Graph showing log internal standard concentration versus log internal standard: target ratio of PCR products after competitive PCR for IL-8

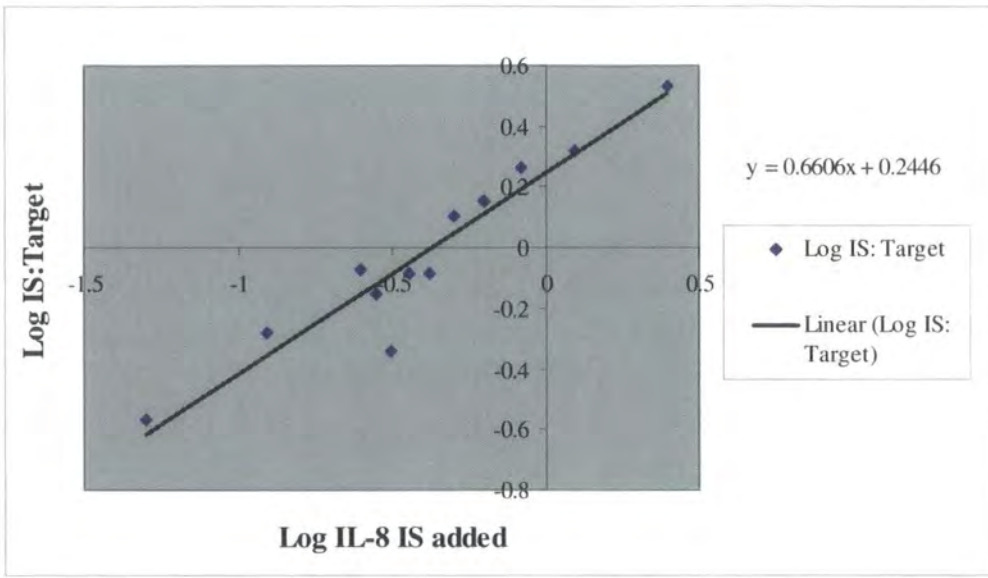

Figure 7.7

Film showing products of competitive RT-PCR between β–actin target and β-actin IS

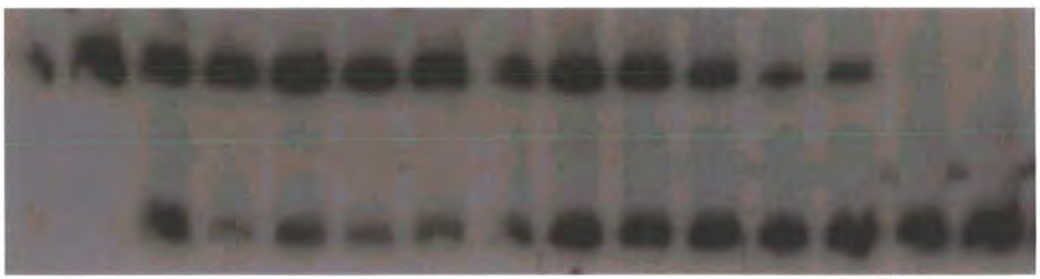

1 2 3 4 5 6 7 8 9 10 11 12 13 14 15

Lane 1 = PCR negative control Lane 2 = 80pg cDNA only

Lane 3 = 80pg cDNA + 1pg IS Lane 4 = 80pg cDNA + 1.1pg IS

Lane 5= 80pg cDNA + 1.3pg IS Lane 6 = 80pg cDNA + 1.4pg IS

Lane 7 = 80pg cDNA + 1.7pg IS Lane 8= 80pg cDNA + 2pg IS

Lane 9 = 80pg cDNA + 2.5pg IS Lane 10= 80pg cDNA + 3.3pg IS

Lane 11 = 80pg cDNA + 5pg IS Lane 12= 80pg cDNA + 10pg IS

Lane 13 = 80pg cDNA + 20pg IS Lane 14= 80pg cDNA + 100pg IS

Lane 15 = 10µg of IS only

Graph 7.4

Graph showing log internal standard concentration versus log internal standard: target ratio of PCR products after competitive PCR for β-actin

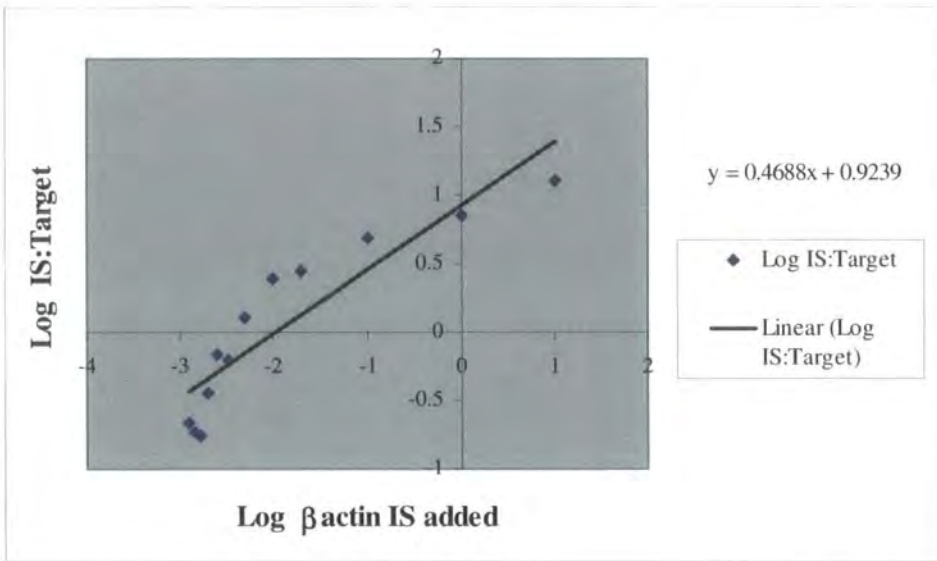

7.4 Discussion

Although RT-PCR is a very powerful technique, the sensitivity of the reaction means that potential errors can arise at any stage from RNA isolation to PCR therefore it is important to use appropriate controls at all steps. It is necessary to prepare controls and understand the dynamics of the PCR reaction in the system being studied. However once achieved this paves the way for the examination of genes of interest.

7.4.1 Problems associated with RT-PCR

A problem associated with RNA isolation is that most techniques used for RNA isolation also yield significant amounts of genomic DNA contamination [261]. Thus it is important when designing primers for RT-PCR is to design primers that span at least one intron. This helps overcome the problems associated with DNA contamination. DNA contamination will be identified because the product that will be generated will be of larger in size than the product obtained from cDNA. In this study primers were routinely designed across an intron. In addition a control DNA sample was included when a new set of primers were used. DNA contamination can also be eliminated adding DNase 1 to the reaction. Hung et al [266] have reported complete inactivation of DNase 1 by heat denaturation at 75°C for 5 minutes. Although this step was not included in the protocol reported here, it will be included in future experimental work

An additional problem is that pseudogenes exist in the mammalian genome for many genes [267], including the most commonly used housekeeping genes (βactin, GAPDH, cyclophilin). Psuedogenes are sequences that arise from the historical integration of retroviral sequence into the human genome. As pseudogenes do not have introns, the size of a PCR product amplified from a pseudogene may be identical to that produced from the cDNA copy. The only way to identify these products is to perform a no RT control. The no RT control yields two fragments; one identical in size to the expected product and a larger product which can be attributed the pseudogene. In this study we routinely performed a no RT control when performing reverse transcription. In addition we also included a no RNA control and tested it with primers that amplify DNA

to show that there was no contamination of RT reagents. No evidence of pseudogenes was found in the experiments performed.

Another problem that can arise is heteroduplex formation. Although an internal standard has the same primer binding sites as the target and is needed so ensure that reaction efficiencies of both the target and standard are similar, this similarity can also be the source of error [268]. As the PCR reaction proceeds, single strands of the internal standard and native amplification products can reanneal to form heteroduplexes. The likelihood of hetroduplex formation has been shown to be reduced by using standards with a deletion or an insertion but increased when point mutation is used [268]. This is thought to be because a deletion or an insertion provides a non-homologous region large enough to prevent annealing between the target and standard. In this study internal standards were prepared containing a deletion to minimise the risk of heteroduplex formation.

7.4.2 Discussion of results

In this study high-density cDNA arrays were used to detect changes in gene expression during macrophage foam cell formation. To confirm these changes, competitive RT-PCR was used in attempt to quantitate these changes independently. Unfortunately due to time limitations the method was not fully optimised in the foam cell model such that it could be used to quantitate genes found to be regulated by native and modified LDL as reported in chapters 5 and 6.

The major steps towards achieving this goal were however performed. Internal standards were successfully prepared for the following genes HPRT, β actin, lipoprotein lipase and interleukin-8. In addition initial set up experiments were also performed. Competitive RT-PCR was performed showing standard and target sequences competing for the PCR in the presence of a dilution series of internal standard (figures 7.2-7.8). Furthermore target and IS products could be easily distinguished from one another by agarose gel and denaturing gel electrophoresis. The results for the genes showed competitive PCR taking place between the target and internal standard. When graphs were plotted for all the genes, at certain concentrations of IS added, a linear relationship

was observed between the amount of internal standard added and the ratio of internal standard to target. However the slope of the graph was not 1 as required. In addition, the slopes did not pass through the origin. This indicates that there may be a difference in the amplification efficiencies of the internal standard and target sequences. This will warrant further investigation to determine the effects of the numbers of cycles required at which amplification efficiencies are the same. These experiments used 30 PCR cycles at which stage the PCR is likely to have reached the plateau stage. Both target and IS are more likely to show similar amplification efficiencies during the earlier linear stages of the PCR reaction.

7.4.3 Future Experiments

Future experiments would first investigate the relative amplification efficiencies of the target and internal standard sequence. This could be performed by removing aliquots from different cycles of a radioactive competitive PCR reaction between targets and IS, separating them on a gel and determining the radioactivity in each aliquot. The amount of radioactivity in each sample at different cycle number for IS and target can then be compared. Graphs can then be plotted of the cycle number versus radioactive incorporation and the two graphs can be compared to ensure that the PCR is only performed up to a cycle number that encompasses the linear phase of the reaction before the plateau phase occurs.

Next internal standards would be cloned into a vector with appropriate transcription sites and transcribed into RNA standards using an RNA polymerase. This would ensure that there is control during the RT step. Subsequently levels of these genes can be quantitated in samples of differentiated THP-1 cells exposed to either native or modified LDL. In addition specific ELISA assays could be used to measure the protein levels of these genes and see if they correlate with the quantitative RT-PCR results.

7.4.4 The future of RT-PCR

Advances in technology have resulted in the development of a new generation of thermocyclers. These thermocyclers allow the real time monitoring of PCR products so that PCR products can be visualised as they are formed thus offering improved quantitation [269]. Such thermocyclers include the ABI 'Taqman' and Roche 'Lightcycler'. Since multiple fluorescent probes can be used, internal standard and target sequences and the DNA melting curves they generate can be differentiated using different fluorescent probes. Different types of fluorescent probes have been used for monitoring [270]. These include molocular beacons (that form a stem-and-loop structure) hydrolysis probes (which take advantage of the 5'- 3' exonuclease activity of Taq), hybridisation probes and DNA specific dyes such as SYBR green.

The advantages of real time monitoring is that a much larger amount of data about the PCR is obtained from the data points for each cycle. In addition errors in sample manipulation that are involved in end-point quantitation and the time taken are minimised. Due to their cost however, these machines are not accessible to everyone and are commonly only found in core facilities.

Changes seen with hybridisation array technologies are commonly reported after they have been confirmed using RT-PCR or northern blots [271]. Furthermore competitive RT-PCR is still popular method for the quantitative analysis of gene expression in those labs that do not yet have access to array technology. In addition when only one or a few genes need to be studied, RT-PCR or northern blots are easier to use and less expensive. Thus RT-PCR will still remain one of the major methods for the analysis of mRNA expression levels.

Chapter 8: Discussion

The overall aim of this study was to gain an insight into gene expression during the transformation of macrophages into foam cells in an *in vitro* model. Information regarding which genes are expressed and their pattern of expression during foam cell formation will help our understanding of the complex nature of the atherosclerotic process. In addition, identification of differentially expressed genes can also help to understand the underlying biochemical pathways and may reveal potential therapeutic targets.

The macrophage plays an important role in normal physiology. It is a major cell of the inflammatory response involved in the removal of pathogenic organisms [54]. The macrophage has also been implicated in a variety of diseases including tuberculosis, AIDS, rheumatoid arthritis and atherosclerosis [54]. During the initial stages of atherosclerosis, accumulation of foam cells leads to the formation of the fatty streak. Although the fatty streak is asymptomatic, it is the precursor lesion that subsequently leads to the development of the intermediate and more complicated lesions of atherosclerosis. In addition, during the advanced stages of atherosclerosis, macrophages are thought to be critical in determining plaque stability through the release of MMPs that may weaken the fibrous cap. Studies have described a variety of foam cell responses that can contribute to the growth and rupture of atheorsclerotic plaques [114]. These include the production of growth factors and cytokines (TGF β, M-CSF, IL-1 and IL-8), chemokines (MCP-1), proteins such as the MMPs and tissue factor.

8.1 Background

At the start of this study, there were few reports of large-scale gene expression studies examining differential expression of genes in the foam cell model. Most of the genes that had been reported were single genes identified through the use of traditional molecular biology techniques such as differential display or northern blots [249,254]. In addition the reporting of these genes were from a variety of different biological models

including human and animal cell lines [120,150] in isolated HMDM grown *in vitro* [183], and in foam cells isolated from both human and animal plaques [58].

The nearest report of an attempt to examine large-scale gene expression study at that time was a report by Wang *et al* [118]. These authors studied the expression of 49 genes in differentiated THP-1 cell line on exposure to AcLDL using a multi-gene assay based on northern blotting. The genes they studied included cytokines, growth factors, chemokines and adhesion molecules. Their study identified only one gene to be differentially expressed namely the cytokine IL-8.

Therefore in an attempt to identify other differentially regulated genes during foam cell formation we attempted to perform a large-scale gene expression study in an *in vitro* model of foam cell formation as the first step of understanding and establishing events that may be occurring *in vivo*. To achieve this goal we used array technology that allows the simultaneous study of the expression of thousands of genes.

8.2 Experimental design

8.2.1 THP-1 cells –use of an in vitro model for foam cell formation

Due to the technical limitations involved, most studies of lipoprotein uptake in macrophages use cell culture models. For these experiments the human monocytic cell line THP-1 was chosen as the experimental model. THP-1 cells can be easily differentiated to macrophages using a phorbol ester and are similar to HMDM in many respects [184]. The decision to use an *in vitro* model rather than an *ex vivo* (HMDM) or *in vivo* model (macrophages isolated from atherosclerotic plaques) was based on practical experimental considerations. These included minimising variability of the source of sample and the fact that THP-1 cells could be grown in relatively large quantities as required with relative ease. The use of an *ex vivo* model (HMDM) was excluded due to the problems associated with variations between individual donors. We wanted to minimise variation as when the study was started we were unsure how cDNA array technology would perform. The use of *in vivo* macrophages from plaques was excluded due to the limited amount material expected to be obtained and the difficulty in isolating

a pure sample of foam cells from the other cell types present in the isolated atherosclerotic lesions.

8.2.2 Use of acetylated and oxidised LDL

Native LDL is taken up by macrophages via the regulated LDL receptor pathway and incubation of macrophages with native LDL does not result in foam cell formation. Thus THP-1 cells exposed to native LDL were chosen to represent the physiological situation since *in vivo* macrophages are exposed to the circulating native LDL. Modification of LDL is known to result in its uptake by unregulated pathways and foam cell formation. Two forms of modified LDL were used in this study, AcLDL and OxLDL. AcLDL is not thought to occur *in vivo* however as shown by Goldstein and Brown [16] in their discovery of the scavenger receptor, incubation of cells with AcLDL results in its uptake, leading to foam cell formation. This form of modified LDL is commonly used as an experimental standard for forming foam cells, although the effects of AcLDL may not be very representative of *in vivo* events.

Modified forms of LDL thought to occur *in vivo* include oxidation, glycation, lipolysis, proteolysis and aggregation. Of these; OxLDL has been implicated as the most likely form of LDL that exists *in vivo* and causes foam cell formation. OxLDL represented a more potent form of lipid loading.

Although aggregated or glycated LDL could have also been used, two extreme conditions were chosen. Exposure to AcLDL represented standard lipid loading. Exposure to OxLDL was a more extreme form of lipid loading, since OxLDL is not a single entity but a heterogeneous mixture consisting of a number of components including oxysterols. This can also raise problems when comparing studies between different investigators since discrepancies in reported genes may be due to differences in techniques used for modification and the concentrations of OxLDL used.

8.2.3 Choice of technology to examine differentially regulated genes.

The original molecular biology method planned to be employed in this study to identify differentially regulated genes was differential display (Chapter 7). However as this PhD was a part of a collaborative research project with an industrial partner (Glaxo Wellcome), the author was given the opportunity to use high density cDNA technology that was utilised within the company.

The decision to proceed with the use of this technology was taken after consideration of a number of factors including the time involved in learning a new technology, the number of experiments that could be performed, the potential of the results that could be obtained using the technology and the risks associated with a method still under development. It should be noted that this technology could only be used due to the collaborative nature of this study. Such collaborations between industry and academia are important for the transfer of scientific knowledge and technological advances between the two institutions. Furthermore they play a valuable role in providing students work experience in an industrial setting.

8.3 Results

8.3.1 Foam cell formation

Although both AcLDL and OxLDL have been reported to induce foam cell formation in macrophages, this had to be achieved by the author of this thesis. To date there are no current standard protocols for modifications of LDL and concentrations of these modified forms of LDL that induce foam cell formation. Commonly however the method reported by Basu *et al* [172] the standard method used for preparation of acetylated LDL and methods of either Steinbrecher *et al* [171] and Hammer *et al* [175] are used for oxidation.

Due to the nature of experimental work, variations will always exist in the experimental procedures used for culturing cells, for isolating and modifying LDL between different investigators. Therefore before gene expression between macrophages

and foam cells could be assessed, foam cell formation had to be confirmed in differentiated THP-1 cells using the experimental conditions used within this study. This was achieved using both quantitative and qualitative methods.

Initially THP-1 cells were differentiated using PMA. PMA stimulates differentiation by binding to and activating protein kinase C in cell membranes and tissues.Both flow cytometric analysis and light microscopy confirmed that differentiation of monocytes to macrophages had occurred (chapter 3) and a change in cell morphology was noted. As was expected and reported by other investigators [163], cells were found to change from a homogenous population of 'round' cells to a more heterogeneous population with cells becoming adherent and spread. This is consistent with previously reported data that the THP-1 cell line responds to PMA treatment by changes in cell morphology with acquisition macrophage like functions including phagocytosis and enhanced secretion of lipoprotein lipase and apoE [190]. Exposure of dividing THP-1 cells to PMA has also been reported to results in loss of LDL receptors and the appearance of scavenger receptors [21]. These factors make THP-1 cells suitable for *in vitro* studies of foam cell formation.

However several disadvantages also exist in using THP-1 cells differentiated with PMA. Firstly it does not truly represent the *in vivo* situation. In addition it has also been reported that there is a degree of heterogeneity in expression of macrophage functions after PMA treatment. Regardless of length of exposure to PMA, a certain population of THP-1 cells remain negative for expression of the scavenger receptor. Another point to consider is the length of time required for differentiation. Although some investigators have reported differentiation after 24 hours, Via *et al* [160] have reported that maximal scavenger receptor activity and morphological differentiation were only achieved consistently after 72 hours of exposure to PMA (cells in this study were differentiated for 7 days to ensure full differentiation). PMA itself can activate the transcription of a number of genes including LpL, apoE, collagenase and metallothionein. To exclude effects of PMA induced genes in this study; cells were exposed to PMA for identical time periods for differential gene expression experiments so that the only variable was the form of lipoprotein treatment received.

Once THP-1 cells had been differentiated using PMA, cells were exposed to native, acetylated or OxLDL. Subsequently cholesteryl ester accumulation was assessed within the cells to show that differentiated cells exposed to modified LDL accumulated more cholesteryl esters than those exposed to native LDL. Cells were exposed at varying concentrations (0, 0.05, 0.1, 0.2 and 0.3mg/ml) of LDL and modified LDL over varying time periods (0, 24, 48 and 72 hours). Cholesterol accumulation was assessed quantitatively by using flow cytometry of nile red stained cells and the ^{14}C oleate loading. These methodologies both of which have been previously reported [163,164] for assessing foam cell formation indicated that cholesterol ester accumulation using AcLDL was greater than native LDL at a concentration of 0.2mg/ml of AcLDL and that this was achieved after 24 hours of exposure. Using OxLDL, cholesteryl ester accumulation was found to occur at a slower rate and cells did not show accumulation greater than native LDL until a concentration of 0.3mg/ml of OxLDL and this was achieved after 72 hours.

Qualitative methods using Oil red O staining and fluorescence microscopy also confirmed that differentiated THP-1 cells exposed to modified lipoprotein accumulated more cholesterol esters than cells exposed to native LDL as visually observed by the presence of increased numbers of lipid droplets and greater fluorescence in cells exposed to modified lipoprotein as compared to native lipoprotein.

Thus an *in vitro* model of foam cells could be established as previously reported. This *in vitro* model of foam cells could subsequently be used to study differential gene expression between cells exposed to native LDL compared to cells exposed to modify LDL (foam cells). For gene expression studies, differentiated THP-1 cells were exposed to native and modified LDL for 24 hours at concentration of 0.2mg/ml lipoprotein. In an attempt to study genes showing differential gene expression during early exposure to modified LDL, samples of differentiated THP-1 cells exposed to AcLDL and OxLDL (0.2 mg/ml) for 4 hours were also prepared.

8.3.2 Array Technology

For array technology experiments two different arrays were used, a custom atheroma array with a pre-selected genes thought to be involved in the CHD and arrays representative of the human genome (containing genes that had been sequenced to date and EST). Both arrays were generated using cDNA clones from the human I.M.A.G.E library.

The custom arrays had the advantage of containing a pre-selected list of genes that were relevant to CHD. In addition the all the genes on the array were gridded at least 4 times and sequenced to determine whether they matched their original given I.M.A.G.E identity. This meant post analysis of the data was easier and reproducibility could be assessed. In addition it confirmed the high error rate present within the I.M.A.G.E collection. Of 769 genes chosen for the custom atheroma array only 579 (75%) matched their original assigned I.M.A.G.E identity.

The I.M.A.G.E arrays had the advantage of containing EST sequences and a much larger number of genes. However due to the large error rate and level of redundancy all gene differences identified had to be sequence confirmed. This meant that post analysis of data took longer since clones corresponding to the genes identified had to be repicked from the library and sequenced. In addition as would expected there I.M.A.G.E arrays gave a larger number of genes to follow compared to the custom arrays and many of the differences identified corresponded to ESTs.

It has been reported by Botwell *et al* [273] that the original Unigene sets (from which the I.M.A.G.E collection results) has significant discrepancies between actual and designated clone sequence and thus many of the I.M.A.G.E clones (up to 30 %) may be assigned incorrect identities. This is consistent with the error rate (25%) found in preparing the custom array.

Another factor to take into consideration for future experiments was the time taken to collate all the data from the I.M.A.G.E arrays. Due to the size of the I.M.A.G.E library the work involved in processing the arrays, collecting and analysing the data was much greater than the custom arrays. In addition the most of the changes identified corresponded to ESTs. It is thus arguable whether the I.M.A.G.E arrays should have been

used in this study. The results however provide a significant database of subsequent genes/EST to follow up and analyse. In addition the results provide a good starting point to follow-up the differential expression of novel genes represented through the ESTs.

8.3.3 Differential gene expression

Results of differential gene expression studies showed fewer genes to be regulated by experimental treatment (AcLDL and OxLDL) than we had hypothesized and expected. Although this result was surprising, reports by other investigators using array technology have also showed the number of genes to be regulated to be less than they had expected with experimental samples. These results also fit those observed from the completion of the sequencing of the human genome project. Although the number of genes expected was though to be around 100,000 before completion of the project, the results have suggested around 20,000-30,000 genes [199]. This could be due to more splice variants of genes being present than previously envisaged.

In this study we found the largest number of genes found to be regulated were found to be in the native versus control sample. The control sample used in this study was sample of differentiated THP-1 cells that had been exposed to serum free medium (as had all the samples) to remove any exogenous lipoprotein stores, however unlike the other samples the cells were not subsequently exposed to any lipoprotein. This sample thus represented lipoprotein deficient cells in which essential cellular processes may have been switched off completely or slowed down due to lack of lipid availability. In other words the control cells may have been in a semi quiescent state and exposure of the cells to native LDL resulted in an active state where normal cellular processes may have been switched on again, hence the large number of changes observed in this comparison.

The results from the experimental treatments did however show genes that were expected to be involved in this process were differentially expressed. These genes included CD36, MMP-2, TIMP-1 and IL-1β all of which have been reported to play a role in the atherosclerotic process [24, 147, 150, 225]. These results indicated both that foam cell formation had occurred and that the array technology used here was capable of detecting these changes. Furthermore in general the genes found to be differentially

expressed showed a tendency to be either inflammatory molecules or genes involved in cell structure and morphology. Since atherosclerosis is now widely accepted to be an inflammatory process [4], the results of this study provide further credence to this claim. Furthermore lipid loading would be expected to result in changes in cell morphology.

Although no new novel genes were detected by this study, this is not unexpected considering that most of the genes on the custom atheroma arrays were selected due to their involvement in CHD and thus most of them have already been reported or studied in foam cell models. As the I.M.A.G.E arrays also contained cDNAs representing EST clusters, the results from the human I.M.A.G.E arrays did provide potential novel transcripts to follow up.

Comparing AcLDL with OxLDL, more changes were found with OxLDL. This was expected since as already noted OxLDL, is not a single entity, but is composed of many oxidised lipid components such as oxysterols. In particular exposure to AcLDL was found to result in the increased expression of IL-1β, a pro inflammatory cytokine which is known to sustain the inflammatory process. Exposure to OxLDL resulted to an increase in CD36, a known receptor for OxLDL and also an increase in expression of MMP-2. An increase in MMP-2 activity has been reported in foam cells isolated from atherosclerotic lesions. MMP-2 is involved in the breakdown of components of the ECM. It has also been implicated in SMC migration. Both AcLDL and OxLDL also showed a decrease in TIMP-1 expression indicating that active MMPs may play an important role during foam cell formation. MMP-1, MMP-2, MMP-3 and MMP-9 have all been reported in lesional macrophages. In this study we only detected the expression of MMP-2 indicating that this may be the one of the MMPs expressed on early exposure to modified LDL. It has demonstrated that levels of MMP-2 increase as the plaques from fatty streaks to fibrous plaques [274].

In hindsight of the large number of changes observed with the native versus control samples, it may have been better to expose all cells to native LDL (use the native LDL sample as a control). After exposure of all samples to native LDL for 24 hours, cells could then have been exposed to native, acetylated and oxidised LDL for 24 hours. This may have resulted in the cells being more representative of the *in vivo* situation where

macrophages are exposed to native LDL in the plasma. However this would not have been realised had these experiments not been performed in the first place. In addition if analysis of the data had been performed for each comparison one at a time this may have identified the situation at an earlier stage of the study. Unfortunately this was not possible due to time limitations and restricted use of the array technology, which meant that experiments had to be performed and analysed in two allocated set time periods.

8.3.4 Temporal gene expression

A second part to this study was to examine temporal gene expression of differentiated THP-1 cells in response to OxLDL. This was performed so that a global picture of the pattern of gene expression taking place upon lipid loading with OxLDL could be obtained. Cells were exposed to OxLDL (0.2mg/ml) for 0, 4, 8, 16, 24, 48 and 72 hours. Probes were prepared and applied to the custom atheroma arrays. This generated an expression level for every gene on the custom array at every time point studied was obtained. These expression levels were corrected (to take into background) to produce a final matrix of data. This showed that 216 genes on the array showed an expression level (after normalisation) at one of the time points studied.

To analyse the data matrix produced by this large number of data points in a manner that was meaningful, the data was coloured so that the data was represented in a manner that was both quantitative and qualitative. This has been one of the main approaches taken to analyse large data sets that are produced by array technology. This allowed easier visualisation of the data and allowed the identification of genes showing low, moderate and high levels of expression. Furthermore from this data set, genes of interest or genes known to be involved in the atherosclerotic process could be selected and their patterns of expression compared to identify genes showing similar patterns of expression. The results showed that members of gene families showed highly similar patterns of expression including members of the annexin, fibronectin and cluster determinant families. Other families however; such as the members of the MMPs did not show similar patterns of expression. Comparison of expression patterns of genes of interest showed that, in particular, two sets of genes showed highly similar patterns of

expression. IL-1β showed a highly similar pattern of expression to TIMP-1. In addition CD36 was found to show a highly similar pattern to a transcription factor STAT6. When different variants/subforms of a gene were present and showed differential regulation, the different variants were found to show highly similar patterns of expression

One point to note here is that the results produced by the temporal study do not take into account the effect that native LDL has on these genes. This is important since when compared to native LDL, the genes may not show up and down regulation. The only conclusions that can be drawn from this data set is that the genes identified are expressed during their exposure to OxLDL and the pattern of expression these genes follow over the time course of exposure to OxLDL over 72 hours. In addition the effects of PMA were not controlled for during this part of the study, all cells were compared to a zero time sample. However since THP-1 cells were differentiated using PMA for 7 days before the time course experiment was started any further changes due to PMA should be minimal. This is because PMA should have fully differentiated the cells by this stage.

Selecting genes known to be involved in the atherosclerotic process or gene families did identify genes showing similar patterns of expression. However this method relied on knowledge of the atherosclerotic field and did not identify any patterns of expression emerging from the full data set of genes showing temporal expression. To achieve this, hierarchical cluster analysis was applied to the results produced from the temporal study in order to identify groups of genes showing similar patterns of expression. The results showed 9 different clusters of genes.

Hierarchical cluster analysis is a commonly reported clustering method that has been applied to data generated using array technology [235]. Hierarchical is an unsupervised technique that builds clusters of genes with similar patterns of expression. However the method does have some disadvantages. One being that it ignores negatives correlations; which may be important in a particular data set. In addition the method is inflexible in that genes that are linked together incorrectly early on the process cannot latter be assigned to different clusters. Thus the temporal gene results presented here show the strength of array technology in terms of number of genes and time points that can be analysed.

Studies similar to the temporal work performed in this study has been reported. An overview of expression profiling in cardiovascular disease has been reported by Henriksen *et al* [158]. Andersson *et al* [275] have reported transcript profiling of cholesterol loaded macrophages, however they employed the method of cDNA representational difference analysis and shotgun sequencing. Shiffman *et al* [276] have reported the results of a temporal study using THP-1 cells exposed to 0.1mg/ml OxLDL for up to 4 days. However there are some fundamental differences between this study and the one reported by Shiffman *et al* [276]. This means that although the results obtained from both studies can be examined they cannot be directly compared. Neither can they support or disprove results at an individual level since the experimental conditions used in both studies were different. These differences include

(a) Time allowed for differentiation of THP-1 cells

Whilst cells in this study were differentiated using PMA for seven day before exposure to OxLDL, Shiffman's group only allowed differentiation for 24 hours before exposure to OxLDL. However Shiffman's group use a time matched PMA control sample at each time point to take into account the effects of PMA. This was not done in this study due to limitations of resources and time.

(b) Concentration of OxLDL used

The concentration of OxLDL used in this study was 0.2mg/ml, the authors of the above study used 0.1mg/ml, half the amount used in this study.

(c) Time course

Cells in this study were exposed to OxLDL for periods of 4, 8, 16, 24, 48 and 72 hours. Shiffmans group exposed cells to OxLDL for 0.5, 2.5, 8, 24, 48 and 96 hours.

(d) Number of genes assessed

In this study we assessed 769 genes that were arrayed on nylon membranes. Shiffman *et al* probed a much larger number of genes 9808 human genes. In addition these genes were arrayed on glass slides.

Both studies however found similar numbers of genes to be differentially expressed during exposure. Here we report the expression of 217 genes from 769 genes. Shiffman et al reported the expression 268 genes from 9808 genes. Although we report a much higher number of genes in term of the percentage of genes probed, this can be accounted for the fact that the genes on the custom arrays used here were pre-selected for their involvement in CHD. In addition, similar to the results of the study presented here Shiffman's group do not exclude the fact these temporally expressed genes may also be regulated by native LDL treatment.

Although as noted above IL-8 was identified by Wang *et al* [114] to be expressed in differentiated THP-1 cells exposed to AcLDL, we did not identify the gene during DGE experiments. However the reason for this became clear when the temporal pattern of expression of IL-8 was examined. This showed that IL-8 expression peaked at 8 hours and by 24 hours it had returned to basal levels. This is consistent with the work of Wang *et al* [114] who despite the fact they used a lower level of OxLDL nevertheless found a similar pattern of expression with IL-8 showing a peak of expression at 8 hours. The fact that we used a time point of 24 hours explains the reason why the gene was not detected during DGE experiments. This highlights the need to perform temporal studies on genes of interest since expression patterns can vary greatly even over small time periods.

8.4 Problems associated with array technology

As shown by the results presented in this study, array technology has the ability to survey a large number of genes and yield large numbers of results. However as with any use of any technology in a developmental stage there are many issues, which must be addressed.

8.4.1 Reverse transcription bias

One of the problems with using technologies that assess mRNA levels via cDNA production is that not all mRNA's are not transcribed with the same efficiency [220].

This fact can lead to reverse transcription bias, which can change the relative amounts of different cDNAs. Another problem caused by this bias is that some mRNA's may be reverse transcribed for only parts of their lengths, making them less likely to bind and stay bound to their corresponding sequences on the array. One way of getting around this problem is to prime reverse transcription from random starting positions on the mRNA rather than always starting from their poly A tails [277].

8.4.2 Oligonucleotide versus cDNA arrays

Two different types of arrays have largely arisen from array technology. Oligonucleotide arrays or cDNA clones that are arrayed onto glass slide or nylon membranes (as used in this study). Compared to oligonucleotide arrays, cDNA arrays have the advantage of potentially improved sensitivity due to the availability of more target sequence to which the probe can hybridise [207]. However clone mix-ups between sequencing and array creation means that interesting clones must be sequenced again to be assured of their identity [273]. Shorter oligonuclotide arrays however have the advantage of allowing detection between highly similar genes and alternative splice variants [220].

The spotting pattern and spot shape of synthesized oligonucleotide arrays are very regular [220]. Printed arrays are more likely to have uneven spot morphology and irregular spacing caused by the printing method used. Some genomic and cDNA clones have repetitive sequences, leading to cross hybridisations on the arrays [220]. Generally the use of oligonucleotide arrays is becoming more widespread, however agreement has yet to be reached on what the optimal length of oligonucleotide to use (25mer or 60 mer oligonucleotides are the currently the most commonly used) [206].In addition reports comparing the different platforms (cDNA arrays versus oligonucleotide arrays) have generated conflicting results on whether the data between the 2 platforms is comparable [278,279].

8.4.3. Controls for array experiments

As shown by this study, expression levels of normally used housekeeping genes such as GAPDH did not remain constant and were actually found to be differentially expressed. Warrington *et al* [280]have identified only 47 genes out of a total of 7000 genes studied in 11 different adult and fetal tissues; whose expression remains at similar levels making them useful as controls.

The best controls that have been suggested are genes from different organisms to the one being studied, so that when using human samples one should use control genes derived from bacteria or plants. This means that the probe should only hybridise to its complement sequence on the array and is not present in the sample. If several different genes are spiked into the sample at different concentrations, subsequent monitoring of these genes can be used as sample to sample normalising factors.

The results from this study indicated that the levels of normally used housekeeping genes between samples did not remain constant during DGE experiments. Thus during the temporal gene expression study, housekeeping genes were not used as controls, instead the median intensity of the arrays was used. This was considered a developmental step in the technology. If the expression levels of housekeeping genes not been found to be differentially regulated during DGE experiments; this step could not be taken when the temporal gene expression study was performed.

8.4.4 Background

Another factor that will affect the results is the background signal of the array and subsequent threshold values used to exclude background. This means genes of low abundance are likely to be excluded. Quantitation of the intensities of each spot on the array can also be affected by noise from surrounding spots. In addition dust on the slide and non-specific hybridisation can also affect results. Furthermore detection intensity might not be uniform across the array, leading to excessive intensity on one side of the array.

8.4.5 Glass slides versus nylon membranes

Arraying of cDNA samples is now more commonly performed on glass slides than nylon membranes although both have their own advantages and disadvantages. Commercially available filter arrays are cheaper than glass arrays because they require no special equipment except phosphorimaging screens [209]. Membranes are also useful for scarce mRNA, as a smaller amount of mRNA is required to prepare the probe in comparison to the amount required for the preparation of fluorescent probes that are applied to glass arrays

8.4.6 Single versus Dual labelling

Both Nylon membranes and Affymetrix GeneChip arrays employ a single label whereas glass slides use two fluoresecet dyes commonly Cy3 and Cy5 [281]. Use of a single dye enables comparison with any subsequent experiments performed; whereas when two samples are hybridised on one slide; only that comparison can be performed. This means that the experimental design process requires careful thought. In addition cross over and gene specific effects of the Cy3 and Cy5 means that dye swapping experiments should be performed [220]. On the other hand use of single label requires two separate arrays which can cause subsequent image comparison issues if image artefacts are present on one of the arrays

8.4.7 Technical versus Biological Replicates

Technical replicates normally indicate identical probes prepared independently from the same RNA. Technical replicates are useful to ensure that the procedures and equipment being used are working consistently and thus replicates are an important part of the set up process. Biological replicates are samples prepared from different preparations of RNA isolated from independent samples. Biological replicates are important as they provide greater statistical power to the analysis of the data generated.

8.4.8. Array technology for the identification of novel genes

One of the potential downfalls of array technology is that generally only known gene/transcripts and EST clusters from the databases such as Unigene are represented on arrays. This could result in a lack of novel transcripts on the arrays. In this study, two such cases are discussed below. A class of molecules called the disintegrins (MDCs) have been identified in atherosclerotic lesions [282]. In particular MDC 15 has been found to be present in lesions of atherosclerosis [282]. However when the list of genes on the custom array were consulted it was found that only MDC 9 was present on the arrays thus even if MDC15 was differentially expressed on the custom arrays we would not have been able to detect it because it was not present on the array. In addition a novel scavenger receptor for OxLDL called SR-PSOX (scavenger receptor for phosphatidyl serine and oxidised lipoprotein) has been recently reported [283]. Similarly this receptor was not represented on the arrays. With sequencing of genomes from the major organisms of interest complete, future array experiments can ensure that all the genes in the genome of the organism being studied can be represented.

8.4.9 Data Storage, Sharing and Interpretation

One of the major problems of array technology has arisen exactly due to the strength of the technology, namely the amount of data produced. Undoubtedly the main advantage of using array technology in this study has been the amount of data generated. For example the time course experiment, which produced 5383 data points would not have been possible in the time scale of a PhD project using traditional molecular biology methods. Thus the greatest challenges are to have standards which allow data from different array platforms to be compared; to allow sharing and storage of data and to be able to interpret the data biologically meaningful manner. Major steps have been taken in the scientific community over the last few years to address some of these issues.

The Microarray Gene Expression Data Consortium (MGED) has been formed and has set standards for the generation and submission of microarray data [284]. These

standards include minimum information about a microarray experiment (MIAME) [285] and microarray gene expression markup language (MAGE-ML) [286]. These standards have also been adopted by the major scientific journals including Nature, Science and The Lancet and microarray data repositories such as Gene Expression Omnibus (GEO; discussed below)

The data from this study and other gene expression studies performed at Glaxo Wellcome was stored in a database so that future comparisons and analysis of this data with other data sets generated within the company could be performed. However access to this database is restricted to Glaxo Wellcome personnel. Unfortunately most academic institutions cannot meet the costs of setting up and managing such databases. In addition such company databases do not allow data to be made available to the scientific community at large. To address these needs, the National Centre for Biotechnology Information in the U.S has set up a medium for the deposition for data generated by array technology experiments. This database is known as GEO [287]. Other such databases include European Bioinformatics Institutes ArrayExpress [288].

The results of most microarray experiments results in a list of differentially expressed genes. Initially researchers spent huge amounts of time going through such lists manually using literature searches and public databases in an attempt to discover relevant biological processes and pathways. Recently tools such as NetAffx [289], GenMAPP [290], Gene Ontology (GO) [291] and KEGG [292] have been developed to assist researchers in this area. As biologists, bioinformations and statisticians continue to work together more such tools can be expected.

8.5 Future work

Although the results provided here provide a comprehensive view of gene expression occurring in during foam cell formation, it should be remembered that this experiment was performed in an *in vitro* cell model. Although this may be highly representative of the *in vivo* model it does still not obviously divert the need for this work to be performed *in vivo* that is ultimately a more complex situation involving other cell types all of which interact to contribute to the atherosclerotic process. The first stage in

this process would be ultimately to use an *ex vivo* model, namely HMDM. However due to the variability with HMDM from different individuals it would be interesting to use array technology to look at the level of HMDM isolated from different individuals. If these differences were minimal then the foam cell model could be established within these cells and differences in gene expression examined. Further experimentation would then look at the *in vivo* model with macrophages isolated from fatty streaks and advanced plaques. However here the problems lie in being able to isolate macrophages from the other cellular components present in lesions and the availability of limited material. In this respect techniques such as Laser capture microdissection will be important. Recently Trogan *et al* [293] used this technique to look at gene expression in macrophages from atherosclerotic lesions in mice. Whilst they used RT-PCR for looking at gene expression because of limited RNA, methods such as linear amplification which decrease the amount of RNA required [294] means that microarray analysis is also possible.

Future experiments will also assess cell viability, since OxLDL has been reported by some investigators to be toxic [38]. In this study cell death was noted in differentiated THP-1 cells exposed to OxLDL for 72 hours. Shiffman *et al* [247] have reported exposure to OxLDL for up to 4 days with no mention of cell death. In fact their study suggested that most up regulation of genes was occurring at this point and that this may possibly still represent the early stage of changes that are thought to occur during lipid loading. If this is the case, this will also warrant further investigation.

Although the genes reported here were not confirmed using independent means, most of the genes here have already been reported or implicated in the atheorsclerotic process. In addition the study by Shiffman *et al* [247] found that in fact array technology was found to under represent the levels of the genes reported. Furthermore they were able to confirm the results of genes identified from array technology using quantitative real time PCR. In an attempt to confirm some of the genes identified here, the methods of quantitative RT-PCR were set up. However due to time limitations the experimentation could not be completed.

When this study was started array technology was limited to industrial environments and large academic institutions that could afford the technology. However since then the technology has become more widespread as costs of the technology have

dropped and the potential of the technology has been exploited. Most institutions have now set up core microarray facilities.

Further developmental progress has also been made with the development of tissue arrays and protein arrays. Tissue arrays allow the expression of one gene to be assessed over thousands of different tissue samples to be assessed. Although it is more difficult to identify proteins that are differentially expressed, protein arrays have been utilised successfully [295].

8.6 Conclusion

This study has demonstrated the application of array technology to identify expression of genes involved in the macrophage to foam cell formation. The study has demonstrated the large amounts of data that such studies can generate and the importance of techniques needed to analyse this data. The data presented here should be viewed as an ideal database for consultation as knowledge of the atherosclerotic field expands. In addition it is a good starting point for designing future experimentation looking at the involvement of genes in the foam cell process in the *in vitro* foam cell model used here.

As technology progresses to protein arrays, arrays looking at differences in levels of mRNA will remain important in establishing how data is correlated between mRNA levels and protein levels and establish the importance of post-transcriptional and post-transcriptional modifications that occur during gene expression.

The data generated from this study supports the role of inflammation in the atherosclerotic process. Advances such as the discovery of statins have had a major impact on mortality from CHD over the last couple of decades. As our understanding of the atherosclerotic process increases further more such advances are expected. Recently Wald *et al* [296] have suggested work on a polypill which would combine six key compounds, aspirin, a statin, folic acid and three blood pressure medications. Such treatment if successful could further dramatically decrease mortality from CHD.

Chapter 9: Bibliography

[1] Cascieri, M.A. The potential for novel anti-inflammatory therapies for coronary artery disease. Nature Reviews Drug Discovery, **1**, 122-130 (2002)

[2] Mangiapane, E.H and Salter, A.M. Diet, Lipoproteins and Coronary Heart Disease. Nottingham University Press, Notthingham, UK (1999)

[3] Ross, R Atherosclerosis: - an inflammatory disease. New England Journal of Medicine, **340**, 115-126 (1999)

[4] Libby, P. Inflammation in atherosclerosis. Nature, **420**, 868-874 (2002)

[5] Feher, M.D. and Richmond, W. *In* Lipids and Lipid Disorders. Gower Medical Publishing, London, UK (1990)

[6] Stary, H.C. Macrophages, macrophage foam cells and eccentric intimal thickening in the coronary arteries of young children. Atherosclerosis, **64**, 91-108 (1987)

[7] Stary, H.C., Chandler, A.B., Seymor, G. and Guyton, J.R. A Definition of Initial, Fatty Streak and Intermediate Lesions of Atherosclerosis. Arteriosclerosis Thrombosis and Vascular Biology, **14**, 840-855 (1994)

[8] Li, A.C and Glass, C.K. The macrophage foam cell as a target for therapeutic intervention. Nature Medicine, **8** (11), 1235-1242 (2002)

[9] Lusis, A.J. (2002).Atherosclerosis, Nature, **407**, 233-241 (2002)

[10] Betteridge, D.J. Lipids: Current Perspectives, volume 1, lipids and lipoproteins. Martin Dunitz Ltd, London, UK (1996)

[11] Kreuzer, J and Hodenberg, E.V. The role of apolipoproteins in lipid metabolism and atherogenesis; apects in man and mice. Journal of Hypertension, **12**, 113-118. (1998)

[12] Brown, M. S. & Goldstein, J. L. The low density lipoprotein pathway and its relation to atherosclerosis. Annual Review of Biochemistry, **46**, 897-930 (1977)

[13] Brown, M. S. & Goldstein, J. L. How LDL Receptors Influence Cholesterol and Atherosclerosis. Scientific American, **257**, 58-66 (1984)

[14] Strickland, D.K., Kounnas, M.A. and Argraves, W.S. LDL receptor-related protein: a multiligand receptor for lipoprotein and proteinase catabolism. FASEB Journal, **9**, 890-898 (1995)

[15] Sakai, J., Hoshino, A., Takahashi, S., Miura, Y., Ishii, H., Kawarabayasi, Y., and Yamamoto, T. Strucure, chromosome location and expression of the human very low density lipoprotein receptor gene. Journal of Biological Chemistry, **269**, 2173-2182 (1994)

[16] Goldstein, J.L., Ho, Y.K., Basu, S.K. and Brown, M.S. Binding site on macrophages that mediates uptake and degradation of acetylated low density lipoprotein, producing massive cholesterol deposition. Proceedings of the National Academy of Science, **76**, 333-337 (1979)

[17] Brown, M.S. and Goldstein, J.L. Lipoprotein metabolism in the macrophage: implications for cholesterol deposition in atherosclerosis. Annual review of Biochemistry, **53**, 223-261 (1983)

[18] Boullier, A., Bird, D.A., Chang, M.K., Dennis, E.A., Friedman, P., Gillotre-Taylor, K., Horkko, S., Palinski, W., Quehenberger, O., Shaw, P., Steinberg, D.,

Terpstra, V., and Witztum, J.L. Scavenger receptors, oxidised LDL and atherosclerosis. Annals of the New York Academy of Sciences, **947**, 214-222 (2001)

[19] Linton, M.F. and Fazio, S. Class A scavenger receptors, macrophages and atherosclerosis. Current Opinion in Lipidology, **12**, 489- 905 (2001)

[20] de Villiers, W.J. and Smart E.J. Macrophage scavenger receptors and foam cell formation. Journal of Leukocyte Biology, **66**, 740-746 (1999)

[21] Geng, Y., Kodma, T and Hansson, G.K. Differential expression of scavenger receptor isoforms during monocyte-macropahge differentiation and foam cell formation. Arterioslerosis, Thrombosis and Vascular Biology, **14**, 798-806 (1994)

[22] Kunjathoor, V.V., Febbraio, M., Podrez, E.A., Moore, K.J., Andersson, L., Koehn, S., Rhee, J.S., Silverstein, R., Hoff, H.F., Freeman, M.W. Scavenger receptors class A-I/II and CD36 are the principal receptors responsible for the uptake of modified low density lipoprotein leading to lipid loading in macrophages. Journal of Biological Chemistry, **277,** (51), 49982-49988 (2002)

[23] Nakagawa-Toyama, Y., Yamashita, S., Miyagawa, J., Nishida, M., Nozaki, S., Nagaretani, H., Sakai, N., Hiraoka, H., Yamamori, K., Yamane, T., Hirano, K., Matsuzawa, Y. Localization of CD36 and scavenger receptor class A in human coronary arteries:- a possible difference in the contribution of both receptors to plaque formation. Atherosclerosis, **156**, 297-305 (2001)

[24] Krieger, M. Scavenger receptor B1 type is a multiligand HDL receptor that influences diverse physiologic systems. Journal of Clinical Investigation, **108**, (6) 793-797 (2001)

[25] Febbraio, M., Hajjar, D.P. and Silverstein, R.L. CD36: a class B scavenger receptor involved in angiogenesis, atherosclerosis, inflammation, and lipid metabolism. Journal of Clinical Investigation, **108**, 785-791 (2001)

[26] Ramprasad, M.P., Terpstra, V., Kondratenko, N, Quehenberger, O. and Steinberg, D. Cell Surface expression of mouse macrosialin and human CD68 and their role as macrophage receptors for oxidised low density lipoprotein. Proceedings of the National Academy of Science, **93**, 14833-14838 (1996)

[27] Sawamura, T., Kume, N., Aoyoma, T., Moriwaki, H., Aiba, Y., Tanaka, T., Miwa, S., Katsura, Y., Kita, T and Masaki, T. A novel receptor for oxidised low density lipoprotein. Nature, **386**, 73-77 (1997)

[28] Kataoka, H., Kume, N., Miyamoto, S., Minami, M., Moriwaki, H., Murase, T., Sawamura, T., Masaki, T., Hashimoto, N. and Kita, T. Expression of Lectin like Oxidised Low-Density Lipoprotein Receptor-1 in Human Atherosclerotic Lesions. Circulation, **99**, 3110- 3117 (1999)

[29] Stary, H.C., Blankenhorn, D.H., Chandler, A.B., Glagov, S. Insull W. Jr., Richarson, M., Rosenfeld, M.E., Schaffer, S.A., Schwartz, C.J. Wagner, W.D. *et al.* A definition of the intima of human arteries and of its atherosclerotic prone regions: a report from the Committee on Vascular Lesions of the Council on Arteriosclerosis, American Heart Association. Circulation, **88**, 391-405 (1992)

[30] Hurt-Camejo, E. Cellular consequences of the association of apoB lipoproteins with proteoglycans. Potential contribution to atherogenesis. Arteriosclerosis, Thrombosis and Vascular Biology, **17**, 1011-1017 (1997)

[31] Heeneman, S., Cleutjens, J.P., Faber, B.C., Creemers, E.E., van Suylen, R.J., Lutgens, E., Cleutjens, K.B., Daemen, M.J. The dynamic extracellular matrix:

intervention strategies during heart failure and atherosclerosis. The Journal of Pathology, **200** (4), 516-25 (2003)

[32] Stary, H.C., Chandler, A.B., Dinsmore, R.E., Fuster, V., Glagov S., Insull W. Jr., Rosenfeld,M.E , Schwartz, C.J., Wagner, W.D. and Wissler, R.W. A Definition of Advanced Types of Atheroscleorotic Lesions and Histological Classification of Atheroscelrosis. A Report from the Committee on Vascular Lesions of the Council on Arteriosclerosis, American Heart Association. Arteriosclerosis, Thrombosis and Vascular Biology, **15** (9), 1512-1531 (1995)

[33] Virmani, R, Kolodgie, F.D., Burke, A.P., Farb, A. and Schwartz, S.M. Lessons from Sudden Coronary Death. A Comprehensive Morphological Classification Scheme for Atherosclerotic Lesions. Arteriosclerosis, Thrombosis and Vascular Biology, **20**, 1262-1275 (2000)

[34] Nakashima, Y., Plump, A.S., Raines, E.W., Breslow, J.L. and Ross, R. ApoE-deficient mice develop lesions of all phases of atherosclerosis throughout the arterial tree. Arteriosclerosis, Thrombosis and Vascular Biology, **14**, 133-140 (1994)

[35] Stary, H.C. Macrophages, macrophage foam cells and eccentric intimal thickening in the coronary arteries of young children. Atherosclerosis, **64**, 91-108 (1987)

[36] Brewer, H.B. The lipid laden foam cell; an elusive target for therapeutic intervention. Journal of Clinical Investigation, **105**, 703-705 (2000)

[38] Ball, R.Y. Evidence that death of macrophage foam cells contribute to the lipid core of atheroma. Atherosclerosis, **114**, 45-54 (1995)

[39] Libby, P and Masanori, A. Stabilisation of atherosclerotic plaques: New mechanisms and clinical targets. Nature Medicine, **8** (11), 1257-1262 (2002)

[40] Takano, M., Mizuno, K., Okamatsu, K., Yokoyama, S., Ohba, T., Sakai, S. Mechanical and structural characteristics of vulnerable plaques: analysis by coronary angioscopy and intravascular ultrasound. Journal of the American College of Cardiology, **38**, 99-104 (2001)

[41] Coombs, B.D., Rapp, J.H., Ursell, P.C., Reilly, L.M and Saloner, D. Structure of plaque at carotid bifurcation: high-resolution MRI with histological correlation. Stroke, **32**, 2516-2521 (2001)

[42] Hoffmann, U., Bodlaj, G., Derfler, K., Bernhard, C., Wicke, L., Herold, C.J., Kostner, K. Quantification of coronary artery classification in patients with FH using EBCT. European Journal of Clinical Investigation, **31**; 471-475 (2001)

[43] Brindle, J.T., Antti, H., Holmes, E., Tranter, G., Nicholson, J.K., Bethell, W.L., Clarke, S., Scholfied, P.M., McKilligin, E., Mosedale, D.E., Grainger, D.J. Rapid and non invasive diagnosis of the presence and severity of coronary heart disease using ^{1}H-NMR-based metabonomics. Nature, **8** (12), 1439-1444 (2002)

[44] Smith, E.B. Transport, interactions and retention of plasma proteins in the intima: the barrier function of the internal elastic lamina. European Heart Journal, **11**, 72-81 (1990)

[45] Ross, R. The pathogenesis of atherosclerosis: a perspective for the 1990s. Nature **362**, 801-809 (1993)

[46] Gerrity, R.G. The Role of the Monocyte in Atherogenesis: I. Transition of Blood-Borne Monocytes into Foam Cells in Fatty Lesions. American Journal of Pathology, **103**, 181-190 (1981)

[47] Faggiotto, A. and Ross, R. Studies of hypercholesterolemia in the non-human primate II: - Fatty streak conversion to fibrous plaque. Arteriosclerosis, Thrombosis, and Vascular Biology, **4**, 341-356 (1984)

[48] Binder, C.J., Chang, M, Shaw, P.X., Miller, Y.I., Hartvigsen, K., Dewan, A. Witztum, J.L. Innate and acquired immunity in atherogenesis. Nature Medicine, **8** (11), 1218-1226 (2002)

[49] Etingin, O.R., Silverstein, R.L., Hahar, D.P. Von williebrand factor mediates platelet adhesion to virally infected endothelial cells **90**, 5153- 5156 (1993)

[50] Wu, K.K and Thiagarajan, P. Role of endothelium in thrombosis and hemostasis. Annual Review of Medicine, **47**, 315-331 (1996)

[51] Campbell, J.H. and Campbell, J.H. The role of smooth muscle cells in atherosclerosis. Current Opinion in Lipidology, **5**, 323-330. (1994)

[52] Raines, E.W. and Ross, R. Smooth muscle cells and the pathogenesis of the lesions of atherosclerosis. British Heart Journal, (supplement 1): S30-S37 (1993)

[53] Davies, M.J. Coronary disease. The pathophysiology of acute coronary syndromes. Heart, **83**, 361-366 (2000)

[54] Gordon, S., Clarke, S., Greaves, D. and Doyle, A. Molecular immunobiology of macrophages: recent progress. Current Opinion in Immunology, **7**, 24-33 (1995)

[55] Camejo, G., Hurt-Camejo, E.Wiklund, O. and Bodjers, G. Association of apoB lipoproteins with arterial proteoglycans: Pathological significance and molecular basis. Atherosclerosis, **139**, 205-222 (1998)

[56] Murata, K., Motayama, T, Kotake C. Collagen types in various layers of the human aorta and their changes with the atherosclerotic process. Atherosclerosis, **60**, 251-262 (1986)

[57] Millonig, G., Schwentner, C., Mueller, P., Mayerl, C., Wick, G. The vascular-associated lymphoid tissue: a new site of local immunity. Current Opinion in Lipidology, **12** (5), 547-553 (2001).

[58] Yla-Herttuala, S., Lipton, B.A., Rosenfeld, M.E., Sarkioja, T., Yoshimura, T., Leonard, E.J., Witztum, J.L. and Steinberg D. Expression of monocyte chemoattractant protein-1 in macrophage-rich areas of human and rabbit atherosclerotic lesions. Proceedings of the National Academy of Science, **88**, 5252-5256 (1991)

[59] Clinton, S., Underwood, R., Sherman, M., Kefe, D., and Libby, P. Macrophage-colony stimulating factor gene expression in vascular cells and in experimental and human atherosclerosis. American Journal of Pathology, **140**, 291-300 (1992)

[60] Skalen, K., Gustafsson, M., Rydberg, E.K., Hulten L.M., Wiklund, O., Innerarity, T.L., Boren, J. Subendothelial retention of atherogenic lipoproteins in early atherosclerosis. Nature, **417**, 750-754 (2002)

[61] Quinn, M.T., Parthasarathy, S., Fong, L.G. and Steinberg, D. Oxidatively modified low density lipoproteins: a potential role in recruitment and retention of monocyte/macrophages during atherogenesis. Proceedings of the National Academy of Sciences, **84**, 2995- 2998 (1987)

[62] Dong, Z. M., Chapman, S.M., Brown, A.A., Frenette, P.S., Hynes. R.O., Wagner, D.D. The combined role of P- and E- selectins in atherosclerosis. Journal of Clinical Investigation, **102**, 145- 152 (1998)

[63] Iiyama, K., Hajra, L., Iiyama, M., Li. H., DiChiara, M., Medoff, B.D. and Cybulsky, M.I. Patterns of vascular cell adhesion molecule-1 and intracellular adhesion molecule -1 expression in rabbit and mouse atherosclerotic lesions and at sites predisposed to lesion formation. Circulation Research, **85**, 199-207 (1999)

[64] Cybulsky M.I., Iiyama, K., Li. H., Zhu. S., Chen, M., Iiyama. M., Davis, V., Gutierrez-Ramos, J.C., Connelly, P.W. and Milstone, D.S. A major role for VCAM-1, but not ICAM-1 in early atherosclerosis. Journal of Clinical Investigation, **107**, 1255-1262 (2001)

[65] Tabata, T., Mine, S., Kawahara, C., Okada, Y. and Tanaka, Y. Monocyte chemoattractant protein-1 induces scavenger receptor expression and monocyte differentiation into foam cells. Biochemical and Biophysical Research Communications, **305** (2), 380-385 (2003)

[66] Boring, L., Gosling, J., Cleary, M., and Charo, I.F. Decreased lesion formation in $CCR2^{-/-}$ mice reveals a role for chemokines in the initiation of atherosclerosis. Nature, **394**, 894-897 (1998)

[67] Nicholson, A.C., Han, J., Febbraio, M., Silverstein, R.L. and Hajjar, D.P. Role of CD36, the macrophage class B scavenger receptor, in atherosclerosis. Annals of the New York Academy of Sciences, **947**, 224-228 (2001)

[68] Itabe H. Oxidized low-density lipoproteins: what is understood and what remains to be clarified. Biological & Pharmaceutical Bulletin, **26** (1), 1-9 (2003)

[69] Marathe, S., Kuriakose, G., Wiiliams, K.J and Tabas, I. Sphingomylenase, an enzyme implicated in atherogenesis, is present in atherosclerotic lesions and binds to specific componenets of the subendothelial extracellular matrix. Arteriosclerosis, Thrombosis and Vascular Biology, **19**, 2648-2658 (1999)

[70] Ghosh, S, St Clair, R.W. and Rudel, L.L. Mobilization of cytoplasmic cholesteryl ester droplets by overexpression of human macrophage cholesterol ester hydrolase. Journal of Lipid Research. Papers in Press published ahead of print on July 1, 2003

[71] Kritharides, L., Christian, A., Stoudt, G., Morel, D. and Rothblat, G.H. Cholesterol metabolism and efflux in human THP-1 macrophages. Arteriosclerosis, Thrombosis and Vascular Biology, **18**, 1589-1599 (1998)

[72] Feng B. and Tabas I. ABCA1-mediated cholesterol efflux is defective in free cholesterol-loaded macrophages. Mechanism involves enhanced ABCA1 degradation in a process requiring full NPC1 activity. The Journal of Biological Chemistry, **277** (45), 43271-43280 (2002)

[73] Veniant, M.M., Withycombe, S., and Soung, S.G Lipoprotien size and atherosclerosis susceptibility in $Apoe^{-/-}$ and $ldlr^{-}$ mice. Arteriosclerosis, Thrombosis and Vascular Biology, **21**, 567-570 (2001)

[74] Brown, M.S., Ho, Y.K and Goldstein, J.L. The Cholesterol Ester Cycle in Macrophage Foam Cells. The Journal of Biological Chemistry, **255** (19), 9344-9352 (1980)

[75] Rudel L.L., Lee R.G. and Cockman, T.L. Acyl coenzyme A: cholesterol acyltransferase types 1 and 2: structure and function in atherosclerosis. Current Opinion in Lipidology, **12** (2):121-127 (2001)

[76] Miyazaki, A., Sakashita, N., Lee, O., Takahashi, K., Horiuchi, S., Hakamata, H., Morganelli, P.M., Chang, C.C.Y. and Chang, T. Expression of ACAT-1 protein in human atherosclerotic lesions and cultured human monocyte-macrophages. Arteriosclerosis, Thrombosis and Vascular Biology **18**, 1568-1574 (1998)

[77] Heinonen, T.M. Acyl coenzyme A:cholesterol acyltransferase inhibition: potential atherosclerosis therapy or springboard for other discoveries? Expert Opinion on Investigational Drugs, **11**(11), 1519-1527 (2002)

[78] Khoo, J.C, Reue, K., Steinberg, D. and Schotz, M.C. Expression of hormone-sensitive lipase mRNA in macrophages .Journal of Lipid Research, **34**, 1963-1973 (1993)

[79] Okazaki, H., Osuga, J., Tsukamoto, K., Isoo, N., Kitamine, T., Tamura, Y., Tomita, S., Sekiya, M., Yahagi, N., Iizuka, Y., Ohashi, K., Harada, K., Gotoda, T., Shimano, H., Kimura, S., Nagai, R., Yamada, N. and Ishibashi, S. Elimination of cholesterol ester from macrophage foam cells by adenovirus-mediated gene transfer of hormone-sensitive lipase. The Journal of Biological Chemistry, **277** (35), 31893-31899 (2002)

[80] Small, C.A, Goodacre, J.A and Yeaman, S.J. Hormone-sensitive lipase is responsible for the neutral cholesterol ester hydrolase activity in macrophages. FEBS letter, **247**, 205-208 (1989)

[81] Harte, R.A., Hultén, L.M., Lindmark, H. Reue, K., Schotz, M.C., Khoo, J. and Rosenfield, M.E. Low level of expression of hormone sensitive lipase in arterial macrophage-derived foam cells: potential explanation for low rates of cholesteryl ester hydrolysis. Atherosclerosis, **149**, 343-350 (2000)

[82] Merkel, M., Eckel, R.H. and Goldberg, I.J. Lipoprotein lipase: genetics, lipid uptake, and regulation. Journal of Lipid Research, **43** (12), 1997-2006 (2002)

[83] Mead, J.R. and Ramji, D.P. The pivitol role of lipoprotein lipase in atherosclerosis in atherosclerosis. Cardiovcascular Research, **55**, 261-269 (2002)

[84] Wilson, K., Fry, G.L, Chappell, D.A., Sigmund, C.D. and Medh, J.D. Macrophage-specific expression of human lipoprotein lipase accelerates atherosclerosis in transgenic apolipoprotein E knockout mice but not C57BL/l mice. Arteriosclerosis, Thrombosis and Vascular Biology, **21**, 1809-1815 (2001)

[85] Landmesser, U. and Harrison, D.G. Oxidant Stress as a marker for cardiovascular events-Ox marks the spot. Circulation, **104**, 2638-2640 (2001)

[86] Kavanagh, I.C., Symes, C.E., Renaudin, P., Nova, E., Mesa, M.D., Boukouvalas, G., Leake, D.S., and Yaqoob, P. Degree of oxidation of low density lipoprotein affects expression of CD36 and PPAR gamma, but not cytokine production, by human monocyte-macrophages. Atherosclerosis, **168** (2), 271-282 (2003)

[87] Gaut, J.P. and Heinceke, J.W. Mechansims for oxidising low-density lipoprotein. Insights from patterns of oxidation products in the artery wall and from mouse models of atherosclerosis. Trends in Cardiovascular Medicine **11**, 103-112 (2001)

[88] Chisolm, G.M and Steinberg, D. The oxidative modification hypothesis of atherogenesis:an overview. Free Radical Biology and Medicine, **104**, 1815-1826 (2000)

[89] Toshima, S., Hasegawa. A., Kurabayashi, M., Itabe, H. Takano, T., Sugano, J, , K, Kimura, J., Michishita. I., Suzuki, T. and Ryozo, N. Circulating Oxidized Low Density Lipoprotein Levels. A Biochemical Risk Marker for Coronary Heart Disease. Arteriosclerosis, Thrombosis and Vascular Biology, **20**, 2243-2247 (2000)

[90] Fuhrman, B., Volkova, N. and Aviram, M. Oxidative stress increases the expression of the CD36 scavenger receptor and thecellular uptake of oxidized low-density lipoprotein in macrophages from atherosclerotic mice: protective role of antioxidants and of paraoxonase. Atherosclerosis, **161**(2), 307-316 (2002)

[91] Wagner, P. and Heinecke, J.W. Copper ions promote peroxidation of low density lipoprotein lipid by binding to histidine residues of apolipoprotein B100, but they are reduced at other sites on LDL. Arteriosclerosis, Thrombosis and Vascular Biology, **17**, 3338- 3346 (1997)

[92] Parathasathy, S. and Steinberg, D. Cell-induced oxidation of LDL. Current Opinion in Lipidology, **3**, 313-317 (1992)

[93] Gordon, S. The role of the macrophage in immune regulation. Research in Immunology, **149**, 685-688 (1998)

[94] Hiramatsu, K, Rosen, H., Heinecke, J.W. Wolfbauer, G., Chait, A. Superoxide initiates oxidation of low density lipoprotein by human monocyte. Arteriosclerosis, **7** (1), 55-60 (1987)

[95] Daugherty, A. Dunn, J.L, Rateri, D.L. and Hienecke, J.W. Myeloperoxidase, a catalyst for lipoprotein oxidation, is expressed in human atherosclerotic lesions. Journal of Clinical Investigation, **107**, 419-430 (2001)

[96] Yamamoto, S. Mammalian lipoxygenases; molecular structures and functions. Biochimica et Biophysica Acta, **1128**, 117-131 (1992)

[97] Mehrabian, M., Allayee, H., Wong, J., Shi, W., Wang, X.P., Shaposhnik, Z., Funk, C.D., Lusis, A.J. and Shih, W. Identification of 5-lipoxygenase as a major gene contributing to atherosclerosis susceptibility in mice. Circulation Research, **91**, 120-126 (2002)

[98] Ylä-Herttuala, S. Rosenfeld, M.E., Parthasarathy, S., Glass, CK, Sigal, E. Witztum, J.L. and Steinberg, D. Colocalisatoin of 15-lipoxygenase mRNA and

protein with epitopes of OxLDL in macrophage-rich areas of atherosclerotic lesions. Proceedings of the National Academy of Sciences, **87**, 6959-6963 (1990)

[99] Cyrus, T., Witztum, J.L., Rader, D.J., Tangirala, R., Fazio, S., Linton, M.F. and Funk, C.D. Disruption of the 12/15 lipoxygenase gene diminishes atherosclerosis in apo E deficient mice. Journal of Clinical investigation, **103**, 1597-1604 (1999)

[100] Carr, A.C., McCall, M.R and Frei, B. Oxidation of LDL by Myeloperoxidase and Reactive Nitrogen Species. Reaction Pathways and Antioxidant Protection. Arteriosclerosis, Thrombosis and Vascular Biology, **20**, 1716-1723 (2000)

[101] Hazen, S.L. and Heinecke, J.W 3-Chlorotyrosine, a specific marker of myeloperoxidase-catalyzed oxidation, is markedly elevated in low density lipoprotein isolated form human atherosclerotic intima. Journal of Clinical Investigation, **99**, 2075-2081 (1997)

[102] Moncada, S. Palmer, R.M. and Higgs, E.A. Nitric Oxide; Physiology, pathophysiology and pharmacology. Pharmacological Reviews, **43** (2), 109-142 (1991)

[103] Heinecke, J.W. Oxidants and antioxidants in the pathogenesis of atherosclerosis: implications for the oxidized low density lipoprotein hypothesis. Atherosclerosis, **141**, 1-15 (1998)

[104] Yates, M. T., Lambert, L.E., Whitten, J.P., MacDonald, I., Mano, M., Ku, G. and Mao, S.J.T. A protective role for nitric oxide in the oxidative modification of low density lipoprotein by mouse macrophages. FEBS letter, **309**, 135-138 (1992)

[105] Shi, W., Wang, X., Shih, D.M., Laubach, V.E., Navab. M., and Lusis, A.J. Paradoxical reduction in fatty streak formation in mice lacking the endothelial nitric oxide synthase. Circulation, **105**, 2078-2082 (2002)

[106] Colles, S.M., Maxson, J.M.Carlson, S.G. and Chisolm, G.M. Oxidized LDL induced injury and apoptosis in atherosclerosis. Potential role for oxysterols. Trends in Cardiovascular Medicine, **11,** 112-116 (2001)

[107] Jha, P., Flather, M., Lonn, E., Farkouh, M. and Yusuf, S. The antioxidant vitamins and cardiovascular disease. A critical review of epidemiological and clinical trial data. Annual of Internal Medicine, **10**; 1189-1192 (1995)

[108] Thomas, S.R., Leichtweis, S.B., Pettersson, K., Croft, K.D., Mori, T.A., Brown, A.J. and Stocker, R. Dietary cosupplementation with vitamin E and coenzyme Q10 inhibits atherosclerosis in apolipoprotein E knockout mice. Arteriosclerosis, Thrombosis and Vascular Biology, **21**, 585- 593 (2001)

[109] Steinberg, D and Witztum, J.L. Is the oxidative modification hypothesis relevant to human atherosclerosis? Do antioxidant trials conducted to date refute the hypothesis? Circulation, **105**, 2107-2111 (2002)

[110] Vivekananthan, D.P., Penn, S. Sapp, S.K. Hsu, A. and Topol E.J. Use of antioxidant vitamins for the prevention of cardiovascular disease: meta-analysis of randomised trials. The Lancet, **361**, 2017- 2023 (2003)

[111] Li, W., Yuan, M., Olsson, A.G., and Brunk, U.T. Uptake of Oxidised LDL by macrophages results in partial lysosomal enzyme inactivation and relocation. Arteriosclerosis, Thrombosis and Vascular Biology, **18**, 177-184 (2000)

[112] Hakala, J.K., Oksjoki, R., Laine, P., Du, H., Grabowski, G.A., Kovanen, P.T. and Pentikainen, M.O. Lysosomal enzymes are released from cultured human macrophages, hydrolyze LDL *in vitro*, and are present extracellularly in human atherosclerotic lesions. Arteriosclerosis, Thrombosis, and Vascular Biology, **23**(8):1430-1436 (2003)

[113] Steinberg, D. Atherogenesis in perspective: hypercholesterolemia and inflammation as partners in crime. Nature Medicine, **8** (11), 1211-1217 (2002)

[114] Hansson, G.K. Immune mechanisms in atherosclerosis. Arteriosclerosis, Thrombosis and Vascular Biology, **21**, 1876-1890 (2001)

[115] Nathan, C.F. Secretory Products of Macrophages. Journal of Clinical Investigation **79**, 319-326 (1987)

[116] Saren, P., Welgus, H.G and Kovanen, P.T. TNF-α and IL-1β selectively induce expression of 92-kDa gelatinase by human macrophages. Journal of Immunolgy, **157**, 4159-4165 (1996)

[117] Nakagawa, T. Nozaki, S., Nishida, M., Yakub, J, Tomiyama, Nakata, A. Matsumoto, K., Funahashi, T., Kameda-Takemura, K., Kurata, Y., Yamashita, S. and Matsuzawa, Y. Oxidized LDL Increases and Interferon-γ decreases expression of CD36 in Human Monocyte-Derived Macrophages. Arteriosclerosis, Thrombosis and Vascular Biology, **18**, 1350-1357(1998)

[118] Wang, N., Winchester, R., Ravalli, S., Rabbani, L.E., Tall, A. Interleukin 8 is Induced by Cholesterol Loading of Macrophages and Expressed by Macrophage Foam Cells in Human Atheroma. The Journal of Biological Chemistry, **271** (15), 8837-8842 (1996)

[119] Gerszten, R.E., Garcia-Zepeda, E.A., Lim, Y., Yoshida, M., Ding, H.A., Gimbrone Jr, M.A,. Luster, A.D., Luscinskas, F.W. and Rosenzweig, A. MCP-1 and IL-1 trigger firm adhesion of monocytes to vascular endothelium under flow conditions. Nature, **398**, 718-723 (1999)

[120] Qiao, J.H. Role of macrophage colony-stimulating factor in atherosclerosis: studies of osteropetrotic mice. American Journal of Pathology, **150**, 1687-1699 (1997)

[121] Mazière, C., Alimardani, G., Dantin, F., Dubois, F., Conte, M. and Mazière, J. Oxidized LDL activates STAT1 and STAT3 transcription factors: possible involvement of reactive oxygen species. FEBS letters, **448**, 49-52 (1999)

[122] Schönbeck, U., Sukhova, G.K., Shimizu, K., Mach, F., Libby, P. Inhibition of CD40 signalling limits evolution of established atherosclerosis in mice. Proceedings of the National Academy of Science, **97**, 7458-7463 (2000)

[123] Daynes, R.A and Jones, D.C. Emerging roles of PPARs in inflammation and immunity. Nature Reviews Immunology, **2**, 748-759 (2002)

[124] Chinetti, G., Lestavel, S., Bocher, PPAR-α and PPAR-γ activators induce cholesterol removal from human macrophage foam cells through stimulation of the ABCA1 pathway. Nature Medicine, 7 (1), 53-58 (2001)

[125] Moore, K.J Rosen, E.D, Fitzgerald, M.L., Randow, F. Andersson, L.P., Altshuler, D., Milstone, D.S., Mortensen, R.M., Spiegelman, B.M., Freeman, M.W. The role of PPAR-γ in macrophage differentiation and cholesterol uptake. Nature Medicine, **7** (1), 41-47 (2001)

[126] Rust, S., Rosier, M., Funke, H., Real, J., Amoura, Z., Piette, J.C., Deleuze, J.F., Brewer, H.B., Duverger, N., Denefle, P. and Assmann G. Tangier Disease is caused by mutations in the gene encoding ATP-binding cassette transporter 1. Nature Genetics, **22**, 352-355 (1999)

[127] Tangirala, R.K., Bischoff, E.D., Joseph, S.B., Wagner, B.L., Walczak, R., Laffitte, B.A., Daige, C.L., Thomas, D., Heyman, R.A., Mangelsdorf, D.J., Wang,

X., Lusis, A.J., Tontonoz, P. and Schulman I.G. Identification of liver X receptors as inhibitors of atherosclerosis. Proceedings of the National Academy of Science, **99**, 11896-11901 (2002)

[128] Repa, J.J and Mangelsdorf, D.J. The liver X receptor gene team: Potential new players in atherosclerosis. Nature Medicine, **11** (8), 1243-1248 (2002)

[129] Joseph, S.B. Castrillo, A., Laffitte, B.A., Mangelsdorf, D.J and Tontonoz, P. Reciprocal regulation of inflammation and lipid metabolism by liver X receptors. Nature Medicine, **9** (2), 213-219. (2003)

[130] Davies, M.J., Richardson, P.D., Woolf, N. Katz, D.R. and Mann, J. Risk of thrombosis in human atherosclerotic plaques: Role of extracellular lipid, macrophage, and smooth muscle content. British Heart Journal, **69**, 377-381 (1993)

[131] Davies, M.J. The pathophysiology of acute coronary syndromes. Heart, **83** (3), 361-366 (2000)

[132] Davies, M.J. Stability and Instability: The two faces of coronary atherosclerosis. The Paul Dudley White Lecture. Circulation, **94**, 2013-2020 (1996)

[133] Galis, Z. Sukhova, G. Lark, M and Libby, P. Increased expression of matrix metalloproteinases and matrix degrading activity in vulnerable regions of human atherosclerotic plaques. Journal of Clinical Investigation, **94**, 2493-2503 (1994)

[134] Wilcox, J.N., Smith, K.M., Schwartz, S.M. and Gordon, D. Localisation of tissue factor in normal vessel wall and in the atherosclerotic plaque. Proceedings of the National Academy of Science, **86**, 2839-2843 (1989)

[135] Kockx, M.M and Knaapen, M.W.M. The role of apoptosis in vascular disease. Journal of Pathology, **190**, 267-280 (2000)

[136] Maron, D.J., Fazio, S. and Linton, M.F. Current perspectives on statins. Circulation, **101**, 207-213 (2000)

[137] Crisby, M., Nordin-Fredriksson, G., Shah, P.K., Yano, J., Zhu, J. and Nilsson, J. Pravastatin treatment increases collagen content and decreases lipid content, inflammation, metalloproteinases, and cell death in human carotid plaques; implications for plaque stabilisation. Circulation, **103**, 926-933 (2001)

[138] Somerville, R.P.T., Oblander, S.A., Apte, S.S. Matrix metalloproteinases: old dogs with new tricks. Genome Biology, **4** (6), 216-231 (2003)

[139] Shapiro, S.D. Matrix metalloproteinase degradation of extra-cellular matrix: biological consequences. Current Opinion in Cell Biology, **10**, 602-608 (1998)

[140] Role of nuclear factor-κB activation in metalloproteinase-1, -3, and -9 secretion by human macrophages in vitro and rabbit foam cells produced *in vivo*. Arteriosclerosis, Thrombosis and Vascular Biology, **22**, 765-771 (2002)

[141] Lee, W., Kim, S., Lee, B.B., Kwon, B., Song, H., Kwon , B.S. and Park, J. Tumor Necrosis Factor Receptor Superfamily 14 is involved in atherogensis by inducing proinflammatory cytokines and matrix metalloproteinases. Arteriosclerosis, Thrombosis and Vascular Biology, **21**, 2004-2010 (2001)

[142] George, S.J. Tissue inhibitors of metalloproteinases and metalloproteinases in atherosclerosis. Current Opinion in Lipidology, **98**; 413-423 (1998)

[143] Bond, M. Chase, A.J., Baker, A.H., Newby, A.C. Inhibition of transcription NF-kappa B reduces matrix metalloproteinase 1, -3 ad -9 production by vascular smooth muscle cells. Cardiovascular Research, **50**, 556-565 (2001)

[144] Shah, P.K. Role of inflammation and metalloproteinases in plaque disruption and thrombosis. Vascular Medicine, **3** (3), 199-206 (1998)

[145] Nikkari, S.T., O'Brien, K.D., Ferguson, M., Hatsukami, T., Welgus, H.G., Alpers, C.E. and Clowes, A.W.. Interstitial collagenase (MMP-1) expression in human carotid atherosclerosis. Circulation, **92**(6), 1393-1398 (1995)

[146] Newby, A.C. and Zaltsman, A.B. Fibrous cap formation or destruction - the critical importance of vascular smooth muscle cell proliferation, migration and matrix formation. Cardiovascular Research, **41**(2), 345- 360 (1999)

[147] Pasterkamp, G. *et al.* Atherosclerotic arterial remodelling and the localisation of macrophages and matrix metalloproteinases 1, 2 and 9 in the human coronary artery. Atherosclerosis, **150**, 245- 253 (2000)

[148] Rajavashisth, T.B., Xu, X., Jovinge, S., Miesel, S., Xu, X., Chai, N, Fishbein, M.C., Kaul, S. Cercek, B., Sharifi, B. and Shah, P.K. Membrane type 1 matrix metalloproteinase expression in human atherosclerotic plaques. Evidence for activation by proinflammatory mediators. Circulation, **99**, 3103-3109 (1999)

[149] Loftus, I.M., Naylor, A.R. Goodall, S. Crowther, M., Jones, L. Bell, P.R. Thompson, M.M. Increased matrix metalloproteinase-9 activity in unstable ceratoid plaques: a potential role in acute plaque disruption. Stroke, **31**, 40- 47 (2000)

[150] Moreau, M., Brocheriou, I., Petit, L. Ninio, E., Chapman, M.J. and Rouis, M. Interleukin-8 mediates downregulation of tissue inhibitor expression of

metalloproteinase-1 expression in cholesterol-loaded human macrophages. Relevance to stability of atherosclerotic plaques. Circulation, **99**, 420-426 (1999)

[151] Fabunmi, R.P., Sukhova, G.K., Sugiyama, S., Libby, P. Expression of tissue inhibitor of metalloproteinase-3 in human atheroma and regulation in lesion-associated cells. A potential protective mechanism in plaque stability. Circulation Research, **83**, 270-278 (1998)

[152] Galis, Z.S., Asanuma, K., Godin, D. Meng, X. N-acetyl-cysteine decreases the matrix-degrading capacity of macrophage foam cells. New target for antioxidant therapy. Circulation, **97**, 2445-2453 (1998)

[153] Packard, C.J., O'Reilly, D.S.J., Caslake, M.J., Mcmahon, A.D., Ford, I., Cooney, J., Macphee, C.H., Suckling, K.E., Krishna, M., Wilkinson, F.E., Rumley, A. and Lowe, G.D.O. Lipoprotein-associated phospholipase A2 as an independent predictor of coronary artery disease. The New England Journal of Medicine, **343**, 1148-1155 (2002)

[154] Ridker, P.M., Rifai, N., Clearfield, M., Downs. J.R., Weis, S.E., Miles, J.S. and Gotto, A.M. Jr. Measurement of C-reactive protein for the targeting of statin therapy in the primary prevention of acute coronary events. New England Journal of Medicine, **344**, 1959-1965 (2001)

[155] Caslake, M.J., Packard, C.J., Suckling, K.E., Holmes, S.D., Chamberlain, P. and Macphee, C.H. Lipoprotein-associated phospholipase A2, platelet-activating acetylhydrolase: a potential new risk factor for coronary artery disease. Atherosclerosis, **150**, 413-419 (2000)

[156] Tew, D.G. Southan, C., Rice, S.Q., Lawrence, M.P., Li. H., Boyd, H.F., Moores, K., Gloger, I.S. and Macphee, C.H. Purification, properties, seqeuencing and cloning of a lipoprotein-associated phospholipase A2, involved in the oxidative

modification of low-density lipoproteins. Arteriosclerosis, Thrombosis and Vascular Biology, **16**, 591-599 (1996)

[157] Laffitte, B.A., Repa, J.J., Joseph, S.B., Wilpitz, D.C., Kast, H.R., Mangelsdorf, D.J., Tontonoz, P. LXRs control lipid-inducible expression of the apolipoprotein E gene in macrophages and adipocytes. Proceedings of the National Academy of Science, **98**, 507-512 (2001)

[158] Henriksen, P.A. and Kotelevtsev, Y. Application of gene expression profiling to cardiovascular disease. Cardiovascular Research, **54**, 16-24 (2002)

[159] Auwerex, J. The human leukaemia cell line, THP-1: a multifaceted model for the study of monoycte-macrophage differentiation. Experientia, **47**, 22-31 (1991)

[160] Via, D.P., Pons, D.K., Dennison, D.K., Fanslow, A.E., Bernini, F. Induction of acetyl-LDL receptor activity by phorbol ester in human monocyte cell line THP-1. Journal of Lipid Research, **30**, 1515-1524 (1989)

[161] Stanton, L.W. Methods to profile gene expression. Trends in cardiovascular medicine, **11**, 49-54 (2001)

[162] Duggan, D.J., Bittner, M., Chen, Y., Meltzer, P, Trent, J.M. Expression profiling using cDNA microarrays. Nature Genetics. **21**(suppl 1), 10-14 (1999)

[163] Hassall, D.G. Three probe flow cytometry of a human foam-cell forming macrophage. Cytometry, **13**, 381-388 (1992)

[164] Via, D.P., Plant, A.L., Craig, I.F., Gotto, A.M. and Smith, L.C. Metabolism of normal and modified low-density lipoproteins by macrophage cell lines of murine and human origin. Biochim. Biophys. Acta, **833**, 417-428 (1985)

[165] Greenspan, P., Mayer, E.P. and Fowler, S.D. Nile red: a selective fluorescent stain for intracellular lipid droplets. Journal of Cell Biology, **100**, 965-973 (1985)

[166] Brown, M.S., Goldstein, J.L., Krieger, M., Ho, Y.K., and Anderson, R.G.W. Journal of Cell Biology, **82**, 597-613 (1979)

[167] Chung, B.H., Wilkinson, T., Geer, J.C. and Segrest, J.P. Preparative and quantitative isolation of plasma lipoproteins: rapid, single discontinuous density gradient ultracentrifigation in a vertical rotor. Journal of Lipid Research, **21** (3), 284-291 (1980)

[168] Chung, B.H., Segrest, J.P., Ray, M.J., Brunzell, J.D., Hokanson, J.E., Krauss, R.M., Beaudrie, K. and Cone J.T. Single vertical spin density gradient ultra centrifugation. Methods in Enzymology, **128,** 118-209 (1986)

[169] Lide, D.R. *In* CRC Handbook of Chemistry and Physics (75th Edition). CRC press, UK (1990)

[170] Bradford, M.M. A rapid and sensitive method for the quantitation of microgram quantities of protein utilising the principle of protein-dye binding. Analytical Biochemistry, **72**: 248-254 (1976)

[171] Steinbrecher U.P., Lougheed, M., Kwan, W.C. and Dirks, M. Recognition of oxidized low density lipoprotein by the scavenger receptor of macrophages results from derivatization of apolipoprotein B by products of fatty acid peroxidation. The Journal of Biological Chemistry **264 (26)**, 15216-15223 (1989)

[172] Basu, S.K., Goldstein, J.L, Anderson, R.G.W. and Brown, M.S. Degradation of cationised low density lipoprotein and regulation of cholesterol metabolism in

homozygous familial hypercholesterolemia. Proceedings of the New York Academy of Sciences, **73**, 3178-2183 (1976).

[173] Kunkel, L.M., Smith, K.D., Boyer, S.H, Borgaonkar, D.S., Wachtel, S.S., Miller, O.J., Breg, W.R., Jones, H.W. and Rary, J.M. Analysis of human Y-chromosome specific reiterated DNA in chromosome variants. Proceedings of the New York Academy of Sciences, **74**, 1245-1249 (1977)

[174] Chomczynski, P. and Sacchi, N. Single-step method of RNA isolation by acid thiocyanate-phenol-choloroform extraction. Analytical Biochemistry, **162** (1), 156-159 (1987)

[175] Wang A.M., Doyle, M.V. and Mark, D.F. Quantitation of mRNA by the polymerase chain reaction. Proceedings of the New York Academy of Sciences, **86** (24), 9717-9721 (1990)

[176] Innis, M.A., Gelfand, D.H., Sninsky, J.J. and White T.J. *In* PCR Protocols, Academic press. UK (1990)

[177] Förster, E. An improved general method to generate internal standards for competitive PCR. Biotechniques, 16 (1), 18-20 (1994)

[178] Fumeron, F., Betoulle, D, Luc, G., Behague, I., Richard, S., Poirier, O., Jemaa, R., Evans, A., Arveiler, D., Marques-Vidal, P. Alcohol intake modulates the effect of a polymorphism of the cholesteryl ester transfer protein gene on plasma high density lipoprotein and the risk of myocardial infarction. Journal of Clinical Investigation, **96**, 1664-1671 (1995).

[179] Sambrook, J., Fritsch, E. F. and Maniatis, T. Molecular Cloning: A Laboratory Manual. Cold Spring Harbour Laboratory Harbour Press, New York (1989)

[180] Steinberg, D., Parthasarathy, S., Carew, T. E., Khoo, J. C. & Witztum, J. L. Beyond cholesterol: modifications of low-density lipoprotein that increases its atherogenicity. The New England Journal of Medicine, **320**, 915-923 (1989).

[181] Tabas, I. The stimulation of the cholerterol eserification pathway by atherogenic lipoproteins in macrophages. Current Opinion in Lipidology, **6**, 260-268 (1995).

[182] Wada, Y., Sugiyama, A, Kohro, T., Kobayashi, M., Takeya, M. Naito, M. and Kodama, T. *In vitro* model of atherosclerosis using coculture of arterial wall cells and macrophages. Yonsei Medical Journal, **41**, (6), 740-755 (2000)

[183] Hussain, M. M., Glick, J. M. & Rothblat, G. H. *In vitro* model systems: cell cultures used in lipid and lipoprotein research. Current Opinion in Lipidology, **3**, 173-178 (1992)

[184] Tsuchiya, S. Yamabe, M., Yamaguchi, Y., Kobayashi, Y., Konno, T and Tada, K. Establishment and characterisation of a human acute monocytic leukaemia cell line (THP-1). International Journal of Cancer, **26** (2), 171-176 (1980)

[185] Banka, C.L., Black, A.S., Dyer, C.A. and Curtiss, L.K. THP-1 cells form foam cells in response to coculture with lipoproteins but not platelets. Journal of Lipid Research, **32**, 35-43 (1991)

[186] Kawai, Y., Saito, A. Shibata, N., Kobayashi, M., Yamada, S., Osawa, T., Uchida, K. Covalent binding of oxidized cholesteryl esters to protein: implications for oxidative modification of low density lipoprotein and atherosclerosis. The Journal of Biological Chemistry, **278** (23), 21040-21049 (2003)

[187] Haberland, M.E. Olch, C.L., Fogelman, A.M. Role of lysines in mediating interaction of modified low-density lipoproteins with the scavenger receptor of

human monocyte macrophages. The Journal of Biological Chemistry, **259** (18), 11305-11311 (1984)

[188] Auwerex, J.H., Chait, A., and Deeb, S.S. Regulation of the low density lipoprotein receptor and hydroxymethylglutaryl coenzyme A reductase genes by protein kinase C and a putative negative regulatory protein. Proceedings of the National Academy of Science, **86,** 1133-1137 (1989)

[189] Hara, H. Tanishita, S., Yokoyoma, S., Tajima, S. and Yamamoto, A. Induction of acetylated low density lipoprotein receptor and suppression of low density lipoprotein receptor. Biochemical and Biophysical Research Communications, **126**, 526-531 (1985)

[190] Tajima, S., Hayashi, R., Tsuchiya,S. Miyake, Y., and Yamamoto, A. Cells of a human monocytic leukaemia cell line (THP-1) synthesize and secrete apolipoprotein E and lipoprotein lipase. Biochemical and Biophysical Research Communications, **26**(1), 526-531 (1985).

[191] Waggoner, A and Seadler, A. Multiparameter fluorescence imaging microscopy: reagents and instruments. Human Pathology, **27**(5), 494-502 (1996)

[192] Clare, K., Hardwick, S.J., Carpenter, K.L.H., Weeratunge, N., Mitchinson, M.J. Toxicity of oxysterols to human monocyte macropahges. Atherosclerosis, **118**, 67-75 (1995)

[193] Mosmann, T. Rapid colorimetric assay for cellular growth and survival: application to proliferation and cytotoxicity assays. Journal of Immunological Methods, **65**, 55-63 (1983)

[194] Rodriguez,A., Kafonek, S.D., Georgopoulos, A. and Bachorik, P.S. Cell density can affect cholesteryl ester accumulation in the human THP-1 macrophage. Journal of Lipid Research, **35**, 1909-1917 (1994)

[195] Chisolm, G.M. Cytotoxicity of oxidized lipoproteins. Current Opinion in Lipodology, **2**, 311- 316 (1991)

[196] McManus, M.T., and Sharp, P.A. Gene Silencing in mammals by small interfering RNAs. Nature Review Genetics, **3**, 737-747 (2002).

[197] Lockhart, D.J. and Winzeler, E.A. Genomics, gene expression and DNA arrays. Nature, **405**, 827-836 (2000)

[198] Yamamot, M., Wakatsuki, T., Hada, A., Ryo, A. Use of serial analysis of gene expression (SAGE) technology. Journal of Immunological methods, **350**, 45-66 (2001)

[199] Lander, E.S. Linton, L.M., Birren, B., Nusbaum. C., Zody. M.C., Baldwin, J., Devon, K., Dewar, K. *et al.* Initial sequencing and analysis of the human genome. Nature, **409**, 860-921 (2001)

[200] Southern, E.M., Maskos, U., Elder, J.K. Analyzing and comparing nucleic acid sequences by hybridization to arrays of oligonucleotides: evaluation using experimental models. Genomics, **13**(4), 1008-1017 (1992)

[201] Lennon, G.G and Lehrach, H. Hybridisation analyses of arrayed cDNA libraries. Trends in Genetics, **7**, 314-317 (1991)

[202] Drmanac, R., Drmanac, S., Labat, I., Crkvenjakov, R., Vicentic, A. and Gemmell, A. Sequencing by hybridization: towards an automated sequencing of one million M13 clones arrayed on membranes. Electrophoresis, **13** (8), 566-573 (1992)

[203] Fodor, S.P., Read, J.L., Pirrung, M.C., Stryer, L., Lu, A.T., Solas, D. Light-directed, spatially addressable parallel chemical synthesis. Science, **251**, 767-773 (1991)

[204] Lipshutz, R.L., Fodor, S.P.A., Gingeras, T.R. and Lockhart, D.J. High density synthetic oligonucleotide arrays. Nutre Genetics Supplement. **21**, 20-24 (1999)

[205] Hughes, T.R. Mao, M., Jones, A.R., Burchard, J., Marton, M.J. Shannon, K.W., Lefkowitz, S.M., Ziman, M. *et al.* Expression profiling using microarrays fabricated by an ink-jet oligonucleotide synthesizer. Nature Biotechnology, **19**; 342-347 (2001)

[206] Rubenstein, K. Commerical Aspects of Microarray Technology. Biotechniques **34**, S52-S54 (2003)

[207] Lennon, G., Auffray, C., Polymeropoulos, M and Soares, M.B. The I.M.A.G.E Consortium: An Integrated Molecular Analysis of Genomes and Their Expression. Genomics, **33**, 151-152 (1996)

[208] Eisen, M.B. and Brown, P.O. DNA arrays for analysis of gene expression. Methods in Enzymology, **303**, 179-205 (2001)

[209] Cox, J.M. Applications of nylon membrane arrays to gene expression analysis. Journal of Immunological Methods, **250**, 3-13 (2001)

[210] The Chipping Forecast, Supplement to Nature Genetics, **21**, 1-60 (1999)

[211] The Chipping Forecast II, Supplement to Nature Genetics, **32**, 461-552 (2002)

[212] Gershon, D. Microarray technology: an array of opportunities. Nature, **416**, 885-891 (2002)

[213] Dong, S., Wang, E, Hsie, L., Cao, Y., Chen. X. and Gingeras, T.R. Flexible use of high-density oligonucleotide arrays for single-nucleotide polymorphism discovery and validation. Genome Research, **11**, 1418 -1424 (2001)

[214] Warrington, J.A., Shah, N.A.,Chen,X., Janis,M., Liu, C., Kondapalli, S., Reyes, V., Savage,M.P., Zhang, Z., Watts, R., DeGuzman, M., Berno, A., Snyder, J. and Baid, J. New Developments in high-throughput resequencing and variation detection using high density microarrays. Human Mutation, **19**, 402-409 (2002)

[215] Williams, N.S., Gaynor, R.B., Scoggin, S. Verma, U., Gokaslan, T., Simmang, C., Fleming, J., Tavana, D., Frenkel, E. and Becerra, C. Identification and validation of genes involved in the pathogensis of colorectal cancer using cDNA microarrays and RNA interference. Clinical Cancer Research, **9**, 931-946 (2003)

[216] Schuler GD. Pieces of the puzzle: expressed sequence tags and the catalog of human genes. Journal of Molecular Medicine, **75**, 694-698 (1997).

[217] Southern, E. Mir, K and Shchepinov, M. Molecular interactions on microarrays. Nature Genetics Supplement, **21**, 5-9 (1999)

[218] Cheung, V.G., Morley, M., Aguilar, F., Massimi, A., Kucherlapati, R. and Childs, G. Making and reading microarrays. Nature Genetics Supplement, **21**, 15-19 (1999)

[219] Li, X., Gu, W., Mohan, S. and Baylink, D.J. DNA Microarrays: Their Use and Misuse. Microcirculation, **9**, 13-22 (2002)

[220] Murphy, D. Gene Expression Studies Using Microarrays: Principles, Problems, and Prospects. Advances in Physiology Education, **26** (4) 256- 270 (2002)

[221] Eberwine, J., Kacharmina, J.E., Andrews,C. Miyashiro, K., McIntosh, T., Becker, K., Barrett, T., Kinklem D., Dent, G., and Marciano, P. mRNA expression analysis of tissue sections and single cells. Journal of Neuroscience, **2**: 8310-8314 (2001)

[222] Bertucci, F., Bernard, K., Loriod, B.,Chang, Y., Granjeaud, S., Birnbaum, D., Nguyen, C., Peck, K., and Jordan, B.R. Sensitivity issues in DNA array-based expression measurements and performance of nylon microarrays for small samples. Human Molecular Genetics, **8** (9), 1715-1722 (1999)

[223] Affymetrix Technical Note 'GeneChip® Eukaryotic Small Sample Target Labeling Assay Version II'. Available at http://www.affymetrix.com/support/technical/technotes/smallv2_technote.pdf

[224] Rebhan, M and Prilusky, J. Rapid access to biomedical knowledge with GeneCards and HotMolecBase: Implications for the electrophoretic analysis of large sets of gene products. Electrophoresis, 18, 2774-2780 (1997). Available at http://nciarray.nci.nih.gov/cards

[225] Subbanagounder, G., Wong, J.W., Lee, H., Faull, K.F., Miller, E., Witztum, J.L and Berliner, J.A. Epoxyisoprostane and epoxycyclopentenone phospholipids regulate monocyte chemotactic protein-1 and interleukin-8 synthesis. Formation of these oxidized phospholipids in response to interleukin-1β. The Journal of Biological Chemistry, **277**, 7271-7281 (2002)

[226] Bottalico, L.A., Kendrick, N.C., Keller, A., Li, Y., and Tabas, I. Cholesteryl ester loading of mouse peritoneal macrophages is associated with changes in the expression or modification of specific cellular proteins, including an increase in an α-Enolase Isoform. Arteriosclerosis and Thrombosis, **12**, 263-275 (1993)

[227] Shi, M.M., Godleski, J.J., Paulauskis, J.D. Molecular cloning and post-transcriptional regulation of macrophage inflammatory protein-1 alpha in alveolar macrophages. Biochemical and biophysical research communications; **211**(1):289-295 (1995)

[228] Fu, Y., Luo, N. and Lopes-Virella, M.F. Oxidized LDL induces the expression of ALBP/aP2 mRNA and protein in human THP-1 macrophages. Journal of Lipid Reseach, **41**, 2017-2023 (2000)

[229] Reddy, V.Y., Zhang, Q.Y. and Wiess, S.J. Pericellular mobilization of the tissue-destructive cysteine proteinases, cathepsins B, L and S, by human monocyte-derived macrophages. Proceedings of the National Academy of Science, **92**, 3849-3853 (1995)

[230] Brown, A.J., Mander, E.L., Gelissen, I.C., Kritharides, L., Dean, R.T., and Jessup, W. Cholesterol and oxysterol metabolism and subcellular distribution in macrophage foam cell: accumulation of oxidized esters in lysosomes. Journal of Lipid Research, **41**, 226-37 (2000)

[231] Frostegård, Kjellman, B., Gidlund, M., Andersson, B., Jindal, S., and Kiessling, R. Induction of heat shock protein in monocytic cells by oxidized low density lipoprotein. Atherosclerosis, **121**, 93-103, (2001)

[232] Chung, C.H., Bernard, P.S. and Perou, C.M. Molecular portraits and the family tree of cancer. Nature Genetics Supplement, **32**, 533- 540 (2002)

[233] Wen, X. Fuhrman, S., Michaels, G.S., Carr, D.B., Smith, S., Barker, J.L. and Somogyi, R. Large-scale temporal gene expression mapping of central nervous system development. Proceedings of the National Academy of Science, **95**, 334-339, (1998)

[234] Lashkari, D.A., DeRis, J.L., McCusker, J.H., Namath, A.F., Gentile, C., Hwang, S.Y., Brown, P.O., Davis, R.W. Yeast microarrays for genome wide parallel genetic and gene expression anaylsis. Proceedings of the National Academy of Science, **93**, 10614-10619 (1997)

[235] Eisen, M.B., Spellman, P.T., Brown, P.O., and Botstein, D. Cluster analysis and display of genome-wide expression patterns. Proceedings of the National Academy of Science, **95**, 14863-14868 (1998)

[236] Quackenbush, J. Computational Analysis of Microarray Data. Nature Reviews Genetics, **2**, 418-427 (2001)

[237] Slonim, D.K. From patterns to pathways: gene expression data analysis comes of age. Nature Genetics Supplement, **32**, 502-508 (2002)

[238] Butte, A. The Use and Analysis of Microarray Data. Nature Reviews, Drug Discovery, **1**, 951- 960 (2002)

[239] Golub, T.R., Slonim, D.K., Tamayo, P., Huard, C., Gaasenbeek, M., Mesirov, J.P., Coller, H., Loh, M.L., Downing, J.R., Caligiuri, M.A., Bloomfield, C.D. and Lander, E.S. Molecular classification of cancer: class discovery and class prediction by gene expression monitoring. Science, **286**, 531-537 (1999)

[240] Brown, M.P., Grundy, W.N., Lin, D., Cristianini, N., Sugnet, C.W., Furey, T.S., Ares, M. Jr, Haussler, D. Knowledge-based analysis of microarray gene expression data by using support vector machines. Proceedings of the National Academy of Science, **97**, 262- 267, (2000)

[241] Weinstein, J.N., Myers, T.G., O'Connor, P.M., Friend, S.H., Fornace, A.J. Jr, Kohn, K.W., Fojo, T., Bates, S.E., Rubinstein, L.V., Anderson, N.L., Buolamwini, J.K., van Osdol, W.W., Monks, A.P., Scudiero, D.A., Sausville,

E.A., Zaharevitz, D.W., Bunow, B., Viswanadhan, V.N., Johnson, G.S., Wittes, R.E. and Paull, K.D. An informative-intensive approach to the molecular pharmacology of cancer. Science, **275**, 343-349 (1997)

[242] Tavazoie,S., Hughes, J.D., Campbell, M.J., Cho, R.J. and Church, G.M. Systematic determination of genetic network architecture. Nature Genetics, **22**, 281-285 (1999)

[243] Toronen, P., Kolehmainen, M., Wong, G and Castren, E. Analysis of gene expression data using self-organizing maps. FEBS letters, 451, 142-146 (1999)

[244] Tamayo, P,, Slonim, D., Mesirov, J., Zhu, Q., Kitareewan, S., Dmitrovsky, E., Lander, E.S. and Golub, T.R. Interpreting patterns of gene expression with self-organizing maps: methods and applications to hematopoietic differentiation. Proceedings of the National Academy of Science, **96**, 2907-2912 (1999)

[245] Butte, A.J., Tamayo, P., Slonim, D., Golub, T.R., and Kohane, I.S. Discovering functional relationships between RNA expression and chemotherapeutic susceptibility using relevance networks. Proceedings of the National Academy of Science, **97**, 12182-12186 (2000)

[246] Raychaudhuri, S., Stuart, J.M. and Altman, R.B. Principle components analysis to summarize microarray experiments: application to sporulation time series. Pacific Symposium on Biocomputing, 455- 466 (2000)

[247] Mikita, T., Porter, G., Lawn, R.M. and Shiffman, D. Oxidized low density lipoprotein exposure alters the transcriptional response of macrophages to inflammatory stimulus. The Journal of Biological Chemistry, 276, **49**, 45729-45739 (2001)

[248] Mikita, T., Campbell, D., Wu, P., Williamson, K. Requirements for Interleukin-4-Induced Gene Expression and Functional Characterization of Stat6. Molecular and Cellular Biology, **16** (10), 5811-5820 (1996)

[249] Parker, R.M., and Barnes, N.M mRNA; detection by in situ and northern hybridisation. Methods in Molecular Biology **106**, 247-283 (1999)

[250] Hod, Y. A simplified ribonuclease protection assay. Biotechniques **13**, 852-854 (1992)

[251] Zamore, P.D., Tuschi, T., Sharp, P.A., and Bartel, D.P. RNAi: double-stranded RNA directs the ATP-dependent cleavage of mRNA at 21 to 23 nucleotide intervals. Cell, **101**, 25-33 (2000)

[252] Mullis, K., Faloona, F., Scharf, S., Saiki R., Horn, G. and Erlich, H. Specific enzymatic amplification of DNA in vitro: the polymerase chain reaction. Cold Spring Harbor symposia on quantitative biology, **52**; 263-273 (1986)

[253] Rappoolee, D.A., Mark, D. and Banda, M.J. and Werb, Z. Wound macrophages express TGF-alpha and other growth factors *in vivo*: analysis by mRNA phenotyping. Science, **241**, 708- 712 (1988)

[254] Liang, P and Pardee, A.B. Recent advances in differential display. Current Opinion in Immunolgy, **7**, 274- 280 (1995)

[255] Sompayrac, L., Jane, S., Burn. T.C., Tenen, D.G., and Danna, K.J. Overcoming limitations of the mRNA differential display technique. Nucleic Acids Research, **23**, 4738-4739 (1995)

[256] Wang, T and Brown, M.J. mRNA quantitation by real time TaqMan polymerase chain reaction: validation and comparison RNase protection, Analytical Biochemistry, **269**, 198-201 (1999)

[257] Wu, D.Y., Ugozzoli, L. Pal, B.K., Qian, J. and Wallace, R.B. The effect of temperature and oligonucleotide primer length on the specificity and efficiency of amplification by the polymerase chain reaction. DNA and Cell Biology, **10**, 233-238 (1991)

[258] Raeymaekers, L. Quantitative PCR: theoretical considerations with practical implications. Analytical Biochemistry, **214**, 582-585 (1993)

[259] Thellin, O., Zorzi, W, Lakaye, B., De Borman, B., Coumans, B., Hennen,G., Grisar, T., Igout, A, and Heinen, E. Housekeeping genes as internal standards: use and limits. Journal of Biotechnology, **65**, 291-295 (1999)

[260] Siebert, P.D., and Larrick, J.W. PCR Mimics: Competitive DNA fragments for use as internal standards in quantitative PCR. Biotechniques, **244**(14), 244-249 (1993)

[261] Freeman, W.M., Walker, S.J. and Vrana, K. E. Quantitative RT-PCR: Pitfalls and Potential. Biotechniques, **26**, 112-125 (1999)

[262] McCulloch, R.K., Choong, C.S. and Hurley, D.M. An evaluation of competitor type and size for use in the in the determination of mRNA by competitive PCR. PCR methods and applications, **4**, 219- 226 (1995)

[263] Siebert, P.D., and Larrick, J.W. Competitive PCR. Nature, **359** (82), 557-558 (1992)

[264] Kephart, D. Quantitative RT-PCR: Rapid Construction of Templates for Competitive Amplification. Promega Notes, **68**, 16-19 (1998)

[265] Nakayama, H., Yokoi, H. and Fujita, J. Quantification of mRNA by non-radioactive RT-PCR and CCD imaging system. Nucleic Acids Research, **20**, 4939 (1990)

[266] Huang, Z., Fasco, M.J., Kaminsky, L.S. Optimization of Dnase I removal of contaminating DNA from RNA for use in quantitative RNA-PCR. Biotechniques. **20**(6), 1012-1020 (1996)

[267] Mutimer, H, Deacon, N., Crowe, S. and Sonza, S. Pitfalls of processed pseudogenes in RT-PCR. Biotechniques, **24**, 954-962 (1991)

[268] Henly, W.N., Schuebel, K.E. and Nielsen, D.A. Limitations imposed by heteroduplex formation on quantitative RT-PCR. Biochemical and biophysical research communications. **226**, 113-117 (1996)

[269] Bustin, S.A. Absolute quantification of mRNA using real-time reverse transcription polymerase chain reaction assays. Journal of Molecular Endocrinology, **25**, 169-193 (2000)

[270] Wittwer C.T., Herrmann, M.G., Moss, A.A., and Rasmussen, R.P. Continuous fluorescence monitoring of rapid cycle DNA amplification. Biotechniques, **22**, 176-181 (1997)

[271] Taniguchi, M., Miura, K., Iwao, H. and Yamanaka, S. Quantitative Assessment of DNA Micorarrays-Compasion with Northern Blot Analyses. Genomics, **71**, 34-39 (2001)

[272] Hammer, A., Kager, G., Dohr, G., Rabl, H., Ghassempur, I., Jurgens G Generation, characterization, and histochemical application of monoclonal antibodies selectively recognizing oxidatively modified apoB-containing serum lipoproteins Arteriosclerosis, thrombosis and vascular biology, **15** (5), 704-713 (1995)

[273] Bowtell, D.D.L. Options available-from start to finish-for obtaining expression data by microarray. Nature Genetics Supplement, **21**, 25- 32 (1999)

[274] Li, Z., Li, L., Zielke, H.R., Cheng, L., Xiao, R., Crow, M.T., Stetler-Stevenson, W.G., Froehlich, J. and Lakatta, E.G. Increased expression of 72-kd type IV collagenase (MMP-2) in human aortic atherosclerotic lesions American journal of pathology, **148** (1), 121-128 (1996)

[275] Andersson, T., Boräng, S., Larsson, M., Wirta, V., Wennborg, A. Lundeberg, J., Odeberg, J. Novel Candidate genes for atherosclerosis are identified by representational difference analysis-based transcript profiling of cholesterol-loaded macrophages. Pathobiology, **69**, 304-314 (2001)

[276] Shiffman, D. Mikita, T., Tai, J.T. Large scale gene expression analysis of cholesterol-loaded macrophages. Journal of Biological Chemistry, **275**, 37324-37332 (2000)

[277] Stears, R.L., Getts, R.C. and Gullans, S.R. A novel, sensitive detection system for high density microarrays using dendrimer technology. Physiological Genomics, **3**, 93-99 (2000)

[278] Li, J., Pankratz, M. and Johnson, J.A. Differential gene expression patterns revealed by oligonucleotide versus log cDNA arrays. Toxicological sciences, **69**, 383-390 (2002)

[279] Barczak, A., Rodriguez, M.W., Hanspers, K., Koth, L.L, Tai, Bolstad, B.M., Speed, T.P and Erle, D.J. Spotted Long Oligonucleotide Arrays for Human Gene Expression Analysis. Genome Research, **13**, 1775-1785 (2003)

[280] Warrington, J. A.; Nair, A.; Mahadevappa, M. and Tsyganskaya, M.. Comparison of human adult and fetal expression and identification of 535 housekeeping/maintenance genes. Physiological Genomics, **2**(3), 143-147 (2000)

[281] Vernon, S.D., Unger, E.R., Rajeevan, M., Dimulescu, I.M. and Nisenbaum, R and Campbell, C.E. Reproducibility of alternative probe sysnthesis approaches for gene expression profiling with arrays. Journal of Molecular Diagnostics, **2**, 124-127 (2000)

[282] Herren, B., Raines E.W. and Ross, R. Expression of a disintegrin-like protein in cultured human vascular cells and *in vivo*. FASEB Journal, **11** (2), 173-180 (1997)

[283] Minami, M., Kume, N., Shimaoka, T., Kataoka, H., Hayashida, K., Akiyama, Y., Nagata, I., Ando, K., Nobuyoshi, M., Hanyuu, M., Komeda, M., Yonehara, S. and Kita, T. Expression of SR-PSOX, a novel cell-surface scavenger receptor for phosphatidylserine and oxidized LDL in human atherosclerotic lesions Arteriosclerosis, Thrombosis and Vascular biology, **21**(11),1796-1800 (2001)

[284] The Microarray Gene Expression Data Consortium available at the internet site http://www.mged.org

[285] Brazma., A., Hugamp, P., Quackenbush, J., Sherlock, G., Spellman, P., Stoeckert, C., Aach, J. Ansorge, W, Ball, C.A., Causton, H.C. Gaasterland, T., Glenisson, P. *et al.* Minimum information about a micorarray experiment (MIAME)- towards standards for microarray data, Nature Genetics, **29**, 365-371 (2001)

[286] Spellman, P.T., Miller, M., Stewart, J., Troup, C., Sarkans, U. Chervitz, Bernhart, D. Sherlock, G., Ball, C., Lepage, M., Swiatek, M., Marks, W.L, Goncalves, J., Markel, S *et al.* Design and implemnentation of microarray gene expression markup language (MAGE-ML). Genome Biology, **3** (9), 46.1-46.9 (2002)

[287] Gene Expression Omnibus (GEO) available at the internet site http://www.ncbi.nlm.nih.gov/geo

[288] Array Express available at available at the internet site http://www.ebi.ac.uk/arrayexpress

[289] Liu, G., Loraine, A.E., Shigeta, R., Cline, M., Cheng, J., Valmeekam, V., Sun. S. Kulp, D., Siani-Rose, M.A. NetAffx: Affymetrix Probesets and annotations. Nucleic Acids Research, **31** (1), 82-86 (2003)

[290] Dahlquist, K.D., Salomonis, N., Vranizan,, K., Lawlor, S.C., Conklin, B.R. GeneMAPP, a new tool for viewing and analyzing microarray data on biological pathways. Nature Genetics, **31**, 19-20 (2002)

[291] Ashburner, M., Ball, C.A., Blake, J., Bootstein, D., Butlerm H.M Cherry, J., Davies, A., Dolinski, K., Dwight, S., Eppig, J. *et al.* Gene Ontology: tool for the unification of biology. The Gene Ontology Consortium. Nature Genetics, **25**(1), 25-29 (2000)

[292] Kanehisa, M., Goto, S. KEGG: Kyoto Encyclopeida of Genes and Genomes. Nucleic Acids Research, **28** (1), 27-30 (2000)

[293] Trogan, E., Choudhury, R.P., Dansky, H.M., Rong, J.X., Breslow, J.L. and Fisher, E.A. Laser capture microdissection analysis of gene expression in macrophages from atherosclerotic lesions of apolipoprotein E-deficient mice. Proceedings of the National Academy of Science, **99** (4), 2234-2239 (2002)

[294] Wang, E., Miller, L.D., Ohnmacht, G.A., Liu, E.T. and Marincola, F.M. Nature Biotechnology, **18**, 457-459 (2000)

[295] MacBeath, G. Protein Microarrays and proteomics. Nature Genetics Supplement, **32**, 526-531 (2002)

[296] Wald, .N.J. and Law, M.R. A strategy to reduce cardiovascular disease by more than 80%. British Medical Journal, **326**, 1419-1425 (2003).

Appendix 1

Density of sodium bromide solution (g/cm^{-3}) versus index of refraction at 20°C (relative to air at a wavelength of 589nm) from reference [169].

Density	Refractive Index
1.0021	1.3337
1.0060	1.3344
1.0139	1.3358
1.0218	1.3372
1.0298	1.3386
1.0380	1.3401
1.0462	1.3415
1.0546	1.3430
1.0630	1.3445
1.0716	1.3460
1.0803	1.3475
1.0892	1.3491
1.0981	1.3506
1.1072	1.3522
1.1164	1.3538
1.1945	1.3647
1.2089	1.3669
1.2236	1.3691
1.2385	1.3713
1.2536	1.3735

Graph 1. Graph showing relationship between KBr density and refractive index

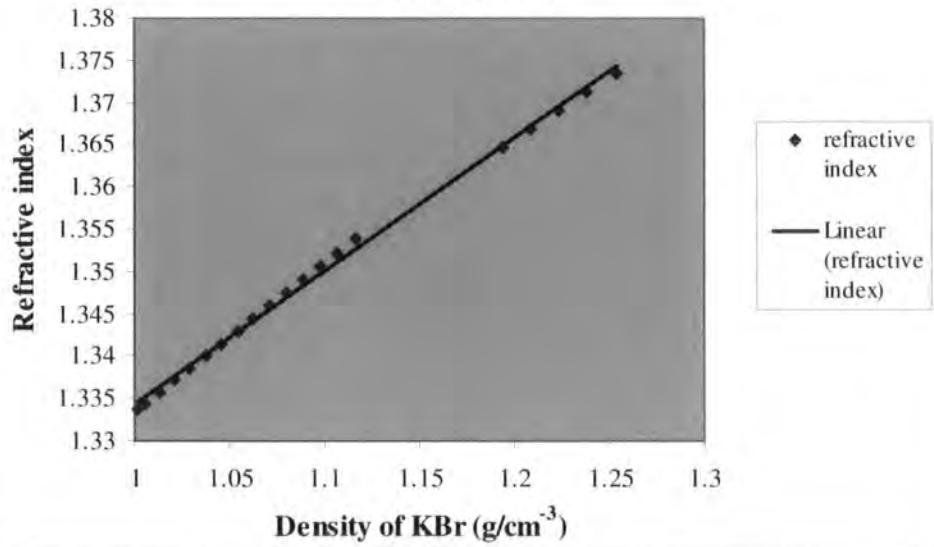

Appendix 2: Array Parameters

Settings used during arraying and subsequent analysis

(a) Parameters used for arraying

Arraying pattern	*Spacing*
Spots/cells in X: 4 or 5	Spot to spot spacing in X: 1
Spots/cells in Y: 4 or 5	Spot to spot spacing in Y: 1
Cells/Field in X: 16	Cell to Cell spacing in X: 4.5
Cells/Field in Y: 24	Cell to Cell spacing in Y: 4.5
Fields in X: 2	Interfield spacing in X: 0.3
Fields in Y: 2	Interfield spacing in Y: 0.5

(b) Parameters used for array processing

General: Spot radius: 0.4

Spot Finding: Spot search

Search range 3

Minimum correlation 0.65

Minimum covariance 0.16

Static Phosphoimager: Template radius modifier: - 0.8

Template Parabola Height: - 6

Intensity Reading

Spot reader 1.0 (for cDNA hybridisation)

0.6 (for DNA loading)

Background Reading

Background reader:

Histogram Method: Expand histogram area by 2 for cDNA hybridisation

Low Fraction Method Background Fraction = 0.1 for DNA loading

Control defaults

Spacing in X and Y: Spacing in X: 4.5

Spacing in Y: 0

Default dilution factor: 2

Other items

Duplicates (replicates) = set to 0.9

Flooding set to 0.5

Appendix 3: Atheroma array

Appendix 3 can be found on the CD enclosed with this thesis. Appendix 3 can be found on the CD as a Microsoft Excel worksheet, named appendix 3 'Atheroma Array'.

The workbook contains three separate worksheets

(a) Alphabetical gene list.

The alphabetic gene list contains a list in alphabetical order of the 770 genes (identity taken to be as given in the I.M.A.G.E library) arrayed on the array.

(b) Sequence verified genes

The sequence verified list contains a list, in alphabetical order of the 579 genes that when sequenced matched their original assigned I.M.A.G.E identity. This list also contains (where available) the corresponding Genbank and EST accession number for each gene.

(c) Array template

The array template contains a list of the gene at each X, Y position on the array.

Appendix 4

Appendix 4; list of comparisons performed between samples and identification number assigned to the subsequent comparison results tables generated

comparison sample1	**comparison sample 2**	**custom atheroma arrays**	**I.M.A.G.E arrays comparison numbers**		
		comparison numbers	*I.M.A.G.E 1*	*I.M.A.GE 2*	*I.M.A.G.E 3*
		up, down (regulated)	up, down (regulated)	up, down (regulated)	up, down (regulated)
Native	Control	2543, 2542	2517, 2516	2519, 2518	2521, 2520
24hrOxLDL	Control	2544, 2546	2522, 2523	2524, 2525	2526, 2527
24hrAcLDL	Control	2548, 2549	2528, 2529	2530, 2531	2540, 2541
24hr OxLDL	Native	2554, 2555	2477, 2478	2479, 0	2480, 2481
24hrAcLDL	Native	2552, 2553	2482, 2483	2484, 2485	2486, 2487
24hrOxLDL	24hrAcLDL	2556, 2557	0, 2489	2490, 2491	2492, 2493
4hr AcLDL	Control	(-)	2534, 2535	2536, 2537	2538, 2539
4hr OxLDL	Control	2560, 2561	2510, 2511	2512, 2513	2514, 2515
4hr OxLDL	4hr AcLDL	(-)	0, 2494	2495, 2496	2497, 2498
24hrOxLDL	4hrOxLDL	2562, 2563	0, 2499	2501, 2500	2503, 0
24hr AcLDL	4hrAcLDL	(-)	2505, 2504	2507, 2506	2509, 2508

Notes to table 1

[1] The I.M.A.G.E library was gridded over three arrays due to its large size. This is denoted by I.M.A.G.E 1, 2 and 3.

[2] Due to the poor image quality of the arrays obtained from hybridisation of the 4hr AcLDL probe to the custom arrays, no comparisons could be performed using these images, this is denoted in the table by (-). I.M.A.G.E grids hybridised to 4 hour AcLDL probe had no problems indicating that gridding of PCR products onto the arrays may have been at fault.

[3] For each set of comparisons, samples were compared in two directions to determine up-regulated and down-regulated genes. This gives two tables of results for most of the comparisons, where only one number is given, genes were only found to be regulated in one direction.

[4] As all samples were prepared in duplicate, four sets of results were obtained for each comparison performed. The four comparison lists were compared against one another and only difference that were common in all lists were identified as definite differences and were listed in a new comparison table and assigned a new comparison identification number. The comparisons numbers given in the table above correspond to these final comparison tables

[5] Comparison numbers correspond to results in tables given in Appendix 5 Excel worksheet.

Appendix 5

Appendix 5 can be found on the enclosed CD as an Excel workbook, named appendix 5 'atheroma results'. For each comparison table listed, the comparison from which the results were derived is listed at the top of the comparison table. The comparison tables are arranged by greatest fold difference. The comparison tables list the gene name, fold difference, the calculated standard deviation of the gene, its position (x,y) on the array (although genes were gridded at more than one position, only one x,y position is given; this x,y position corresponds to those given in appendix 3.3; array template). The next column contains a unique identification number assigned by the DGE group, Glaxo Wellcome, Stevenage, UK. The final column lists the comparison identification number; this corresponds to the comparison numbers given in the table in appendix 4.

Appendix 6

Appendix 6 can be found on the enclosed CD as an Excel workbook, named appendix 6 'I.M.A.G.E results'.

Appendix 6 I.M.AG.E workbook contains worksheets named by comparison numbers, except the first worksheet. The first worksheet is labelled 'summary of results' gives a summary of the top up and down regulated genes identified in each the comparisons listing the gene name and the fold difference observed. The rest of the workbook contains worksheets labelled with comparison identification numbers. These comparison numbers correspond to comparisons identification numbers given in the table in appendix 4.

As explained in the text, genes/EST sequences identified from the I.M.A.G.E array comparisons as showing differential expression were repicked from the library and resequenced. The data provided in these worksheets is the sequencing data obtained. Sequencing was performed by the Sequencing group, Department of Genetics, Glaxo Wellcome. The worksheets have been modified by the author to provide the data in each worksheet by greatest fold difference.

Appendix 7

Appendix 7 can be found on the enclosed CD as an Excel workbook, named appendix 7 'Data Analysis'. This shows the data obtained from performing the temporal gene expression part of this study and the subsequent analysis performed. Appendix 7.4 lists genes showing expression during at least one time point (listed alphabetically) on exposure of differentiated THP-1 cells to OxLDL.

Appendix 8

Appendix 8 can be found on the enclosed CD as an Excel workbook, named appendix 8 'Pearson Correlation'. The workbook contains separate worksheets, each of which represent one of the nine clusters obtained after performing hierarchical clustering.